ABSTRACT

HOLLOWAY, BLAIR STERLING. The Role of the Great Lakes in Northwest Flow Snowfall Events in the Southern Appalachian Mountains. (Under the direction of Gary M. Lackmann.)

Northwest flow snowfall (NWFS) events are a regional forecasting challenge that affects much of the southern Appalachian Mountains. These events can be defined as snowfall accompanying upslope flow and low-level northwesterly winds in this region, and typically feature irregular snowfall distributions and highly variable total accumulations. Previous research done by Perry and Konrad (2004–2007) provides an excellent climatology of NWFS events, and shows that NWFS accounts for nearly 50% of mean annual snowfall along the higher elevations of the southern Appalachians. Additionally, through analysis of backward air parcel trajectories, their research shows that NWFS events that featured a Great Lakes connection exhibited increases in composite mean and maximum snowfall totals. This body of work clearly suggests that the Great Lakes can enhance snowfall in NWFS events by warming and moistening the low-level airmass upstream of the southern Appalachians.

The specific objective of this study is to quantify and evaluate the role of the Great Lakes in NWFS events for select cases via model experiments using the Weather Research and Forecast (WRF) model. The selected cases occurred 5–6 March 2001, 18–20 December 2003, and 10–11 February 2005, and were investigated using a case study approach. In order to determine the effect of the Great Lakes on NWFS precipitation in these cases, two experimental runs were designed to isolate the role of the lakes. First, surface fluxes of heat and moisture were set to zero across the entire model domain (NOFLX). Second, surface fluxes of heat and moisture were set to zero across only water points (LKNOFLX). The

sensitivity of the selected NWFS events to planetary boundary layer (PBL) scheme was also tested (MYJPBL).

Overall, it was found that the Great Lakes play an important role in some NWFS events and can be responsible for 20–30% of the precipitation that occurs in these events. Of the selected cases, the March 2001 and February 2005 events showed large decreases in precipitation in the LKNOFLX model run compared to the control (CTRL) run. In these two events, the role of the Great lakes was to destabilize the upstream airmass and increase the Froude number. At a point roughly halfway between the Great Lakes and the southern Appalachians, the LKNOFLX model run in the February 2005 event had an average 950–850 hPa Froude number of 0.99, which was 0.40 less than the CTRL value of 1.39. Similarly in the March 2001 event, the LKNOFLX model run had an average 950–850 hPa Froude number of 1.28, which was 0.42 less than the CTRL value of 1.70. In both cases, the reduced average low-level Froude number in the LKNOFLX run compared to the CTRL shows that when the effect of warming and moistening of the low-level upstream airmass caused by the Great Lakes is removed, a more stable upstream airmass occurs which reduces the Froude number and reduces NWFS precipitation.

The Role of the Great Lakes in Northwest Flow Snowfall Events in the Southern Appalachian Mountains

by
Blair Sterling Holloway

A thesis submitted to the Graduate Faculty of
North Carolina State University
in partial fulfillment of the
requirements for the Degree of
Master of Science

Marine, Earth, and Atmospheric Sciences

Raleigh, North Carolina

2007

APPROVED BY:

_____	_____
Dr. Sethu Raman	Dr. Yuh-Lang Lin

_____
Dr. Gary M. Lackmann
(Chair of Advisory Committee)

BIOGRAPHY

Blair Holloway was born and raised in Durham, NC, about thirty minutes from the NC State campus. He came to NC State in the fall of 2000 and completed his Bachelor's degree in Meteorology in 2004 with a minor in Environmental Science. As an undergraduate, Blair worked as an intern at NBC-17 in Raleigh, NC and also participated in the first National Weather Service (NWS) Internship Class offered at the NWS Forecast Office in Raleigh. Blair began graduate school in the fall of 2004 at NC State and spent the summer leading up to that time working as a Student Career Experience Program (SCEP) employee at the Greenville-Spartanburg, SC NWS Forecast Office. He was fortunate to do his Master's research as part of a National Science Foundation grant, studying the role of the Great Lakes in northwest flow snowfall events in the southern Appalachian Mountains. After completing his required coursework for the Master's degree, Blair left NC State to take a full-time position as a meteorologist with the NWS in Greenville-Spartanburg, SC, with the plan to finish his thesis remotely. Upon completion of his Master's degree, Blair plans to continue his career as a meteorologist with the NWS.

ACKNOWLEDGMENTS

First, financial support for this research was received from the National Science Foundation (Grant - ATM-0342691). I also want to express my sincere thanks to my committee members, Drs. Gary Lackmann, Sethu Raman, and Yuh-Lang Lin. Their advice and guidance during the writing of this thesis was very helpful and very much appreciated. In particular I would like to thank my advisor Dr. Lackmann for his constant support while writing this thesis from afar. He never gave up on me as time passed and constantly provided encouragement and focus for this project. This certainly would not have been possible without him.

Next I would like to thank everyone else who had such a positive impact on this research project. First, thanks to Drs. Baker Perry and Chip Konrad for laying the groundwork in this topic area. Their research really cleared the path and gave me a solid base on which to begin my own research. They were also always easily accessible and provided excellent support and feedback throughout the project. I also must thank the management team at the Greenville-Spartanburg, SC National Weather Service Forecast Office, including Larry Gabric, Larry Lee, and Terry Benthall. Thank you so much for the opportunity for employment and for providing such a great start to my career. Also, thanks for constantly supporting and encouraging me to finish my thesis. Lastly, and certainly not least, thanks to everyone involved in the Northwest Flow Snowfall Discussion Group. The feedback provided by the group through e-mail and conference calls was excellent and provided a great forum for me to present my research progress.

Also, thanks to everyone in the Forecasting Lab and all the other graduate students I had the pleasure of interacting with during my time in graduate school at NC State. Thanks

for the friendships and always lending a helping hand for various technical things that were encountered along the way. I wish you all nothing but the best in your future endeavors.

Finally, a very special thank you is in order for my entire family. All of you helped give me the love and support necessary to make it through the graduate school years. To my wife, Anna, thank you for your personal sacrifices throughout this process. Your love and encouragement got me through the tough times and pushed me to continue forward even when I didn't want to. To my parents, Sterling and Hilda, thank you for teaching me early on the importance of education and challenging yourself along the way. You gave me the opportunities in life that were never made available to you, and for that I will be forever grateful.

TABLE OF CONTENTS

LIST OF TABLES

LIST OF FIGURES

1. Introduction

1.1. Motivation

Northwest flow snowfall (NWFS) events in the southern Appalachian Mountains present a significant challenge to operational forecasters at National Weather Service (NWS) forecast offices in the region. NWFS can be defined as snowfall accompanying upslope flow and low-level northwesterly winds in the southern Appalachian Mountains. These events are typically accompanied by cold temperatures, strong winds (leading to blowing and drifting of snow), as well as irregular snowfall distributions and highly variable total accumulations (Lee 2005; Perry 2006; Perry et al. 2007). NWFS events occur across a broad spectrum of impacts: from low-impact events characterized by flurries or trace accumulations, all the way up to major events, such as the 18–20 December 2003 event in which total accumulations exceeded 1–2 feet (Lee 2005). Even moderate NWFS events can greatly disrupt everyday life and hinder travel for residents of the southern Appalachian region.

From an operational forecasting standpoint, motivation for this study was provided and fostered by direct communication with forecasters at NWS offices located in the vicinity of the southern Appalachian Mountains. Their knowledge and expertise was solicited through two main avenues; the Mid-Atlantic Collaborative, Science, Technology, and Applied Research (CSTAR) NWFS Discussion Group, as well as personal communication with the staff at the Greenville-Spartanburg (GSP) NWS forecast office. For operational forecasters, the main aspects of NWFS events that present challenges during the forecasting process include total snowfall accumulations and spatial extent and variability. Many different parameters are taken into consideration during the forecast process for NWFS

events including the horizontal and vertical extent of moisture west of the mountains, temperature, stability, and wind speed and direction (Lee 2005).

Additional motivation for this study was provided by the Perry and Konrad studies (2004–2007) focusing on the climatological aspects of NWFS in the southern Appalachian Mountains. These studies, discussed more thoroughly later in this chapter, investigate the relationships between NWFS events and such parameters as wind direction, terrain, and the Great Lakes (Perry and Konrad 2005; Perry et al. 2007). Not only do these studies provide excellent background climatology for NWFS events over a 25 year time period, 1975–2000, but they also lay the groundwork for further investigation of the role of the Great Lakes in NWFS events. These studies suggest that the Great Lakes provide a significant contribution to the moisture supply in NWFS events. However, in their studies, this role was not quantified, and limited to NWFS events characterized by large-scale subsidence. Further, the role of the lakes was not separated into contributions of moistening versus destabilization.

This study analyzes NWFS events in the southern Appalachian Mountains from an observational and modeling perspective, focusing on the role of the Great Lakes in such events. The main objective of this study is to:

- *Quantify and evaluate the role of the Great Lakes in NWFS events for select cases via model experiments using the Weather Research and Forecast (WRF) model.*

The current chapter discusses the hypotheses and background research related to NWFS. Chapter 2 highlights the methodology used to approach the problem, the experimental design, and features the tools used for analysis. Chapters 3, 4, and 5 each outline a separate NWFS case study including an event analysis and model experiments used to test research hypotheses. Chapter 6 then places the results within the context of operational forecasting

applications as well as summarizing the conclusions of the work and highlighting possible future research.

1.2. Questions and hypotheses

The scientific questions to be emphasized here deal directly with the role of the Great Lakes in NWFS events and are as follows:

1) Does the presence of the Great Lakes matter in NWFS events in the southern Appalachians? If so, when, and by how much?
2) If the lakes matter, what is the role of Great Lakes in contributing to the destabilization the upstream airmass?
3) If the lakes matter, how is the coverage of precipitation affected by lake-induced instability changes?
4) What parameters might forecasters consider in accounting for the lake influence in NWFS events?

The research questions presented here address some fundamental aspects of NWFS events. First, instability, especially potential instability, could be instrumental in determining the spatial distribution and structure of accumulated snowfall. We might expect larger spatial extent with lighter/more homogeneous accumulations in stable conditions versus lesser spatial extent with larger/more concentrated areas of accumulations when unstable. Potential instability occurs when $\partial\theta_e/\partial z<0$, and is characterized by a column of air that is warm and/or moist near the surface and cold and/or dry aloft (Bluestein 1992). If saturated, when the lower part of a column of air in which $\partial\theta_e/\partial z<0$ is lifted, it warms relative to the top of the column and becomes unstable if the column is lifted to saturation. The presence and

magnitude of potential instability in NWFS events could lead to localized areas of enhanced snowfall accumulations and may help decrease the spatial homogeneity. The Great Lakes could contribute the low-level heat and moisture necessary for generation of potential instability through strong upward surface fluxes that occur as cold, dry air moves over the relatively warm lakes between fall and early spring.

Finally, understanding the effect of potential instability and the role of the Great Lakes in generating potential instability in NWFS events could help operational forecasters in preparing for such events. This would allow forecasters to fine-tune forecast products and better alert users of the societal impacts expected from a NWFS event. Two specific hypotheses have been developed from the research questions presented here. They focus mainly on the scientific aspects of NWFS events as well as the possible operational effects.

1) The Great Lakes are a major source of moisture and instability in some NWFS events and precipitation amounts would be strongly decreased in their absence.
2) Lake-induced instability can affect the spatial extent and amount of snowfall in NWFS events.

1.3. Background study and research

There are three main areas of research that are important to this study. Section 1.3.1 provides a brief summary of flow over mountains. Section 1.3.2 describes research done on lake-effect snowfall and the affect that the Great Lakes have on the structure of the lower levels of the atmosphere and the synoptic flow around the Great Lakes region. While many of these studies were conducted in the immediate vicinity of the Great Lakes, it follows that these modifications remain some distance downstream, perhaps even reaching the southern

Appalachian Mountains. Section 1.3.3 discusses previous climatological work dealing directly with NWFS events.

1.3.1. Flow over mountains background

This background area of research closely pertains to this study because of the importance of orographic forcing for ascent in NWFS events in the southern Appalachian Mountains. Some previous studies of orographic precipitation have investigated the effects that a mesoscale mountain range can have on the generation and propagation of a convective system in different regimes of conditionally unstable flow (e.g. Chu and Lin 2000; Chen and Lin 2001, 2005). Others have focused on identifying similarities between heavy orographic rainfall events and have created a list of common ingredients that include: 1) a conditionally or potentially unstable airstream impinging on the mountains, 2) the presence of a very moist and moderate to intense low-level jet (LLJ), 3) the presence of steep orography to help release the conditional or convective instability, and 4) the presence of a quasi-stationary synoptic-scale system to impeded or slow the progress of the orographically forced convective system (Lin et al. 2001). This list of common ingredients will be revisited in the conclusions sections in order to place NWFS events into the broader context of orographic precipitation.

As seen in previous studies (Chu and Lin 2000: Chen and Lin 2001, 2005), the moist Froude number (F_w) can be used to determine the occurrence of orographic precipitation. This dimensionless parameter is defined as $F_w = U/N_w h_m$ where U is the wind velocity perpendicular to the mountain range, N_w is the moist static stability of the incoming airstream, and h_m which is the mountain height. It is reasonable then to assume that the

Froude number (F_r) could be useful in determining the occurrence of NWFS precipitation in the southern Appalachian Mountains. Similar to its counterpart F_w, F_r takes into account the same parameters except for including the Brunt-Väisälä frequency, N (a measure of the static stability), instead of the moist static stability (N_w). To summarize, F_r is the ratio of the kinetic energy available to the energy necessary for air to rise over a barrier. The Froude number is a good indicator of the extent of blocking caused by a mountain barrier, with larger values leading to less blocking and smaller values leading to more blocking. Therefore, it follows that less blocking and larger values of F_r, would lead to more air being lifted over a mountain barrier such as the southern Appalachians which would lead to the generation of more NWFS precipitation. Within the F_r equation, there are two ways to create a larger value assuming that the height of the mountain barrier is constant. The first way is by increasing the wind velocity perpendicular to the mountain barrier, U, which increases the kinetic energy available. The second way is to decrease the static stability (N) of the incoming airstream. In a NWFS event, a decrease in the static stability could occur due to destabilization of the airmass upstream of the southern Appalachians by the Great Lakes. This would effectively increase F_r and allow for more air flow over the southern Appalachians and thus more precipitation in a NWFS event. Therefore, F_r is expected to be lower when the influence of the lakes is removed.

1.3.2. Great Lakes background

There are a plethora of studies available that focus on the Great Lakes and their impacts on the atmosphere and surrounding weather patterns. Much work has been done describing the effect that surface fluxes of heat and moisture have on the structure PBL and

its evolution over time (e.g. Chang and Braham 1991; Niziol et al. 1995; Kristovich et al. 2003). These studies have shown how temperature and moisture increases in the lower-levels of the atmosphere as cold, dry air moves across the relatively warm waters of the Great Lakes. Typically this effect occurs in the late fall and winter months and is primarily responsible for the lake-effect snows experienced in the region (Niziol et al. 1995). However, the presence of lake-effect snow has been hypothesized and shown to extend significant distances away from the Great Lakes (Schmidlin 1992). This makes it reasonable to expect that moisture from the Great Lakes, resulting from surface fluxes as cold, dry air movies across the lakes in northwesterly flow, can help enhance snowfall along the southern Appalachian Mountains in NWFS events, provided favorable trajectories in the lower troposphere.

The Great Lakes have also been shown to have large effects on many different parameters at great distances from the lakes themselves, dubbed the "lake-aggregate" effect (Sousounis and Fritsch 1994; Sousounis and Mann 2000). In numerical simulations performed to show the effect of the Great Lakes on synoptic and local scale phenomena, the water surface of the lakes in the Pennsylvania State University-National Center for Atmospheric Research Mesoscale Model version 4 (MM4) was altered such that it would be treated as forest and field types of land use within the model (Sousounis and Fritsch 1994; Sousounis and Mann 2000). As a result, significant changes in the structure and path of weather systems traveling near and through the region were seen, in addition to changes in wind speed and direction of the surface wind flow (Sousounis and Fritsch 1994). Furthermore, changes in temperature, moisture, stability, and precipitation resulted and

extended upwards of a few hundred kilometers away from the Great Lakes (Sousounis and Mann 2000).

Finally, the effect of even small topographic influences on lake-effect snowfall has been shown to affect snowfall rate and total accumulation around the Great Lakes (Hjelmfelt 1992; Niziol et al. 1995). In a comparison of two numerical simulations, one with flat topography and one with regular topography, results show that even modest topographic rises of a few hundred meters can locally enhance precipitation and mesoscale updrafts (Hjelmfelt 1992). Overall, precipitation rate and large-scale precipitation patterns were increased with the local precipitation rate enhanced by as much as a few millimeters per hour (Hjelmfelt 1992). Because topographic rises in the southern Appalachians are as much as 1500–2000 kilometers, a similar and potentially much larger effect is a reasonable expectation, provided that Great Lakes induced instability and moisture can reach this geographical region without substantial modification.

1.3.3. Northwest Flow Snowfall (NWFS) background

Operational forecasters at NWS offices in the vicinity of the southern Appalachian Mountains have many years of experience forecasting and making observations about NWFS events. This has led to the identification of a few fundamental parameters that are considered during the forecast process, for these events, including moisture characteristics of an air mass west of the mountains, temperature, stability, and wind speed and direction (Lee 2005). In addition to the forecasting aspects of these events, an informal classification scheme has been developed at the GSP NWS forecast office based on years of observation (Lee 2005):

1) Type I - Post Frontal

2) Type II - Comma Head

3) Type III - Cut-off Low

The Type I events are referred to as "classical" NWFS since snowfall occurs after a cold frontal passage (Lee 2005). These events are marked by cold advection across the mountains as a deepening surface low pressure system moves northeastward along the east coast (Lee 2005). Type II events are defined by the presence of "comma head" precipitation or moisture wrapping around to the northwestern sector of a surface low pressure system (Lee 2005). These events can evolve into Type I events as the surface low moves northeastward away from the southern Appalachians, and the upper level flow becomes northwesterly (Lee 2005). Finally, Type III cases occur in the presence of a cut-off upper level low (Sabones and Keeter 1989; Fishel and Businger 1993), typically in the late winter and spring (Lee 2005). Such events can last in excess of 24 hours because of the slow movement of many cut-off lows (Lee 2005).

Most of the research done concerning winter storms affecting the eastern United States has focused on cyclogenesis and precipitation type forecasting for areas along and near the East Coast (Maglaras et al. 1995; Gurka et al. 1995; and Keeter et al. 1995). To our knowledge, until very recently, very little research was done dealing directly with NWFS events in the southern Appalachian Mountains. However, the idea of the Great Lakes influencing remote snowfall in northwesterly flow is hardly new and was first investigated in the mountains of West Virginia (Schmidlin 1992). From 1976–1988, 38 snow events were found to be potentially caused by lake-effect snow processes at Snowshoe, West Virginia, accounting for 25–30% of the total snowfall during this period (Schmidlin 1992). It was also

concluded that the moisture necessary for the snowfall at Snowshoe came from the Great Lakes (Schmidlin 1992).

Similar work was done more recently and focuses on the entire area of the southern Appalachian Mountains (Fig. 1.1). For the period from October 1980 to May 1990, it was found that up to 30% of average annual snowfall was attributable to NWFS events in the southern Appalachians (Perry and Konrad 2004). The spatial patterns of NWFS were highly variable because orographic enhancement leads to higher totals on the windward slopes with little or no snow on downwind slopes at lower elevations (Perry and Konrad 2004). Also, the magnitude of the NWFS event depends greatly on higher relative humidity values in the lower levels of the atmosphere (Perry and Konrad 2004).

Furthermore, NWFS events have been shown to have a significant relationship with various topographic and geographic variables in the southern Appalachian Mountains (Perry and Konrad 2006). The interaction of local topography and circulation greatly influences precipitation patterns through the processes of orographic lift and downslope flow, creating precipitation shadowing effects (Perry 2006; Perry and Konrad 2006). Overall, elevation and exposure to the northwest had the greatest influence on spatial patterns of NWFS in the southern Appalachians, especially for the higher elevations (Perry and Konrad 2006).

More recent efforts in research pertaining to NWFS events have shifted to classification based on backward air parcel trajectory analysis (Perry and Konrad 2005; Perry 2006; and Perry et al. 2007). Using the NOAA Hysplit Trajectory Tool (Draxler and Rolph 2003), nearly ~50% of NWFS events exhibited a Great Lakes connection out of a sample of 191 events from 1975–2000 (Perry et al. 2007). A Great Lakes connection was defined as an event that had $\geq$ 6 hours of a trajectory within trajectory grids emanating from the central

Great Lakes (Fig. 1.2; Perry et al. 2007). Furthermore, of events that displayed northwesterly directed backward trajectories, 63.8% of NWFS events exhibited a Great Lakes connection (Perry and Konrad 2005a). Overall, NWFS events with a Great Lakes connection showed increases in composite mean and maximum snowfall totals (Perry et al. 2007). This body of work clearly suggests that the Great Lakes can enhance snowfall in NWFS events through the warming and moistening of the lower levels of the atmosphere.

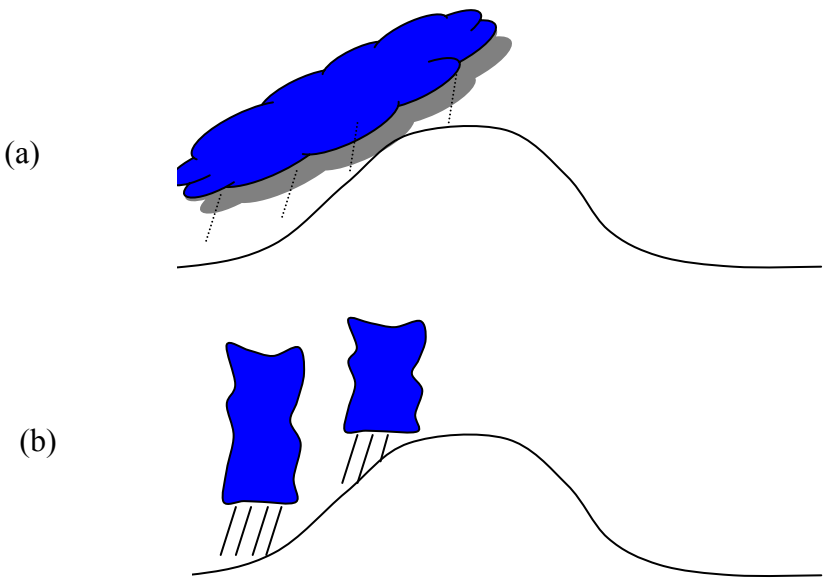

Figure 1.1. (a) Idealized schematic of an event in stable conditions; (b) as in (a) but for an event with convective instability present.

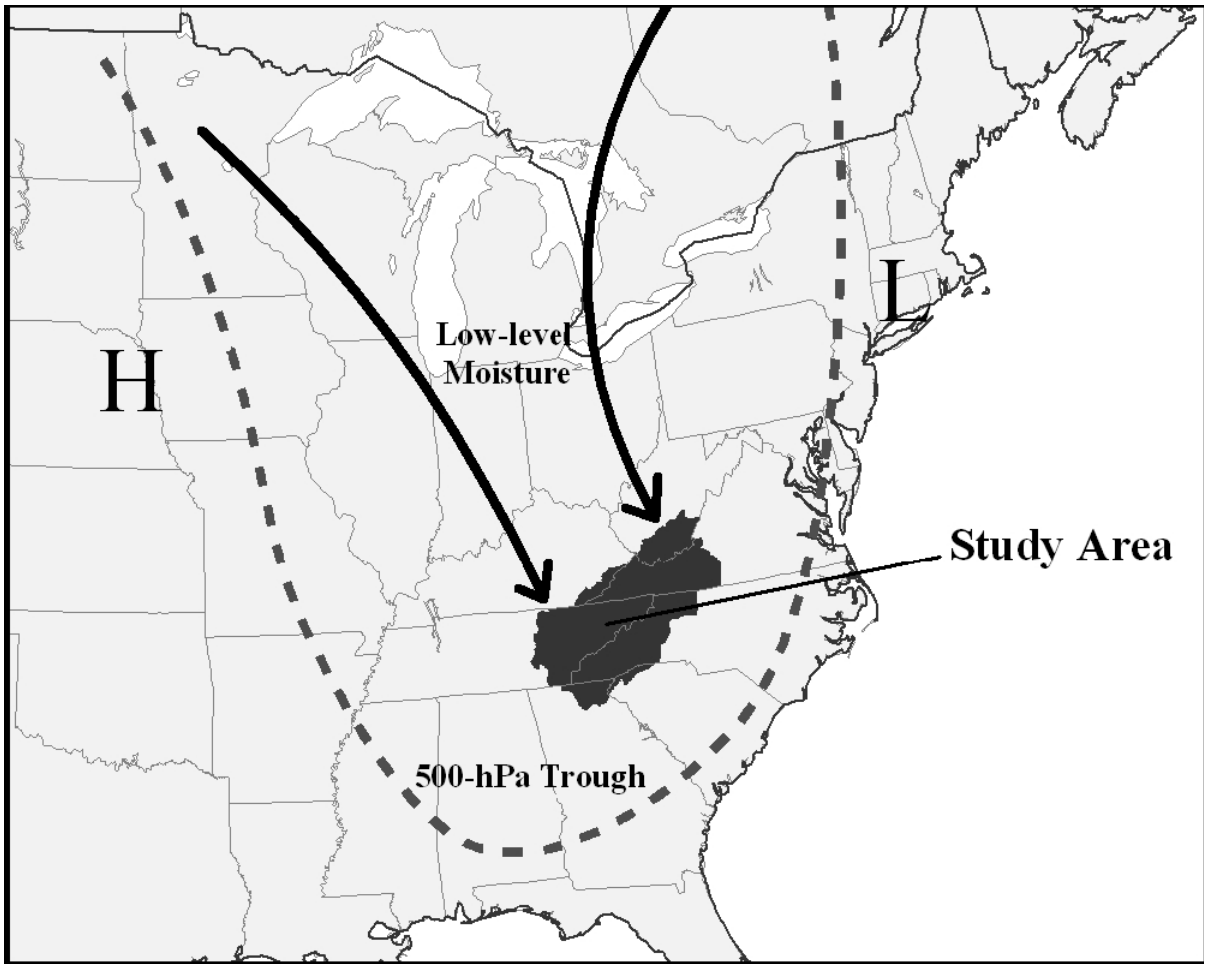

Figure 1.2. Map showing location of southern Appalachian Mountains study area (from Perry and Konrad 2005).

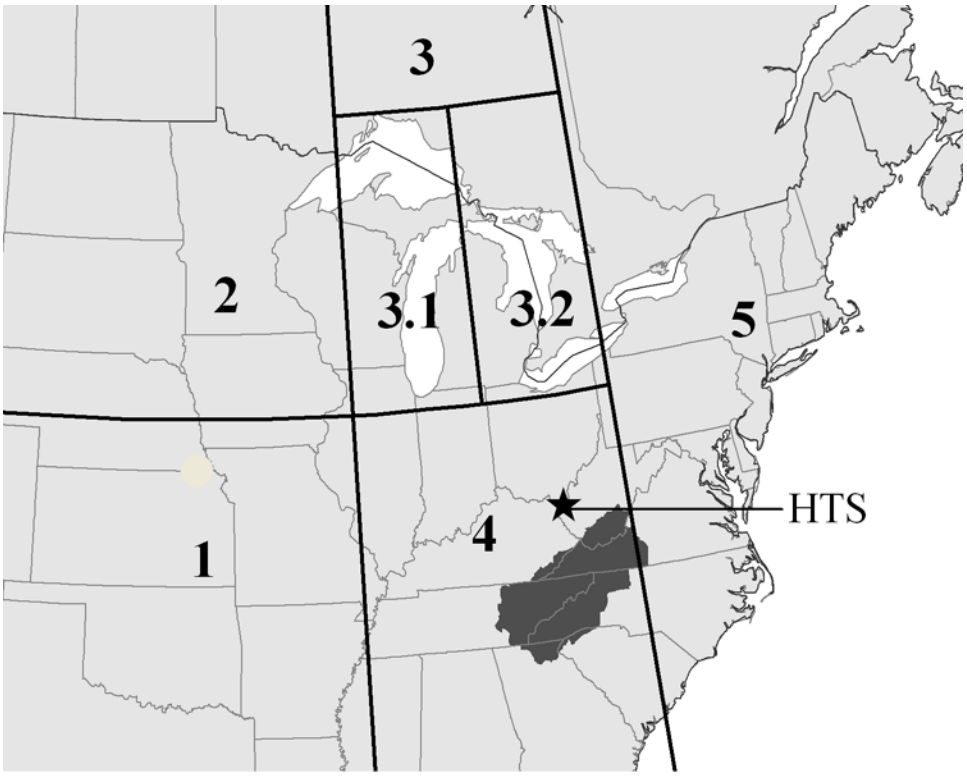

Figure 1.3. Map showing grid division system used for backward trajectory analysis by Perry et al. 2007.

2. Methodology

This chapter describes the overall methodology that was used to conduct this study and followed in the chapters to come. Section 2.1 describes the basic experimental design used in this project, 2.2 describes the case selection process, and 2.3 highlights the details of the numerical model used and the model simulations.

2.1. Experimental design

The experimental design used in this study was adopted with the purpose of quantifying the influence of the Great Lakes on NWFS events in the southern Appalachian Mountains via model experiments. The first task was to identify a set of NWFS cases that exhibited a range of seasonal variability, synoptic variability, and overall snowfall accumulation. The three cases chosen include the 10–11 February 2005 event, the 18–20 December 2003 event, and the 5–6 March 2001 event and will be discussed more thoroughly in section 2.2 as well as in the chapters to come. The next task was to perform a numerical simulation of each event to create a control run. Once a control run was attained, a series of experimental runs was performed and compared to the control runs for each case. The experimental runs were designed in such a way that the Great Lakes were altered in the model atmosphere to achieve the goal of analyzing their collective effects on NWFS events. Also, the choice of PBL parameterization schemes was changed in one of the experimental runs to investigate the sensitivity of NWFS model simulations to PBL scheme selection.

2.2. Selected cases

The three cases selected for this study represent a wide range of variability in several different areas. Seasonally, each case represents a different part of the typical time period climatologically favored for NWFS events. Case 1 occurs in February and represents a mid-winter event. Case 2 takes place in the latter half of December and is an early winter event. Finally, Case 3 occurs in March and represents a late winter event in this study. The time period that these cases span allows for an inspection of NWFS events across the entire winter season. Different background atmospheric stability regimes and lake surface conditions are expected at each of these different points in the winter season. These differences throughout the season could have a substantial effect on F_r due mainly to the degree of instability present, determining the magnitude of F_r and degree of blocking that occurs in the southern Appalachians during a NWFS event.

These cases also provide differing degrees of snowfall accumulations and impacts along the spectrum of NWFS events. The 18–20 December 2003 event produced the greatest snowfall accumulations across the southern Appalachian Mountains of the three selected. Snowfall totals for the event ranged from 1–30 inches, with many areas receiving over a foot of total accumulations (Fig. 2.1). The 5–6 March 2001 event was a medium impact event characterized by a smaller area of significant snowfall totals in excess of 4 inches (Fig. 2.2). As much as 12 inches of snow accumulated in some areas across the southern Appalachian Mountains but the event only produced a general area of 4 inch totals across the region with a lesser eastward extent (Fig. 2.2). Finally, the 10–11 February 2005 event had the lowest snowfall totals as well as the least spatial extent across the area. This event produced two

isolated 7 and 8.1 inch reports but had only a small area of 1–3 inch accumulations across the region (Fig. 2.3).

Regarding the selected cases, the snowfall analyses referenced above must be taken into further consideration. These analyses were created using snowfall data provided by cooperative observers stationed across the southern Appalachians. These data can often be quite variable due to the volunteer nature of the observations and the irregular spatial distribution of stations. Also, the majority of observers only report snowfall during winter situations and not liquid-water equivalent, making comparisons between observed data and model data difficult, since the parameters are not the same. Therefore, for the purposes of this study, model liquid precipitation will be used as the primary means of investigating the selected cases because of the disconnect between observed and model data. The fact that a rigorous comparison of model results to observations is so difficult because of this inconsistency, is a potential limitation of the study.

Finally, the synoptic environment varies greatly amongst the three selected cases as well. Specifics regarding the observational overview and synoptic evolution of each event will be closely examined in each chapter detailing the individual cases.

2.3. Numerical model simulations

To perform the numerical model simulations required by the experimental design used for this study, the Weather Research and Forecast (WRF) model, Advanced Research WRF (ARW) core, was used exclusively. Using the WRF allowed for the production of consistent datasets to analyze the selected case studies. Most of the data used to perform the WRF model runs was accessed through the National Operational Model Archive &

Distribution System (NOMADS) web interface provided by the National Climatic Data Center (NCDC). Both model input and output was displayed using the General Meteorological Package (GEMPAK, desJardins et al. 1991). This section discusses the WRF model and the various configurations used in the model experiments performed on the three selected cases.

2.3.1. Weather Research and Forecast (WRF) model

WRF is an advanced mesoscale modeling system that was created jointly by the National Centers for Environmental Prediction (NCEP) and the National Center for Atmospheric Research (NCAR). More detailed information regarding the WRF model is available in Michalakes et al. (2001) and Skamarock et al. (2005). In this study, all WRF model simulations were performed using Version 2.1.2 of the ARW dynamical core and Version 2.1.1 of the WRF Standard Initialization (WRFSI) package.

The WRF model was chosen for use in this study for a number of reasons. First, the WRF is the preeminent emerging mesoscale model and is widely used by scientists in the private research sector, the university academic realm, and the operational community. Secondly, the flexibility of the WRF and the WRFSI program makes the model user friendly and allows for quick setup of the model domain as well as the initial and boundary condition files. Finally, the expansion of the WRF modeling system has now extended to its implementation in the North American Mesoscale (NAM) model time slot at NCEP. On 20 June 2006, the Eta model in the NAM time slot was replaced by the WRF Nonhydrostatic Mesoscale Model (NMM) dynamical core. With the operational slant of this study it is only natural to use a model that will continue to have an operational significance for years to

come. The differences between the ARW and NMM cores are not believed to profoundly affect the results of this study.

2.3.1.1. Altering the Great Lakes in the WRF model

Since one of the main purposes of this study was to analyze and investigate the role of the Great Lakes in NWFS events in the southern Appalachian Mountains, a few different ways of altering the representation of the Great Lakes in the model atmosphere were attempted including:

1) Editing the sea-surface temperature (SST) file used in the initial conditions such that lake water temperatures over the Great Lakes region were set to 0 °C.
2) Setting the model sea-ice threshold to a value <271 K and then editing the lake water temperatures in the method mentioned above to a value less than the new model sea-ice threshold.
3) Editing the land-sea mask in the model in a manner that all water points within the Great Lakes region would be changed to land points.
4) Manipulating the surface-layer parameterization scheme used in the model so that the heat and moisture fluxes are set to zero over water points.

Of the methods attempted to alter the model representation of the Great Lakes, only the option manipulating the surface-layer scheme was successful in creating the desired effect of shutting off the fluxes of heat and moisture from the Great Lakes. This method enabled the isolation of the Great Lakes necessary to test the hypotheses laid out for this study and was used in two of the experimental runs for each of the cases that are described in the next section.

2.3.1.2. Representation of the southern Appalachians

One aspect of the WRF model that could have strong implications on the results of this study is its representation of the terrain of the southern Appalachians. Because of the relationship between topography and NWFS in the southern Appalachians (Perry and Konrad 2006), knowing the strengths and limitations of the WRF model topography is vital to interpreting the results of the model experiments performed on the three selected cases. Overall, the southern Appalachians are made up of a large area of >2000 ft terrain that extends from northern Georgia to southern West Virginia (Fig. 2.4). Also, there are large areas, especially in western North Carolina and far eastern Tennessee, where the southern Appalachians rise to >5000 ft. across the Great Smokey Mountains and the Black Mountains (which contain Mt. Mitchell, the highest peak in eastern North America at 6684 ft.). Two other important features are the sharp changes in elevation that occur along the North Carolina/Tennessee border and to the east along the Blue Ridge Escarpment (Fig. 2.4). Along the North Carolina/Tennessee border, the terrain abruptly rises from ~1000 feet in parts of east Tennessee, to >5000 ft. in far western North Carolina (Fig. 2.4), creating upslope flow when northwesterly winds prevail. Finally, to the east of the higher terrain in the southern Appalachians, elevations quickly drop back to around 1000 ft. which favors downsloping east of the southern Appalachians when northwesterly winds are in place (Fig. 2.4).

Overall, our WRF model domain topography captures the basic structure of the southern Appalachians but does not adequately represent the magnitude of the higher terrain especially across western North Carolina due to the very coarse grid spacing on our model domain grid (Fig. 2.5). As shown in the actual topography (Fig. 2.4), western North Carolina

contains many areas where elevations >5000 ft. In the coarse model domain however, this area is represented by terrain that only reaches to a maximum height of ~3400 ft. (Fig. 2.5). This could mean a difference of 2000 ft or more in some locations along the southern Appalachians, greatly affecting the upslope flow that occurs in NWFS. However, our model domain does seem to capture the abrupt change in terrain along both the western and eastern edges of the southern Appalachians (Fig. 2.5). The coarse WRF model domain also does well with the Cumberland Plateau in Tennessee. This band of ~2000 ft. terrain in eastern Tennessee is reasonably represented in the WRF with ~1600 ft. elevations (Fig. 2.4).

Due to the representation of the southern Appalachians caused by our use of a very coarse WRF model domain, several potential effects could occur. First, because the WRF model domain captures the abrupt rise/fall in terrain along the western/eastern edge of the southern Appalachians, it is anticipated that the model will be able to create a precipitation structure similar to that of the various NWFS events studied. This includes features such as sharp gradients in precipitation both along the upwind and downwind slopes of the southern Appalachians. Also, it is anticipated that the WRF will be able to produce a general maxima in NWFS precipitation along the higher terrain in the southern Appalachians, despite the coarse grid spacing used on the model domain. These features are readily seen in the snowfall analyses of the 3 selected cases (Figs. 2.1, 2.2, 2.3). However, despite expecting the WRF to emulate the overall precipitation structure of these NWFS events, it is anticipated that the model will fail to reproduce the local maxima in precipitation as seen in the 3 cases. This is due to the fact that our coarse grid spacing prevents a more true representation of the southern Appalachians on the WRF model domain, thus reducing the overall magnitude of upslope flow with northwesterly winds in the model atmosphere.

2.3.2. WRF model configuration

Four different WRF model runs were performed on each of the three individual cases in order to address the questions set forth in this study, and to quantify the influence of the Great Lakes in NWFS. Table 2.1 shows the differences between the model runs, highlighting the differences between the control run and the experimental runs. The model domain, used for all of the model runs, covered the entire eastern half of the continental United States including the Great Lakes, the western portion of the Atlantic Ocean, and much of the Gulf of Mexico (Fig. 2.6). The model grid was 150x150 in size with 24 km grid spacing and was centered at 36.96 °N, -81.09 °W placing the center of the model domain over the southern Appalachian Mountains. Half-degree latitude/longitude SST data were used with the North American Regional Reanalysis (NARR) dataset (Mesinger et al. 2006) designated as the initial and boundary conditions, respectively. Boundary conditions were updated every 3 hours. Each model run was a 141 hour simulation initialized at 0000 UTC 6 February 2005, 0000 UTC 15 December 2003, and 0000 UTC 2 March 2001, respectively, for each NWFS event investigated. The model runs were initialized well before the actual NWFS event occurred in an attempt to avoid any preconditioning of the atmosphere by the Great Lakes, primarily for the various experimental runs.

The first model run was the control run (CTRL). The main purpose of the CTRL was to serve as the basis for comparison for the experimental runs that followed. For the CTRL, the WRF was configured with the following parameterization schemes: the Lin et al. (1983) microphysics scheme, RRTM longwave radiation scheme (Mlawer et al. 1997), Dudhia shortwave radiation scheme (Dudhia 1989), the Rapid Update Cycle (RUC) land-surface model (Smirnova et al. 1997, 2000), the Yonsei University (YSU) PBL scheme (Hong and

Pan 1996; Hong et al. 2006), the Betts-Miller Janjic (BMJ) convective scheme (Janjic 1994, 2000), and a Monin-Obukhov surface-layer scheme. The second model run, also the first experimental run (MYJPBL), was done with the purpose of testing the sensitivity to PBL scheme selection for NWFS events. To do this, the same configuration was used as in the control run except for the use of the Mellor-Yamada-Janjic (MYJ) PBL scheme (Janjic 1990, 1996, 2002) and the Monin-Obukhov-Janjic surface-layer scheme (Janjic 1996, 2002). The next model run and second experimental run (NOFLX) uses the exact same configuration as CTRL but has the surface fluxes shut off across the entire domain. To achieve this, the surface heat and moisture flux flag, "isfflx", in the WRF namelist file was changed to zero prior to running the model. However, it should be pointed out that NOFLX is exposed to surface fluxes of heat and moisture as the model boundary conditions are updated every 3 hours with the NARR data. These NARR data do contain these surface fluxes, but they are not computed (set to zero) by the model in between boundary updates. Finally, in experimental run 3 (LKNOFLX), the fourth method of altering the Great Lakes that was discussed earlier was used with an identical configuration to CTRL. In LKNOFLX, the heat and moisture fluxes computed in the Monin-Obukhov surface-layer scheme were set equal to zero for all water points across the entire domain.

2.3.2.1. PBL scheme comparison

In the first experimental run (MYJPBL), the PBL and surface layer schemes used are changed from the CTRL to test the sensitivity to PBL scheme selection for NWFS events. In the CTRL the YSU PBL scheme is used, and in MYJPBL the MYJ PBL scheme is used. The main difference between the two schemes is the fact that the YSU PBL scheme allows for

nonlocal turbulent mixing (Hong et al. 2006) and the MYJ PBL features local turbulent mixing (Janjic 1990, 1996, 2002). The nonlocal turbulent mixing allows for vertical mixing between non-adjacent model layers in the PBL. The YSU PBL scheme, as labeled by Hong et al. (2006), is a revision of the Medium-Range Forecast (MRF) PBL (Hong and Pan 1996) to include an explicit treatment of entrainment processes at the top of the PBL. The nonlocal mixing in the YSU PBL scheme promotes a deeper boundary layer and provides a more realistic representation of the boundary layer in the model atmosphere compared to the MYJ PBL scheme. Also, the YSU PBL scheme resolves some known problems of the MRF PBL scheme including excessive boundary layer mixing in the presence of strong winds and overly rapid growth of the PBL (Hong et al. 2006).

2.4. Froude number calculations

In order to further quantify the effect of the Great Lakes on NWFS precipitation in the southern Appalachians, the Froude number is calculated at a point upstream of the region. This point, located at Lexington, KY (38.03°N;-84.44°W), is approximately half-way between the lakes and the southern Appalachians. F_r is calculated in the 950–850 hPa layer, in order to determine the average F_r of the low-level airmass upstream of the region during the selected NWFS events. First, N is averaged in the 950–850 hPa layer. Next, the average wind magnitude perpendicular to the mountains in this layer is solved. This wind calculation is done assuming that the southern Appalachian Mountains run at a 40° angle from southwest to northeast. At this angle, a wind direction of 320° would yield a flow perpendicular to the mountain barrier. To calculate the component of the flow that is normal to the mountains, the u and v components of the wind at Lexington, KY are averaged in the 950–850 hPa layer

to determine the overall wind magnitude. Then this is adjusted by taking the average wind direction in this layer and subtracting 320° to find the difference in the angles. Finally, by taking the cosine of the angle difference and multiplying it by the overall wind magnitude, the component of the flow normal to the southern Appalachians is determined for use in the F_r calculation. Also, a barrier height of 1000m is assumed and held constant for all F_r calculations.

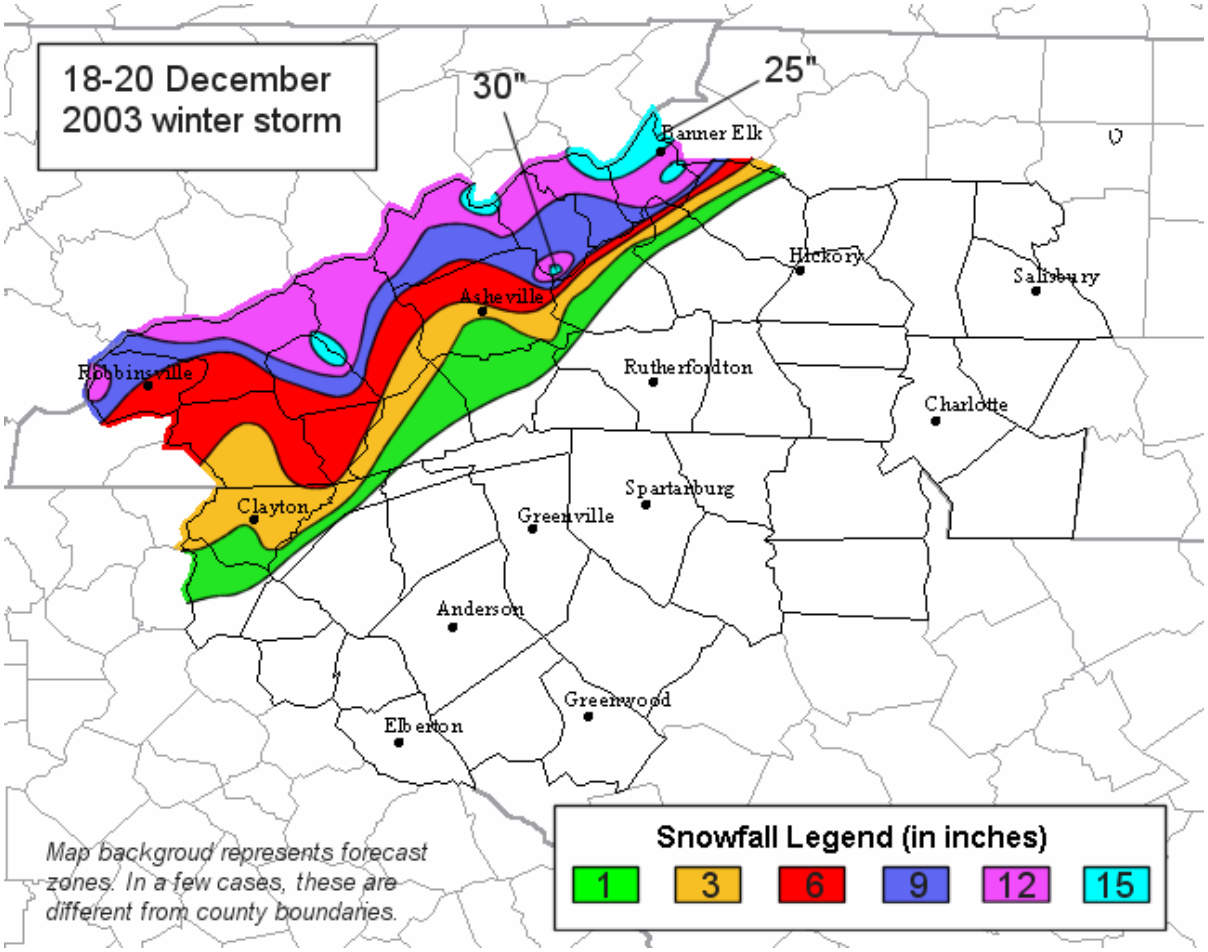

Figure 2.1. Snowfall accumulations map for the 18–20 December 2003 NWFS event from NWS WFO GSP (http://www.erh.noaa.gov/gsp/localdat/December_18–20.htm).

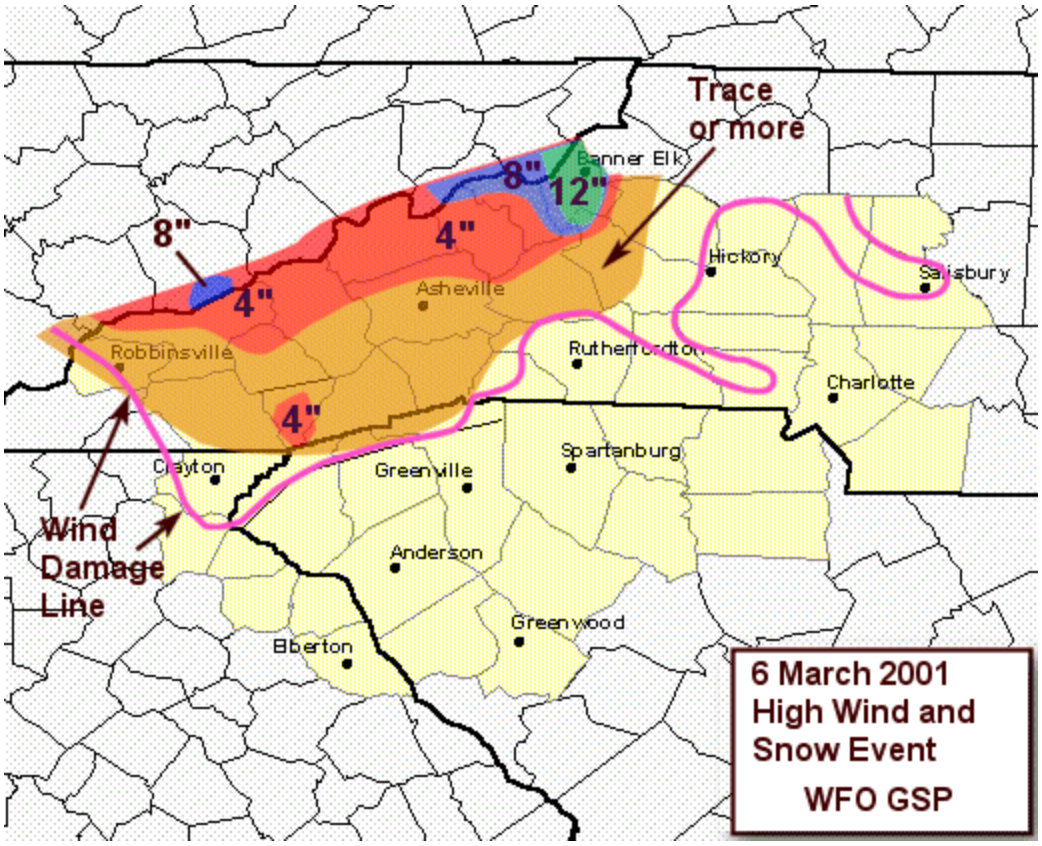

Figure 2.2. Snowfall accumulation map for the 5–6 March 2001 NWFS event from NWS WFO GSP (http://www.erh.noaa.gov/gsp/localdat/headline/6march2001wind-snow/6march2001map.gif).

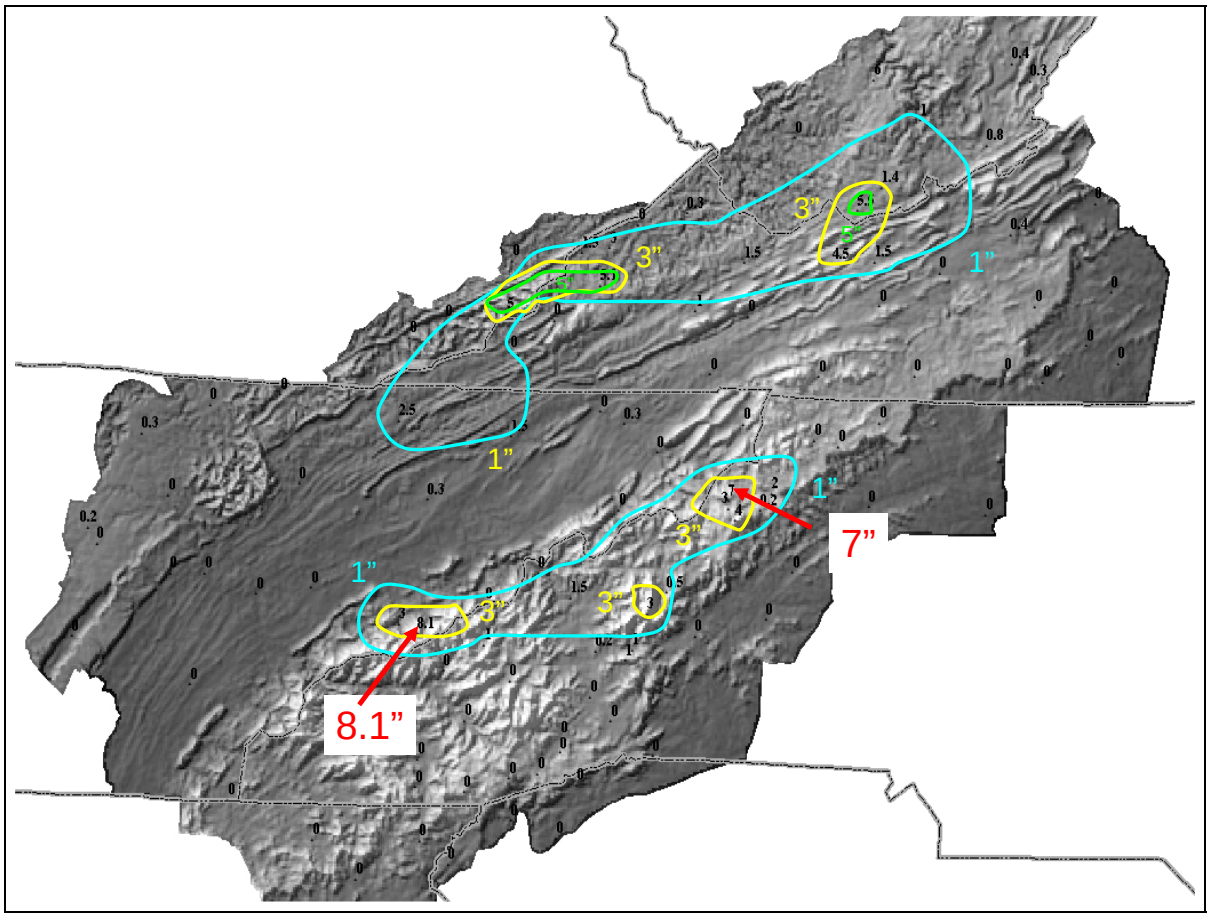

Figure 2.3. Snowfall accumulations map for the 10–11 February 2005 NWFS event (image courtesy of Baker Perry).

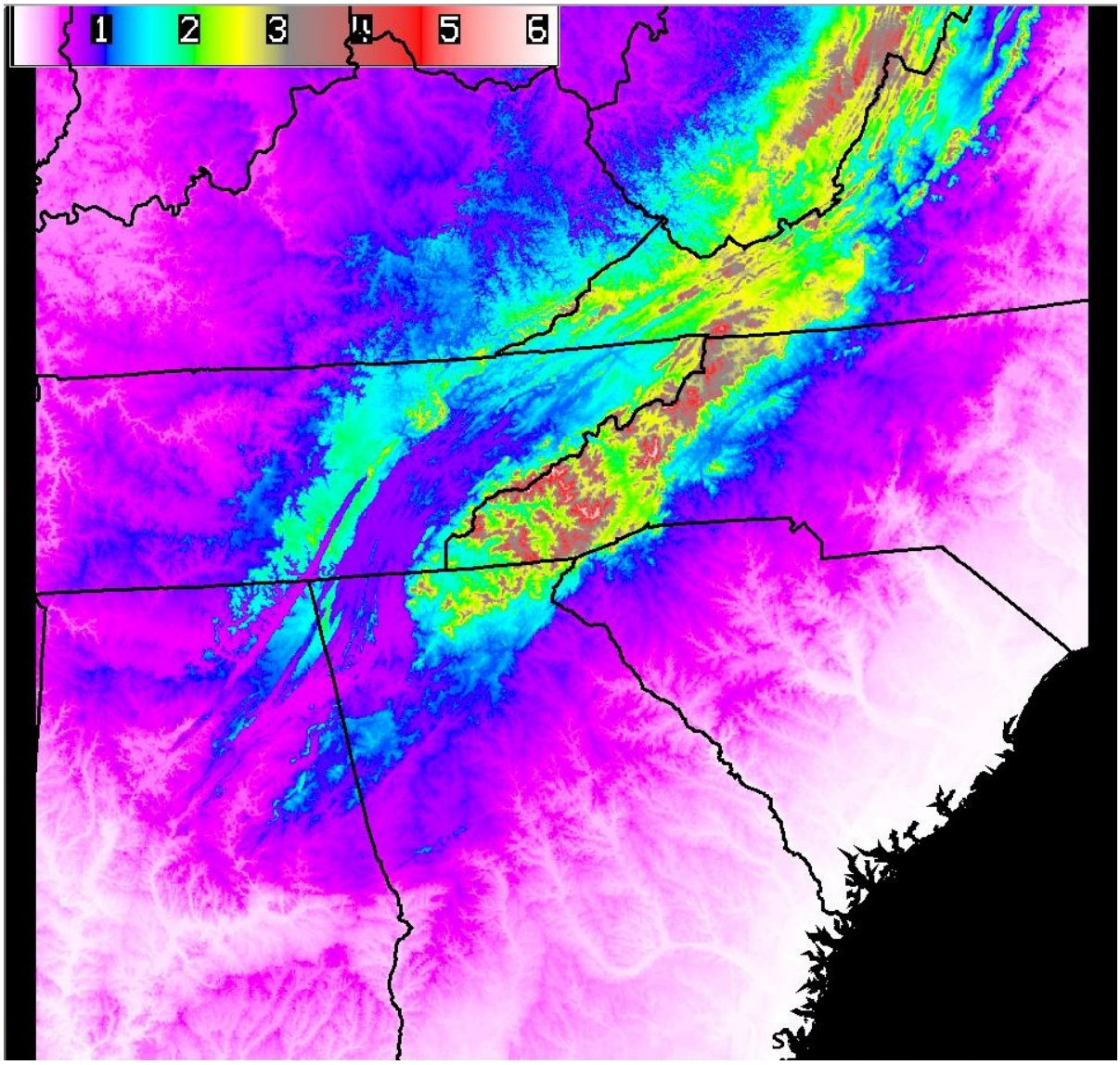

Figure 2.4. Image of the terrain of the southern Appalachians (as in color bar at top, in Kft.). Image taken from Advanced Weather Information Processing System (AWIPS).

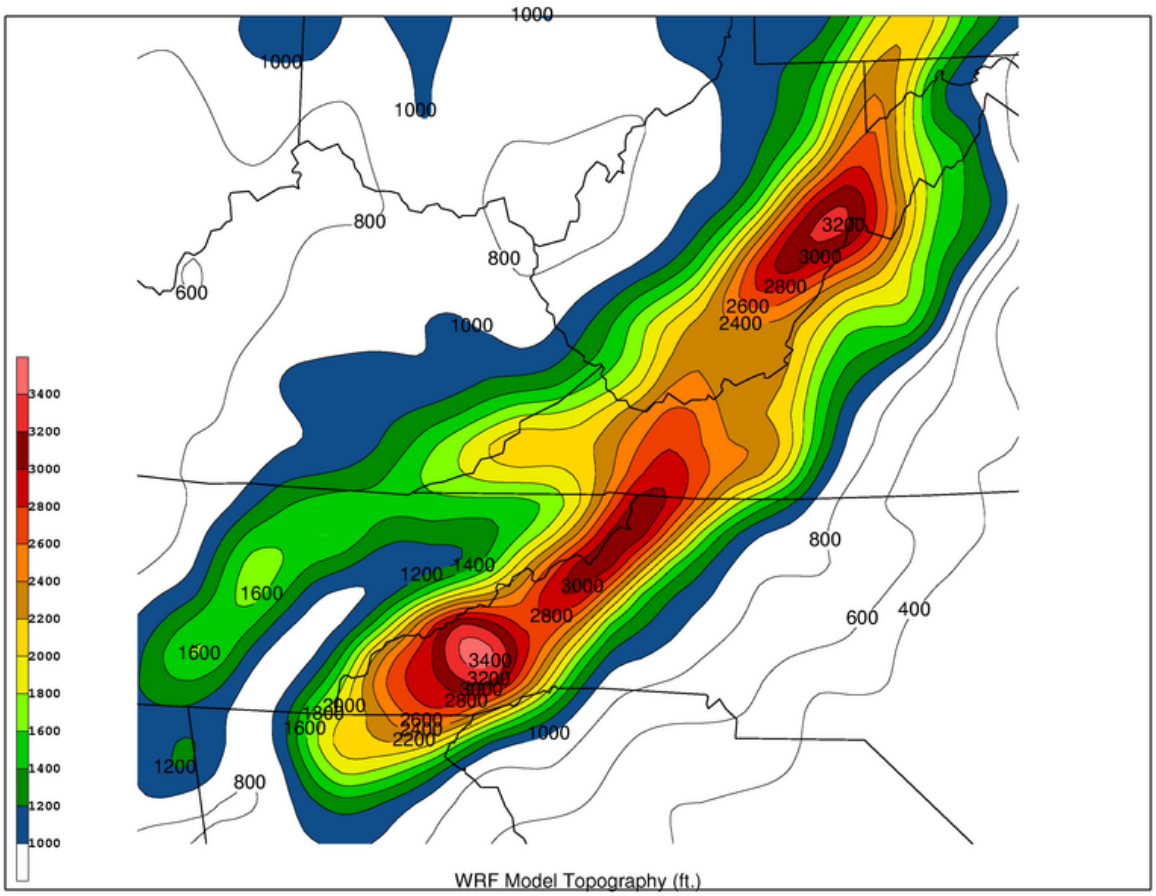

Figure 2.5. Topography of the southern Appalachians in the WRF model (contours every 200 ft, shaded as in color bar at lower left).

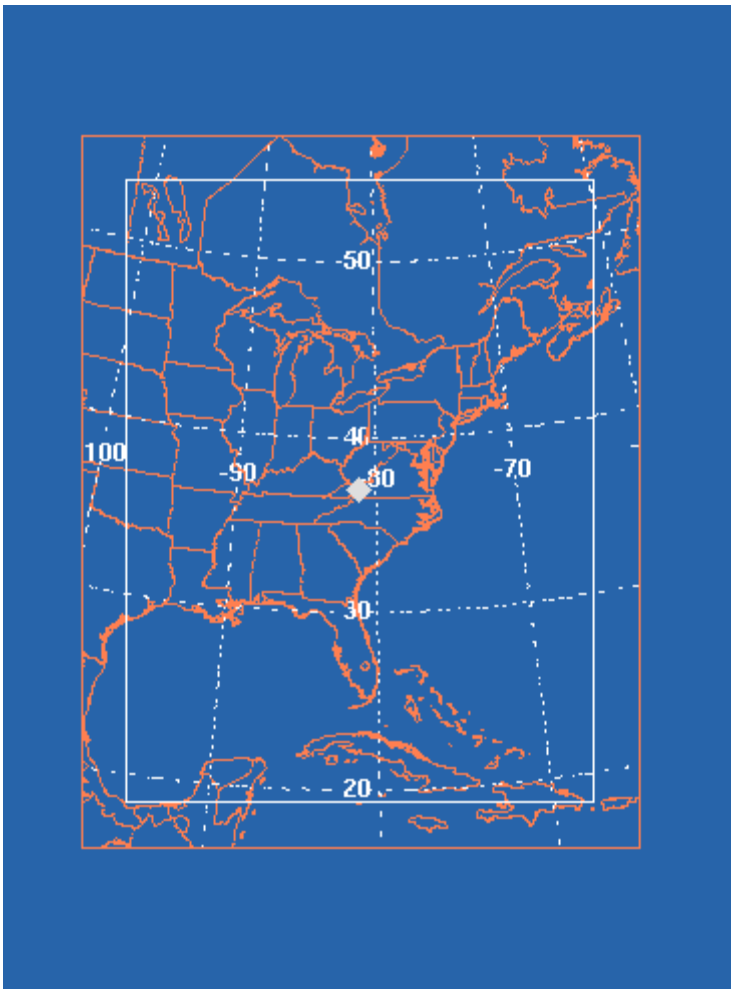

Figure 2.6. Model domain used for all WRF model simulations.

Table 2.1. Brief description distinguishing the WRF model runs.

MODEL RUN	DESCRIPTION
CTRL	Control run, configuration as discussed in 2.3.2
MYJPBL	Same as control but with MYJ PBL
NOFLX	Same as control but no surface fluxes over the model domain.
LKNOFLX	Same as control but no heat or moisture flux over water points.

3. Case 1: 10–11 February 2005

3.1. Event analysis

The first NWFS event examined occurred on 10–11 February 2005 and featured a post-frontal (Type I) event. This case also serves as an example of a lower impact, mid-winter NWFS event. In this section, Case 1 is discussed from a synoptic and observational point of view with numerical simulations of the event discussed in 3.2.

3.1.1. Synoptic overview

On the synoptic scale, the 10–11 February 2005 NWFS event is defined by an eastward moving upper level trough, and low level northwesterly flow occurring in the wake of a cold front associated with a low pressure system developing over the mid-Atlantic United States. At 1200 UTC on the 9th, the upper level trough is easily seen immediately to the west of the Great Lakes, extending southward across the Northern Plains (Fig. 3.1). By 0000 UTC on the 10th, the upper trough had progressed eastward into the Mississippi River Valley (Fig. 3.2) and by 1200 UTC it had shifted further east into the southern Appalachian Mountains (Fig. 3.3). A transition to northwesterly flow aloft occurs along the southern Appalachian Mountains at 0000 UTC on the 11th (Fig. 3.4) with the upper trough axis offshore over the western Atlantic by 1200 UTC (Fig. 3.5).

At 850 hPa, the transition to northwesterly flow takes place earlier than at 500 hPa, occurring between 0000 UTC (Fig. 3.6) and 1200 UTC on the 10th (Fig. 3.7). Also, by 1200 UTC, cold advection is well underway across the southern Appalachians as 850 hPa temperatures had cooled from around 6°C at 0000 UTC to around -8°C at 1200 UTC. The

low level northwesterly flow continues across the southern Appalachians through 0000 UTC on the 11th with 30–40 kts observed (Fig. 3.8). At 1200 UTC on the 11th northwesterly flow persists across the southern Appalachians with more westerly flow occurring upstream toward the Great Lakes (Fig. 3.9).

At the surface, an elongated stationary frontal boundary extended from New England south to the Texas coast at 1200 UTC on the 9th (Fig. 3.10). By 0000 UTC on the 10th, a surface low had developed over western Pennsylvania with a southwestward trailing cold front (Fig. 3.11). The cold front progressed eastward across the western Carolinas over the next 12 hours with northwesterly flow at the surface observed all the way upstream over the Great Lakes region (Fig. 3.12). This northwesterly flow continued through 0000 UTC on the 11th (Fig. 3.13) before turning more westerly by 1200 UTC (Fig. 3.14).

3.1.2. Observational overview

At 0300 UTC on the 10th, composite radar reflectivity shows a band of cold frontal precipitation lingering along the southern Appalachians (Fig. 3.15). However, by 0900 UTC, this precipitation had shifted eastward with light snow showers beginning to develop along the North Carolina/Tennessee border as well as in southwestern Virginia (Fig. 3.16). Surface observations from 0900 UTC show northwesterly flow from the southern Appalachians extending all the way back to the Great Lakes with light snow reported across Kentucky and Indiana (Fig. 3.17). By 1200 UTC, the NWFS event was well underway (Fig. 3.18) with light snow falling from far western North Carolina, northeast to southern West Virginia (Fig. 3.19). The NWFS event continued over the next 18 hours before tapering off by 0900 UTC on the 11th (Fig. 3.20). At 0000 UTC on the 11th low level flow over the Great Lakes had

shifted to more westerly with northwesterly flow only extending back to across Indiana (Fig. 3.21). Finally, by 0600 UTC flow over the Great Lakes had become westerly to southwesterly with only light northwesterly surface winds across the southern Appalachians, signaling the end of the NWFS event (Fig. 3.22).

Another source of data for NWFS events is visible satellite data which can show bands of clouds extending southeastward of the lakes and towards the southern Appalachians. The 1531 UTC 10 February visible satellite image indicates the presence of a band of clouds across central Lake Michigan that extends southeastward toward the southern Appalachian region (Fig. 3.23). This is a persistent feature that can be seen continuously at 1731 UTC (Fig. 3.24), 1931 UTC (Fig. 3.25), and 2131 UTC (Fig. 3.26).

Overall, it appears that the trajectory of air between the Great Lakes and the southern Appalachians in the lower levels of the atmosphere is good enough to support a Great Lakes influence. At 850 hPa, near the beginning of the NWFS event, observed winds are nearly due northerly over the Great Lakes and northwesterly further downstream over the southern Appalachians (Fig. 3.7). At the surface, observed winds along the western and eastern shoreline of Lake Michigan are northerly to northwesterly, with northwesterly flow extending all the way to the southern Appalachians (Fig. 3.18). The presence of nearly due northerly flow over the Great Lakes is believed to be integral to the relative importance of the Great Lakes in NWFS events as that particular directional flow allows air parcels to spend the optimal amount of time over the lakes and Lake Michigan in particular. This type of trajectory is similar to grid division 3.1 from Perry et al. 2007 (Fig. 1.3), which showed increases in composite mean and maximum snowfall totals relative to events defined by trajectories that did not exhibit a Great Lakes connection.

Since much of the precipitation that occurs during NWFS events falls across locations that do not have first-order reporting stations such as Automated Surface Observing Systems (ASOS) stations, daily Cooperative Observer (COOP) reports must be relied upon as the best source of "ground-truth" data. For the 10–11 February 2005 NWFS event, snowfall totals generally ranged from 1–3 inches across Kentucky, southern West Virginia, and southwestern Virginia, with a few isolated 5 inch reports (Fig. 2.3). Across the Tennessee/North Carolina border, similar accumulations resulted but with a few higher maximum amounts of 8.1 inches at Mount Leconte, Tennessee and 7 inches at Mount Mitchell, NC.

3.2. Numerical simulations

To further investigate the 10–11 February 2005 NWFS event, as well as the other events referenced in this study, a series of WRF model runs was completed to create a surrogate observational dataset (Keyser and Uccellini 1987) as well as for use in investigating the physical processes involved in the event. The setup for the various model runs is as was discussed in chapter 2.

3.2.1. Control run (CTRL)

At 0000 UTC on the 10th, CTRL shows a 1012 hPa low pressure center over the central Appalachians with a cold front extending southwestward across the western Carolinas and into central Alabama (Fig. 3.27a). The placement of the low and the cold front is in good agreement with the surface analysis from the same time (Fig. 3.11), though the strength of the low is a bit underestimated in CTRL (Fig. 3.27a). By 1200 UTC, the low pressure

center in CTRL has shifted eastward near the Chesapeake Bay area (Fig. 3.27b), similar to the surface analysis (Fig. 3.12) which indicates that the cold front has moved through the southern Appalachians.

At the 850-hPa level, winds are due westerly across the southern Appalachians at around 0000 UTC on the 10th (Fig. 3.28a) shifting around to northwesterly by 0900 UTC (Fig. 3.28b), the beginning of the NWFS event. Temperatures at the 850-hPa level over the southern Appalachians also cool during this time period from around -2 °C at 0000 UTC, to around -8 °C at 0900 UTC. Surface winds show a similar directional trend with the presence of a wind shift and precipitation associated with cold front across the southern Appalachians at 0000 UTC (Fig. 3.29a). By 0900 UTC on the 10th, the 10 m winds have become northwesterly and the cold frontal precipitation has moved east of the mountains (Fig. 3.29b). Therefore, the beginning of the NWFS event evident in this WRF model run is noted as approximately 0900 UTC 10 February, which is also supported by observational data from the event.

For the event, CTRL shows liquid equivalent precipitation totals ranging from a few hundredths to around 0.40 inches across the southern Appalachians (Fig. 3.30). Overall, the maximum in precipitation lines up along the higher terrain on the North Carolina/Tennessee border, stretching northeastward into West Virginia. Also, accumulating precipitation quickly diminishes east of the region, with a strong precipitation gradient across western North Carolina. On a larger view, it is interesting to note that a swath of >0.05 in. accumulations extends back to the northwest, stretching towards the southern end of Lake Michigan (Fig. 3.31), suggestive of a Great Lakes influence for this event.

Over the Great Lakes, response to the movement of cold air across the warmer lake waters is easily seen in the sensible and latent heat fluxes. At the beginning of the event, 0900 UTC on the 10th, sensible and latent heat fluxes are both >100 W/m^2 across Lake Superior and Lake Michigan with nearly northerly 10 m flow (Fig. 3.32). By 0000 UTC on the 11th northwesterly flow remains across the southern Appalachians with 10 m winds shifting to westerly and southwesterly across western portions of the Great Lakes (Fig. 3.33). The event is essentially over by 1200 UTC on the 11th as the 10 m winds have taken on a stronger westerly component across the Great Lakes, including locations further to the southeast (Fig. 3.34).

One of the scientific questions to be addressed in this study was to investigate the presence and importance of potential instability in NWFS events. As discussed in Chapter 1, potential instability occurs when equivalent potential temperature (θ_e) decreases with height, $\partial\theta_e/\partial z<0$, and can be seen on vertical cross sections of θ_e. Therefore, such cross-sections were plotted from CTRL along a line from La Crosse, IN to Albemarle, NC which is shown in Fig. 3.31. At 0000 UTC on the 10th, θ_e decreases with height as the isentropes fold over a fairly shallow layer, indicative of potential instability extending from La Crosse, IN to near the windward slopes of the southern Appalachians (Fig. 3.35a). There is some potential instability present along the higher terrain, but not of the same magnitude present further upstream. By the beginning of the NWFS event, 0900 UTC, the layer of potential instability has shifted further downstream into the southern Appalachians (Fig. 3.35b) and continues to increase through 1800 UTC (Fig. 3.35c). At the end of the NWFS event, 0900 UTC on the 11th, potential instability is no longer present between the Great Lakes and the southern Appalachians (Fig. 3.35d). This is noteworthy because the potential instability begins to

wane as the 10 m winds become more westerly across the Great Lakes. One explanation for this decrease in potential instability is that because of this wind shift, the lakes are no longer able to contribute heat and moisture to the lower levels of air moving toward the southern Appalachians. Therefore, the potential instability of the air mass moving southeastward towards the southern Appalachians is greatly decreased compared to earlier in the event. However, it is important to note that other processes could be at work. These include a reduction in the height of the PBL due to synoptic-scale subsidence or a general slackening of the winds, as well as the expected diurnal cycle of the PBL.

3.2.2. Experimental run 1 (MYJPBL)

The first experimental run done on the February 2005 NWFS event was MYJPBL. This model run has the same initial setup as CTRL except it uses the MYJ PBL scheme instead of the YSU PBL scheme. In general, the YSU PBL scheme is expected to produce a deeper boundary layer than the MYJ PBL scheme at least partially due to its non-local mixing scheme which allows mixing between non-adjacent model layers (Hong and Pan 1996; Hong et al. 2006). For the event, MYJPBL produced its precipitation maxima along the higher terrain on the North Carolina/Tennessee border extending northeastward into West Virginia (Fig. 3.36), much like CTRL. The pattern on the larger-scale view is also very similar to that of the CTRL with a swath of heavier accumulations extending from the southern Appalachians back to the northwest (Fig. 3.37). However, when directly compared to CTRL, MYJPBL produced much greater precipitation along the southern Appalachians with increases as great as 0.25 inches (Fig. 3.38). Though there are a few areas that received

slightly less precipitation from MYJPBL, the overwhelming majority of locations experienced increased precipitation.

The degree of increase or decrease in potential instability from CTRL to MYJPBL is difficult to ascertain by looking at θ_e cross-sections alone. For example, the 0900 UTC on the 10th cross-section (Fig. 3.39) looks very similar to the same time from the CTRL (Fig. 3.35b). So, for a better comparison, θ_e profiles at different points near and downwind of the Great Lakes as well as along the southern Appalachians were plotted with both CTRL and MYJPBL shown. Beginning at 0900 UTC on the 10th at La Crosse, IN (at the southern tip of Lake Michigan), CTRL exhibits a warmer and deeper boundary layer than MYJPBL (Fig. 3.40a). This continues through 1800 UTC though the difference is smaller in magnitude (Fig. 3.40b). By 0600 UTC on the 11th, the winds in the lower levels have become more westerly and both runs are now devoid of any potential instability (Fig. 3.40c).

At Lexington, KY (nearly halfway between the lakes and the southern Appalachians), differences in the PBL between the two model runs throughout the event are similar to those seen upstream at La Crosse, IN. At 1200 UTC on the 10th at Lexington, KY, MYJPBL has a boundary layer that is ~50 hPa shallower than CTRL (Fig. 3.41a). This continues through 0000 UTC on the 11th, though the depth of the boundary layer has decreased in both model runs (Fig. 3.41b). Finally, by the end of the NWFS event, CTRL continues to exhibit a deeper and warmer boundary layer than MYJPBL (Fig. 3.41c).

Looking further downstream, along the southern Appalachians, the same differences continue between the two model runs throughout the NWFS event. At Banner Elk, NC which is at an elevation of ~3800 feet in the northern mountains of North Carolina, similar differences in the lower levels of the atmosphere are seen at 1500 UTC on the 10th (Fig.

3.42a). By 0000 UTC on the 11th February the differences continue (Fig. 3.42b) though both model runs stabilize greatly by 1200 UTC on the 11th (Fig. 3.42c).

3.2.3 Experimental run 2 (NOFLX)

For the second experimental run performed on the February 2005 NWFS event, surface fluxes of heat and moisture across the entire model domain were set to zero. This was done with the purpose of determining the extent to which upstream destabilization contributed to precipitation in this event. Turning off the fluxes leads to an increase in the stability in the lower levels of the atmosphere, but we still expect some precipitation due the forcing of stable ascent. However, the amount and distribution of NWFS precipitation will change substantially. For NOFLX, total NWFS precipitation amounts ranged from a few hundredths to a maximum value of 0.18 inches across the southern Appalachians (Fig. 3.43). On a larger-scale view, a few features are absent in comparison to CTRL liquid equivalent precipitation. First, there is no swath of precipitation that extends back upstream to the northwest (Fig. 3.44). Also, precipitation over the Great Lakes appears to be largely decreased in amount and extent. Difference plots between CTRL and NOFLX really highlight these differences (Figs. 3.45 and 3.46). In the southern Appalachian region liquid equivalent precipitation is decreased by as much as 0.27 inches, with a large area of differences greater than one tenth of an inch noted (Fig. 3.45). The larger view of precipitation differences again shows the absence of the swath extending back across Kentucky and toward the Great Lakes (Fig. 3.46), consistent with a Great Lakes influence in the CTRL run that has been removed by turning off the fluxes in the NOFLX run.

As anticipated, NOFLX created a much more stable atmosphere than CTRL, with a shallower PBL. Cross-sections of θ_e at 0900 UTC on the 10th show a layer of very stable air extending from La Crosse, IN toward the southern Appalachians (Fig. 3.47a). Though there is some folding of the isentropes in the vicinity of the mountains this is much different than in CTRL (Fig. 3.35b). By 0000 UTC on the 11th the stability has continued to increase from the lakes to the southern Appalachians with the absence of surface fluxes (Fig. 3.47b). The presence of the increased stability in NOFLX is highlighted even more by looking at profiles of θ_e in the southern Appalachians. The 1200 UTC on the 10th profile from Banner Elk shows how much more stable NOFLX is compared to the CTRL (Fig. 3.48a). This difference, due to increased stability in NOFLX, is even more exaggerated by 0000 UTC on the 11th (Fig. 3.48b).

As a result of the increased stability in NOFLX, the strength of vertical velocity is decreased on the upslope side of the southern Appalachians relative to CTRL. One possible reason for this decreased vertical velocity is the fact that this coarse grid with 24km grid spacing may not adequately resolve the process of convective overturning. Also, it is important to note that the increased stability creates a greater resistance to vertical displacement, thereby reducing the vertical motion due to orographic lift from the CTRL run. But, it is also conceivable that this decrease occurs because without the presence of potential instability in NOFLX, additional lift is not realized through the release of this instability in the upslope flow. Instead, lift is created through forced stable ascent caused by upslope northwesterly flow. At both 1500 UTC (Figs. 3.49a and 3.49b) and 2100 UTC (Figs. 3.49c and 3.49d) on the 10th, the CTRL and NOFLX vertical motion fields have similar structure with upward motion maximized on the upwind side of the terrain of the southern

Appalachians. Starting at 1500 UTC on the 10th, the lower levels on the windward side of the southern Appalachians show that CTRL exhibits stronger vertical motion by as much as 4 μbar/sec (Fig. 3.50a). By 2100 UTC on the 10th, this difference becomes greater with vertical velocity in NOFLX as much as 7 μbar/sec less than CTRL (Fig. 3.50b). Differences in the strength of vertical velocity begin to dwindle by 0300 UTC on the 11th (Fig. 3.50c), and lessen further by 0900 UTC on the 11th (Fig. 3.50d), though at both times the net affect is weaker vertical velocity in NOFLX.

Another field that highlights differences between CTRL and NOFLX is the water vapor mixing ratio. Since surface fluxes of heat and moisture are set to zero across the entire model domain, decreases in the water vapor mixing ratio can be expected especially in the lower levels of the atmosphere. A plot of the 950–875 hPa layer-averaged difference field of water vapor mixing ratio between CTRL and NOFLX from 0900 UTC on the 10th shows a swath of decreased moisture extending from the Great Lakes southeastward toward the southern Appalachians (Fig. 3.51a). By 1500 UTC, these differences continue to show a swath that runs up the long axis of Lake Michigan and across Lake Superior (Fig. 3.51b). This pattern persists through 2100 UTC (Fig. 3.51c) and 0300 UTC on the 11th (Fig. 3.51d).

3.2.4. Experimental run 3 (LKNOFLX)

For the third experimental run, surface fluxes were set to zero only over water across the model domain with the purpose of isolating the Great Lakes; this model experiment is dubbed LKNOFLX. For the event, LKNOFLX produced total NWFS accumulations (Fig. 3.52) that appear to look fairly similar to the CTRL (Fig. 3.30). However, a difference field between the two runs shows decreases in precipitation at many locations along the southern

Appalachians (Fig. 3.53). The majority of the differences are decreases with a maximum decrease of 0.16 inches in eastern Tennessee. On a larger scale these decreases in precipitation again show a northwestward extension upstream toward the Great Lakes, but not quite with the same magnitude as NOFLX (Fig. 3.54). In order to quantify the amount of precipitation decrease in LKNOFLX relative to CTRL, a percent of decrease was calculated highlighting only decreases in precipitation. In the southern Appalachians the percent of decrease in the LKNOFLX run was roughly 20% along the North Carolina/Tennessee border (Fig. 3.55). This shows that the Great Lakes are responsible for about 1/5 of NWFS precipitation at some locations in the region for this particular event.

Profiles of θ_e from LKNOFLX are shown in Fig. 3.56. Starting at La Crosse, IN at the beginning of the NWFS event, 0900 UTC on the 10th, LKNOFLX is extremely stable compared to CTRL (Fig. 3.56a). This continues through 2100 UTC (Fig. 3.56b), until the low-level flow turns more westerly thereafter. Further downstream over Lexington, KY a similar result is found but with much less variation between the two runs. At 1200 UTC in Lexington, KY CTRL has a much deeper and warmer boundary layer than LKNOFLX as well as greater potential instability in the lower levels (Fig. 3.56c). This remains a feature at Lexington through 0000 UTC on the 11th (Fig. 3.56d).

Going further downstream into the southern Appalachians we find that differences in the θ_e profile between the two model runs have lessened to only minute variations. At 2100 UTC at Erwin, TN (right along the central North Carolina/Tennessee border) we see that CTRL is now only slightly deeper and more unstable than LKNOFLX (Fig. 3.57a). Similar differences can be seen just to the southwest of Erwin in Marshall, NC at the same time (Fig. 3.57b).

With the differences in instability between CTRL and LKNOFLX generally becoming less defined further downstream from the Great Lakes to the southern Appalachians, the instability is increasing through some other mechanism. To explore this increase in the instability, difference plots between the CTRL and LKNOFLX of surface sensible and latent heat fluxes were created. At the beginning of the NWFS event, a stripe of enhanced sensible heat flux values (>200 W/m^2) appears over southern Indiana and northern Kentucky (Fig. 3.58). This area persists through the next 12 hours and continues to move southeastward toward the southern Appalachians (Fig. 3.59). The enhanced surface fluxes present in LKNOFLX relative to the CTRL could be due to such effects as a decrease in the amount of cloud cover and precipitation between the Great Lakes and the southern Appalachians. In such a scenario stronger surface fluxes over these areas would be expected due to increased insolation because of less cloud cover and reduced albedo caused by a reduction in snow cover, both helping to strengthen the surface fluxes.

Another explanation as to the cause of this area of enhanced surface fluxes in LKNOFLX is due to the change in how the Great Lakes are able modify the low-level air mass moving southeastward toward the southern Appalachians. The air directly over the lakes is expected to be much colder in LKNOFLX due to the absence of surface fluxes over the lake waters. However, this decrease in temperature should lessen in magnitude downstream toward the southern Appalachians as the surface fluxes increase across southern Indiana/northern Kentucky and points southward. In fact, that is exactly what occurs. At 0900 UTC on the 10th an elongated pool of much cooler surface air extends down the long axis of Lake Michigan and southeastward (Fig. 3.60a). The temperature decrease continues to lessen the further downstream, becoming negligible over northern Kentucky. By 2100

UTC, a similar pattern is visible but with the temperature differences having moved a bit further southeastward (Fig. 3.60b). This pattern continues through 0300 UTC on the 11th where the temperature differences have slid further southeastward but are much less in magnitude than they were nearly 24 hours prior just off the southern tip of the Great Lakes (Fig. 3.60c). Therefore, the low-level air mass warms as it moves southeastward toward the southern Appalachians due to increased fluxes over land. This enhanced warming helps destabilize the lower levels and mask the absence of warming and moistening by the Great Lakes that would otherwise be present.

Finally, differences between the CTRL and LKNOFLX extend to the 950–875 hPa layer averaged water vapor mixing ratio. Beginning at 0900 UTC on the 10th, a swath of decreased moisture is present from the Great Lakes to areas immediately to the southeast (Fig. 3.61a). Six hour later, 1500 UTC on the 10th, the pattern is the same as the area of decreased moisture dissipates just to the northwest of the southern Appalachians (Fig. 3.61b). This persists through 2100 UTC on the 10th (Fig. 3.61c), before the swath begins to break up and shift to the east by 0300 UTC on the 11th (Fig. 3.61d). Though differences between the CTRL and LKNOFLX are virtually nonexistent over the southern Appalachians, the presence of decreased moisture upstream of the region is consistent with a similar Great Lakes connection seen in NOFLX (Fig. 3.51). The minimization of the moisture differences near the southern Appalachians is also consistent with the masking effect noted in the 2m temperature difference fields. Overall, these moisture difference fields suggest that the Great Lakes likely contribute at least some of the moisture for this NWFS event.

3.3. Froude number calculations

In order to further quantify the effect of the Great Lakes during this NWFS event, a layer-averaged Froude number was calculated following the procedure discussed in section 2.4. This calculation was done for Lexington, KY, located roughly half-way between the lakes and mountains for the 950–850 hPa layer. The time period investigated runs from 0600 UTC on the 10th to 0600 UTC on the 11th, which effectively covers when this NWFS event occurred. Between the three model runs F_r is highest in CTRL for the majority of the event, with both the LKNOFLX and NOFLX runs having lower values (Fig. 3.62). The CTRL also exhibits a strong diurnal signal with its highest F_r values occurring during the afternoon and evening on the 10th. Overall, the average F_r for each model run during this 24 hour time period is as follows: CTRL=1.39, NOFLX=0.40, and LKNOFLX=0.99. The fact that the CTRL has a higher average F_r during the NWFS event than LKNOFLX, points to effect that the Great Lakes have on the destabilizing the upstream low-level airmass that impinges on the southern Appalachians. Because the LKNOFLX has a lower average F_r than the CTRL, more blocking of the low-level airmass occurs. This allows less air to move up and over the mountains, therefore contributing to the decrease in NWFS precipitation.

3.4. Summary

The 10–11 February 2005 NWFS event is an example of a mid-winter, Type I post-frontal case. NWFS precipitation began across the southern Appalachian Mountains around 0900 UTC 10 February and lasted approximately 24 hours. Total snowfall accumulations for the event were not excessive, with most areas receiving 1–3 inches and an event maximum total of 8.1 inches at Mount Leconte, Tennessee. To study the event further and investigate

the physical processes involved, a series of four model runs was performed with the intent of quantifying the role of the Great Lakes in this NWFS event.

Overall for this event, the Great Lakes were responsible for approximately 20% of NWFS precipitation at some locations in the southern Appalachians. This decrease in precipitation is attributable to increased stability in the low-level airmass upstream of the southern Appalachians in the LKNOFLX experimental run, where the effect of the Great Lakes was removed. The increased stability of the upstream airmass can be clearly seen on θ_e profiles between the lakes and the mountains, where potential instability is decreased in the LKNOFLX run relative to the CTRL. The stabilization of the upstream airmass is further supported by calculations of F_r at a point about half-way between the Great Lakes and the southern Appalachians. At this location for LKNOFLX, the average F_r for the NWFS event in the 950–850 hPa layer is 0.99, which is 0.40 less than the CTRL value of 1.39. This variation in F_r between CTRL and LKNOFLX shows that when the lakes are removed, F_r is decreased as well as the amount of NWFS precipitation. Therefore, the overall effect of the Great Lakes in this NWFS event is to contribute to the destabilization of the airmass upstream of the southern Appalachians, thereby increasing F_r.

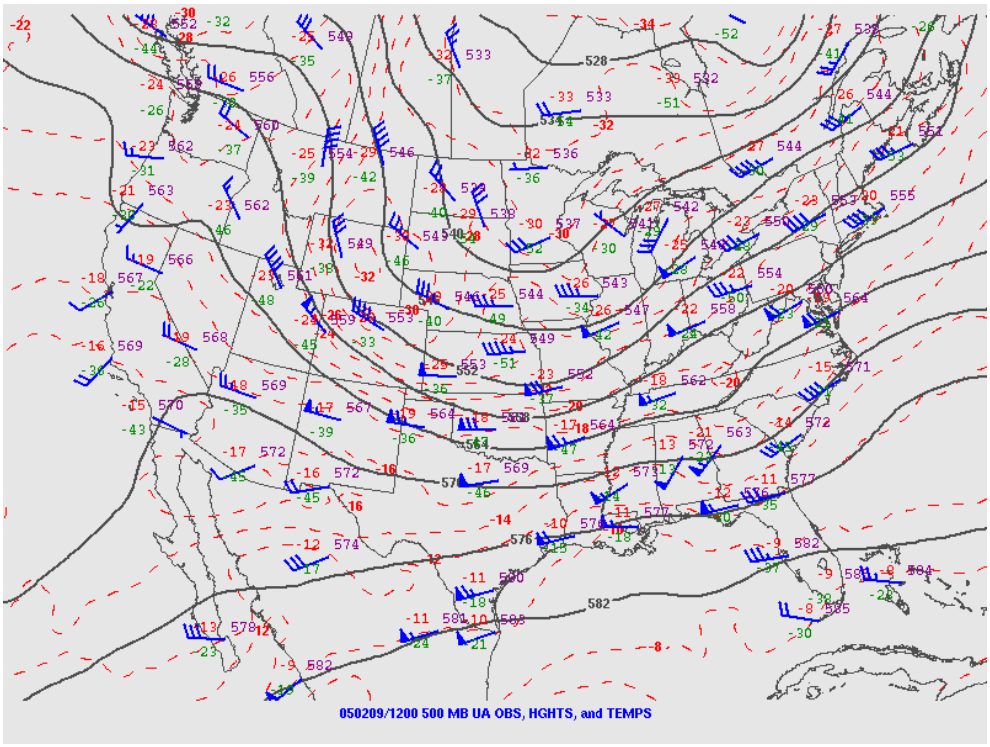

Figure 3.1. Plot of 500 hPa upper air observations, heights, and temperatures from 1200 UTC 9 February 2005. Image from http://www.spc.noaa.gov/obswx/maps/.

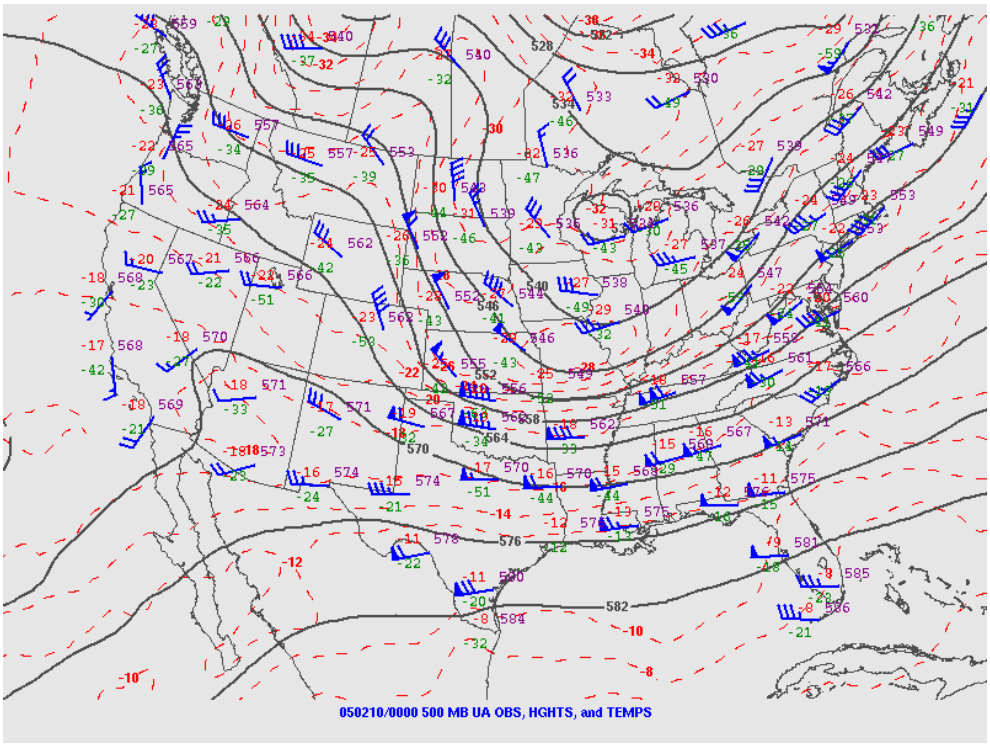

Figure 3.2. Same as in Figure 3.1 except for 0000 UTC 10 February 2005.

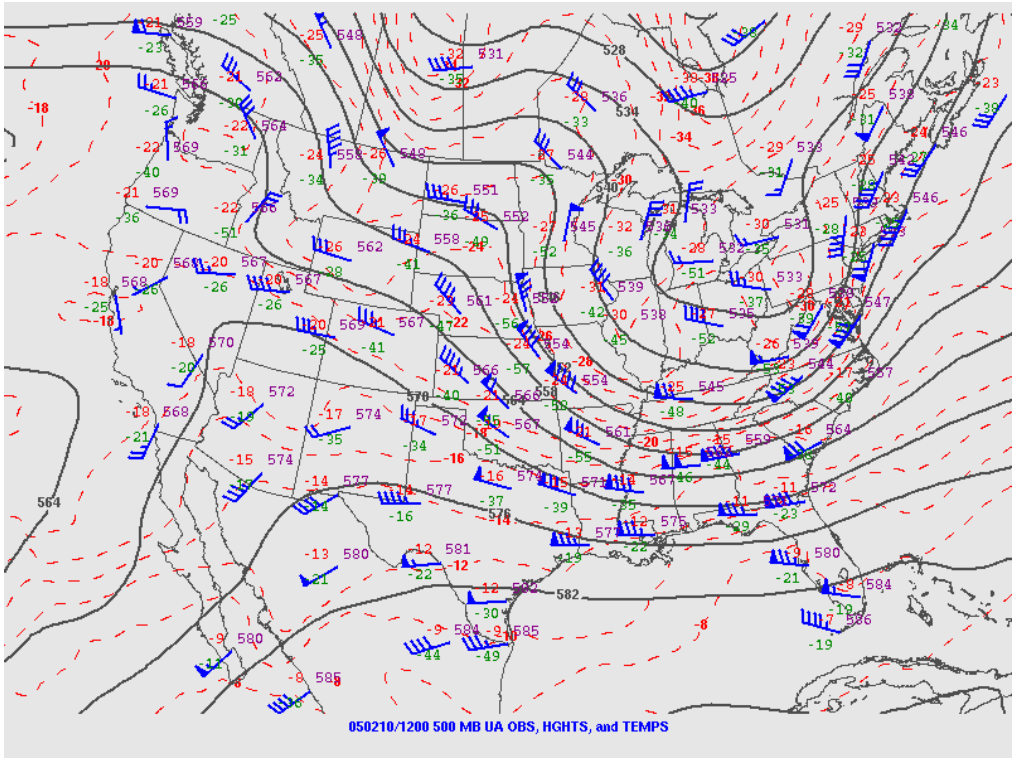

Figure 3.3. Same as in Figure 3.1 except for 1200 UTC 10 February 2005.

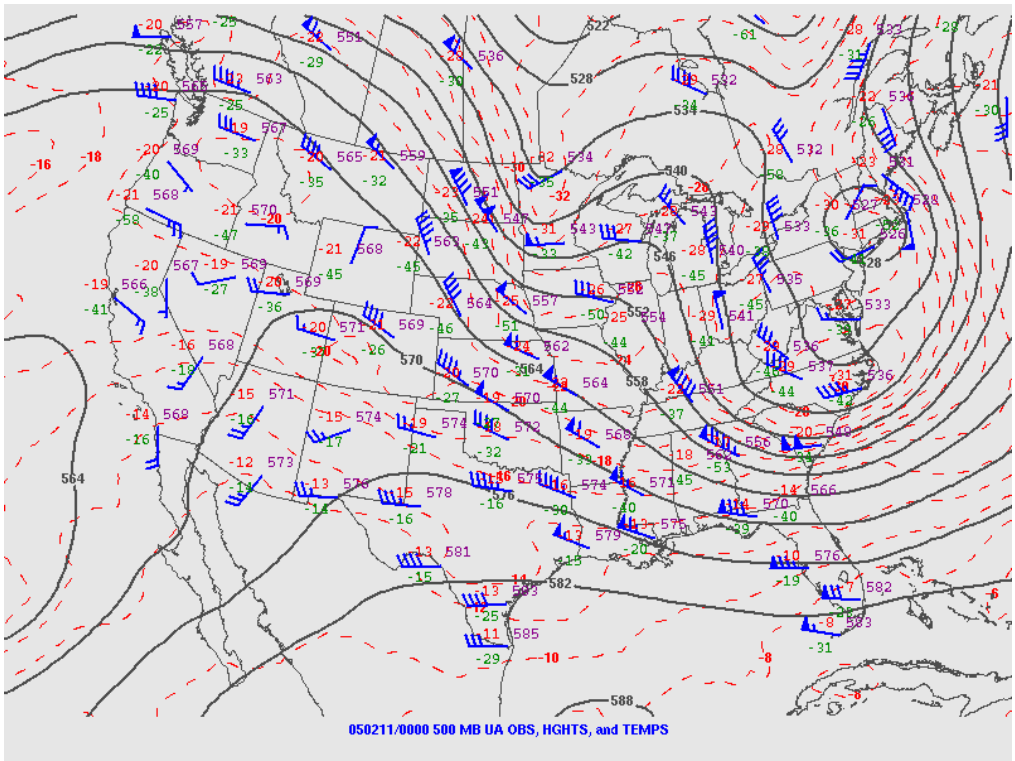

Figure 3.4. Same as in Figure 3.1 except for 0000 UTC 11 February 2005.

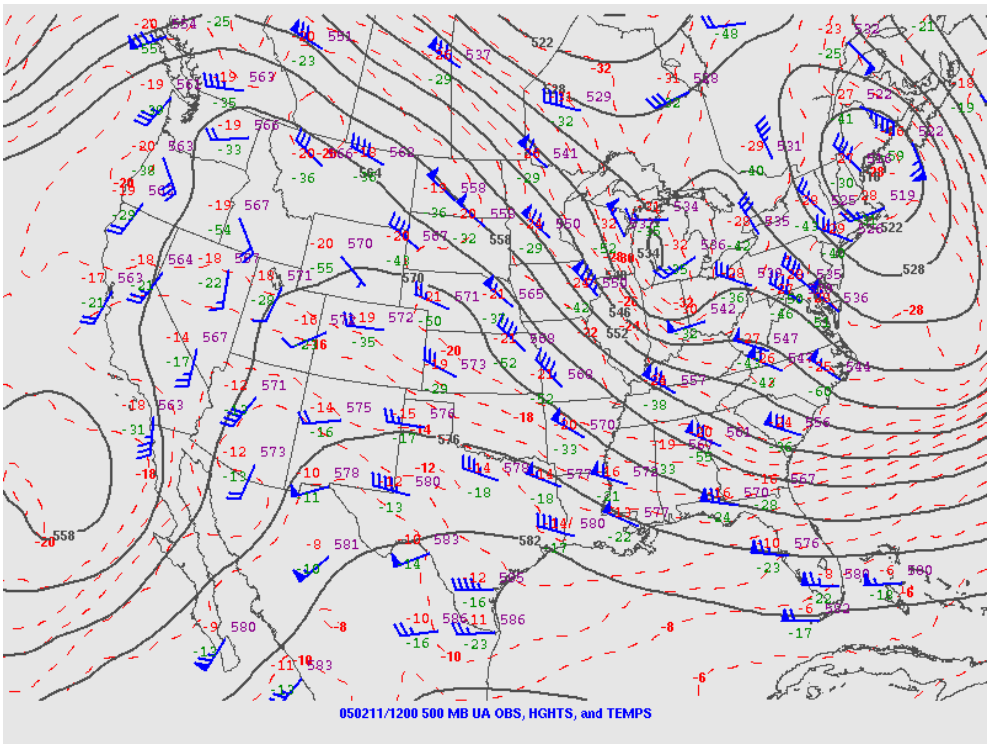

Figure 3.5. Same as in Figure 3.1 except for 1200 UTC 11 February 2005.

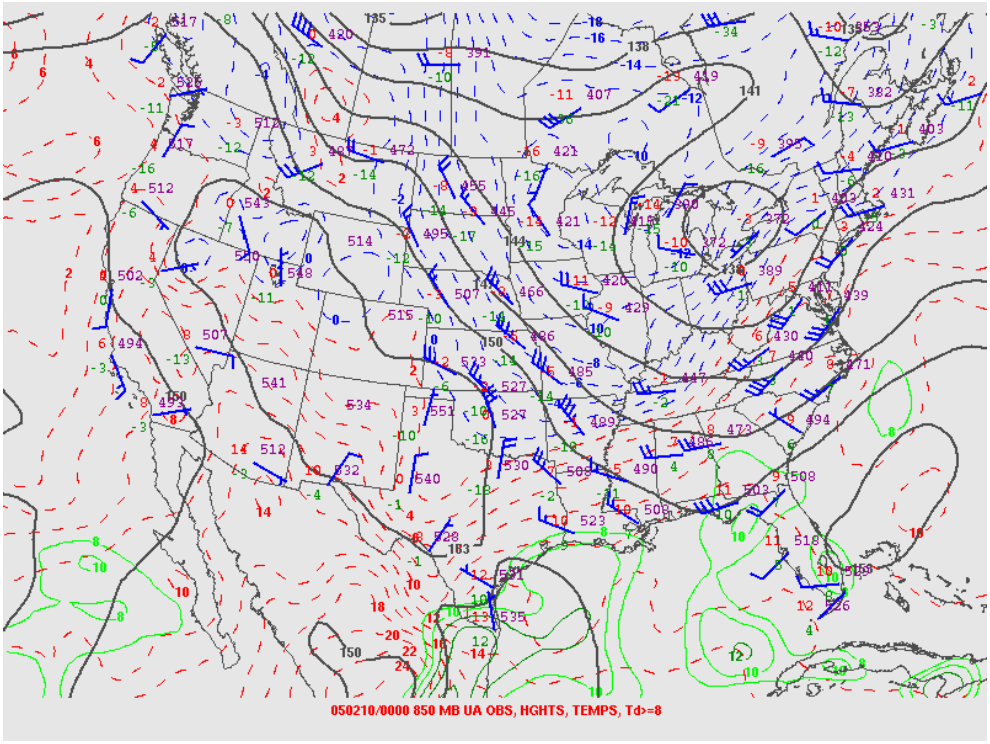

Figure 3.6. Plot of 850 hPa upper air observations, heights, temperatures, and dew point >8 °C from 0000 UTC 10 February 2005.

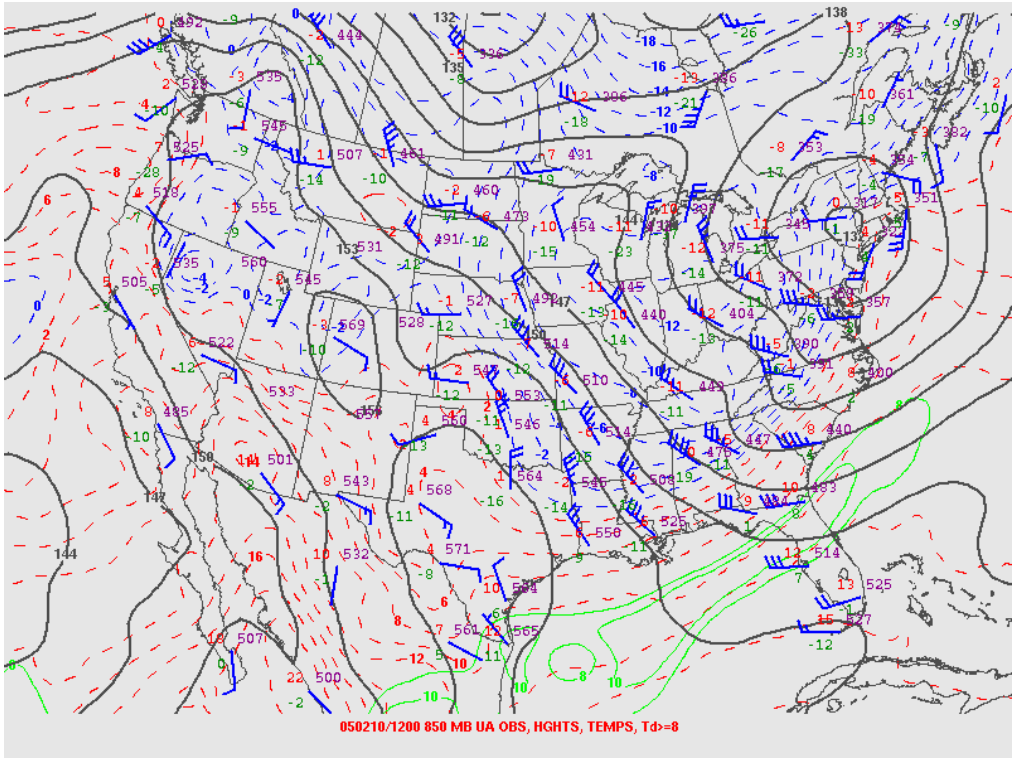

Figure 3.7. Same as in Figure 3.6 except for 1200 UTC 10 February 2005.

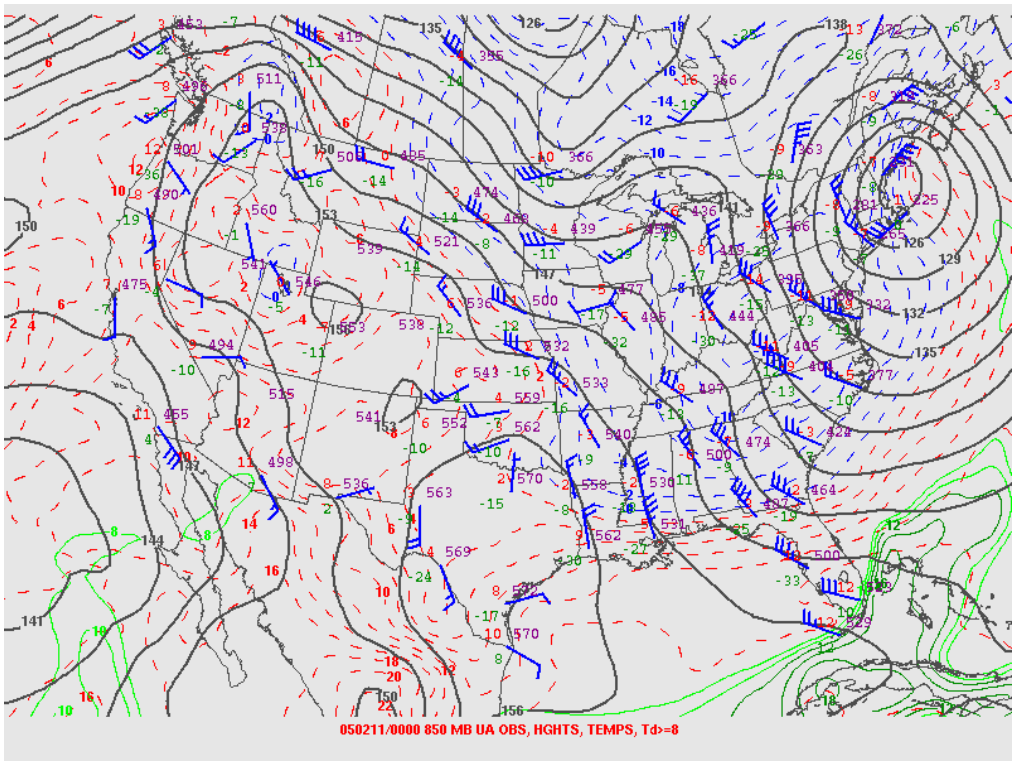

Figure 3.8. Same as in Figure 3.6 except for 0000 UTC 11 February 2005.

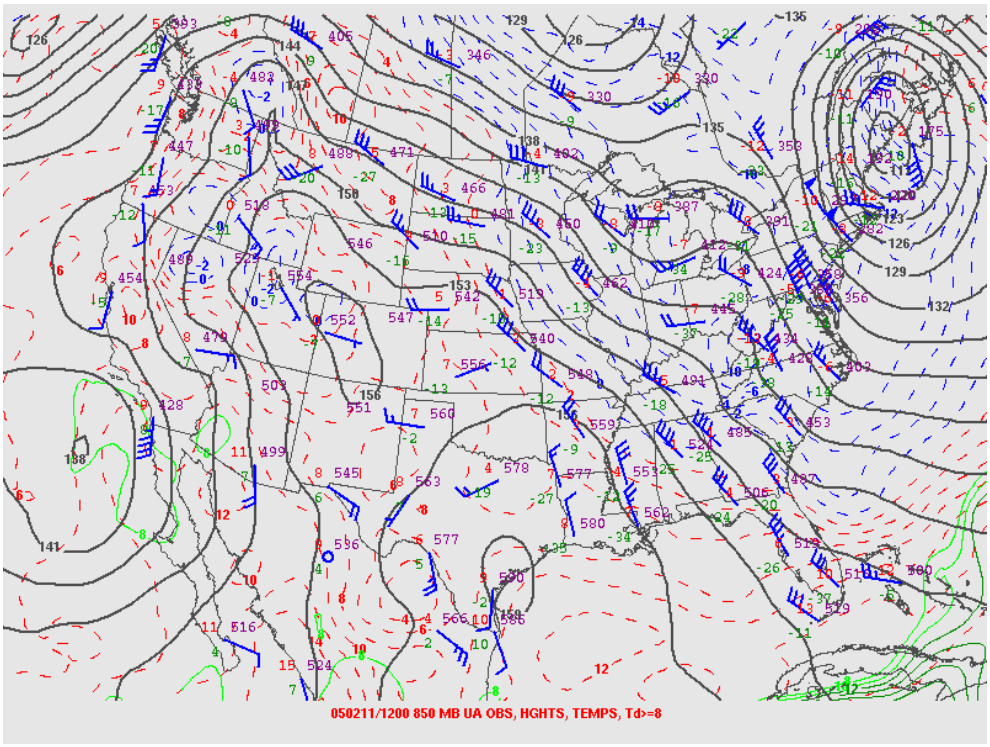

Figure 3.9. Same as in Figure 3.6 except for 1200 UTC 11 February 2005.

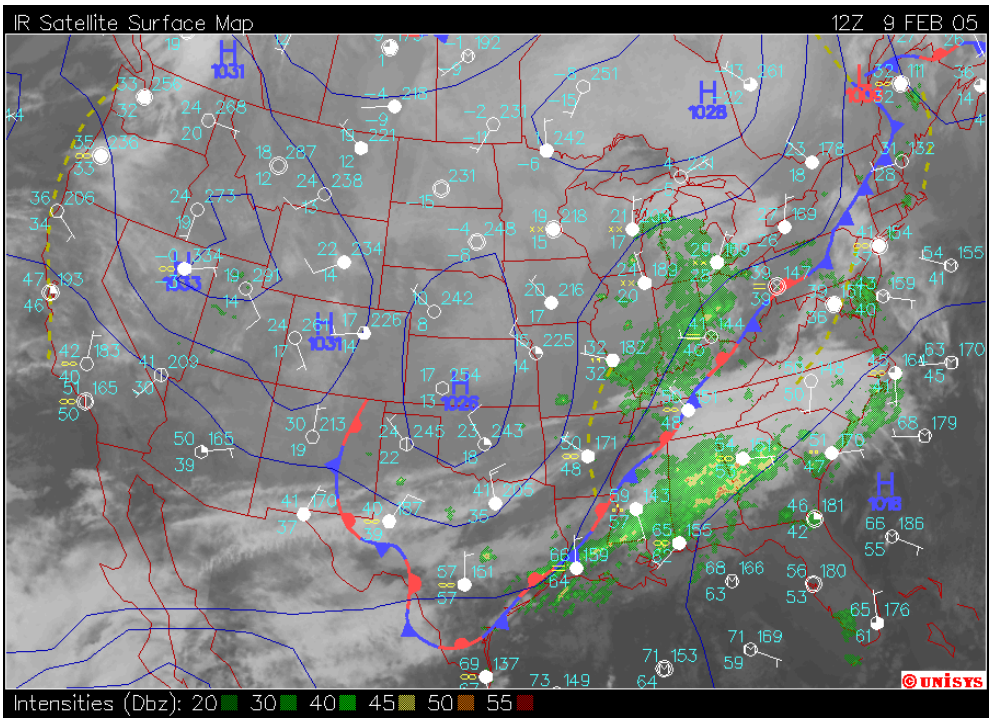

Figure 3.10. Plot of surface analysis, infrared (IR) satellite, surface observations, and composite radar reflectivity from 1200 UTC 9 February 2005. Image from http://weather.unisys.com/archive/sfc_map/0312/.

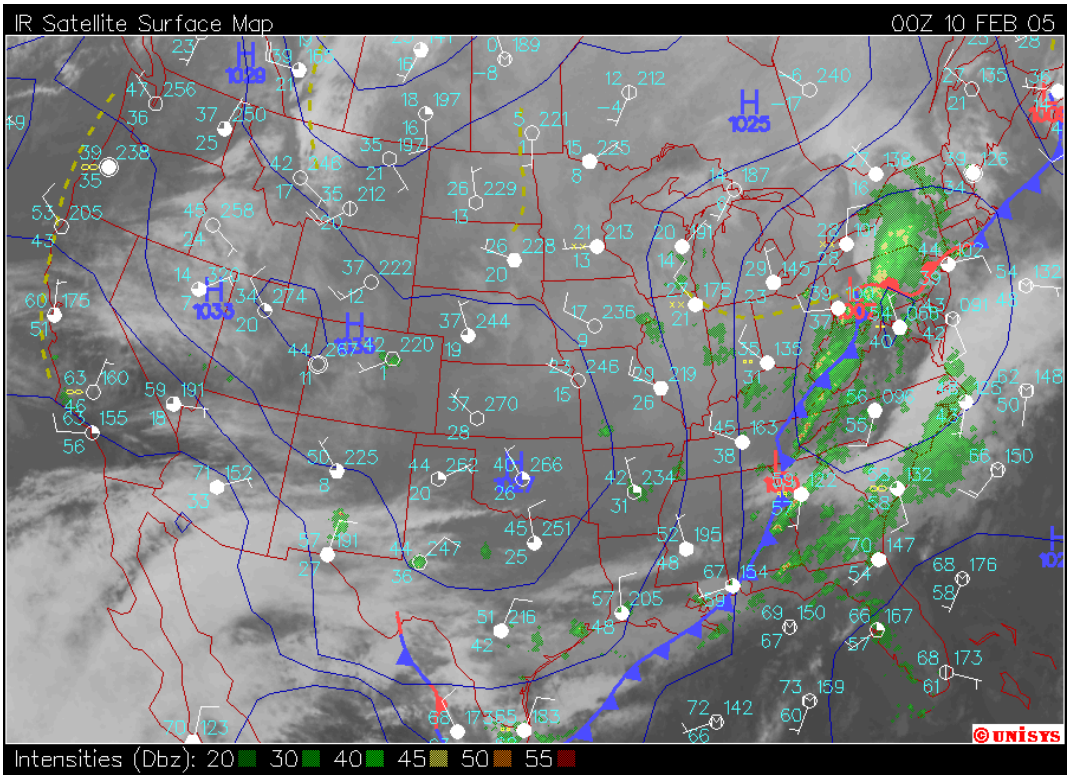

Figure 3.11. Same as in Figure 3.10 except for 0000 UTC 10 February 2005.

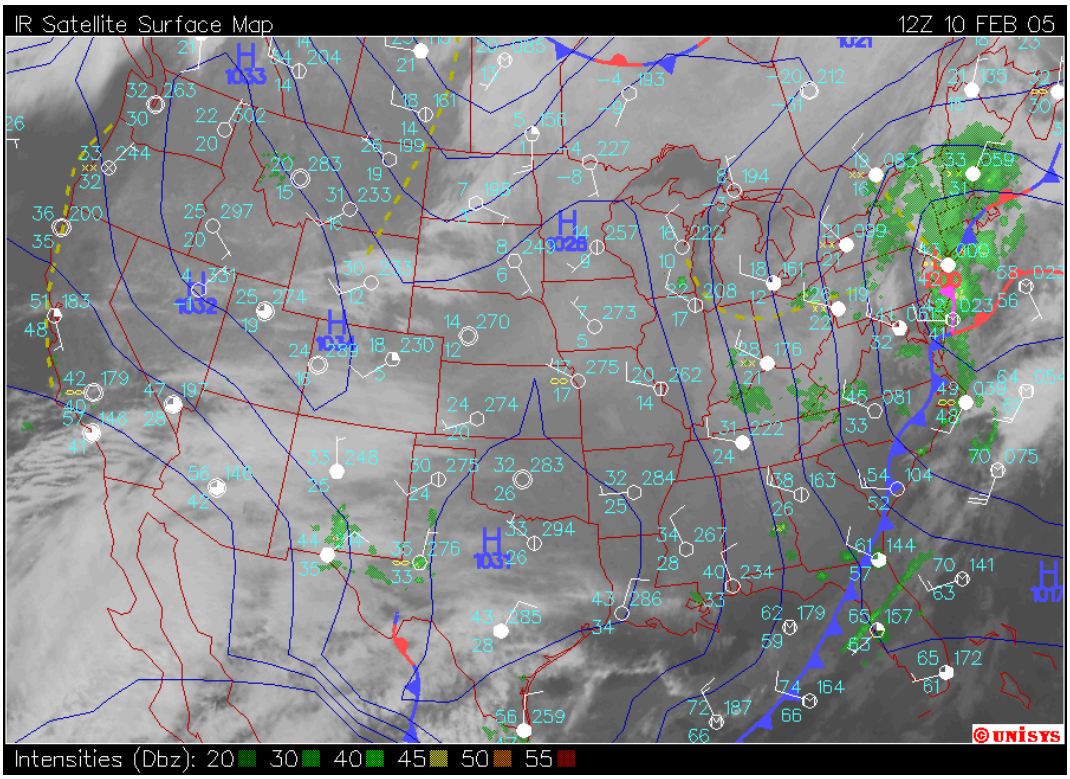

Figure 3.12. Same as in Figure 3.10 except for 1200 UTC 10 February 2005.

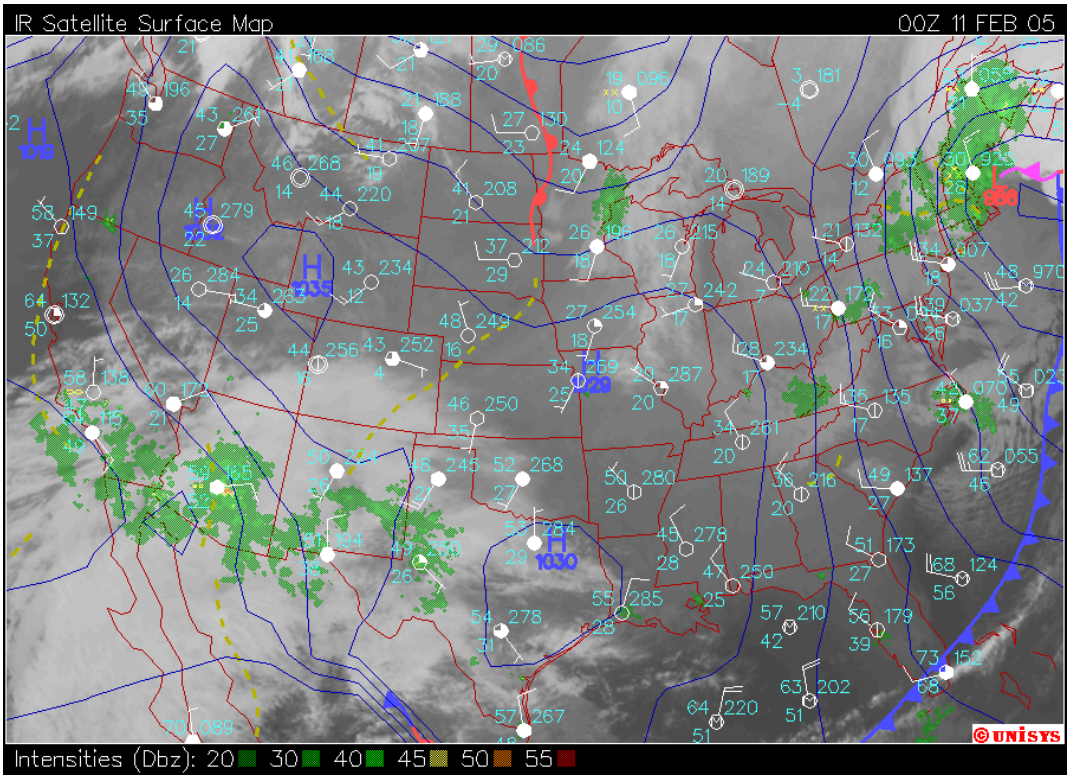

Figure 3.13. Same as in Figure 3.10 except for 0000 UTC 11 February 2005.

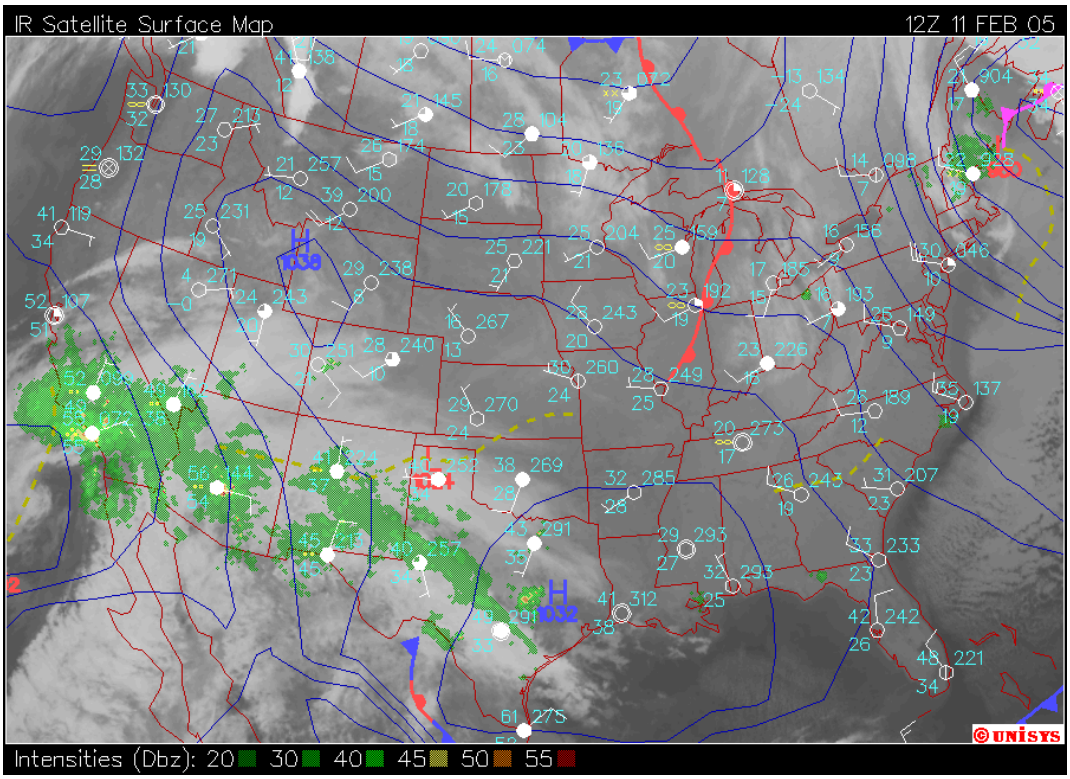

Figure 3.14. Same as in Figure 3.10 except for 1200 UTC 11 February 2005.

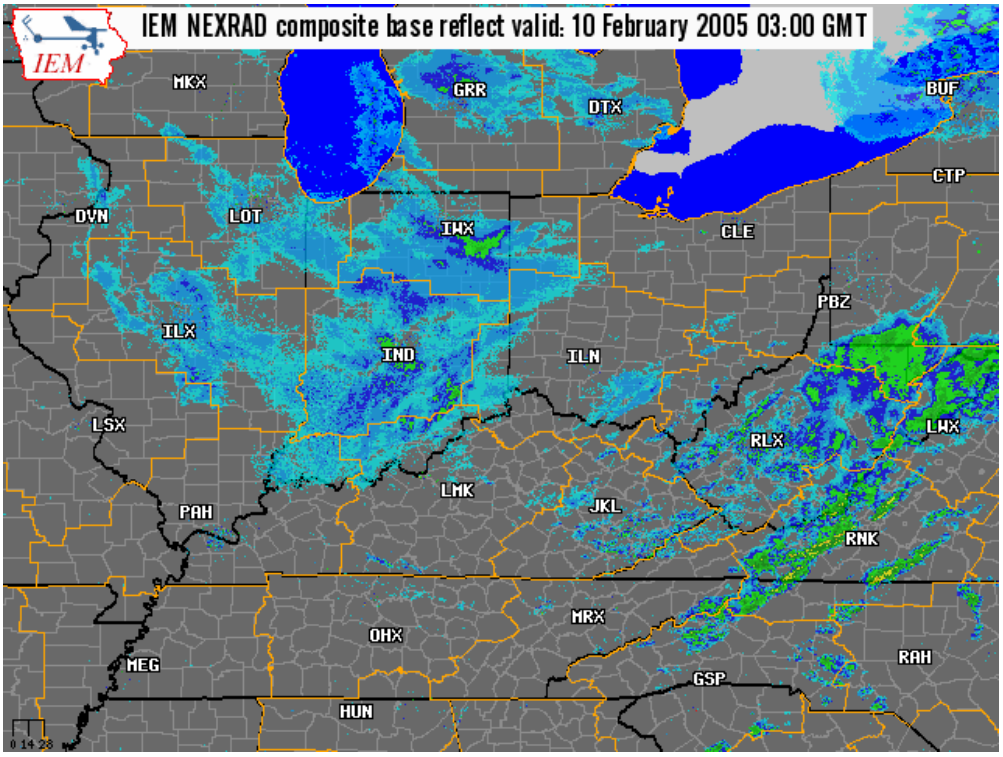

Figure 3.15. Composite radar reflectivity image from 0300 UTC 10 February 2005. Image from http://mesonet.agron.iastate.edu/GIS/apps/rview/warnings.phtml.

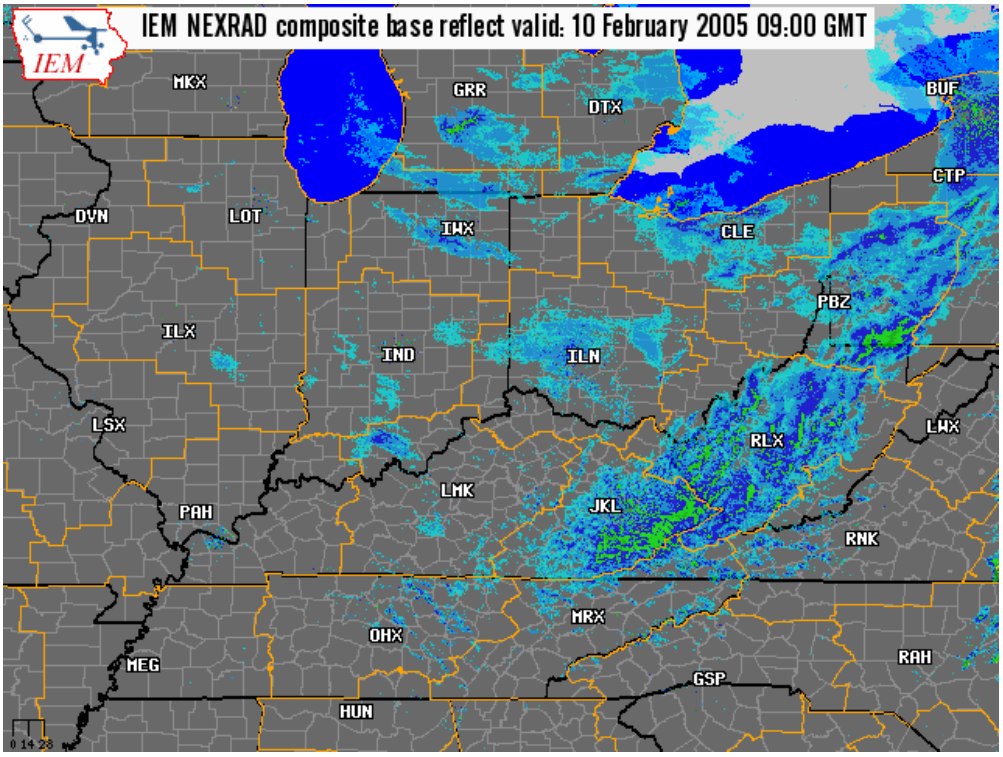

Figure 3.16. Same as in Figure 3.15 except for 0900 UTC 10 February 2005.

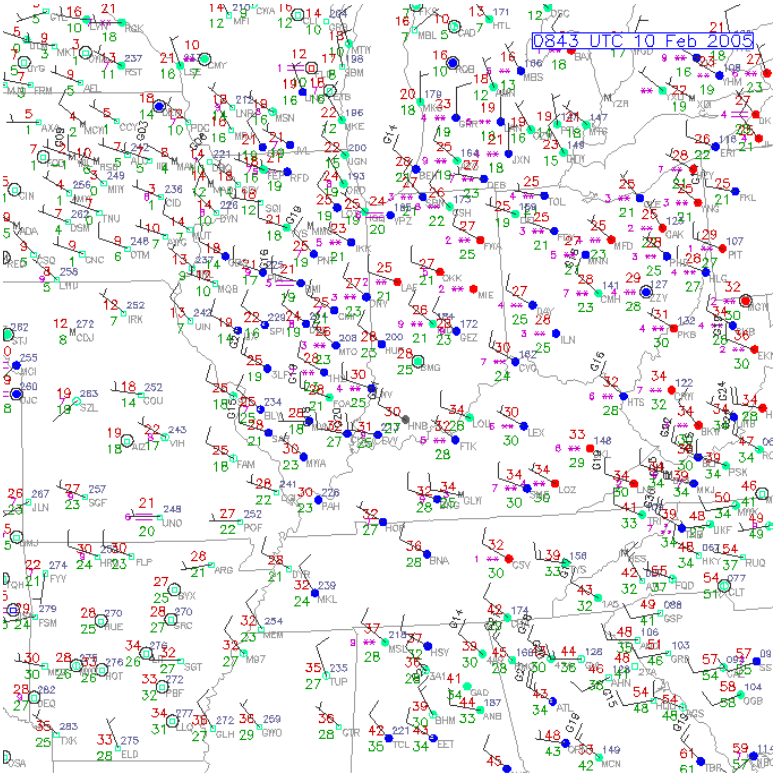

Figure 3.17. Plot of surface observations from 0800 UTC 10 February 2005.

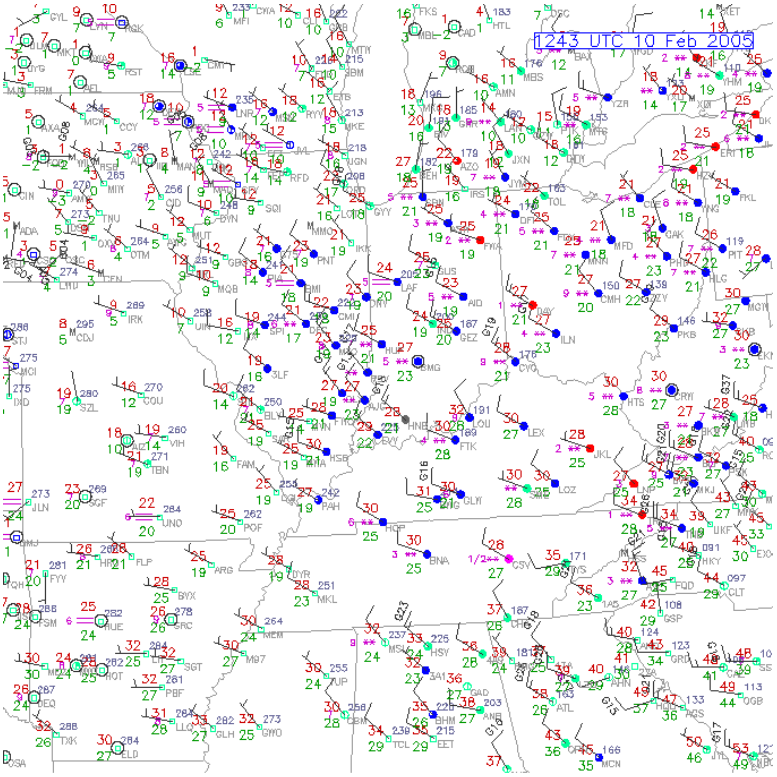

Figure 3.18. Same as in Figure 3.17 except for 1200 UTC 10 February 2005.

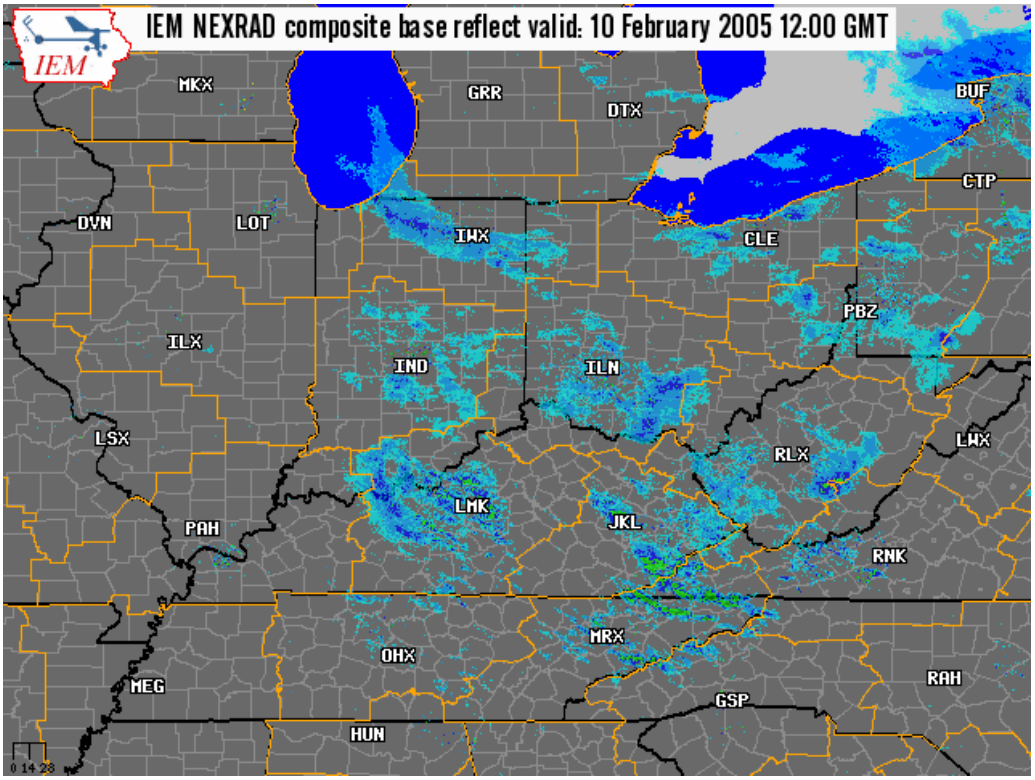

Figure 3.19. Same as in Figure 3.16 except for 1200 UTC 10 February 2005.

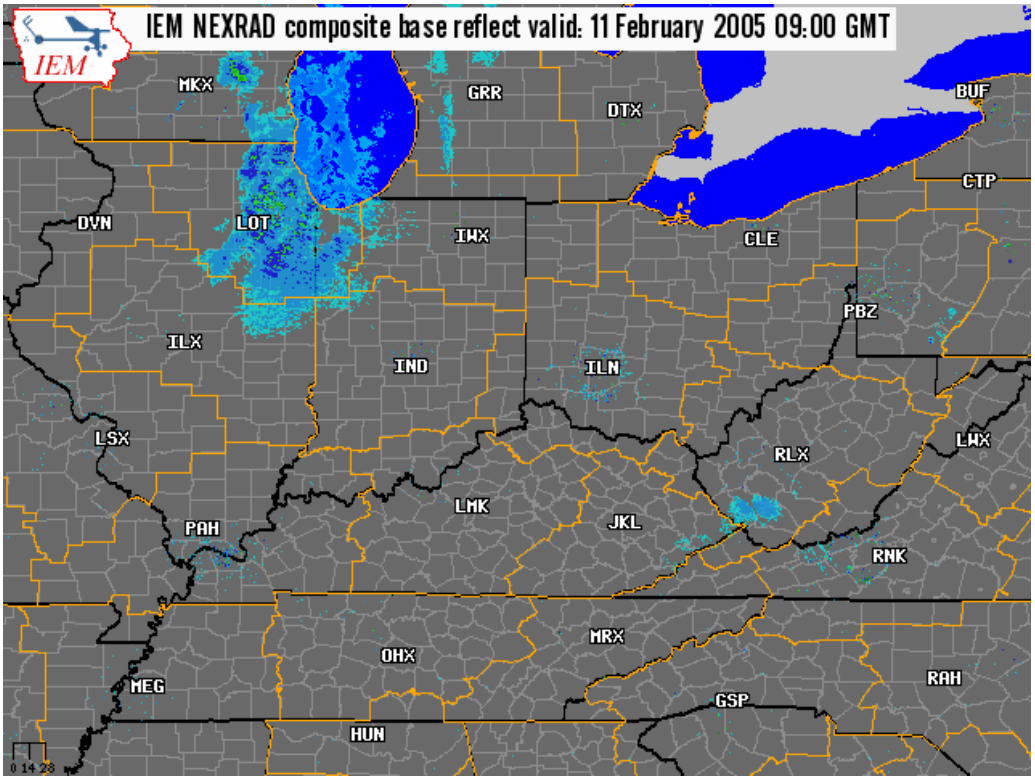

Figure 3.20. Same as in Figure 3.15 except for 0900 UTC 11 February 2005.

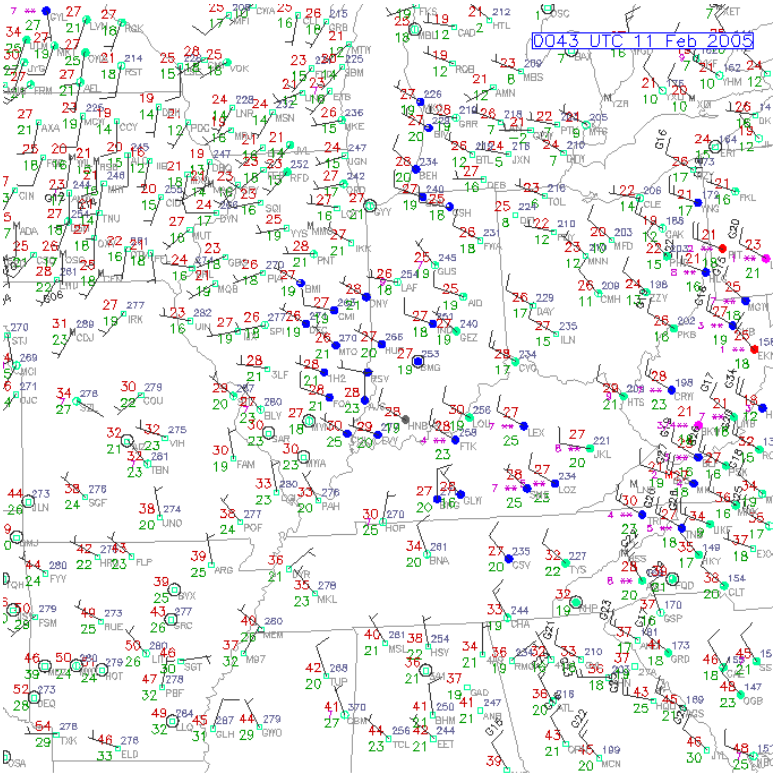

Figure 3.21. Same as in Figure 3.17 except for 0000 UTC 11 February 2005.

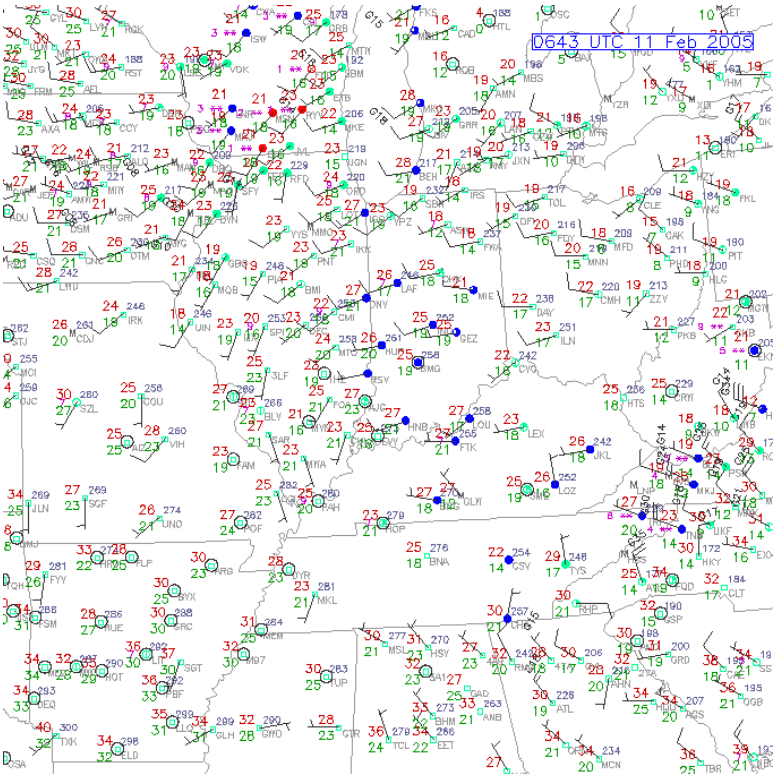

Figure 3.22. Same as in Figure 3.17 except for 0600 UTC 11 February 2005.

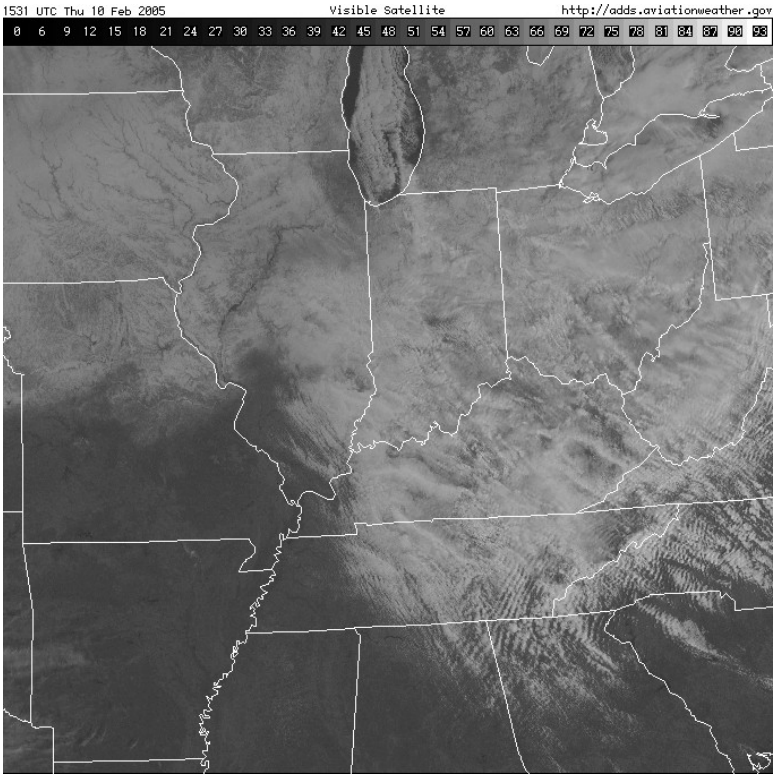

Figure 3.23. Visible satellite image from 1531 UTC 10 February 2005.

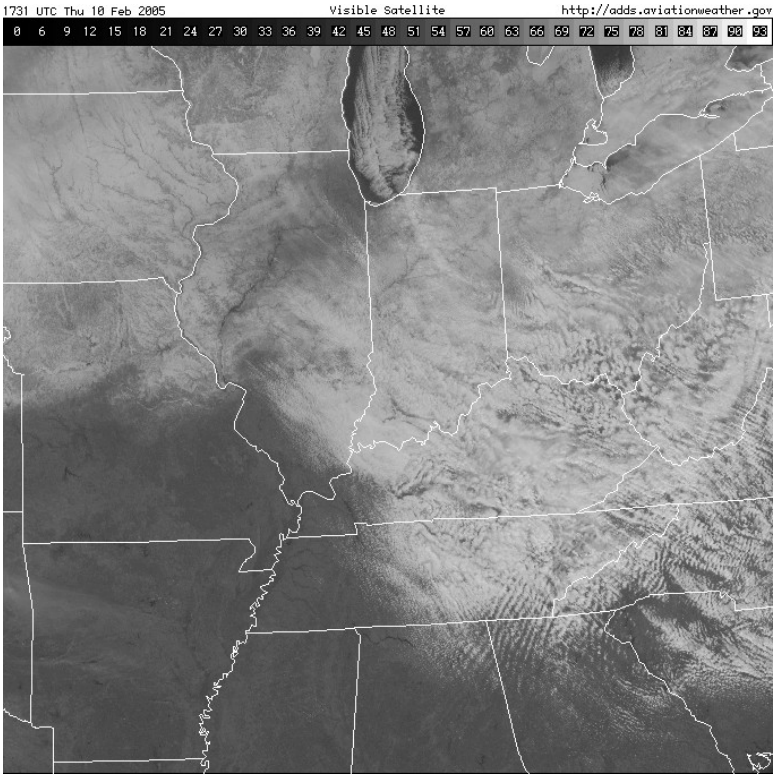

Figure 3.24. Same as in Figure 3.23 except for 1731 UTC 10 February 2005.

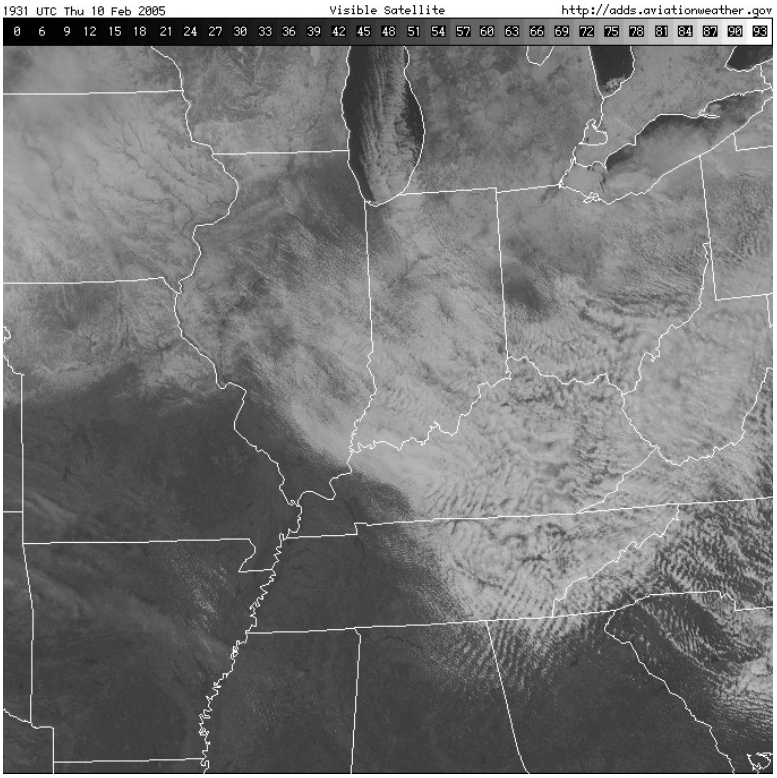

Figure 3.25. Same as in Figure 3.23 except for 1931 UTC 10 February 2005.

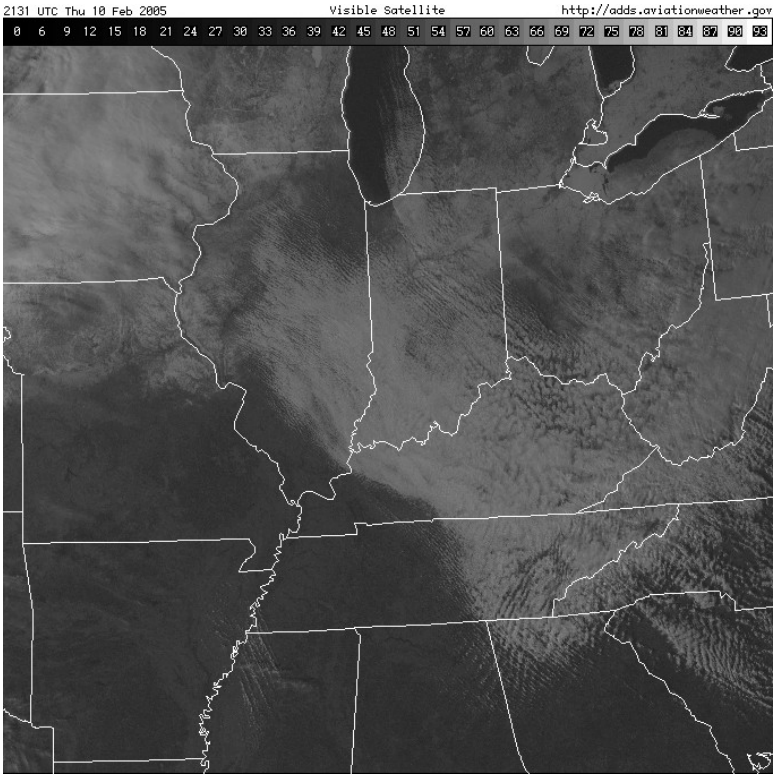

Figure 3.26. Same as in Figure 3.23 except for 2131 UTC 10 February 2005.

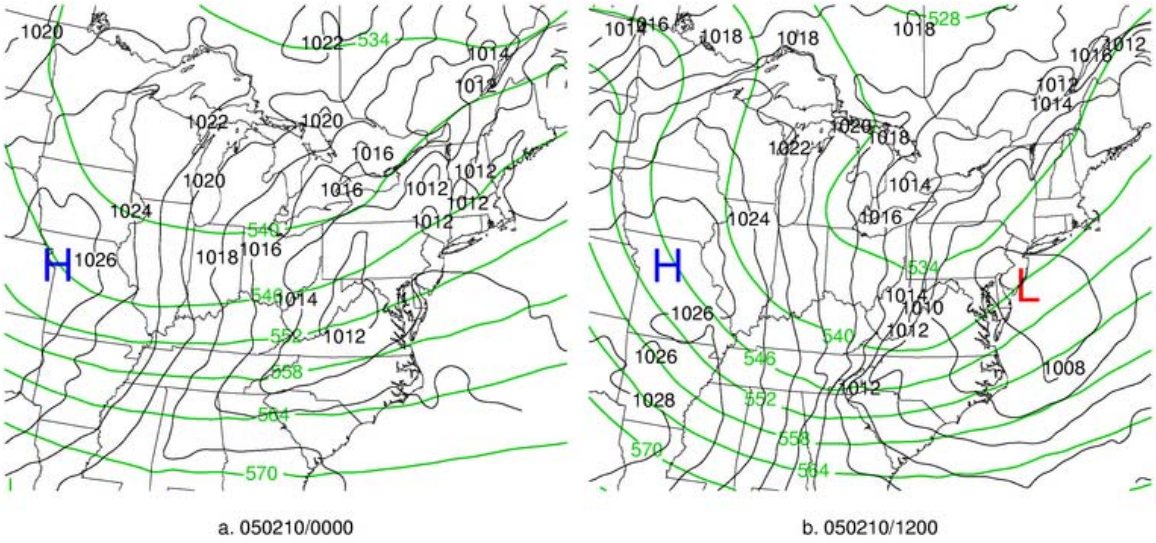

Figure 3.27. CTRL sea-level pressure (black solid contours, interval 2 hPa) and 500 hPa Geopotential height (green solid contours, interval 6 dam): (a) 0000 UTC 10 February 2005; and (b) 1200 UTC 10 February 2005.

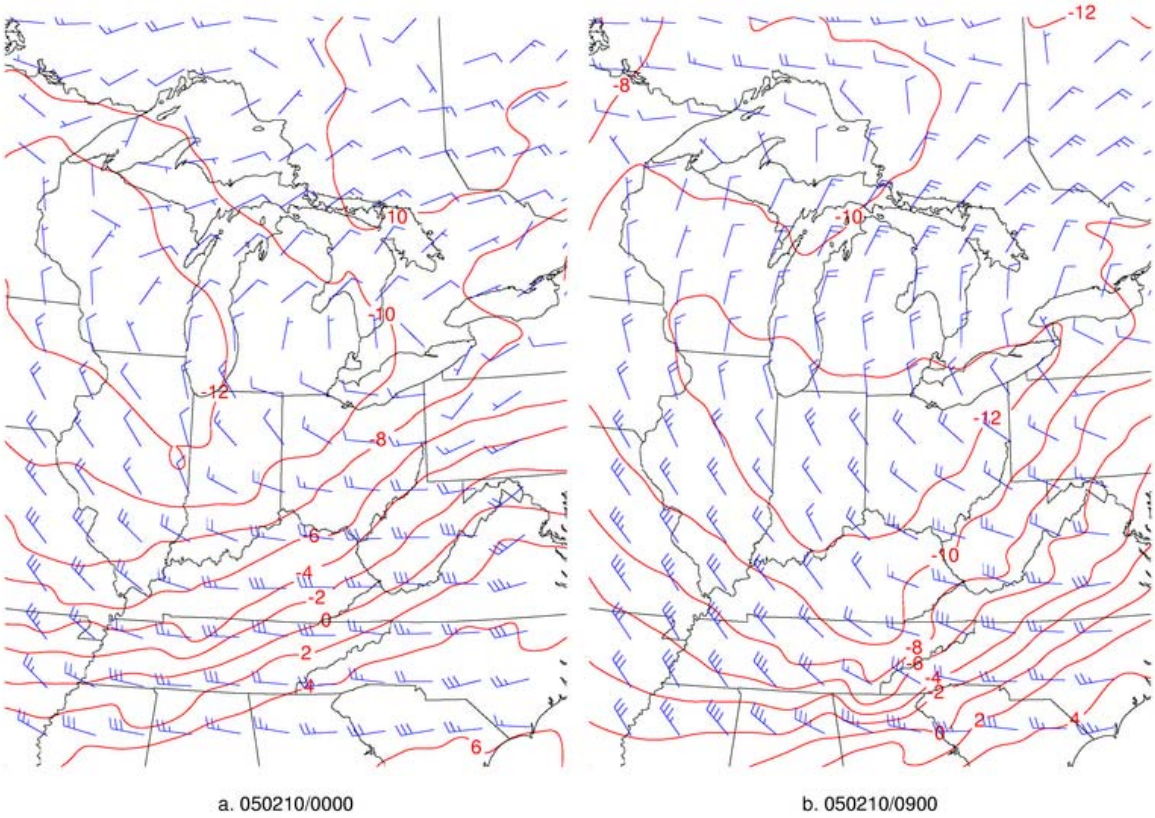

Figure 3.28. CTRL 850 hPa temperature (°C, red solid, interval 2°C) and winds (kt, barbs): (a) 0000 UTC 10 February 2005; and (b) 0900 UTC 10 February 2005.

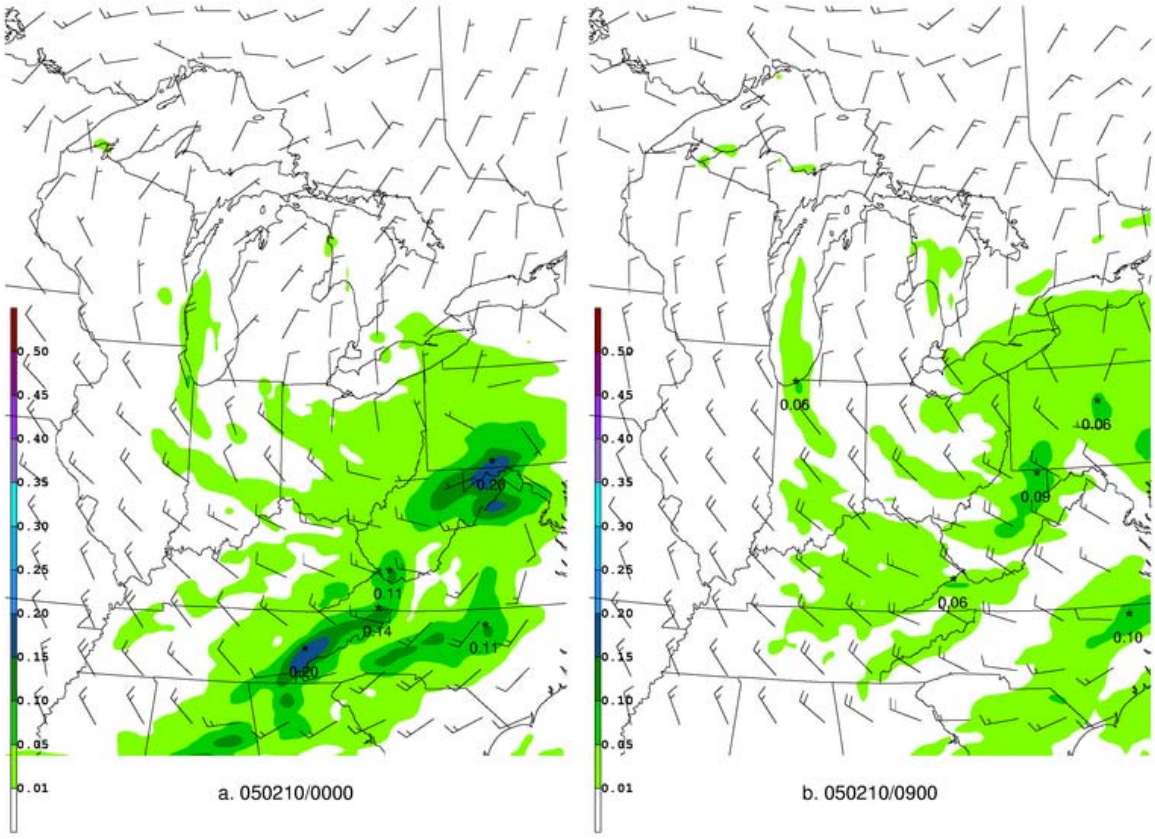

Figure 3.29. CTRL 3 hour liquid equivalent precipitation (inches, shaded as colorbar in lower left corner), and 10 m winds (kt, barbs): (a) 0000 UTC 10 February 2005; and (b) 0900 UTC 10 February 2005.

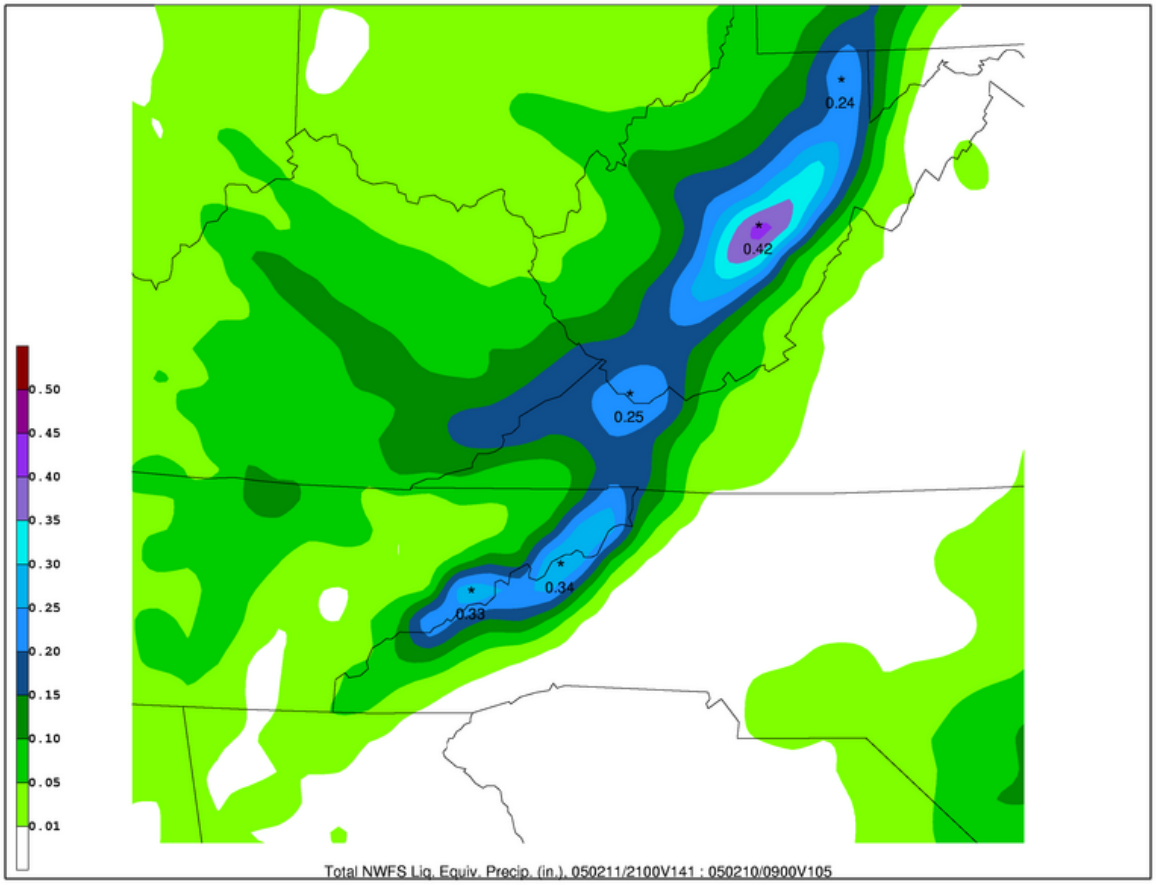

Figure 3.30. CTRL total liquid equivalent precipitation from 0900 UTC 10 February 2005 to 2100 UTC 11 February 2005 (inches, shaded as in colorbar in lower left corner).

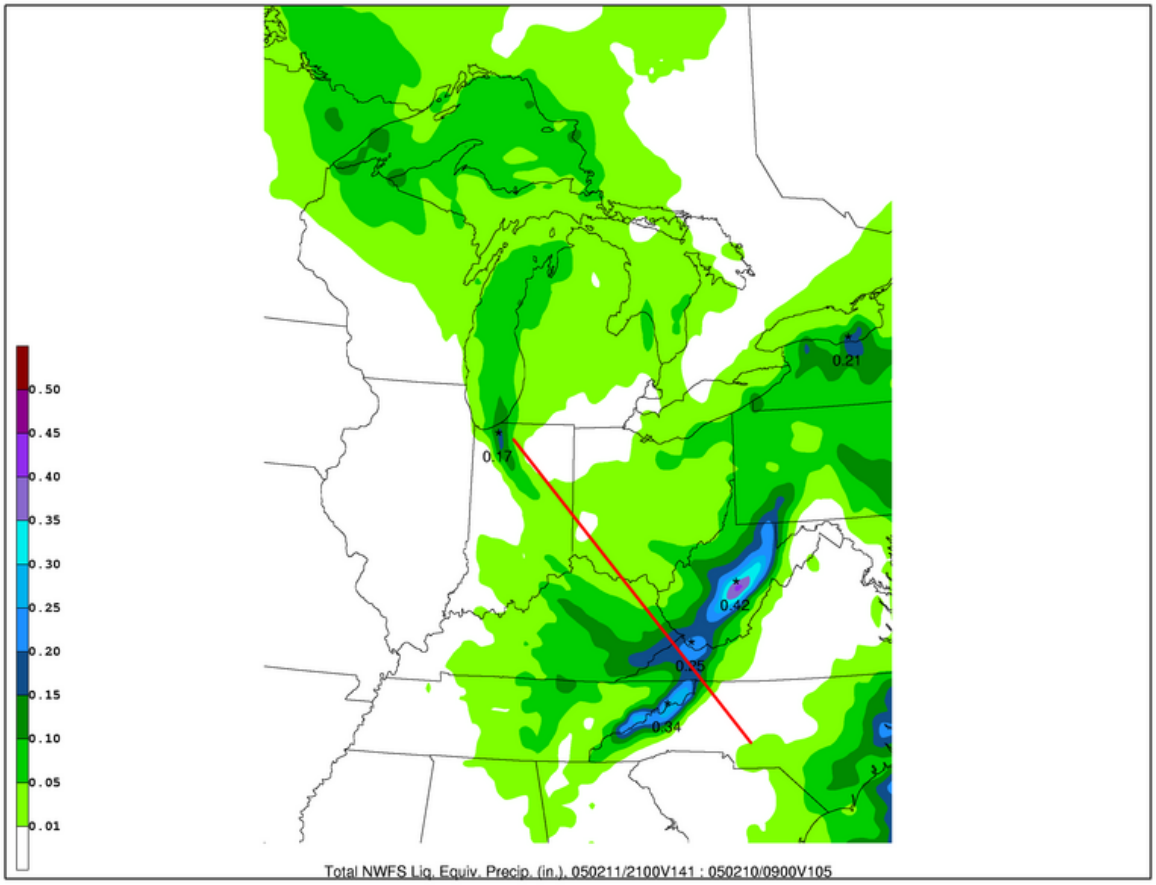

Figure 3.31. As in Figure 3.30, except for larger view. Solid red line denotes plane along which θ_e cross sections were taken.

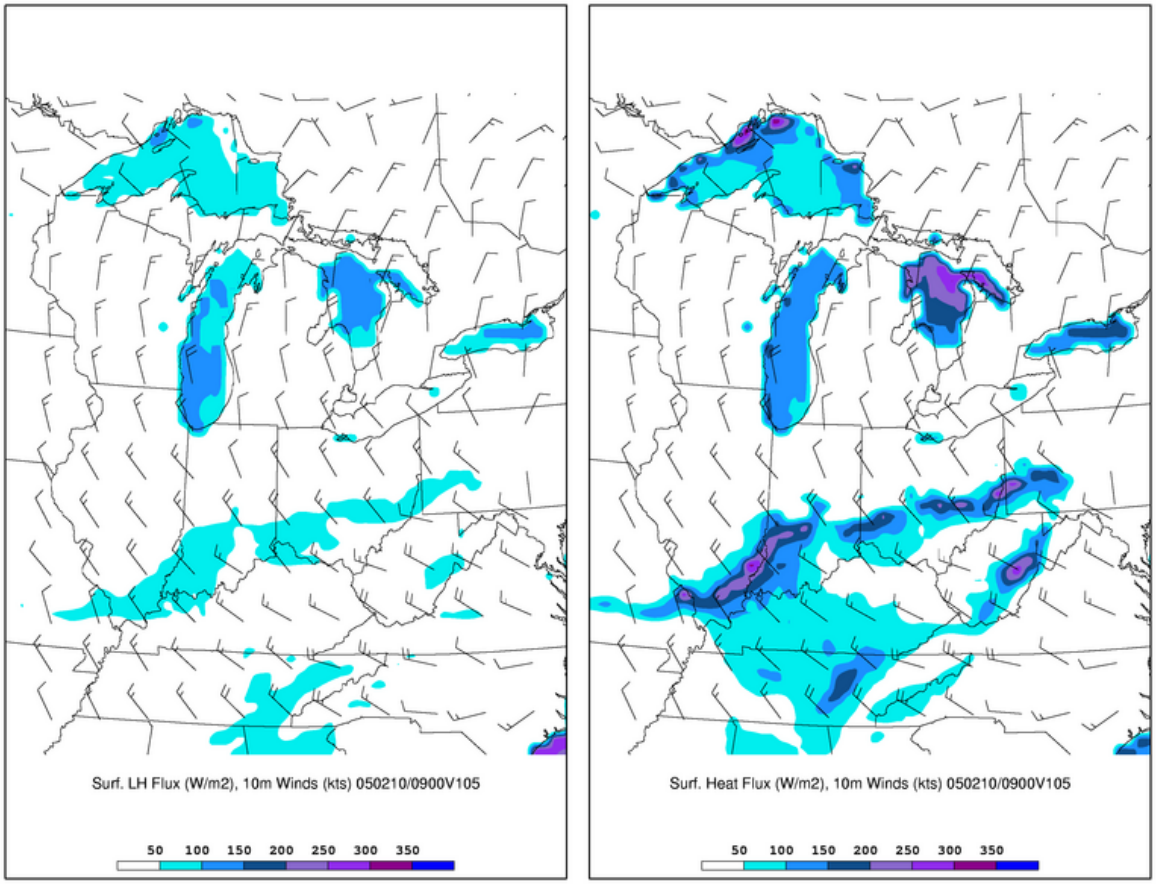

Figure 3.32. CTRL surface latent and sensible heat fluxes (W/m^2), shaded as in colorbar in lower center), and 10 m winds (kt, barbs) for 0900 UTC 10 February 2005.

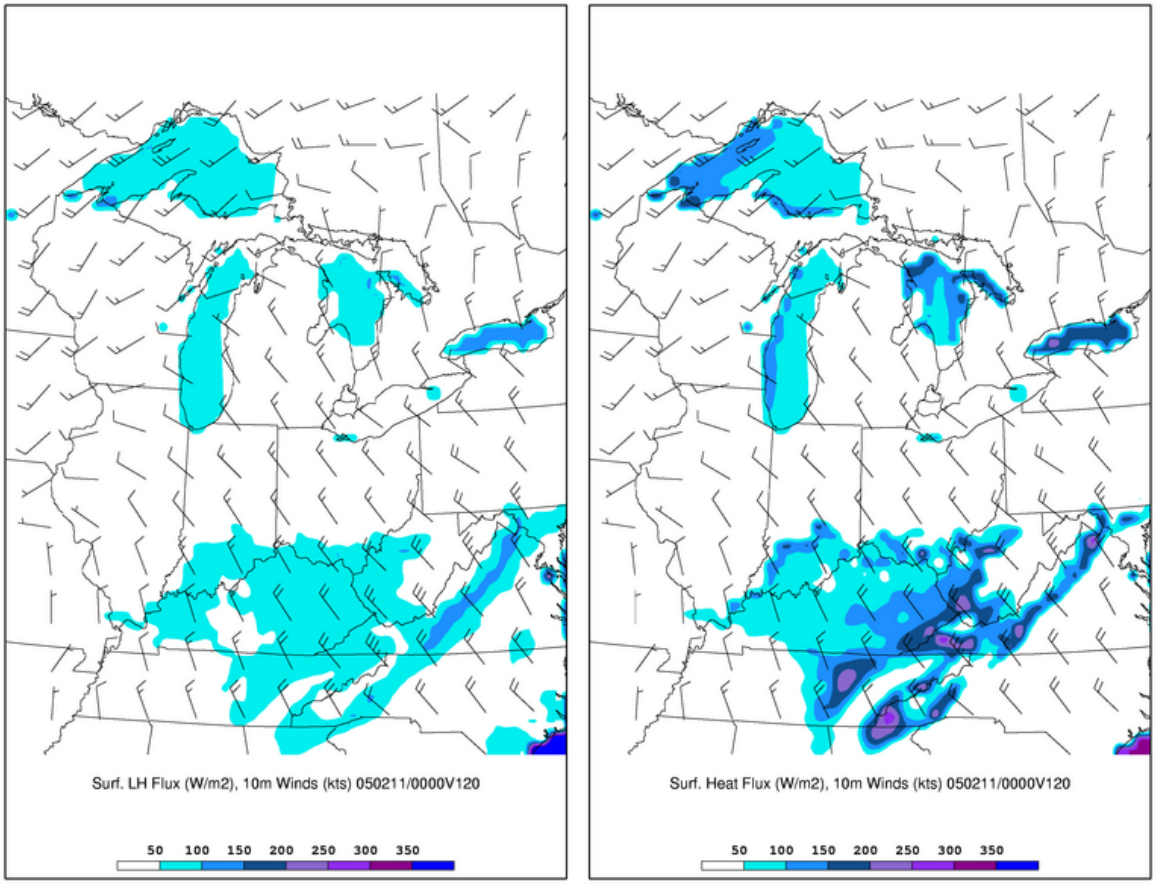

Figure 3.33. As in Figure 3.32, except for 0000 UTC 11 February 2005.

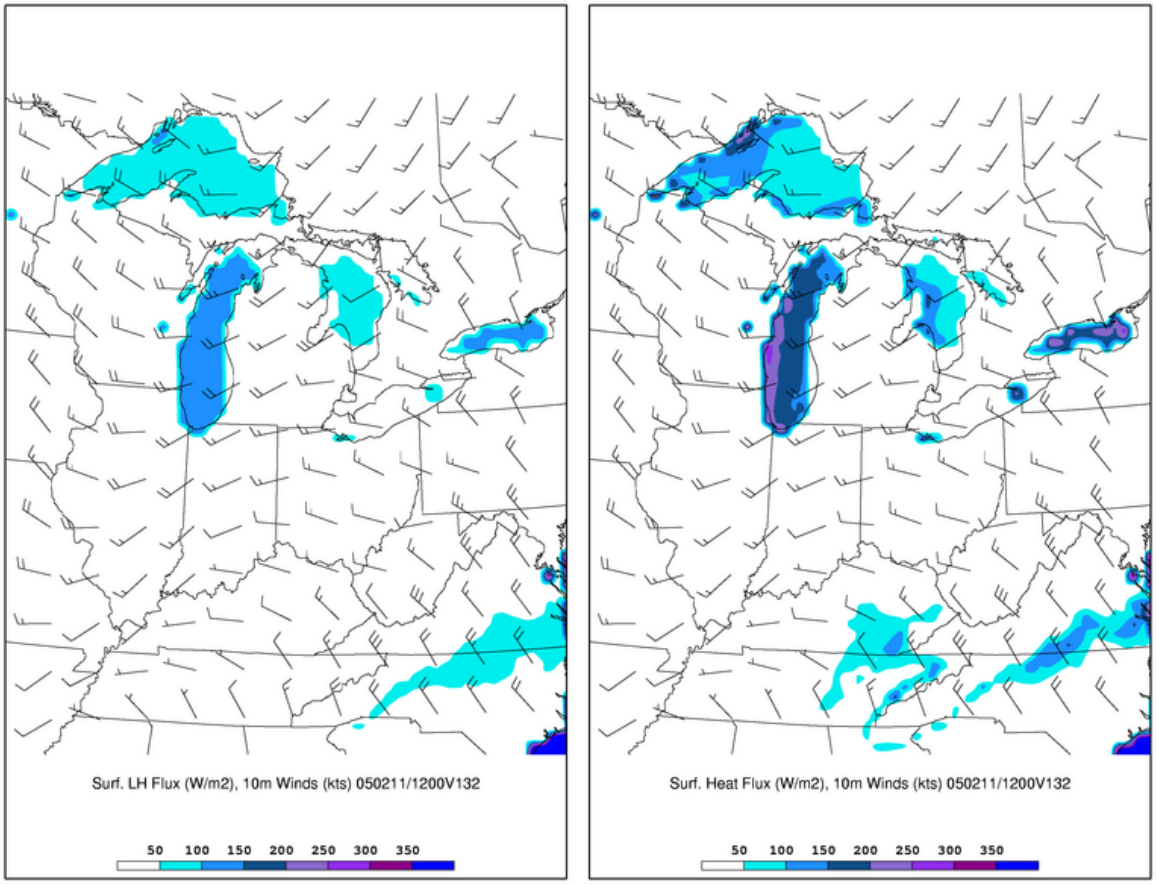

Figure 3.34. As in Figure 3.32, except for 1200 UTC 11 February 2005.

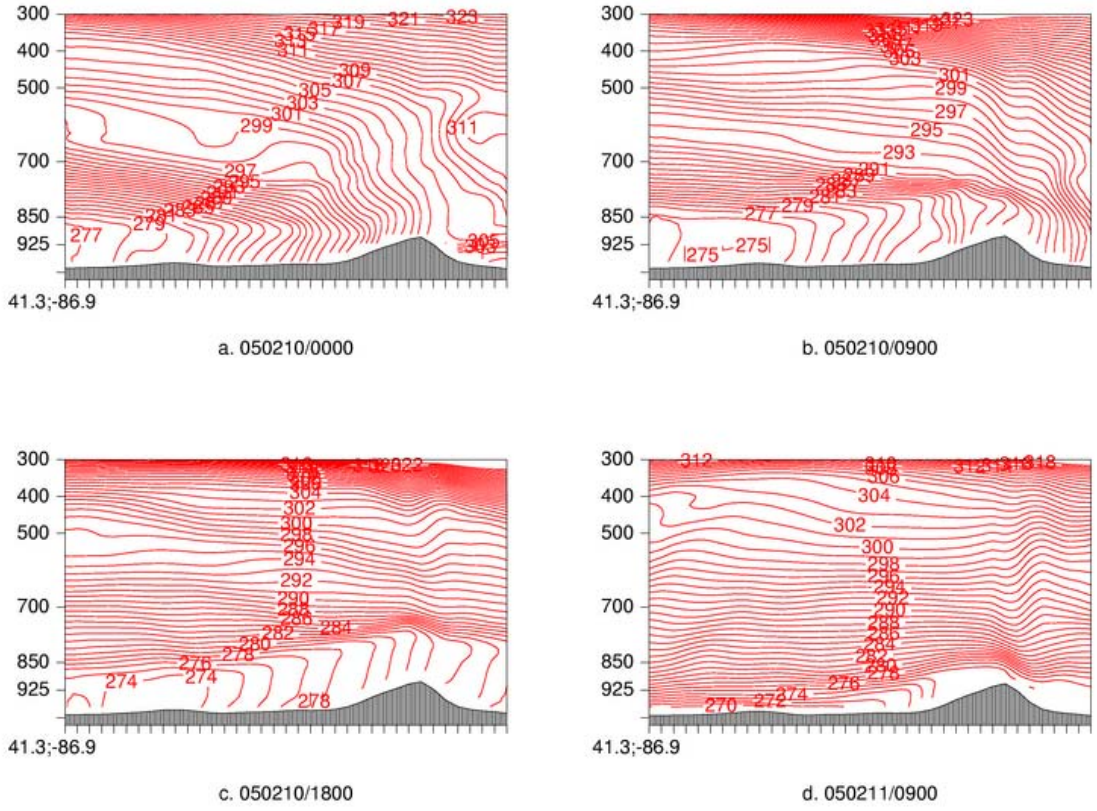

Figure 3.35. θ_e cross sections along the line shown in Figure 3.31 from CTRL: (a) 0000 UTC 10 February 2005; (b) 0900 UTC 10 February 2005; (c) 1800 UTC 10 February 2005; (d) 0900 UTC 11 February 2005.

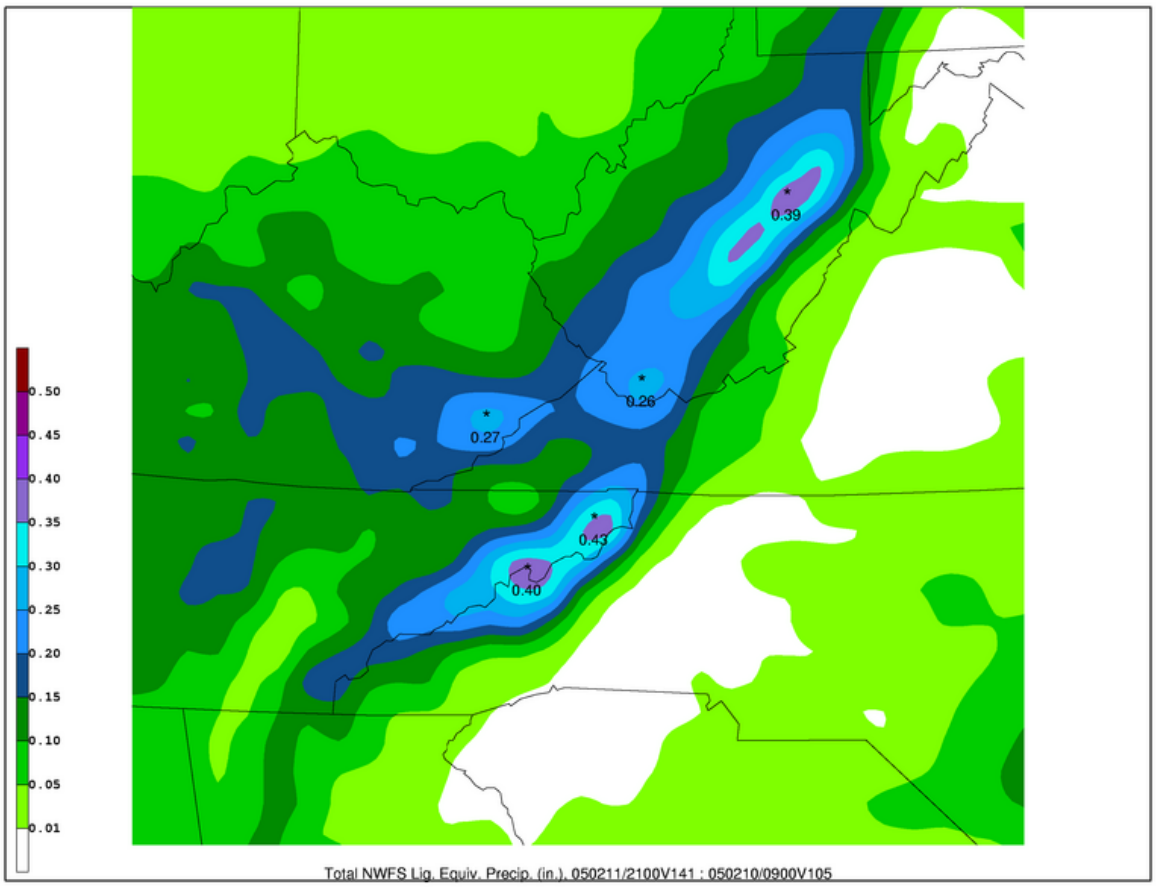

Figure 3.36. As in Figure 3.30, except from MYJPBL.

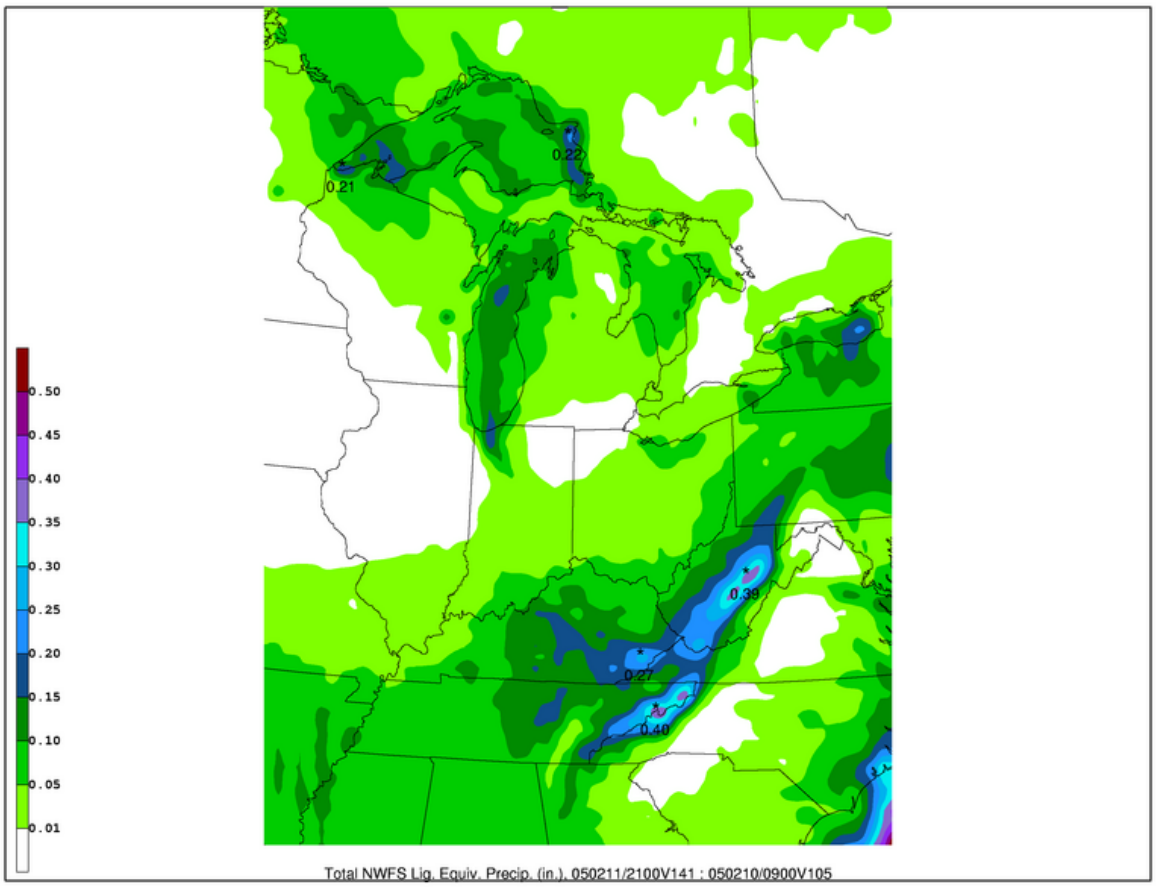

Figure 3.37. As in Figure 3.31, except for MYJPBL.

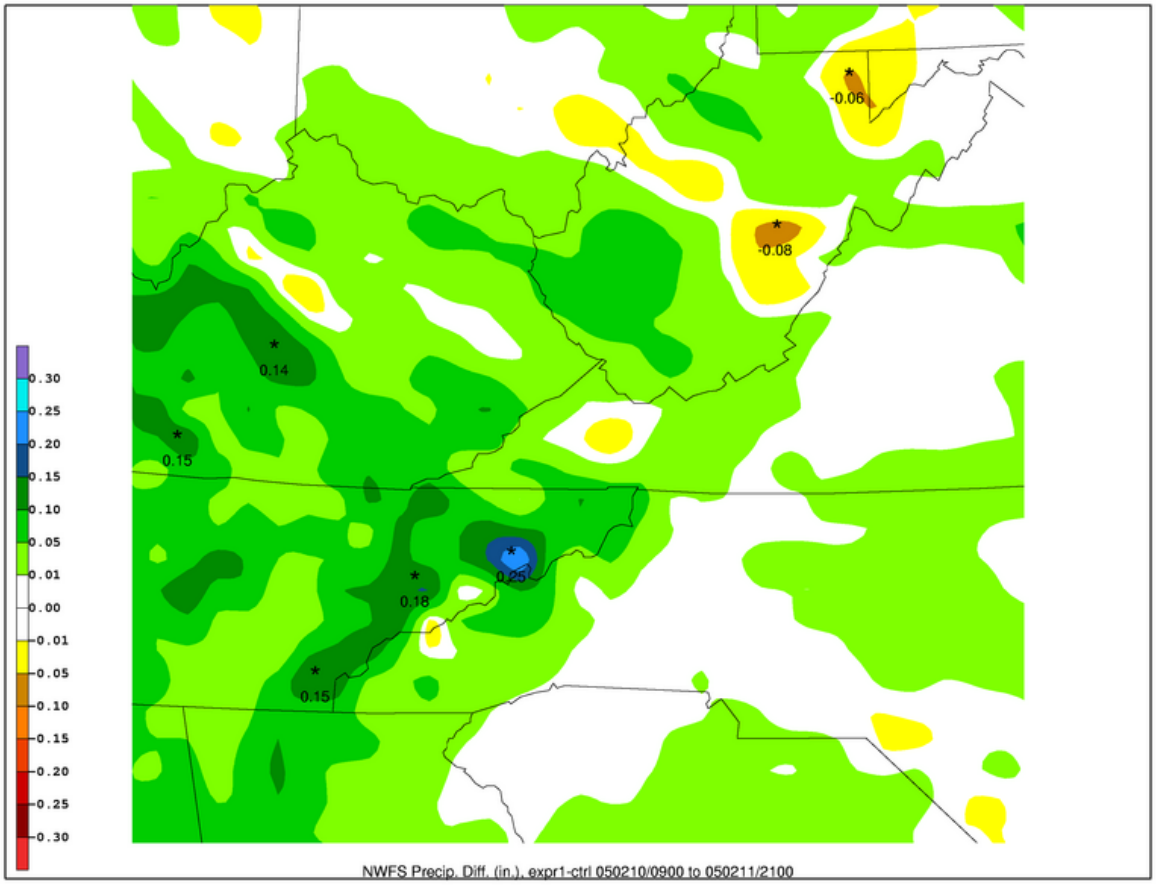

Figure 3.38. Difference field of liquid equivalent precipitation, MYJPBL-CTRL, from 0900 UTC 10 February 2005 to 2100 UTC 11 February 2005 (inches, shaded as in colorbar in lower left).

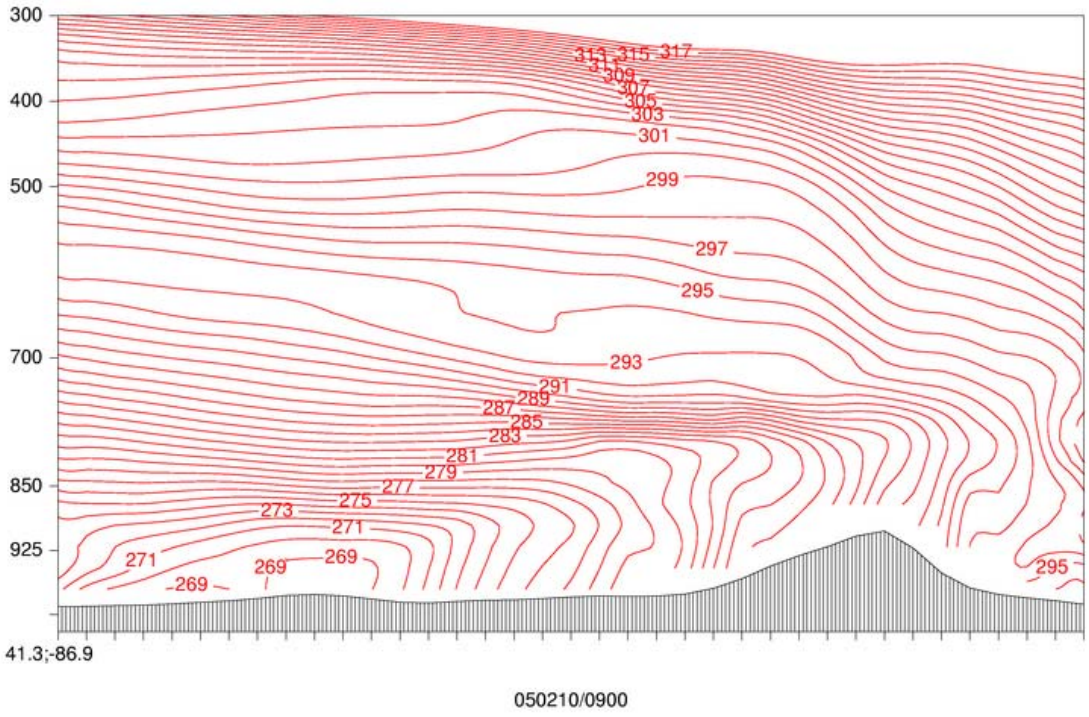

Figure 3.39. As in Figure 3.35, except for MYJPBL at 0900 UTC 10 February 2005.

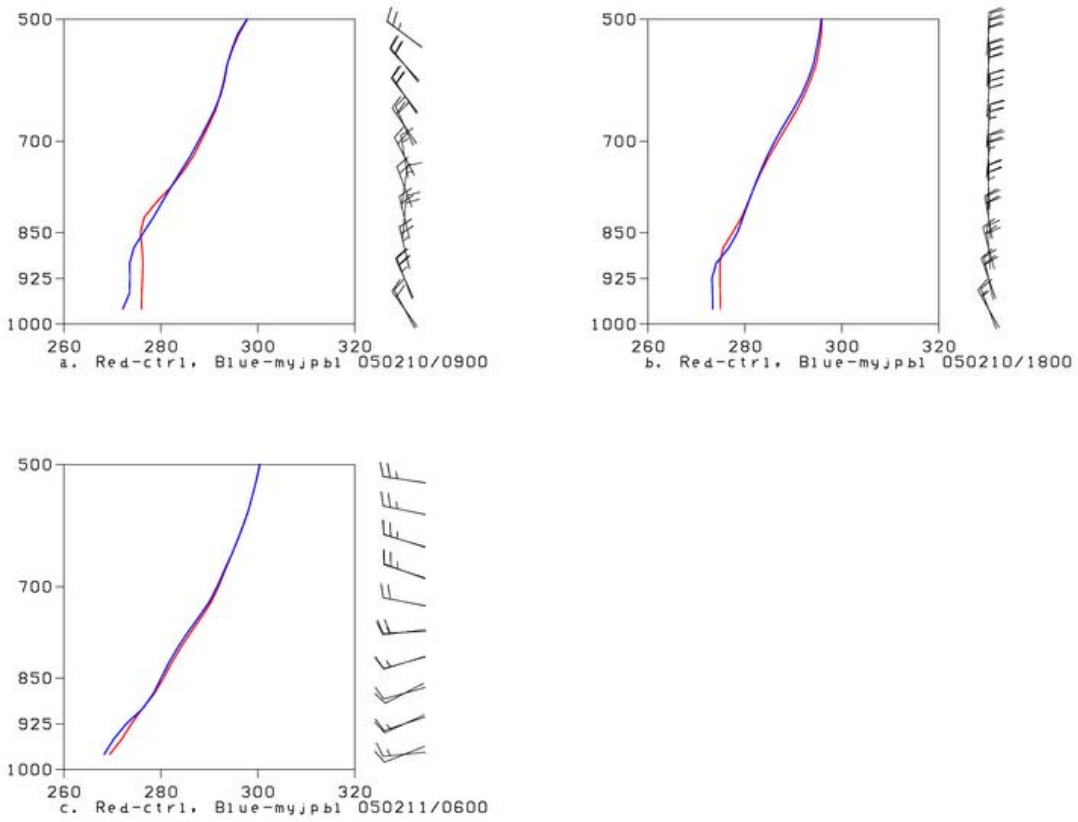

Figure 3.40. θ_e (K) profiles at La Crosse, IN (41.3 N;-86.9 W) for CTRL (red) and MYJPBL (blue): (a) 0900 UTC 10 February 2005; (b) 1800 UTC 10 February 2005; (c) 0600 UTC 11 February 2005.

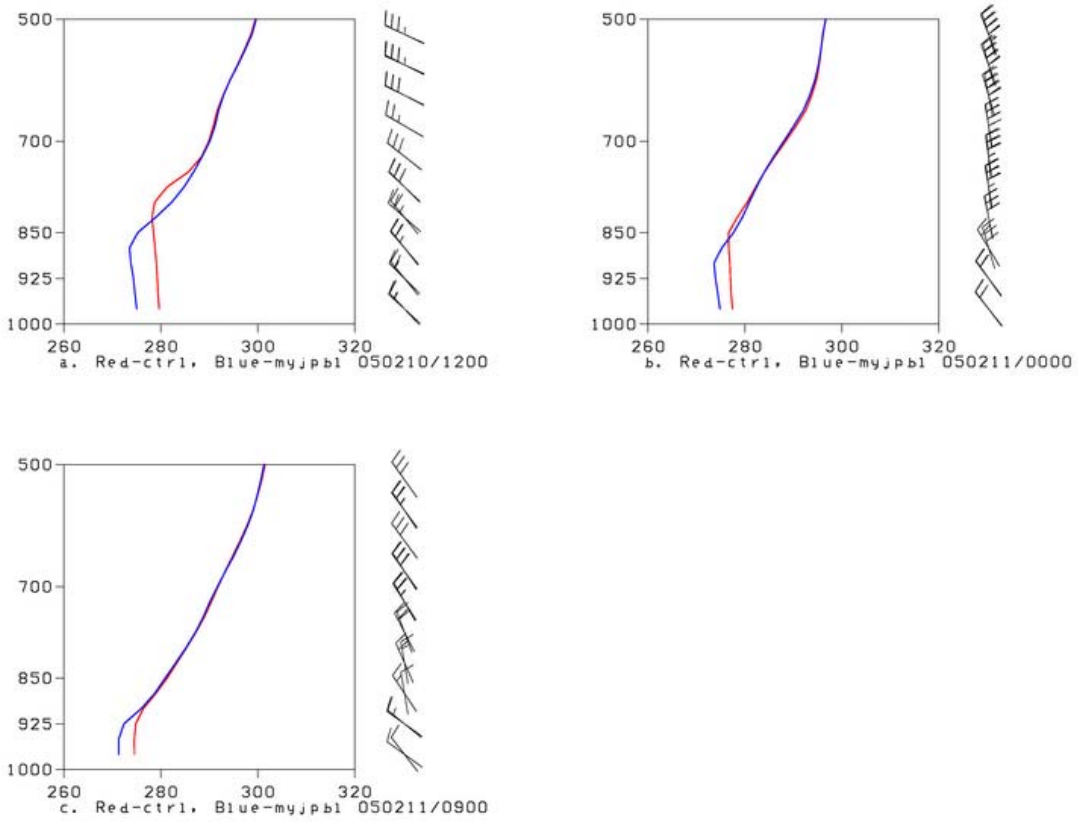

Figure 3.41. θ_e (K) profiles at Lexington, KY (38.03 N; -84.44 W) for CTRL (red) and MYJPBL (blue): (a) 1200 UTC 10 February 2005; (b) 0000 UTC 11 February 2005; (c) 0900 UTC 11 February 2005.

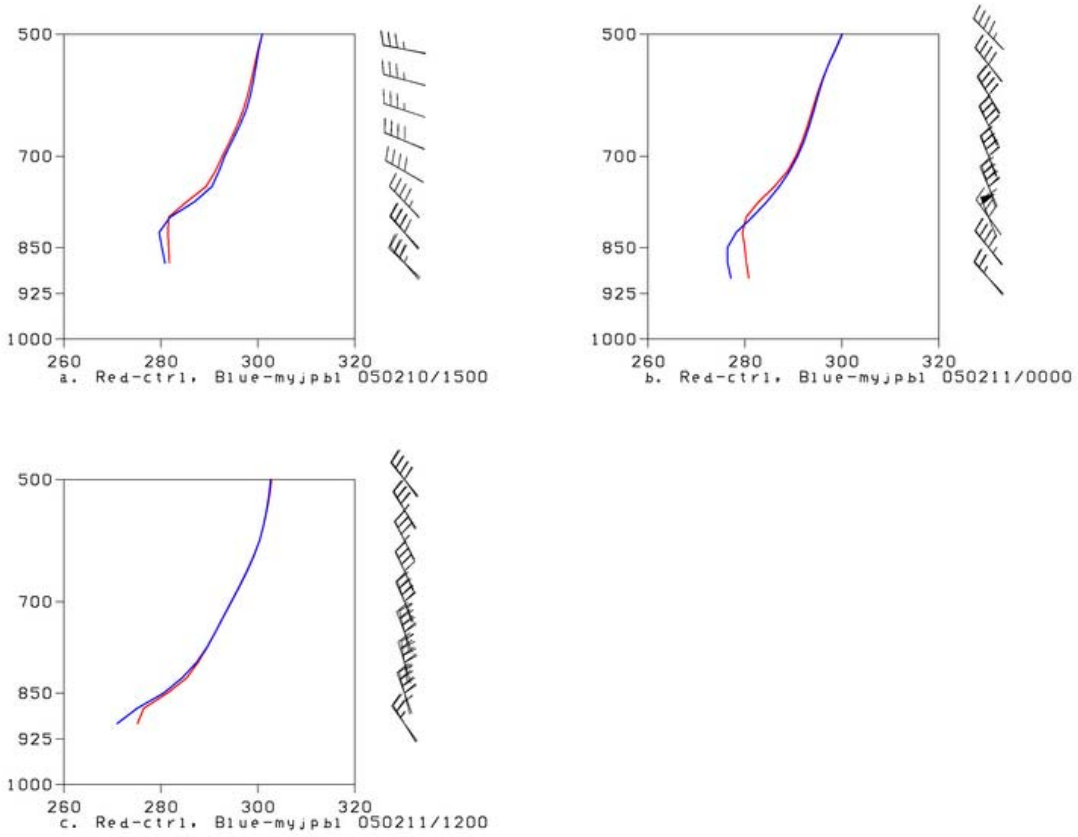

Figure 3.42. θ_e (K) profiles at Banner Elk, NC (36.15 N;-81.89 W) for CTRL (red) and MYJPBL (blue): (a) 1500 UTC 10 February 2005; (b) 0000 UTC 11 February 2005; (c) 1200 UTC 11 February 2005.

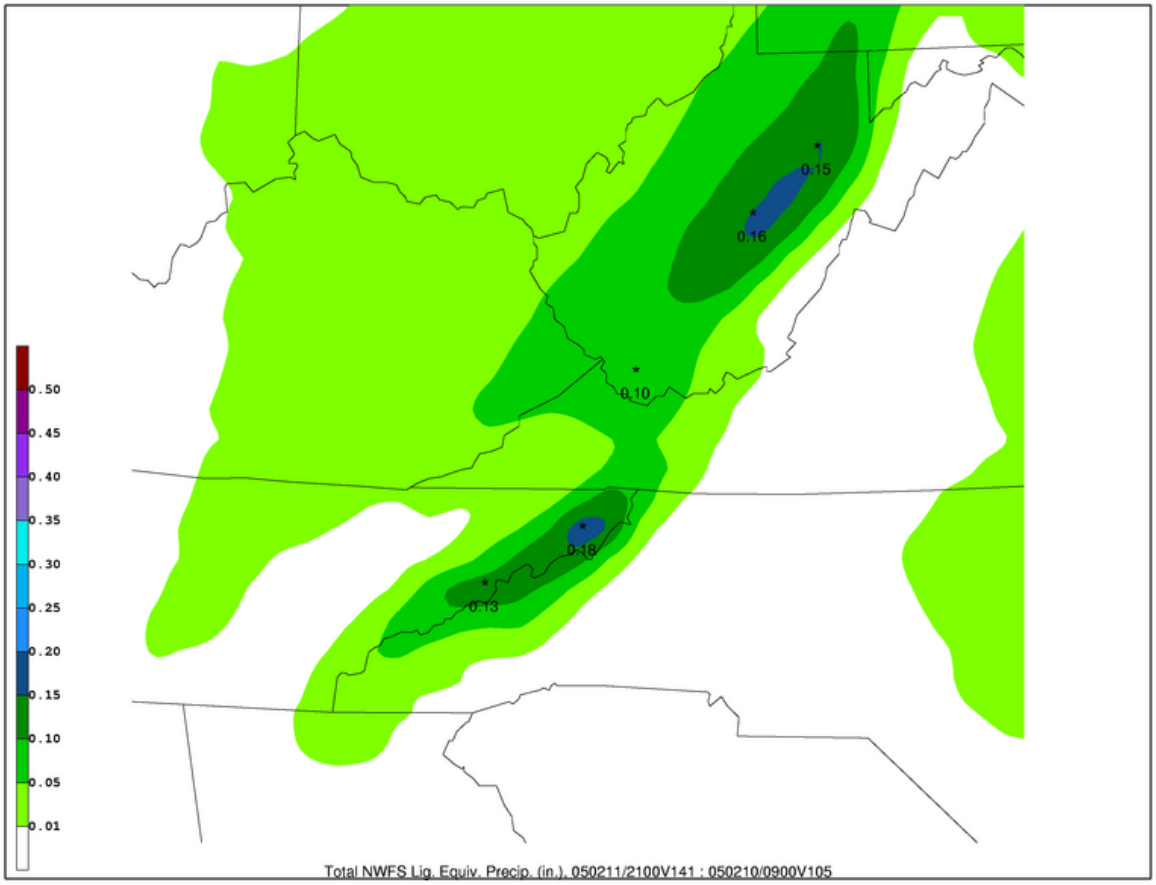

Figure 3.43. As in Figure 3.30, except for NOFLX.

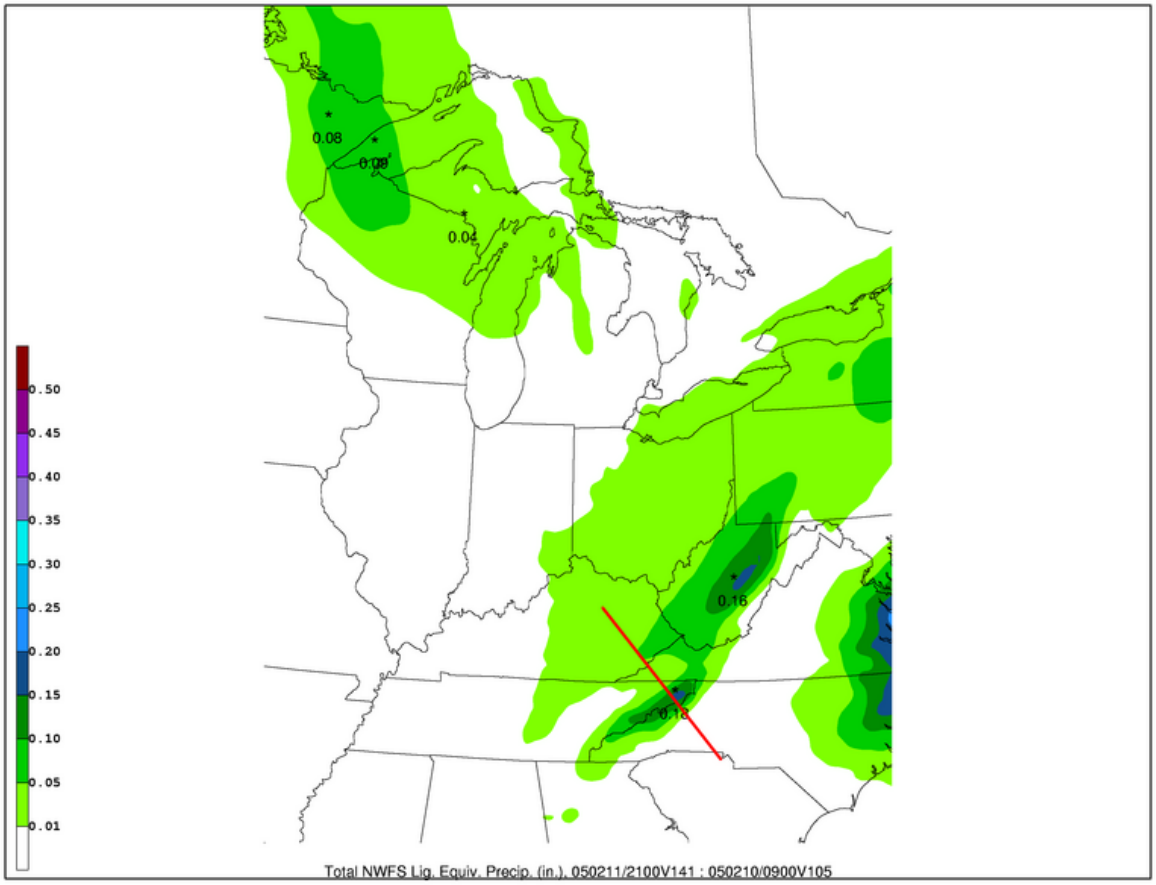

Figure 3.44. As in Figure 3.31, except for NOFLX. Solid red line denotes plane along which ω cross-sections were taken.

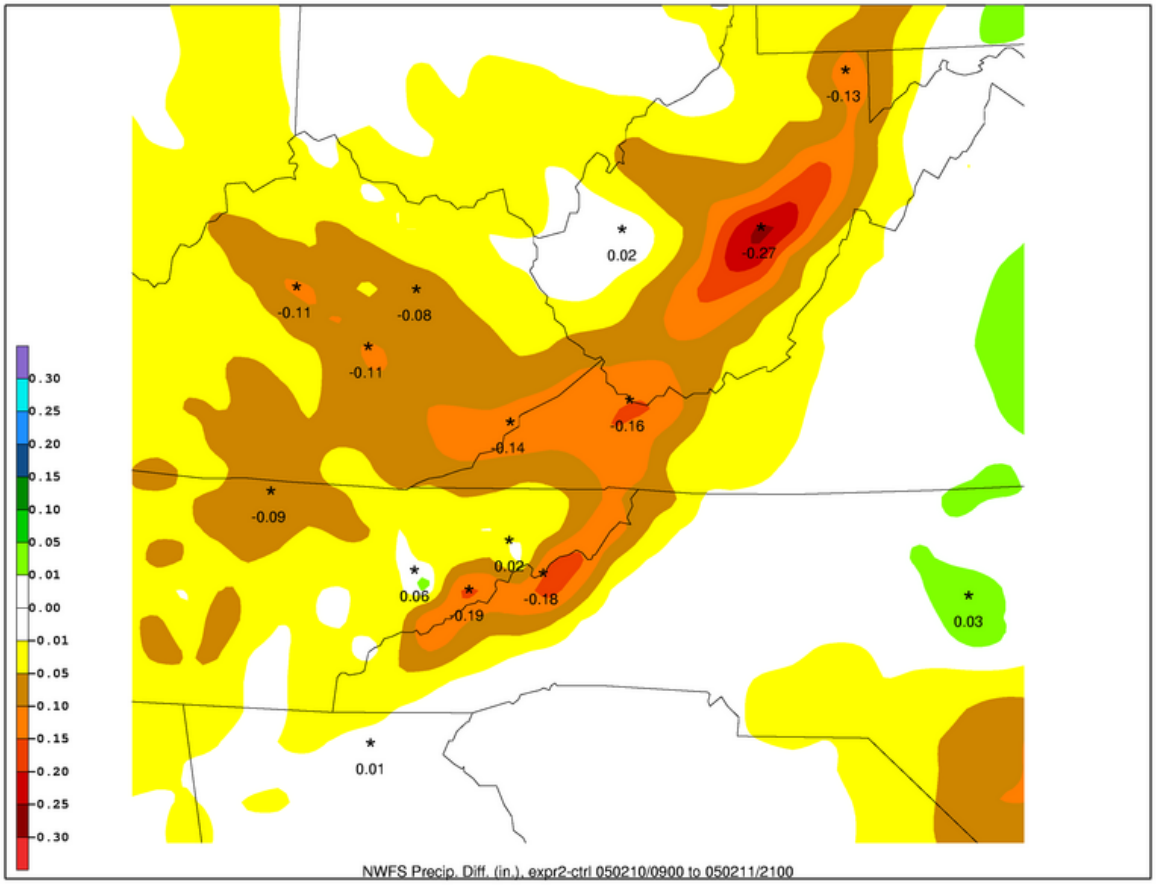

Figure 3.45. As in Figure 3.38, except for NOFLX-CTRL.

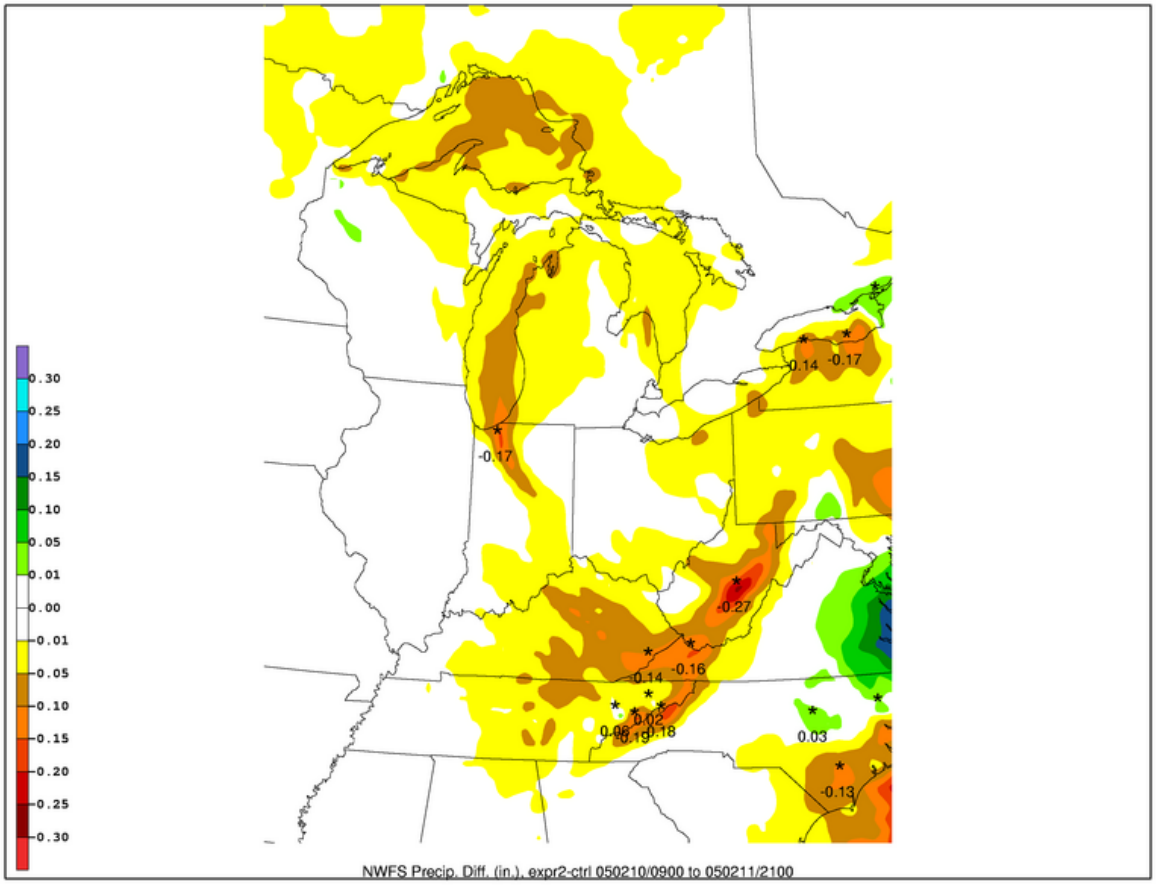

Figure 3.46. As in Figure 3.45, except larger view.

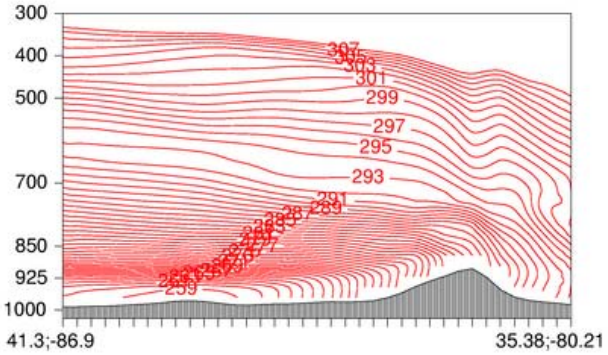

a. 050210/0900

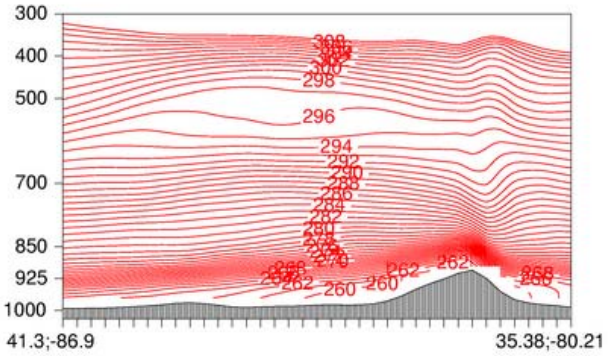

b. 050211/0000

Figure 3.47. θ_e cross sections along the line shown in Figure 3.31 from NOFLX: (a) 0900 UTC 10 February 2005; (b) 0000 UTC 11 February 2005.

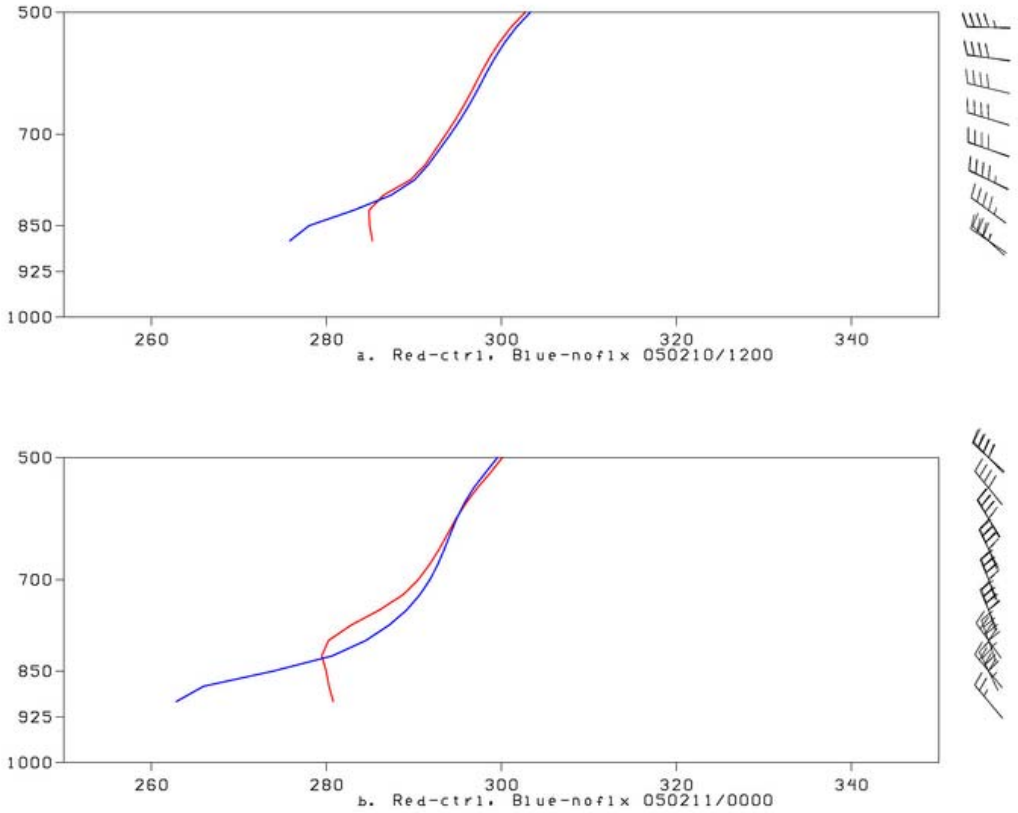

Figure 3.48. θ_e (K) profiles at Banner Elk, NC (36.15 N;-81.89 W) for CTRL (red) and NOFLX (blue): (a) 1200 UTC 10 February 2005; (b) 0000 UTC 11 February 2005.

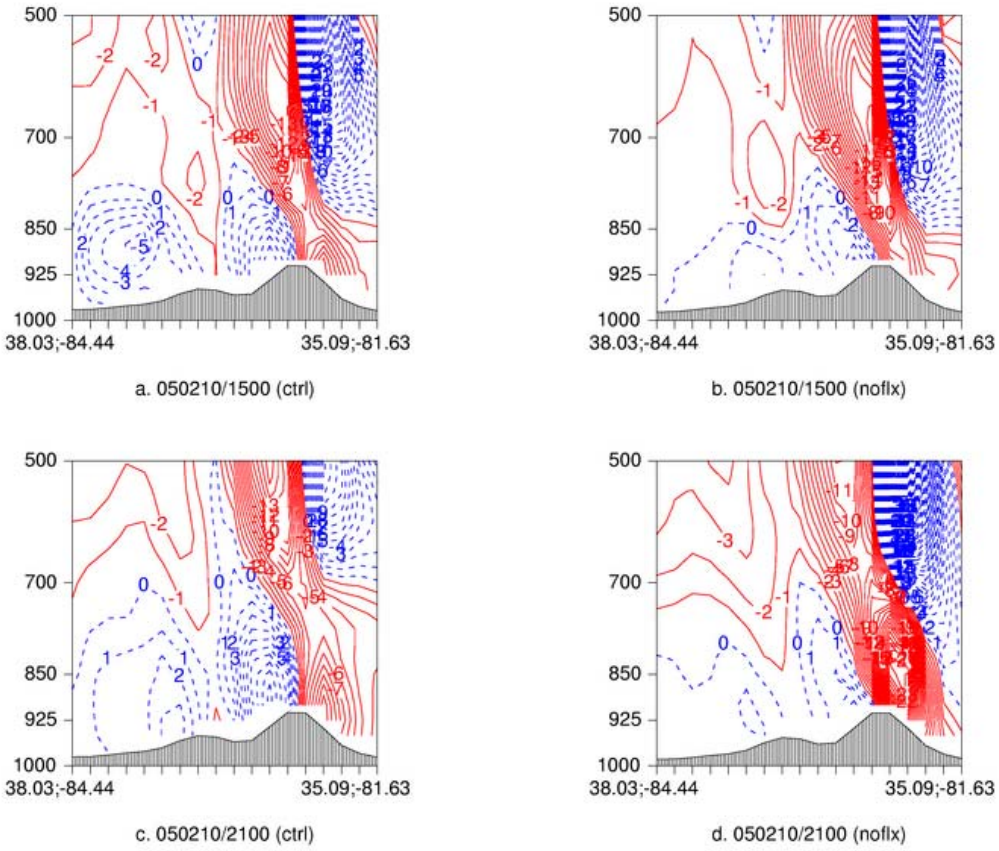

Figure 3.49. Plot of ω (μbar/sec) for CTRL and NOFLX: (a) CTRL at 1500 UTC 10 February 2005; (b) NOFLX at 1500 UTC 10 February 2005; (c) CTRL at 2100 UTC 10 February 2005; and (d) NOFLX at 2100 UTC 10 February 2005.

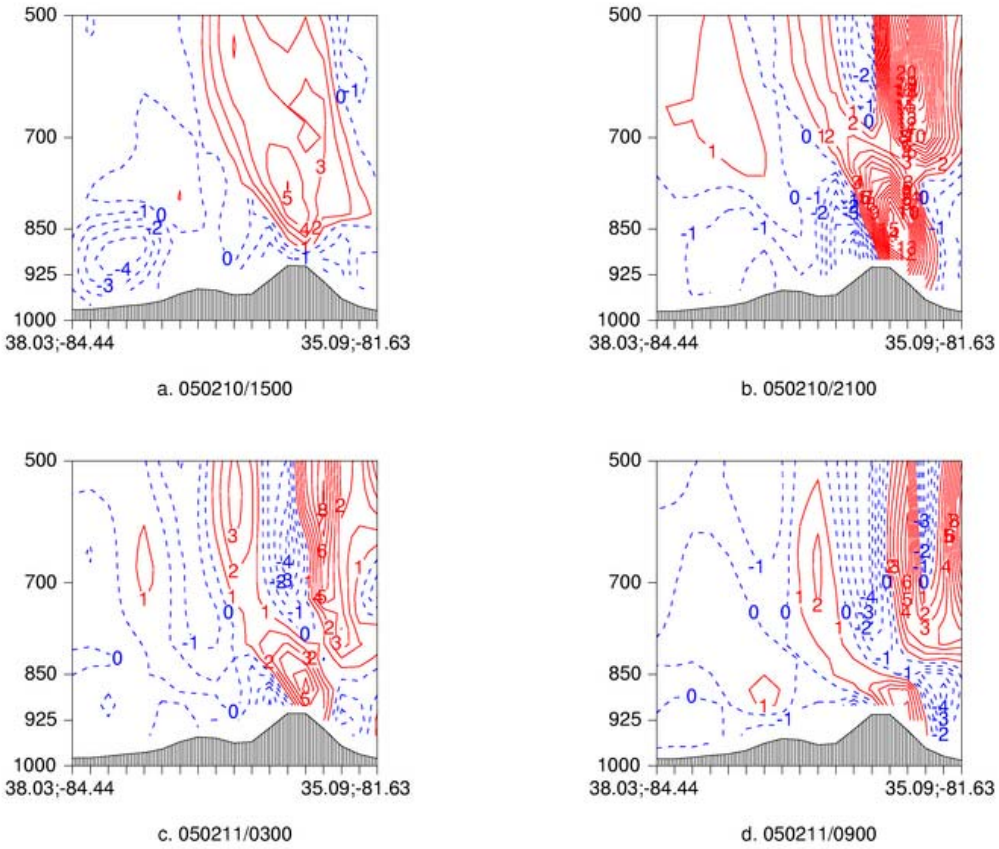

Figure 3.50. Difference plot of ω (μbar/sec) for CTRL-NOFLX, from: (a) 1500 UTC 10 February 2005; (b) 2100 UTC 10 February 2005; (c) 0300 UTC 11 February 2005; and (d) 0900 UTC 11 February 2005.

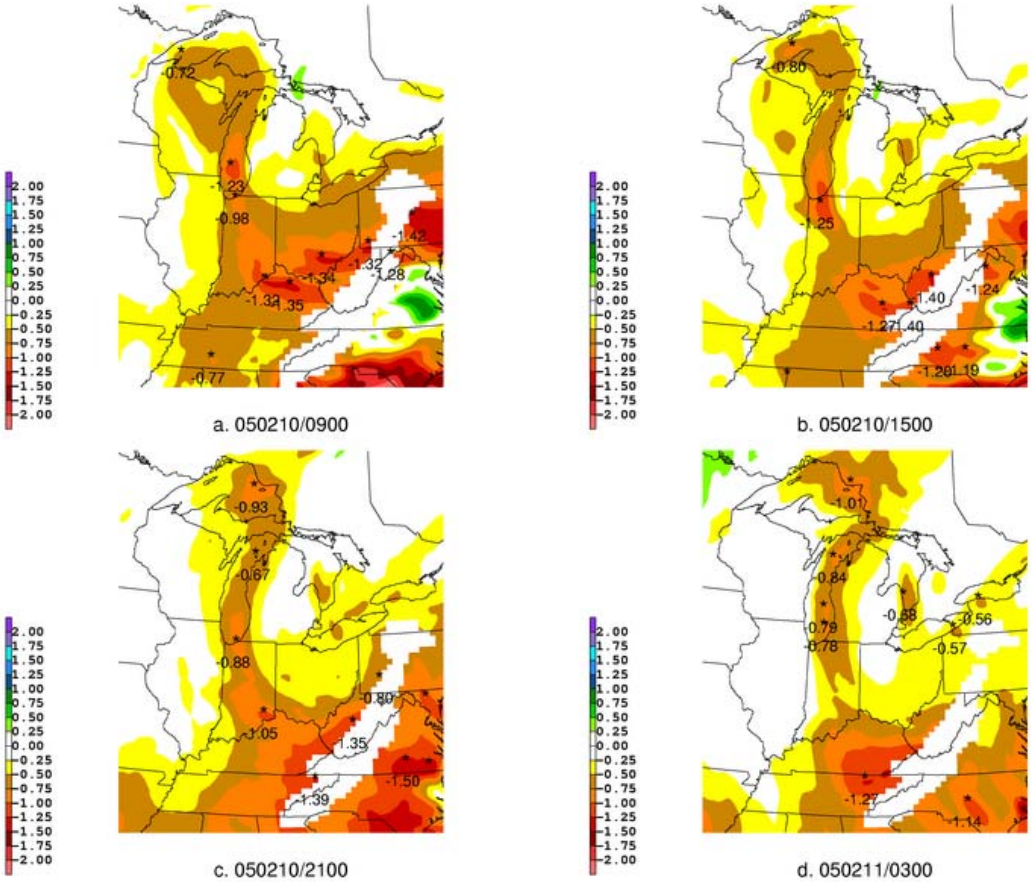

Figure 3.51. Difference field of the 950–875 hPa layer averaged water vapor mixing ratio (g/kg), (shaded as in color bar in lower left), NOFLX-CTRL for: (a) 0900 UTC 10 February 2005; (b) 1500 UTC 10 February 2005; (c) 2100 UTC 10 February 2005; and (d) 0300 UTC 10 February 2005.

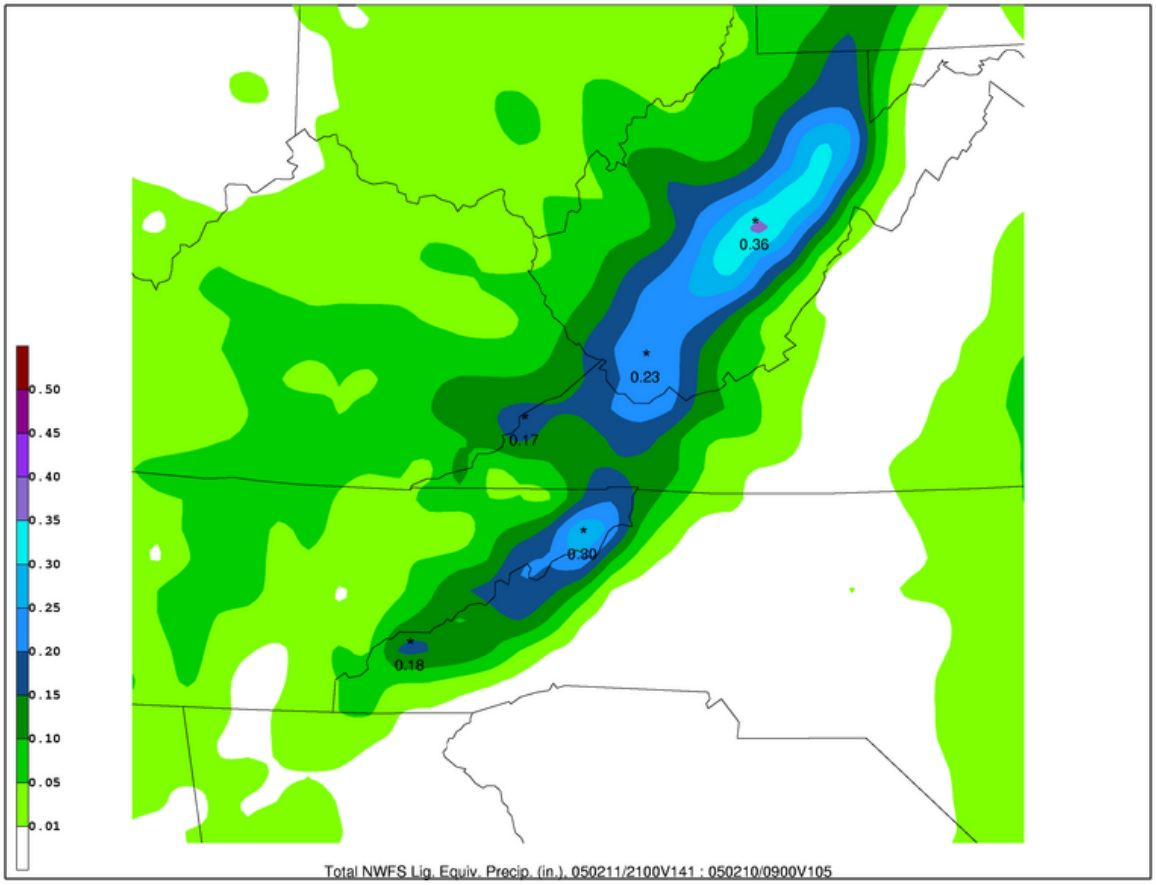

Figure 3.52. As in Figure 3.30, except for LKNOFLX.

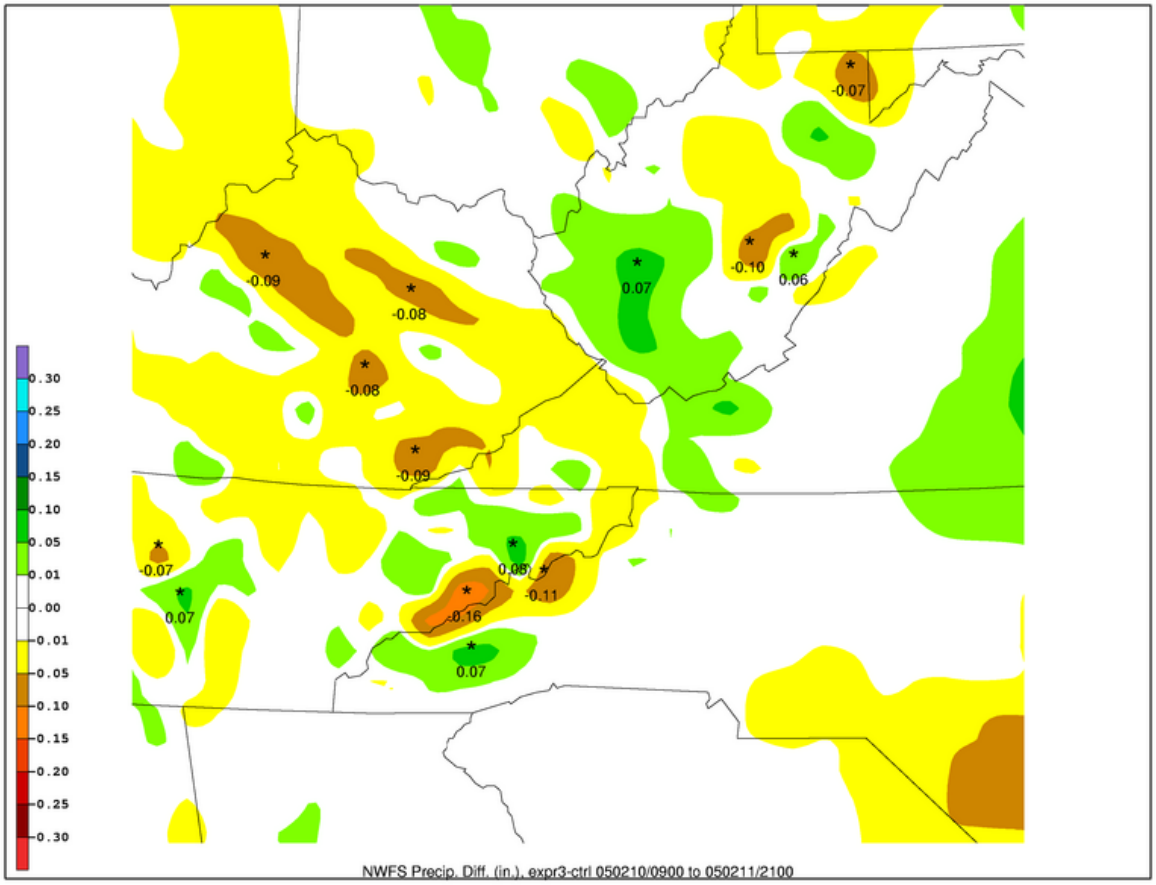

Figure 3.53. As in Figure 3.38, except for LKNOFLX-CTRL.

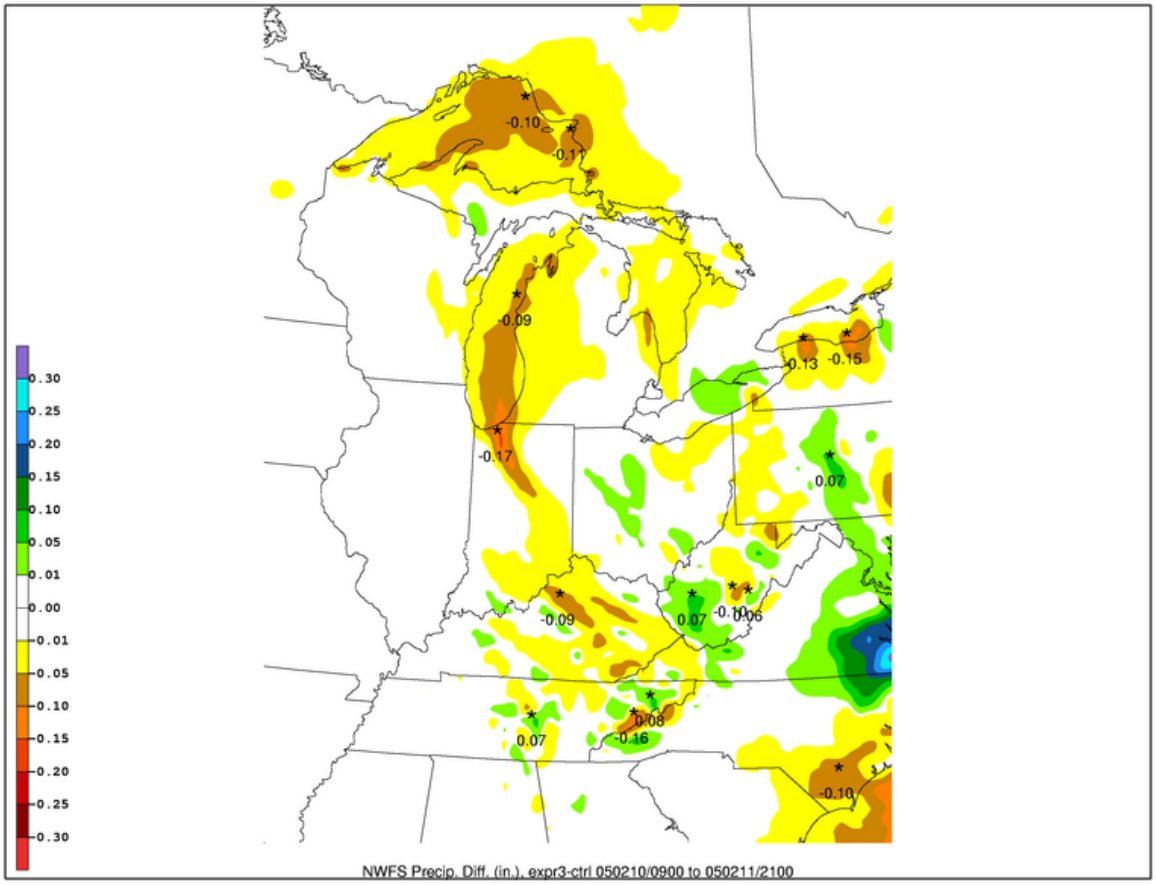

Figure 3.54. As in Figure 3.53, except larger view.

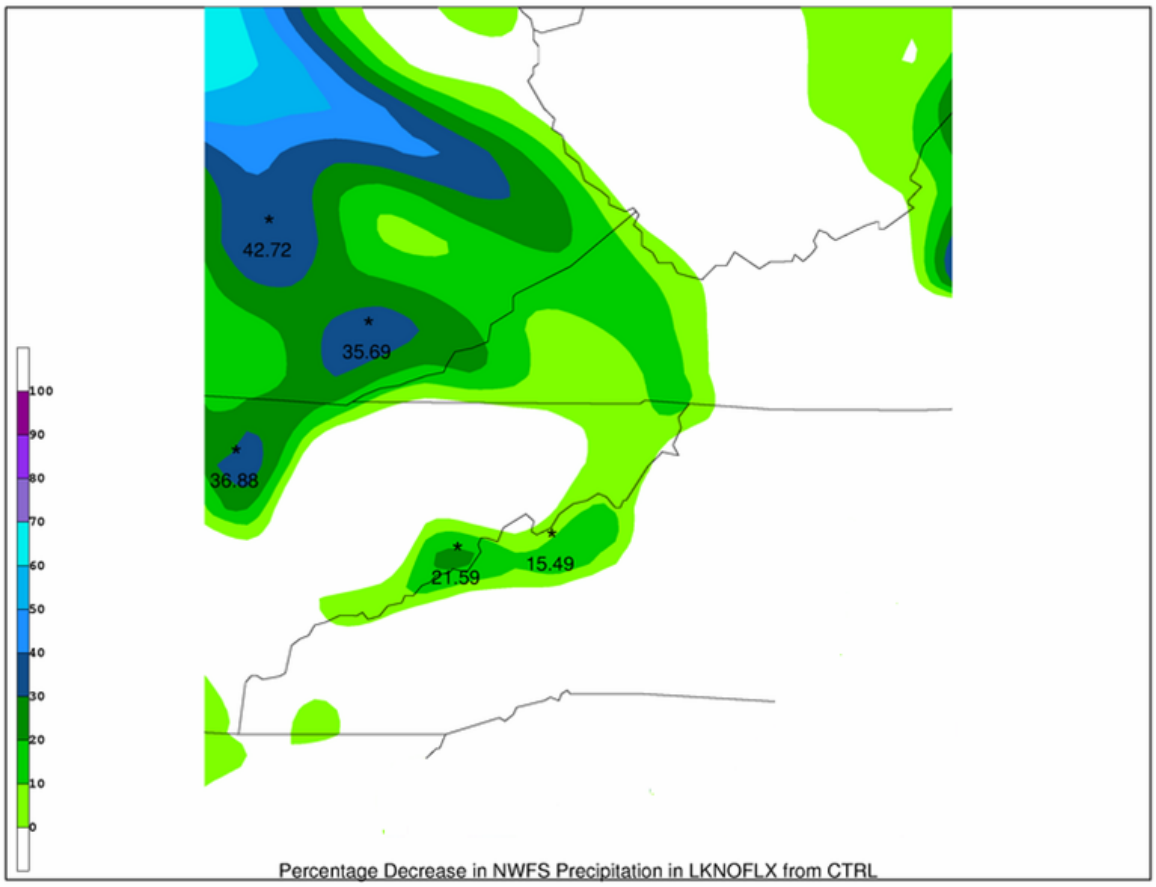

Figure 3.55. Percent of decrease in liquid equivalent precipitation for total NWFS precipitation in LKNOFLX from CTRL for areas of decreased precipitation (shaded as in colorbar in lower left corner).

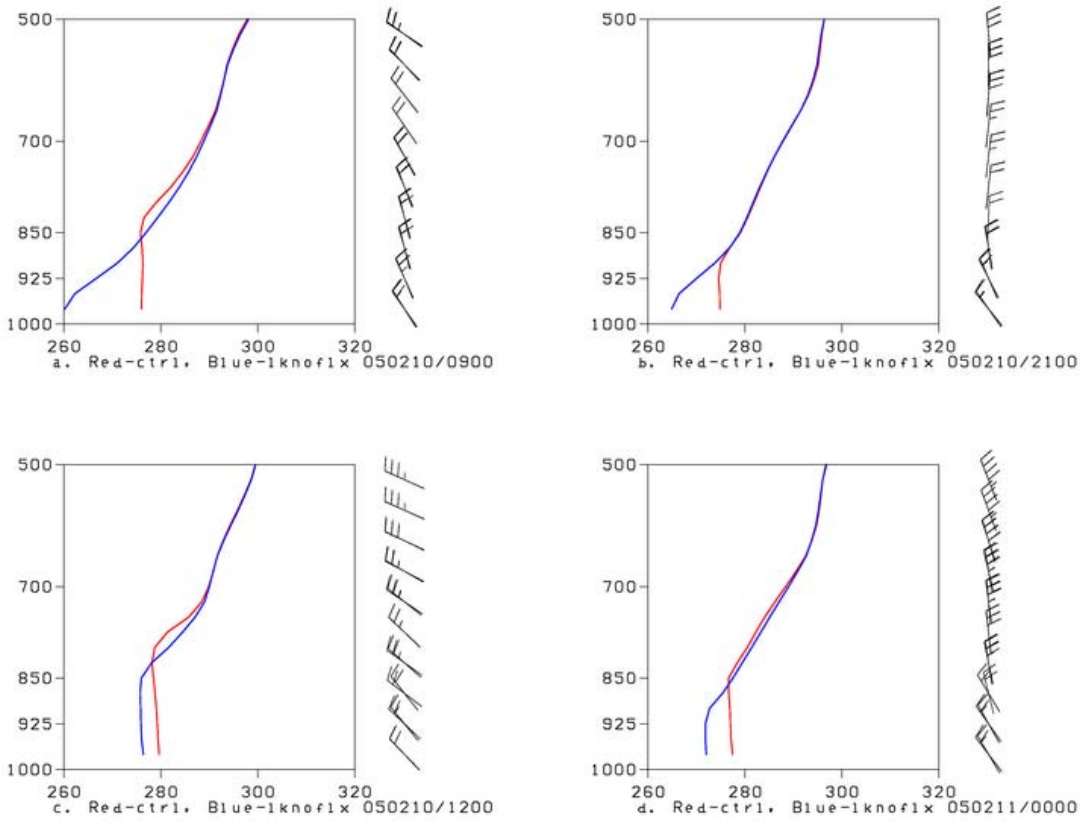

Figure 3.56. θ_e (K) profiles at La Crosse, IN (41.3 N;-86.9 W) for CTRL (red) and LKNOFLX (blue): (a) 0900 UTC 10 February 2005; (b) 2100 UTC 10 February 2005; and at Lexington, KY (38.03 N; -84.44 W): (c) 1200 UTC 11 February 2005; (d) 0000 UTC 11 February 2005.

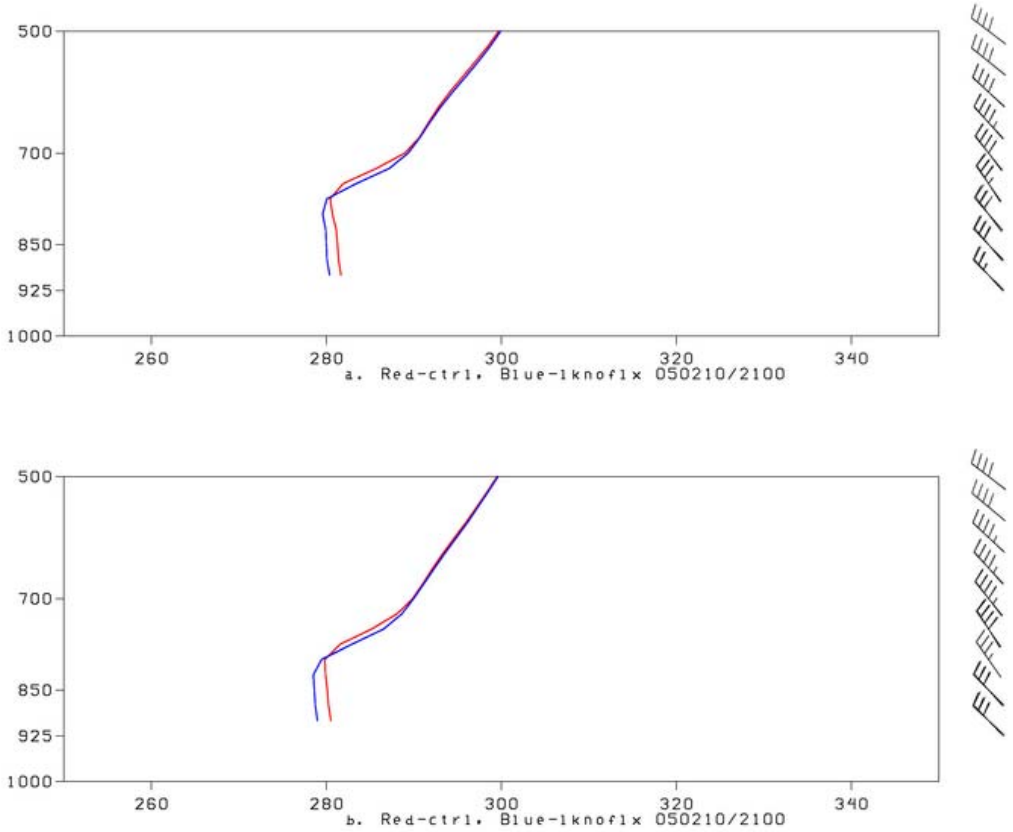

Figure 3.57. θ_e (K) profiles at Erwin, TN (36.14 N;-82.39 W) for CTRL (red) and LKNOFLX (blue): (a) 2100 UTC 10 February 2005; and at Marshall, NC (35.81 N;-82.71 W): (b) 2100 UTC 10 February 2005.

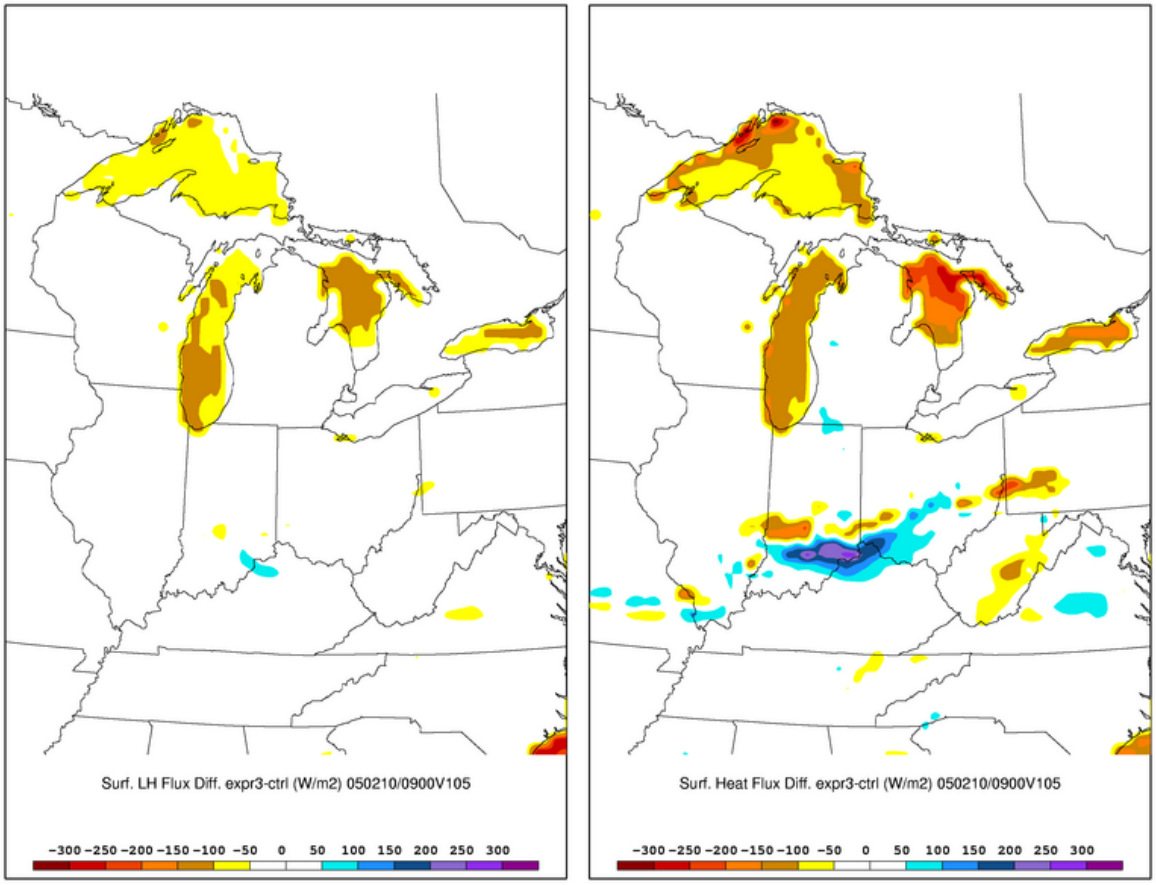

Figure 3.58. Difference field of surface latent and sensible heat flux (W/m^2, shaded as in colorbar in bottom center), LKNOFLX-CTRL, for 0900 UTC 10 February 2005.

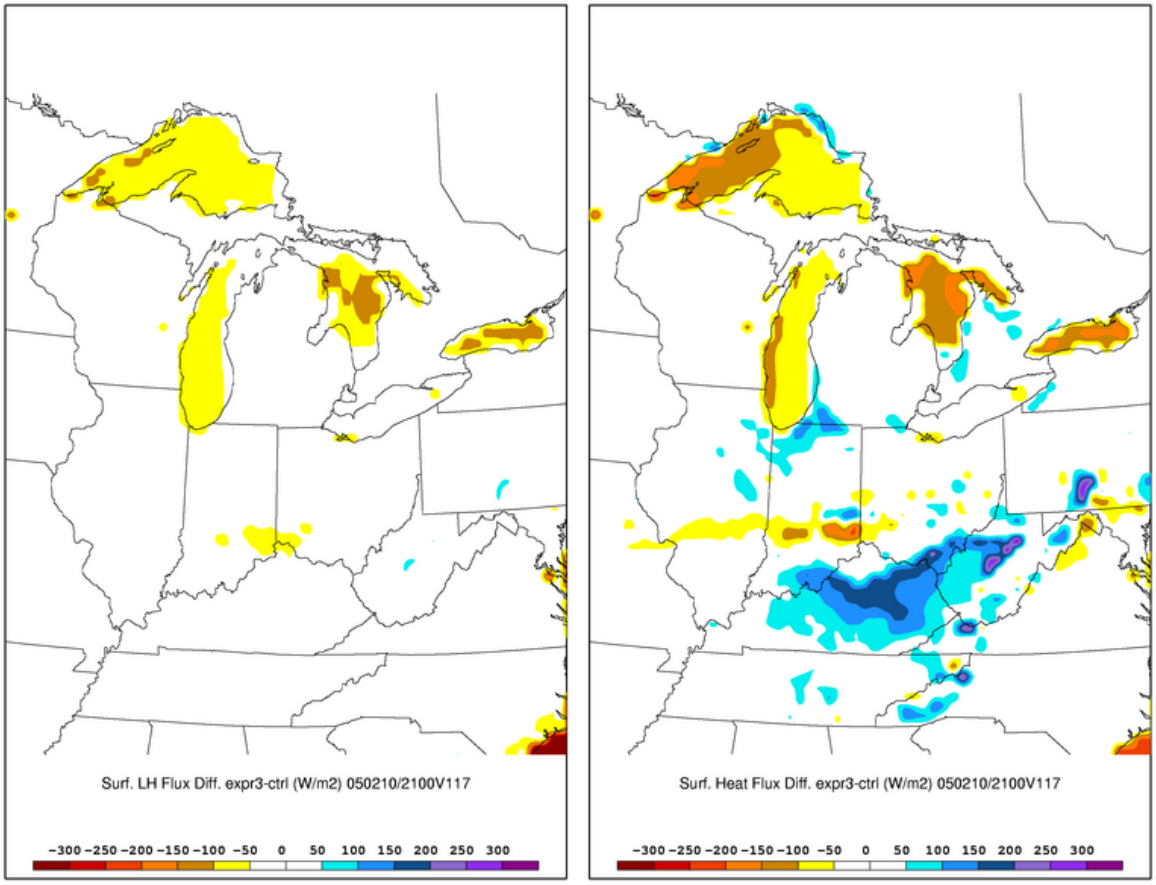

Figure 3.59. As in Figure 3.58, except for 2100 UTC 10 February 2005.

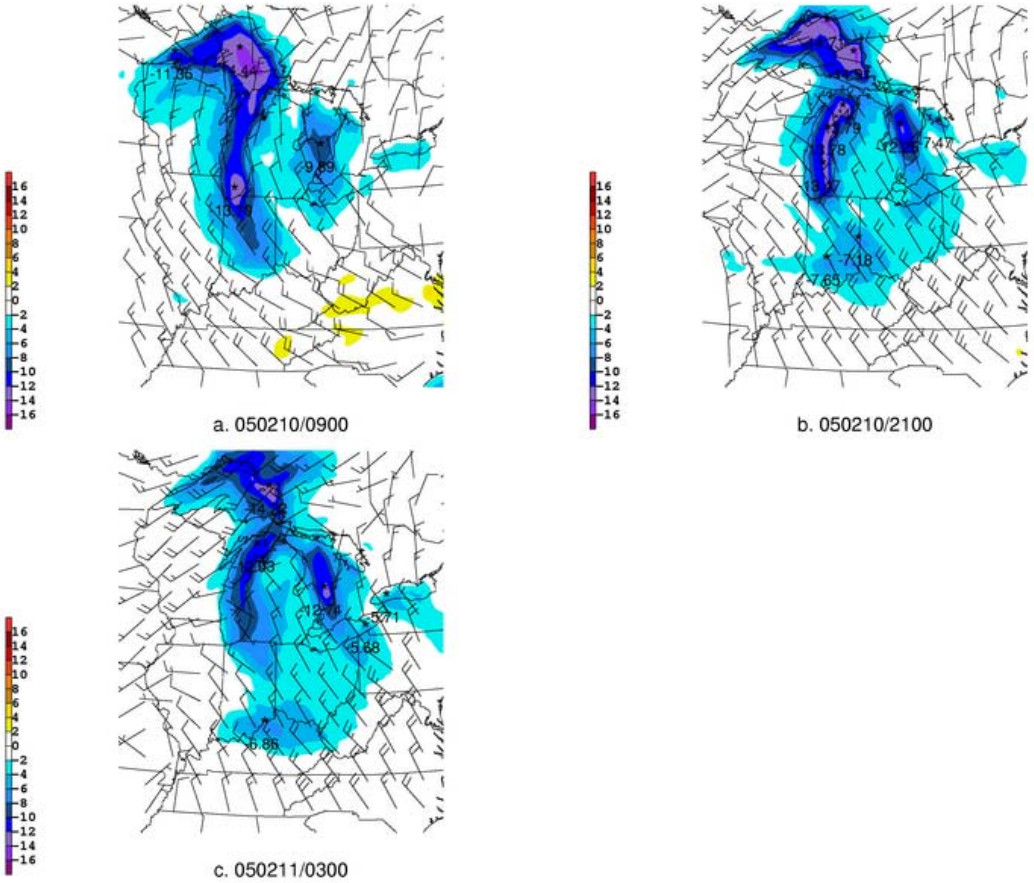

Figure 3.60. Difference field of 2 m temperatures (°C, shaded as in colorbar on lower left), LKNOFLX-CTRL, and CTRL 10 m winds (kt, barbs) from: (a) 0900 UTC 10 February 2005; (b) 2100 UTC 10 February 2005; and (c) 0300 11 February 2005.

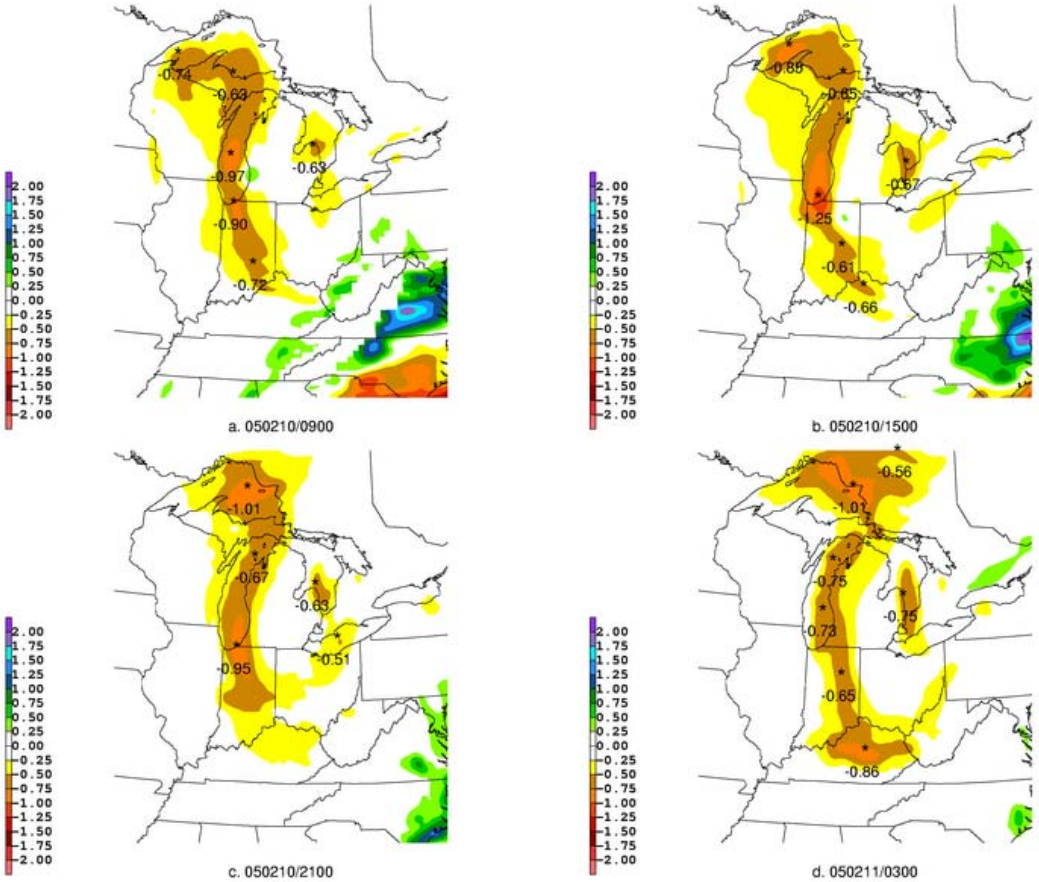

Figure 3.61. Difference field of the 950–875 hPa layer averaged water vapor mixing ratio (g/kg), (shaded as in color bar in lower left), LKNOFLX-CTRL for: (a) 0900 UTC 10 February 2005; (b) 1500 UTC 10 February 2005; (c) 2100 UTC 10 February 2005; and (d) 0300 UTC 10 February 2005.

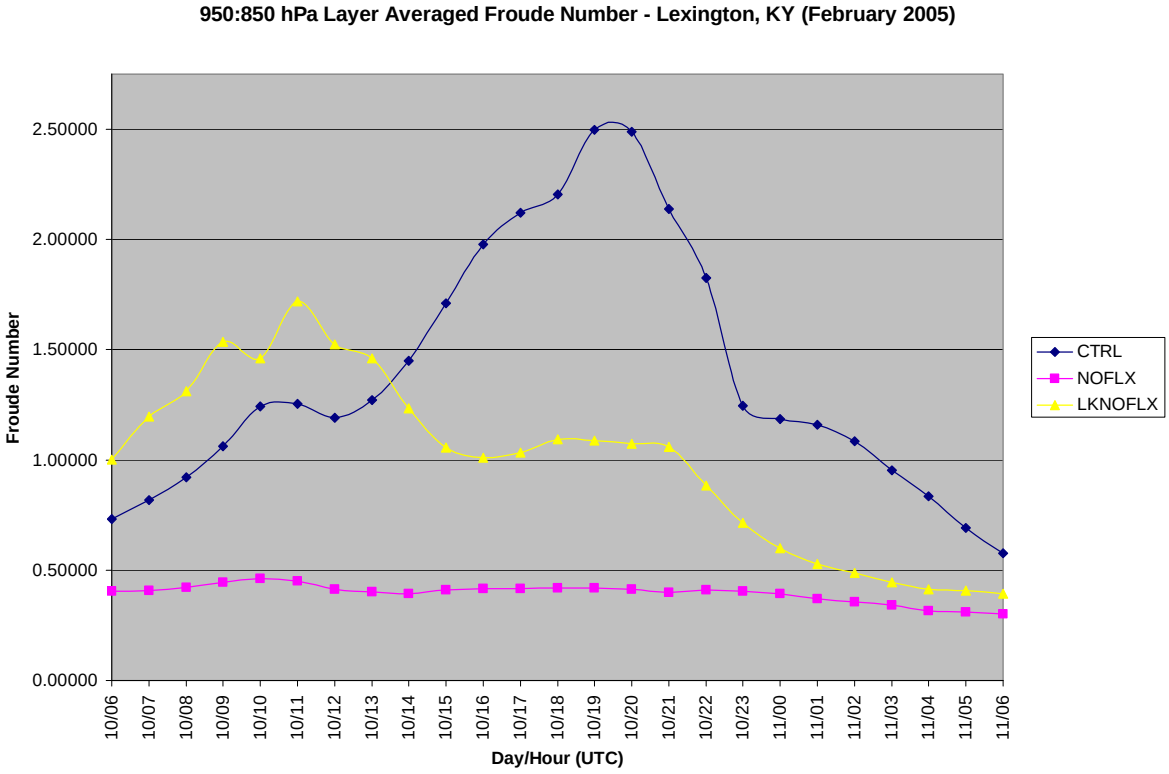

Figure 3.62. 950–850 hPa layer averaged Froude number for Lexington, KY (38.03°N;-84.44°W) from 0600 UTC 10 February to 0600 UTC 11 February for CTRL (blue), NOFLX (pink), and LKNOFLX (yellow).

4. Case 2: 18–20 December 2003

4.1. Event analysis

The second NWFS event analyzed occurred 18–20 December 2003 and does not clearly fall into one of the event categories previously discussed in section 1.3.3. Instead, this event featured a prolonged period of westerly to northwesterly flow in the lower levels of the atmosphere, including the passage of an upper level shortwave trough and associated surface low pressure system. This case serves as an example of a high impact, early-winter NWFS event. In this section, Case 2 is discussed from a synoptic and observational point of view with numerical simulations of the event discussed in section 4.2.

4.1.1. Synoptic overview

At 0000 UTC on the 18th, there was northwesterly flow aloft at 500 hPa across the southern Appalachians, a sharp trough axis centered just east of the region, and a shortwave trough located over the Northern Plains (Fig. 4.1). By 1200 UTC on the 18th, this shortwave trough tracked southeastward across the Mississippi Valley (Fig. 4.2) and into the broad base of the larger longwave trough at 0000 UTC on the 19th (Fig. 4.3), leaving the southern Appalachians under westerly flow aloft. The upper trough shifted slowly eastward over the next 12 hours, turning the flow over the region slightly more northwesterly by 1200 UTC on the 19th (Fig. 4.4). Slow progression of the upper trough continued through 0000 UTC on the 20th (Fig. 4.5), with upper level northwesterly winds noted over the southern Appalachians at 1200 UTC on the 20th as the event was ending (Fig. 4.6).

The lower levels of the atmosphere exhibit more northwesterly flow than the upper levels for the duration of the event. Beginning at 0000 UTC on the 18th at 700 hPa, ~50 kt northwesterly flow is seen from the southern Appalachians, back upstream across the northern plains (Fig. 4.7). However, flow turns more westerly by 1200 UTC on the 18th as the trough digs southeastward (Fig. 4.8). Northwesterly flow returns 24 hours later (Fig. 4.9) and continues through the end of the event at 1200 UTC on the 20th (Fig. 4.10). The 850-hPa level shows similar features to those seen at the 700-hPa level as the winds are westerly for a period of time between 1200 UTC on the 18th (Fig. 4.11), and 0000 UTC on the 19th (Fig. 4.12). Strong northwesterly flow, in excess of 30 kts, continues at 850 hPa through 1200 UTC on the 19th (Fig. 4.13), till the end of the event at 1200 UTC on the 20th (Fig. 4.14). Temperatures at the 850-hPa level remain below freezing for the entire NWFS period; beginning between -4 and -8°C at 1200 UTC on the 18th (Fig. 4.11), continuing through 0000 UTC on the 19th between -4 and -6°C (Fig. 4.12), then cooling back to around -8 °C at 0000 UTC on the 20th (Fig. 4.15).

At the surface at 0000 UTC 18 December 2003, the event begins with a weak low pressure system located northwest of the southern Appalachians over the northern plains (Fig. 4.16), associated with the upper-level shortwave seen at the 500-hPa level at the same time (Fig. 4.1). By 1200 UTC on the 18th, the surface low moved southeastward with the 500-hPa shortwave trough (Fig. 4.2), and crossed the upper Mississippi river valley (Fig. 4.17). The low continues moving toward the southern Appalachians, centering just west of the area at 0000 UTC on the 19th with westerly to northwesterly surface winds seen across the region and back upstream (Fig. 4.18). After the low pressure system moves out of the southern Appalachians by 1200 UTC on the 19th (Fig. 4.19), northwesterly flow continues

over the region, diminishing with the eastward progression of high pressure by 1800 UTC on the 20th (Fig. 4.20).

4.1.2. Observational overview

The 18–20 December 2003 NWFS event began around 1200 UTC on the 18th (Fig. 4.21), and continued through around 0300 UTC on the 19th (Fig. 4.22). A relative lull in precipitation then took place until resuming during the following afternoon, around 1500 UTC on the 19th across the southern Appalachians (Fig. 4.23). Precipitation continued through 2100 UTC on the 19th (Fig. 4.24), before tapering off around 0300 UTC on the 20th (Fig. 4.25).

Overall, the event resulted in large snowfall totals across the southern Appalachians. This includes a large area of over a foot of total accumulations along the North Carolina/Tennessee border (Fig. 2.1). The maximum total for the event was 30 inches, recorded on Mt. Mitchell in Yancey County, North Carolina and as much as 25 inches occurred in the Banner Elk area in Avery County, North Carolina. Despite being such a high impact event when compared to more typical NWFS cases such as the 10–11 February 2005 event, the 18–20 December 2003 event shows a similar spatial structure with accumulations creating a tight gradient of snowfall along the eastern boundary of the higher terrain. Also, the snowfall accumulations are focused generally on the higher terrain along the North Carolina/Tennessee border.

Although surface winds throughout the event were westerly to northwesterly across much of the southern Appalachians, the event never exhibited a good trajectory of low-level winds that would lead the low-level airmass to be modified by the Great Lakes. Unlike the

February 2005 case presented in section 3, this event never showed low-level winds that were almost due northerly across the Great Lakes region. Therefore the low-level trajectory of air flow was not conducive to air being modified by the Great Lakes and being advected downstream toward the southern Appalachians. Beginning at 1800 UTC on the 18th, surface winds are northwesterly upstream from the southern Appalachian region, as well as across the Great Lakes (Fig. 4.26). This situation continues through 0600 UTC on the 19th where northwesterly flow is shown by surface observations across the Upper Midwest (Fig. 4.27). Even after the lull in precipitation, surface winds on the afternoon of the 19th continue to show a low-level trajectory of air that comes from regions located west of the Great Lakes (Fig. 28). Overall, the event never shows a trajectory of surface winds that would support the low-level transport of air coming from the Great Lakes.

4.2. Numerical simulations

In this section, the 4 model runs completed are discussed for the 18–20 December 2003 NWFS event. These model runs are setup as discussed in section 2.3.2.

4.2.1. Control run (CTRL)

Beginning at 0000 UTC on the 18th, CTRL shows the axis of a sharp upper trough just to the east of the southern Appalachians with a closed contour 1010-hPa low center located northeast of the area over western Minnesota (Fig. 4.29a). This low, associated with a 500-hPa shortwave trough, moved southeastward in conjunction with the shortwave over the next 12 hours, to a position over southern Indiana (Fig. 4.29b). The movement of the low is a bit more difficult to follow as it encounters the higher terrain of the Appalachians around

0000 UTC on the 19th (Fig. 4.29c), but clearly appears again off the East Coast by around 0900 UTC on the 19th (Fig. 4.29d). For the rest of the event, the southern Appalachians would remain under the influence of relatively deep west-northwesterly to northwesterly oriented flow as seen at 1500 UTC on the 19th (Fig. 4.30a) and 0000 UTC on the 20th (Fig. 4.30b), with surface ridging and high pressure building across locations upstream of the area by around 0900 UTC on the 20th (Fig. 4.30c).

At the 850-hPa level, northwesterly flow begins across the region at around 0000 UTC on the 18th with 850-hPa temperatures ranging between -8 and -12°C (Fig. 4.31a). Flow turns slightly more westerly with the approach of the surface low pressure system and 500-hPa shortwave trough by around 1500 UTC on the 18th (Fig. 4.31b), but returns to northwesterly at 0600 UTC on the 19th (Fig. 4.31c). This pattern of northwesterly flow and cooling 850-hPa temperatures continued through the remainder of the event as 850 hPa temperatures cooled to around -14°C at 0000 UTC on the 20th (Fig. 4.31d). Still, much like the surface observations noted in section 4.1.2, the flow at 850 hPa never exhibits an optimal trajectory to allow the Great Lakes to influence the incoming low-level airmass. Upstream of the southern Appalachians, 850 hPa winds remain primarily northwesterly instead of being nearly northerly as in the February 2005 event.

Precipitation during the event spanning from 0000 UTC on the 18th and ending around 2100 UTC on the 20th results in a large area of greater than 0.50 inches of liquid equivalent, mainly along the North Carolina/Tennessee border, with lesser, though still significant amounts elsewhere across the southern Appalachians (Fig. 4.32). On a larger view, the swath of precipitation extending back to the northwest is quite apparent follows the track of the shortwave trough and attending surface low pressure system (Fig. 4.33). This

swath of precipitation also follows the area of northwest flow noted in the wind field upstream to across the Upper Midwest. Overall, the CTRL does a reasonable job of capturing the high-impact nature of the event though there are some fundamental differences from the snowfall accumulations seen from the event. The band of highest totals from CTRL along the North Carolina/Tennessee border appears to be too far to the west over eastern Tennessee (Fig. 2.1). Also, even applying a rather high snow to liquid ratio of 20:1 would only yield an event maximum snowfall total of ~16 inches. Though this pales in comparison to the observed maximum snowfall total of 30 inches, it does match up well with the large area of more than a foot of snowfall seen across the far western North Carolina counties (Fig. 2.1).

Like the 10–11 February 2005 NWFS case presented in Ch. 3, θ_e profiles were plotted to assess the presence and relative importance of potential instability in the 18–20 December 2003 event. The profiles were also taken along a plane between La Crosse, IN and Albemarle, NC which is denoted by the red line in Figure 3.31. Again, potential instability occurs when $\partial\theta_e/\partial z<0$ and can be seen in vertical cross sections of θ_e. Starting at 0000 UTC on the 18th, potential instability is fairly shallow and only exists along and near the southern Appalachians (Fig. 4.34a). This decreases slightly across the southern Appalachians by 1200 UTC on the 18th (Fig. 4.34b), before increasing over the same area through 0600 UTC on the 19th (Fig. 4.34c). This slight increase in potential instability continues through 2100 UTC on the 19th (Fig. 4.35a) but only over locations about half-way upstream between the lakes and the southern Appalachians. Then, by 0600 UTC on the 20th (Fig. 4.35b), the end of the event, potential instability dwindles across the entire cross section area. For this case, the

overall magnitude of potential instability is less than that seen in the 10–11 February 2005 event (Fig. 3.35).

4.2.2. Experimental run 1 (MYJPBL)

MYJPBL was run with the same setup as the CTRL except for using the MYJ PBL scheme instead of the YSU. Overall, MYJPBL produced a similar precipitation structure to that of CTRL, with large differences in liquid equivalent totals. From 0000 UTC on the 18th to 2100 UTC on the 20th, liquid equivalent totals are in excess of 0.50 inches along the North Carolina/Tennessee border (Fig. 4.36). The differences between MYJPBL and the CTRL are quite clear as MYJPBL has significantly less precipitation across the southern Appalachians (Fig. 4.37). However, there mixed results as seemingly all other locations outside of the southern Appalachians region experience precipitation increases. This effect is even more noticeable on a large scale view as most areas, especially those across the southeastern portion of the country, see an increase in precipitation (Fig. 4.38).

Along the southern Appalachians, similar differences between MYJPBL and the CTRL appear in profiles of θ_e. At Erwin, TN, which is located along the central portion of the North Carolina/Tennessee border, neither model run shows much in the way of potential instability at 0000 UTC on the 18th (Fig. 4.39a). Both runs continue to indicate a relatively stable boundary layer through 1800 UTC on the 18th (Fig. 4.39b), with potential instability increasing in both model runs by 0300 UTC on the 19th (Fig. 4.39c). The CTRL continues to portray a deeper and more unstable boundary layer by this time. Such differences between the model runs continue through 1800 UTC on the 19th (Fig. 4.40a). Though both model runs stabilize greatly from 0300 UTC on the 19th, CTRL is still more unstable. Stabilization

continues greatly in these model runs through 200 UTC on the 20th as the event came to a close (Fig. 4.40b).

4.2.3. Experimental run 2 (NOFLX)

For the 18–20 December 2003 NWFS case, NOFLX produced much less clear-cut results than Case 1. Overall, the NOFLX experimental run for Case 2 still produced large amounts of NWFS precipitation across the southern Appalachians. A large area of over 0.50 inches of liquid equivalent is positioned along the North Carolina/Tennessee border (Fig. 4.41). Precipitation differences when compared to the CTRL show that a general decrease occurred from the southern Appalachians upstream across the Upper Midwest (Fig. 4.42). Again, the trajectory of the precipitation decreases also track back to locations well west of the Great Lakes region.

Overall, cross sections of θ_e do not show the greatly stabilized lower levels of the atmosphere expected between the Great Lakes and the southern Appalachians. Beginning at 0000 UTC on the 18th, through the isentropes do not exhibit as much folding as in CTRL (Fig. 4.34a) in the lower levels, they also are not as tightly packed in the lower levels, indicative of strong stability (Fig. 4.43a), and continues through 1200 UTC on the 19th (Fig. 4.43b). More specifically, profiles of θ_e taken along the southern Appalachians further highlight the small change in potential instability between the two simulations. At Erwin, TN at 0000 UTC on the 18th, though the NOFLX is more stable than CTRL, differences between the two model runs are minute (Fig. 4.44a). Although the differences are more noticeable at some later times, such as 0900 UTC on the 18th (Fig. 4.44b), they remain quite small through 1800 UTC on the 19th (Fig. 4.44c).

4.2.4. Experimental run 3 (LKNOFLX)

In LKNOFLX, where surface fluxes of heat and moisture were set to zero only over water in the model domain, a similar precipitation structure to CTRL emerges (Fig. 4.45). Overall, only relatively small changes in precipitation occur compared to the CTRL (Fig. 4.46). Across the southern Appalachians, as well as areas located upstream, a mix of increases and decreases in precipitation occur (Fig. 4.47). These differences further support the fact that this case did not have an optimal low-level flow for the Great Lakes to contribute to NWFS precipitation. Across the lakes, large decreases in precipitation occur as would be expected since surface fluxes were removed there. These decreases do extend downstream of the lakes, but only to the southeast along a trajectory that extends to northern portions of West Virginia (Fig. 4.47). This differs greatly from the results found in the February 2005 case where decreases in precipitation occurred from the Lakes downstream to locations across the southern Appalachians.

Profiles of θ_e for LKNOFLX show similar results to those of the NOFLX model run. At Erwin, TN, beginning with 0000 UTC on the 18th, LKNOFLX and CTRL are virtually identical with the LKNOFLX run only slightly cooler (Fig. 4.48a). These similarities continue to 1200 UTC on the 19th (Fig. 4.48b). Again, LKNOFLX and the CTRL continue to show very little difference in θ_e with height and potential instability through 0000 UTC on the 20th (Fig. 4.48c) as the NWFS event was coming to a close. The fact that these profiles are virtually identical when the effect of the lakes is removed again supports the lake of a lake influence in this case.

4.3. Summary

The 18–20 December 2003 NWFS event is an example of a high-impact, early winter event, which does not clearly fall into any of the three previously discussed event categories from section 1.3.3. Instead it is an event defined by nearly 72 hours of westerly to northwesterly flow over the southern Appalachians, including the passage of a surface low pressure system associated with a southeastward moving upper level shortwave trough. For the event, large snowfall totals occurred over the southern Appalachians including the mountains of North Carolina near the Tennessee border. A large area of >12 in. of snow fell across 10 counties in North Carolina with an event maximum of 30 in. reported at Mount Mitchell. The event was studied within the context of the scientific questions and hypotheses laid out in Ch. 1 using a series of 4 WRF model runs.

Overall, this event did not exhibit a low-level wind flow trajectory necessary for the lakes to effect the airmass that would impinge on the southern Appalachians. Unlike the February 2005 event, northwesterly flow extended well upstream of the southern Appalachians which led to a low-level air flow that tracked back to locations across the Upper Midwest. This was clearly seen on observed surface winds as well as in 850 hPa level winds in the CTRL. Also, a large view precipitation plot for the event showed a large swath of precipitation extending from the southern Appalachians back upstream to areas west of the Great Lakes. In the LKNOFLX run, precipitation differences were relatively small across the southern Appalachians and any significant decreases were confined to over the lakes and areas extending southeast of there, well northeast of the southern Appalachian region. Also, a comparison of θ_e profiles throughout the event along the southern Appalachians revealed

that the stability was essentially the same between the CTRL and LKNOFLX, supporting the absence of a lake influence.

Despite the fact that this case did not exhibit any influence by the Great Lakes, it serves well as a comparison case since no significant changes were noted when the lakes were removed in LKNOFLX. This case also stresses the fact that a Great Lake influence is not a necessary characteristic of all NWFS events. Instead, this case shows that even a high-impact NWFS event can occur without the presence of lake-induced instability.

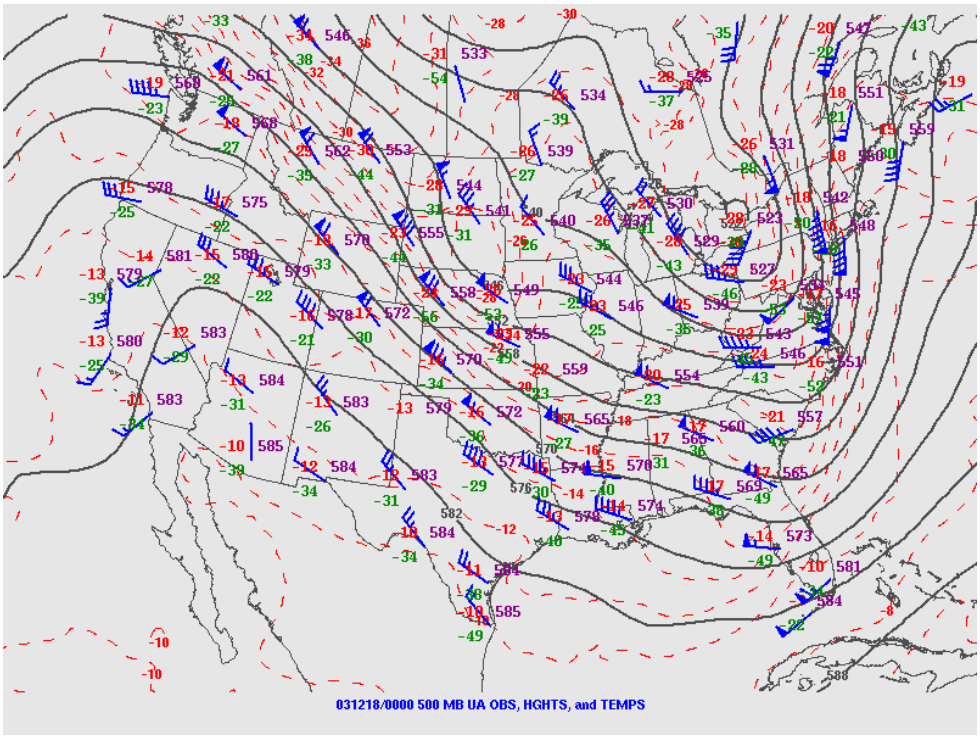

Figure 4.1. Plot of 500 hPa upper air observations, heights (solid black contours), and temperatures (dashed red contours) from 0000 UTC 18 December 2003. Image from http://www.spc.noaa.gov/obswx/maps/.

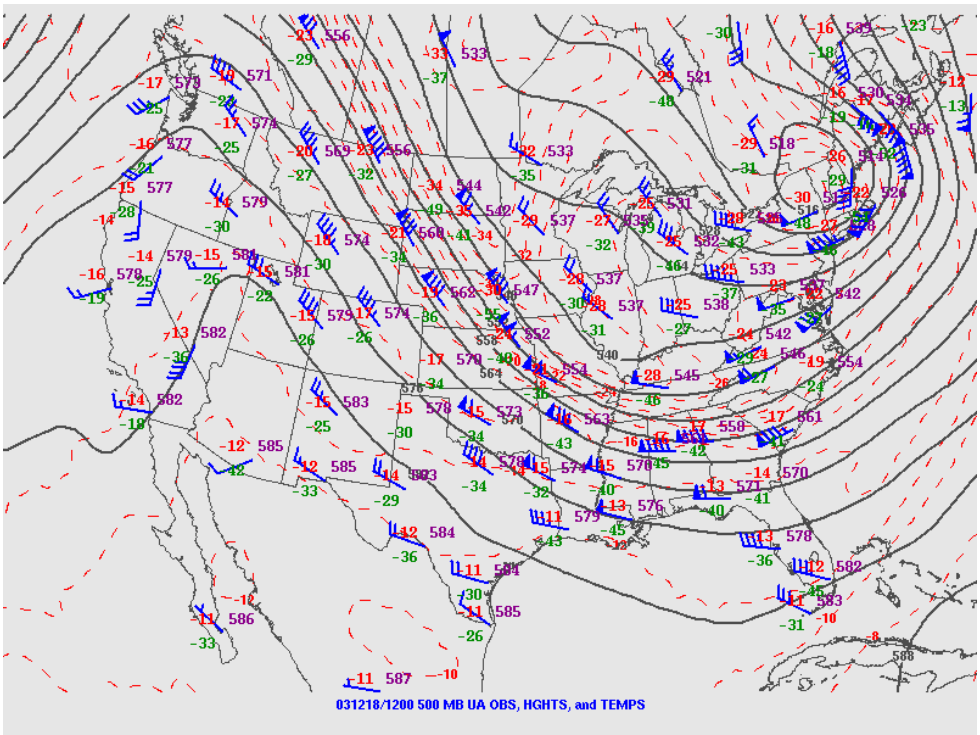

Figure 4.2. As in Figure 4.1 except for 1200 UTC 18 December 2003.

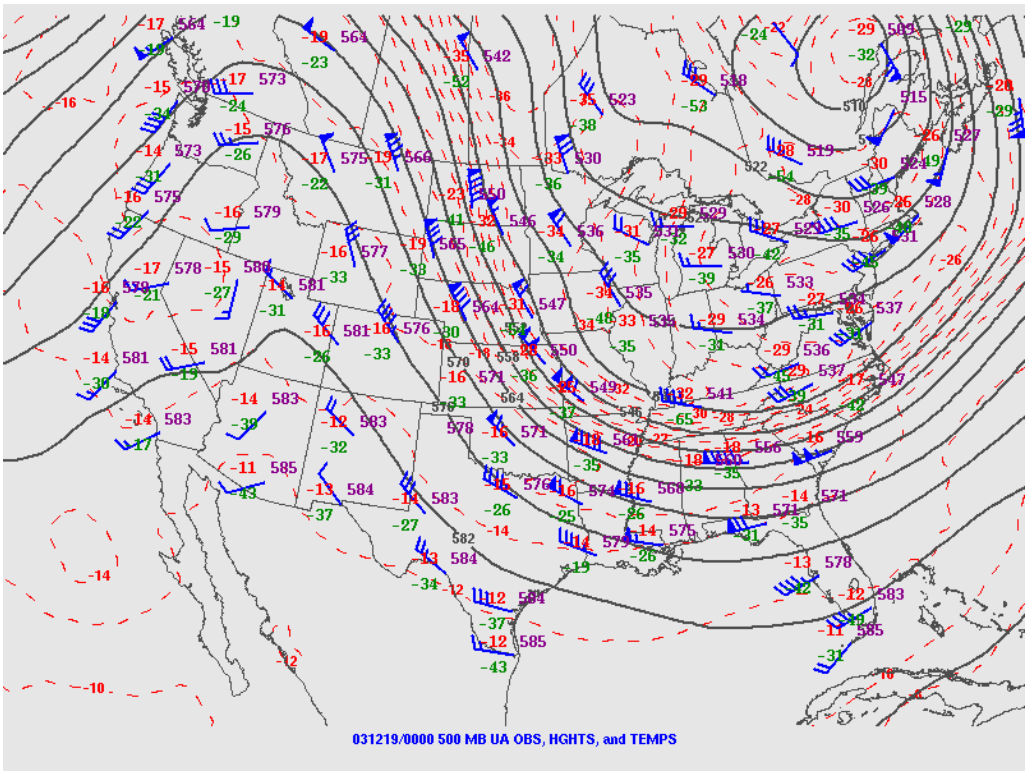

Figure 4.3. As in Figure 4.1 except for 0000 UTC 19 December 2003.

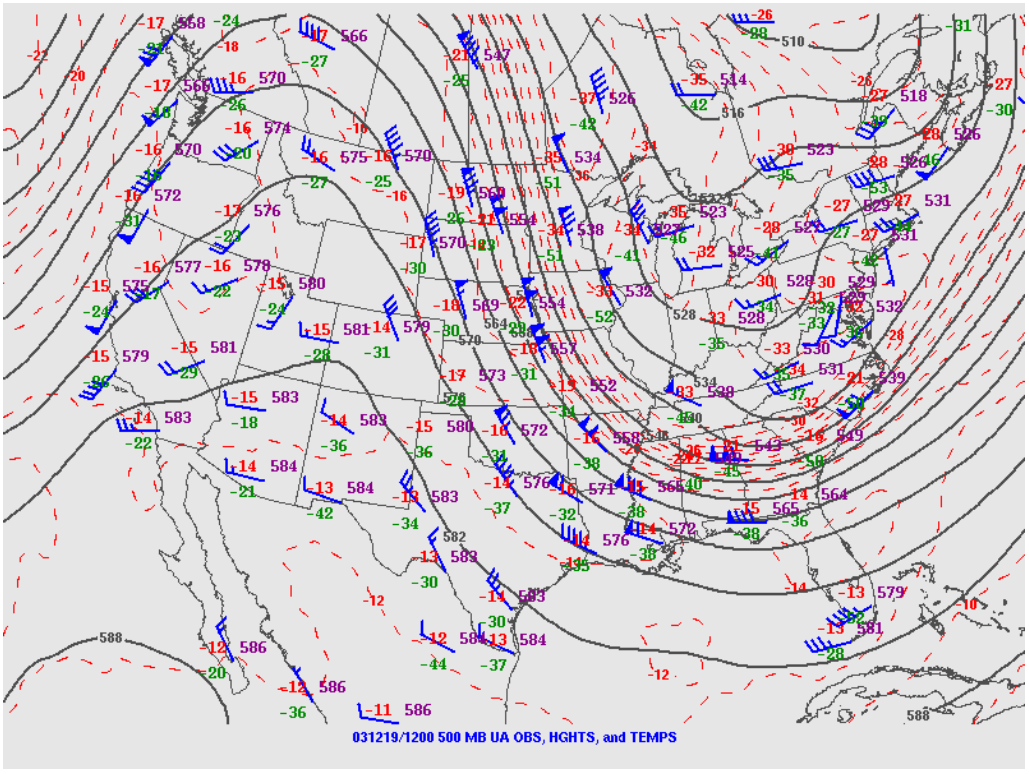

Figure 4.4. As in Figure 4.1 except for 1200 UTC 19 December 2003.

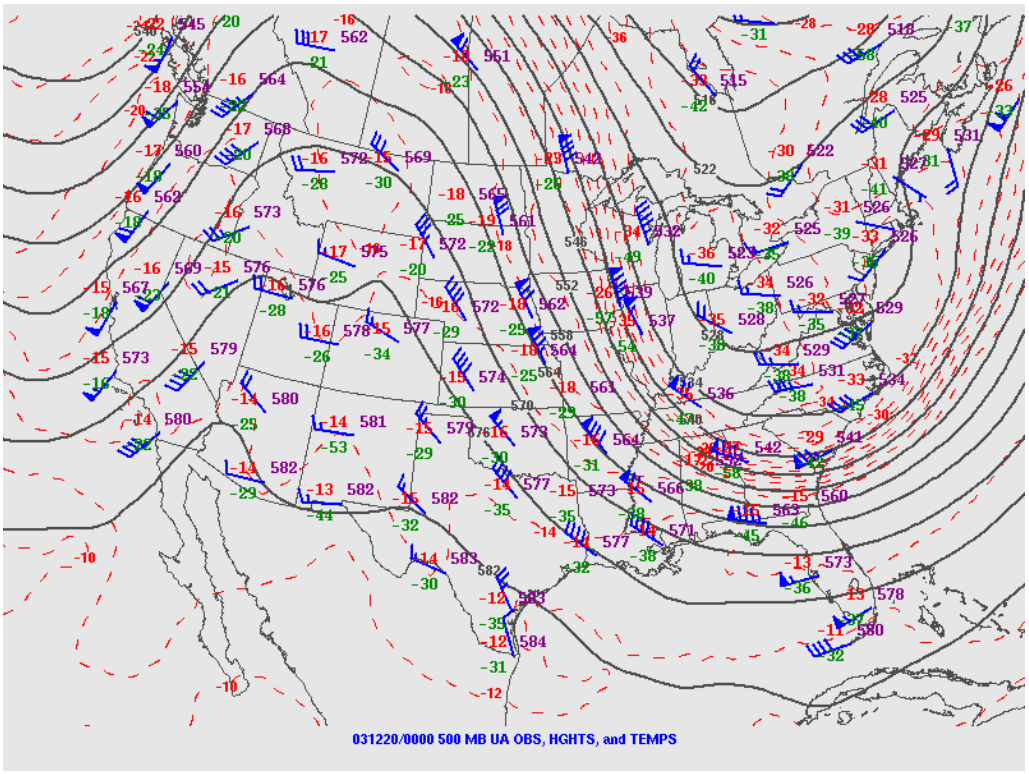

Figure 4.5. As in Figure 4.1 except for 0000 UTC 20 December 2003.

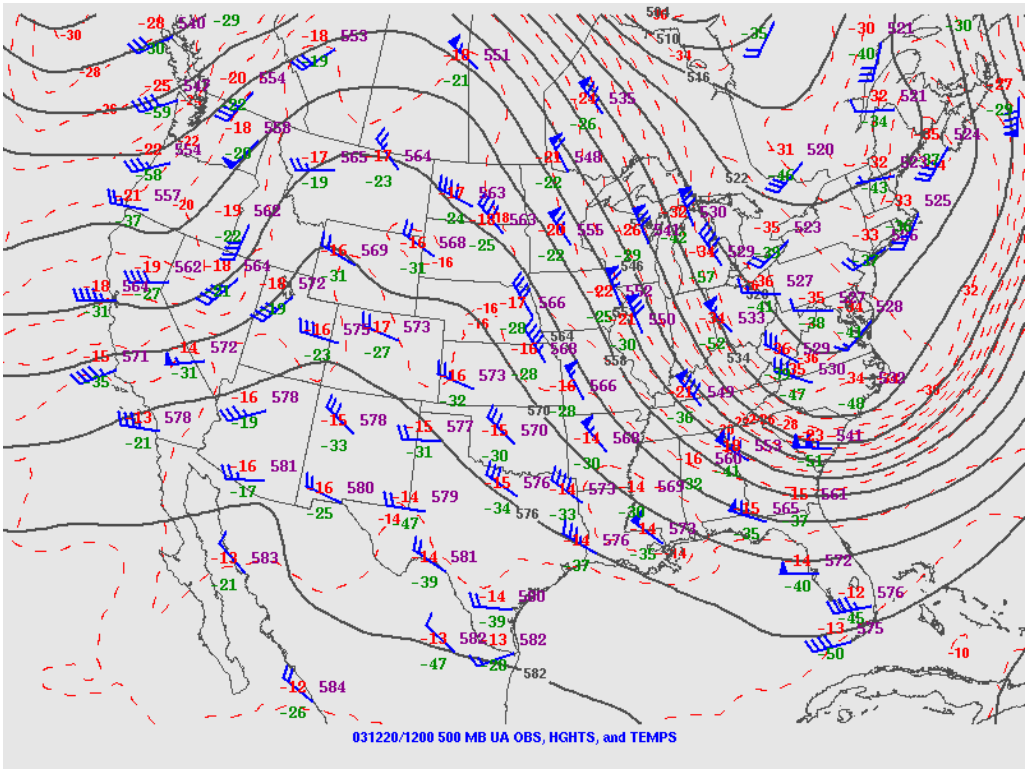

Figure 4.6. As in Figure 4.1 except for 1200 UTC 20 December 2003.

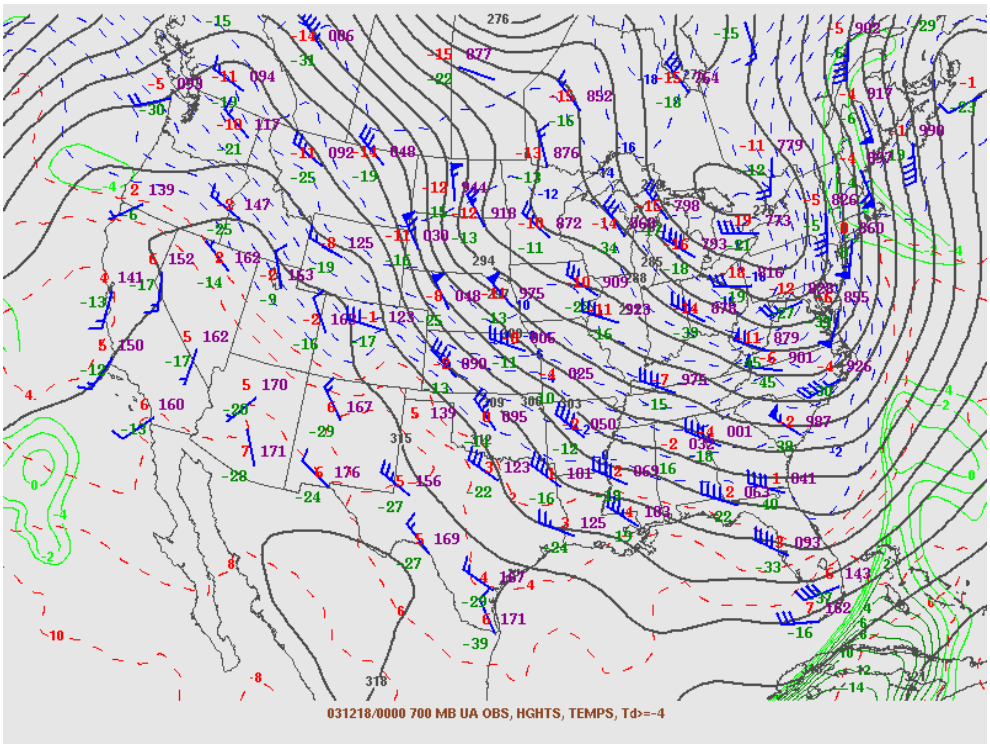

Figure 4.7. Plot of 700 hPa observations, heights (solid dark contours), temperatures (dashed contours), and dew point (solid green contours) from 0000 UTC 18 December 2003.

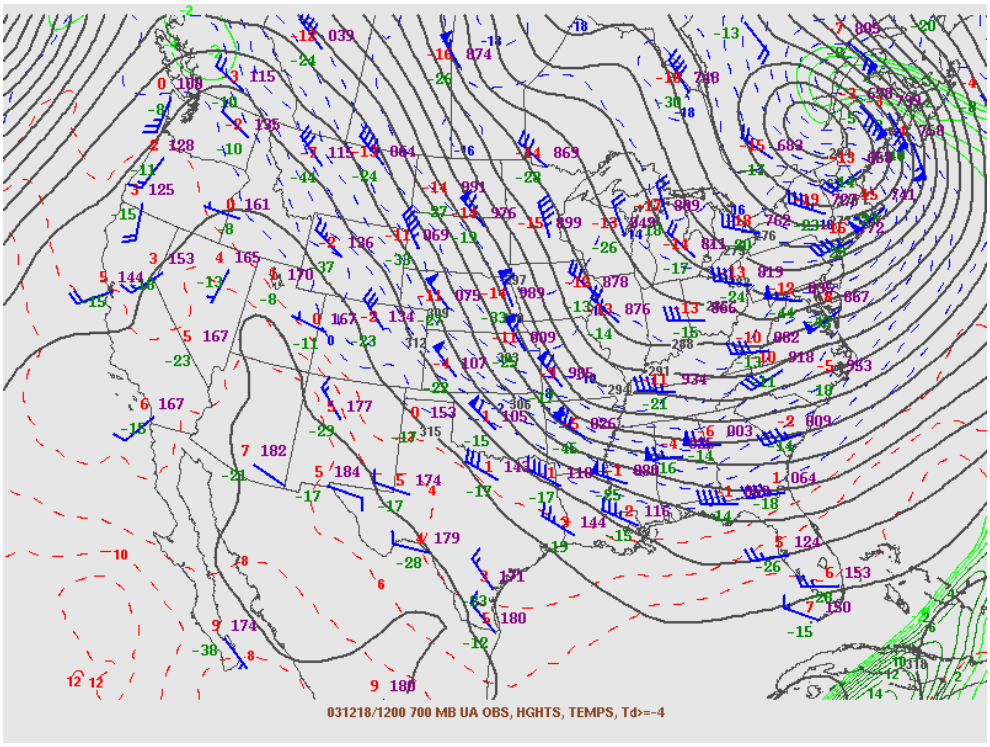

Figure 4.8. As in Figure 4.7 except for 1200 UTC 18 December 2003.

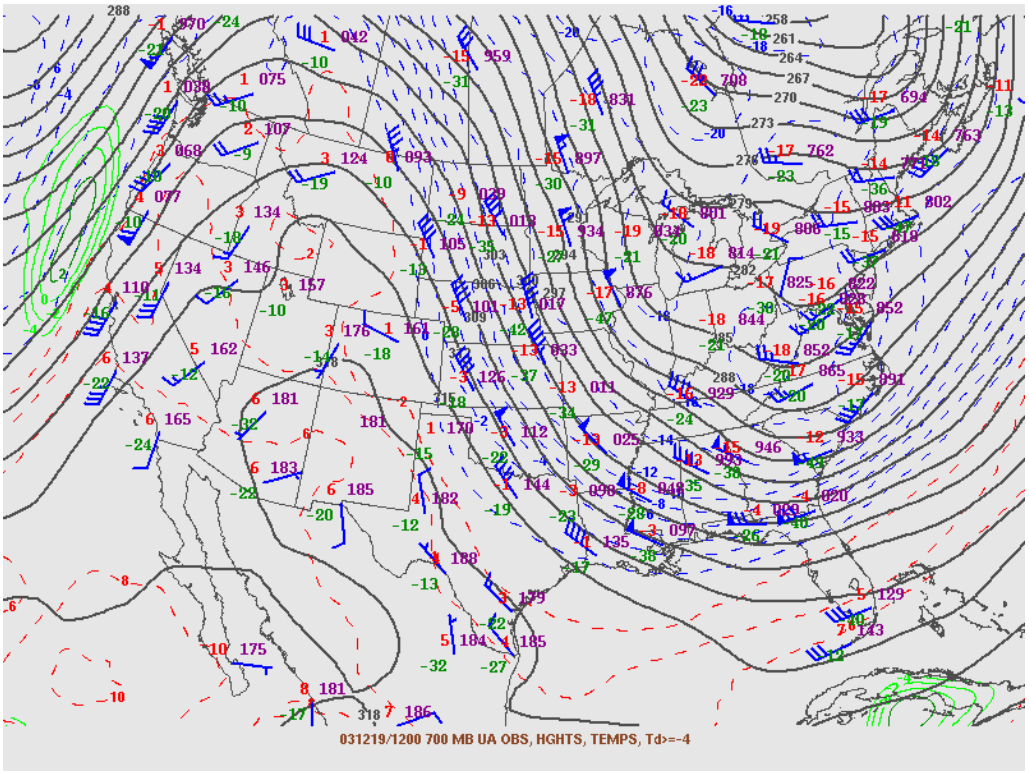

Figure 4.9. As in Figure 4.7 except for 1200 UTC 19 December 2003.

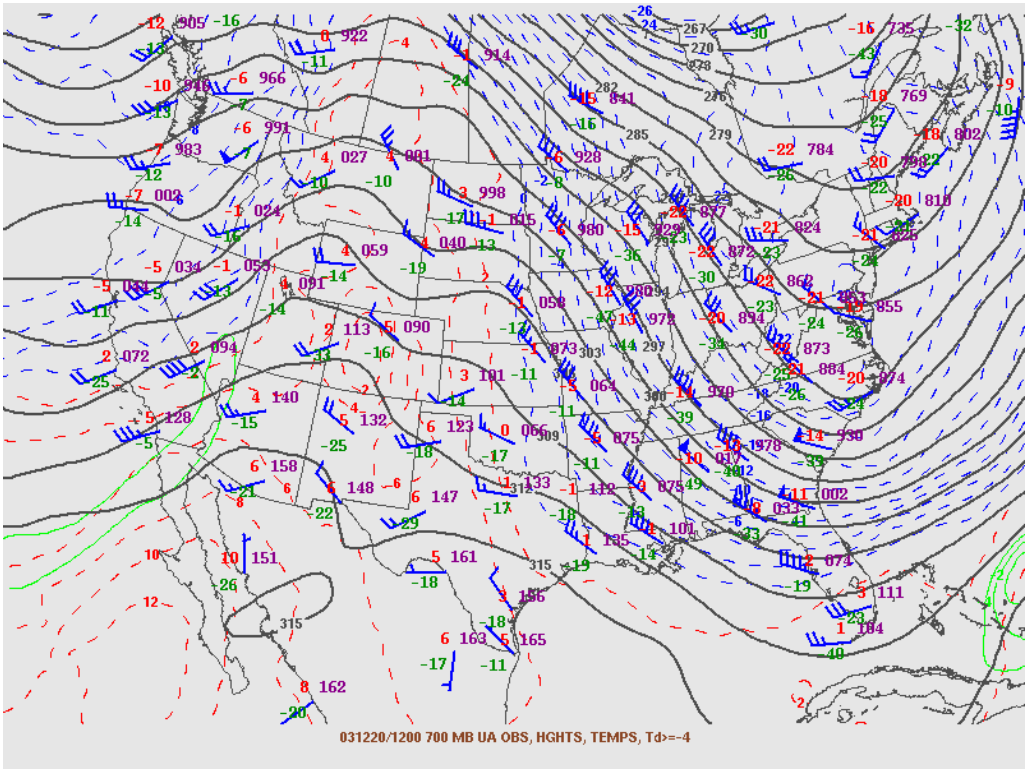

Figure 4.10. As in Figure 4.7 except for 1200 UTC 20 December 2003.

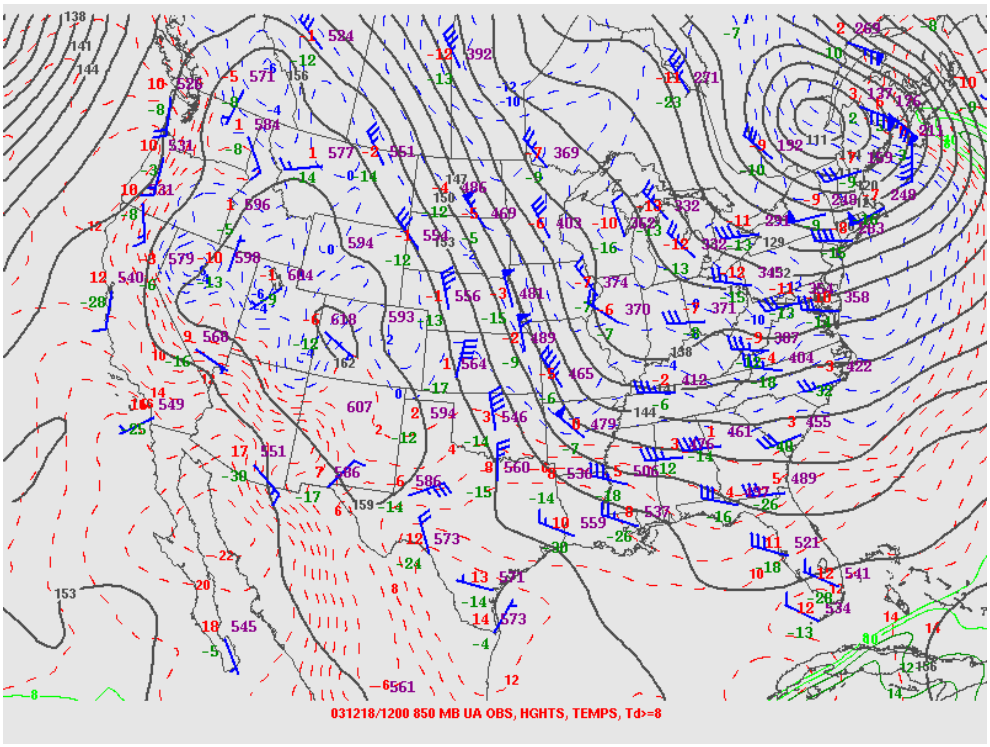

Figure 4.11. Plot of 850 hPa observations, heights (solid dark contours), temperatures (dashed contours), and dew point (solid green contours) from 1200 UTC 18 December 2003.

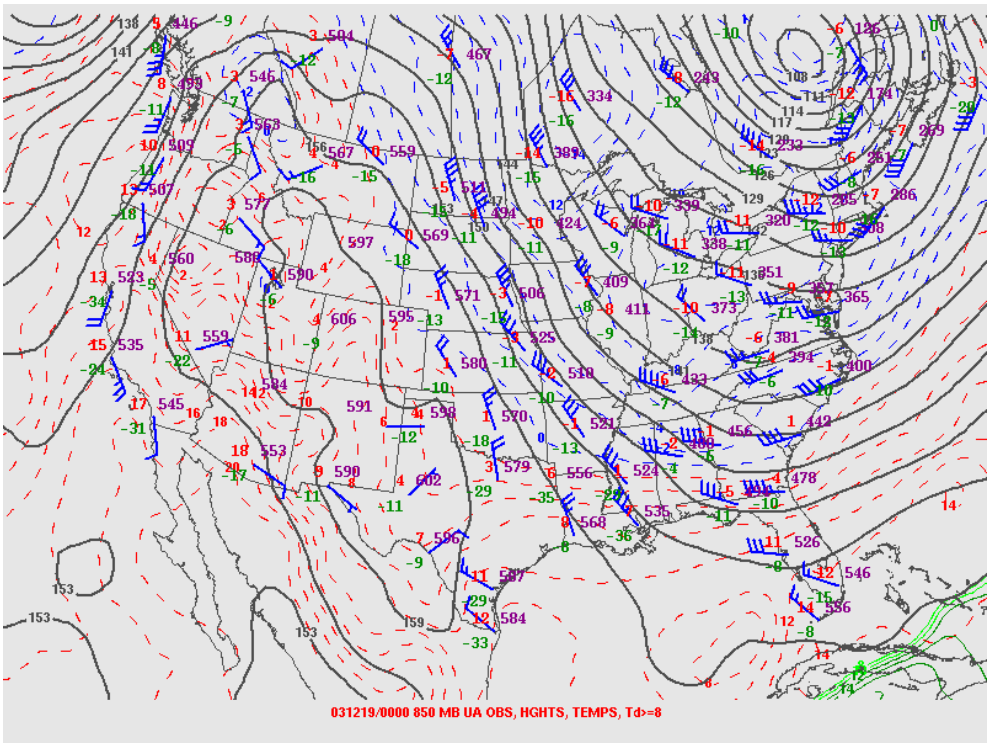

Figure 4.12. As in Figure 4.11 except for 0000 UTC 19 December 2003.

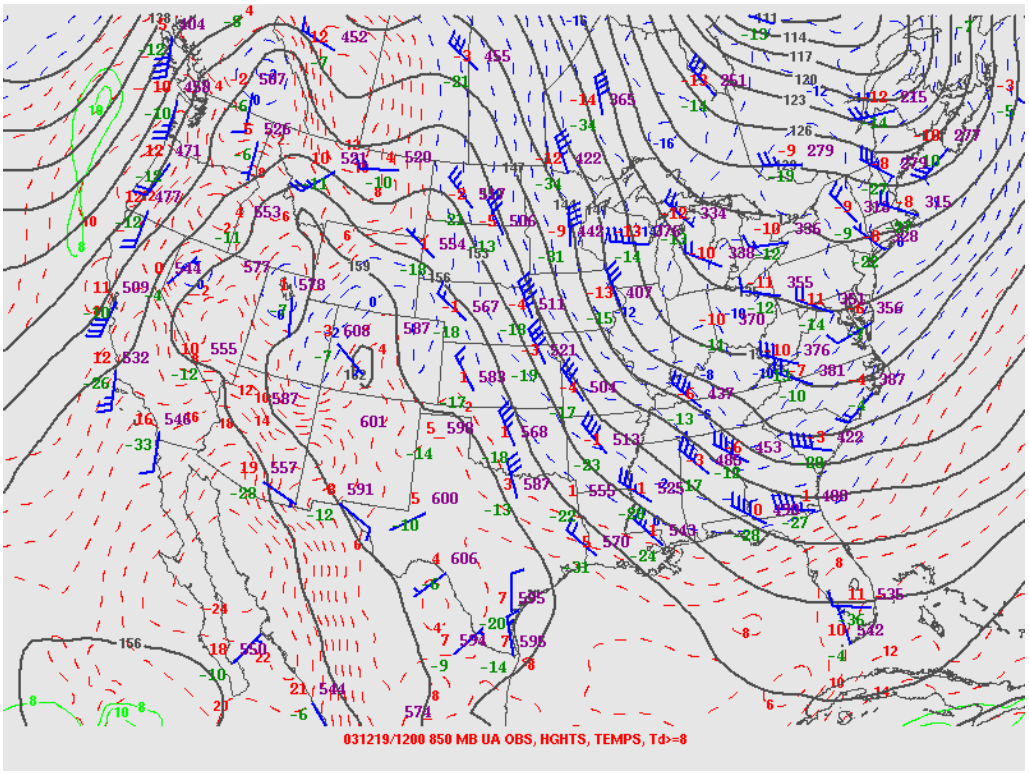

Figure 4.13. As in Figure 4.11 except for 1200 UTC 19 December 2003.

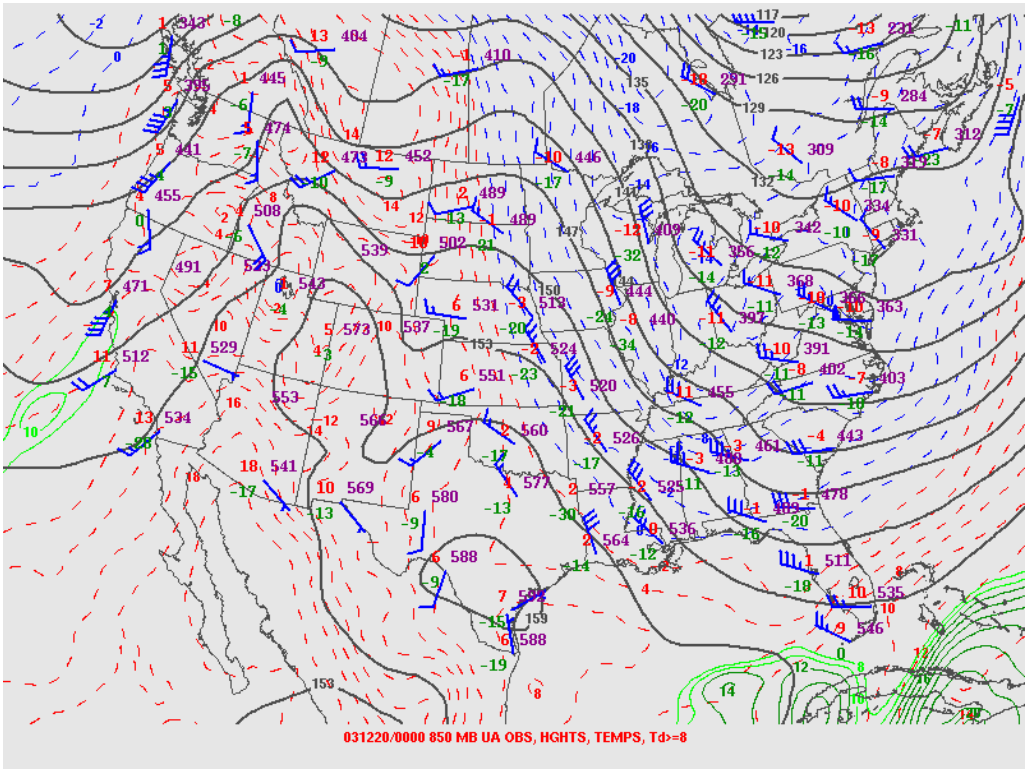

Figure 4.14. As in Figure 4.11 except for 0000 UTC 20 December 2003.

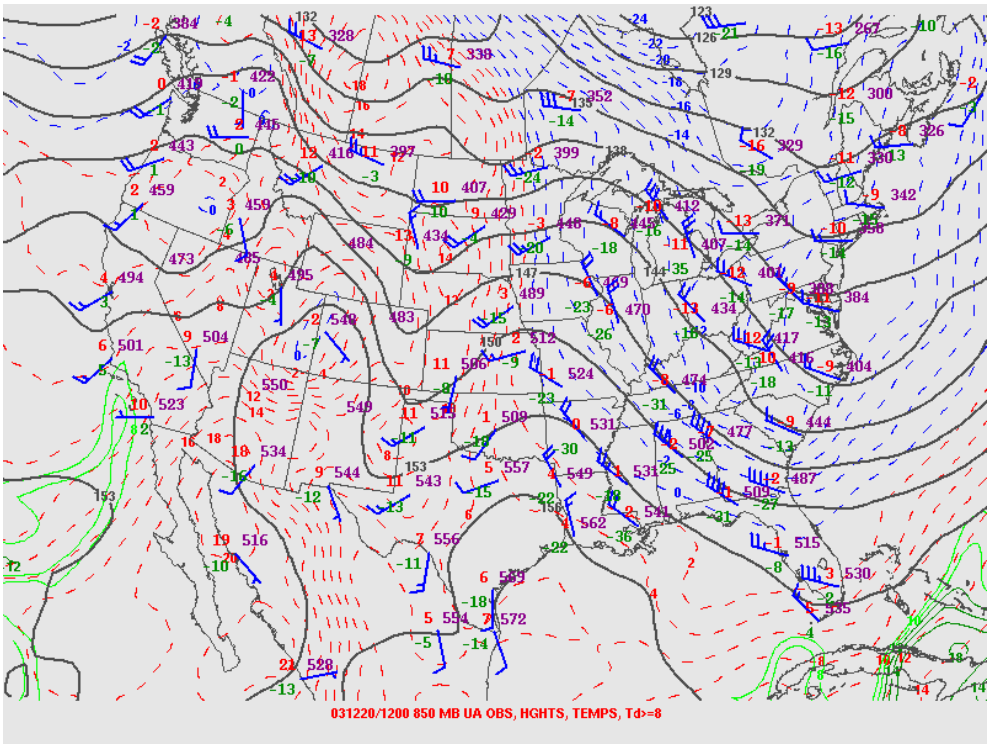

Figure 4.15. As in Figure 4.11 except for 1200 UTC 20 December 2003.

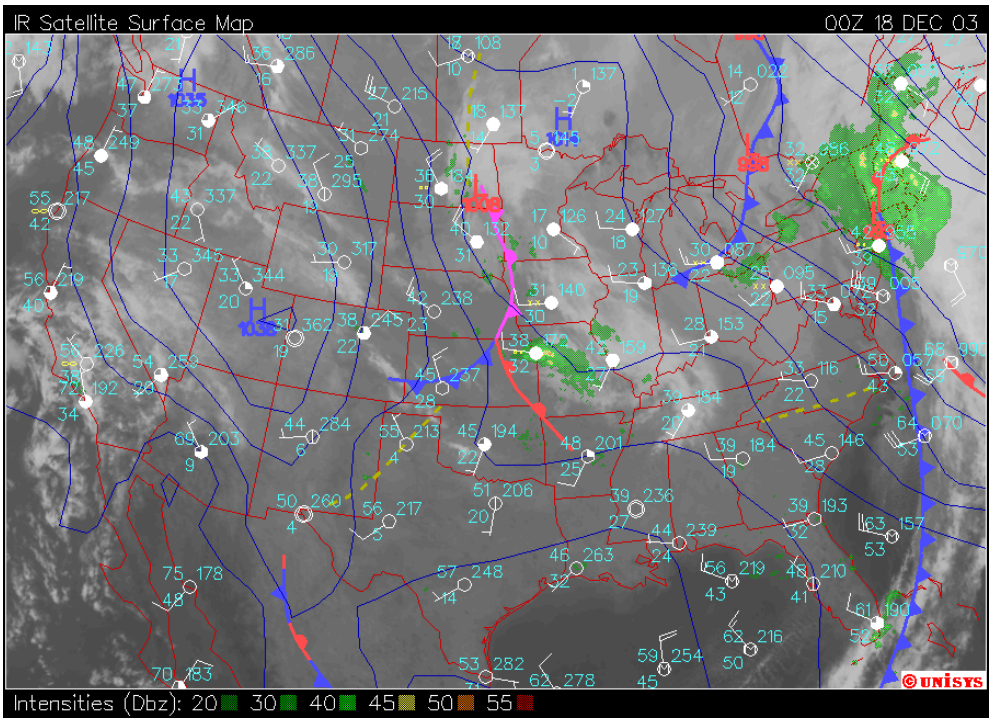

Figure 4.16. Plot of surface analysis, infrared (IR) satellite, surface observations, and composite radar reflectivity from 0000 UTC 18 December 2003. Image from http://weather.unisys.com/archive/sfc_map/.

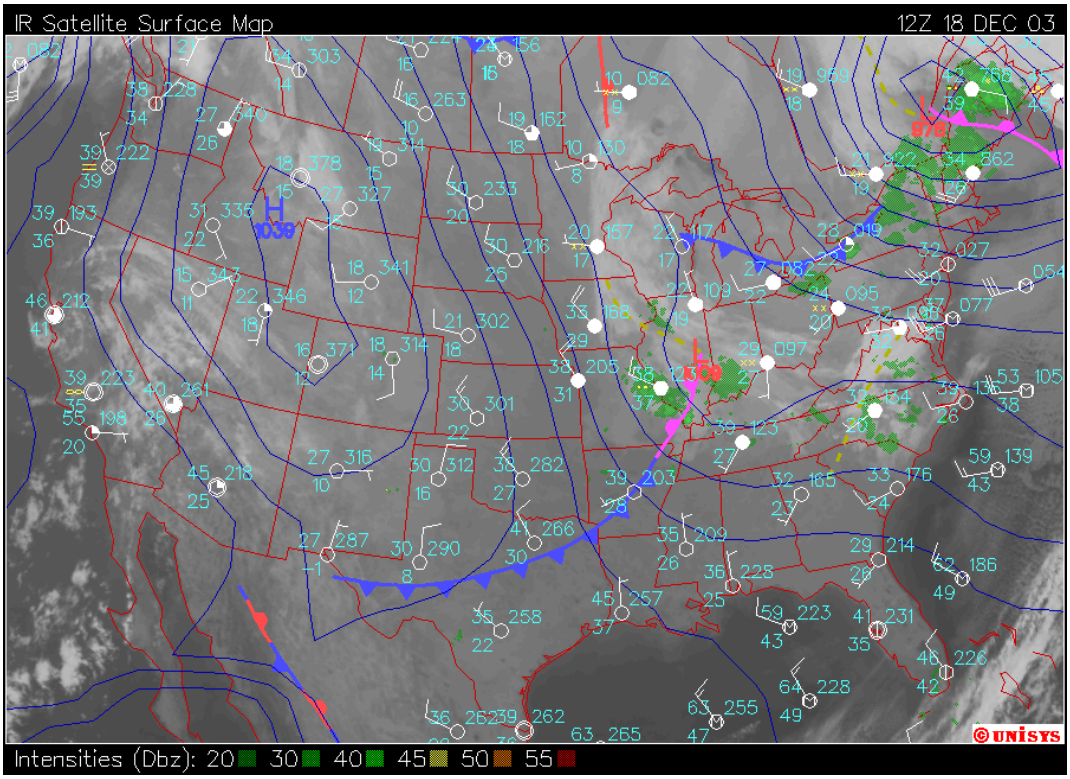

Figure 4.17. As in Figure 4.16 except for 1200 UTC 18 December 2003.

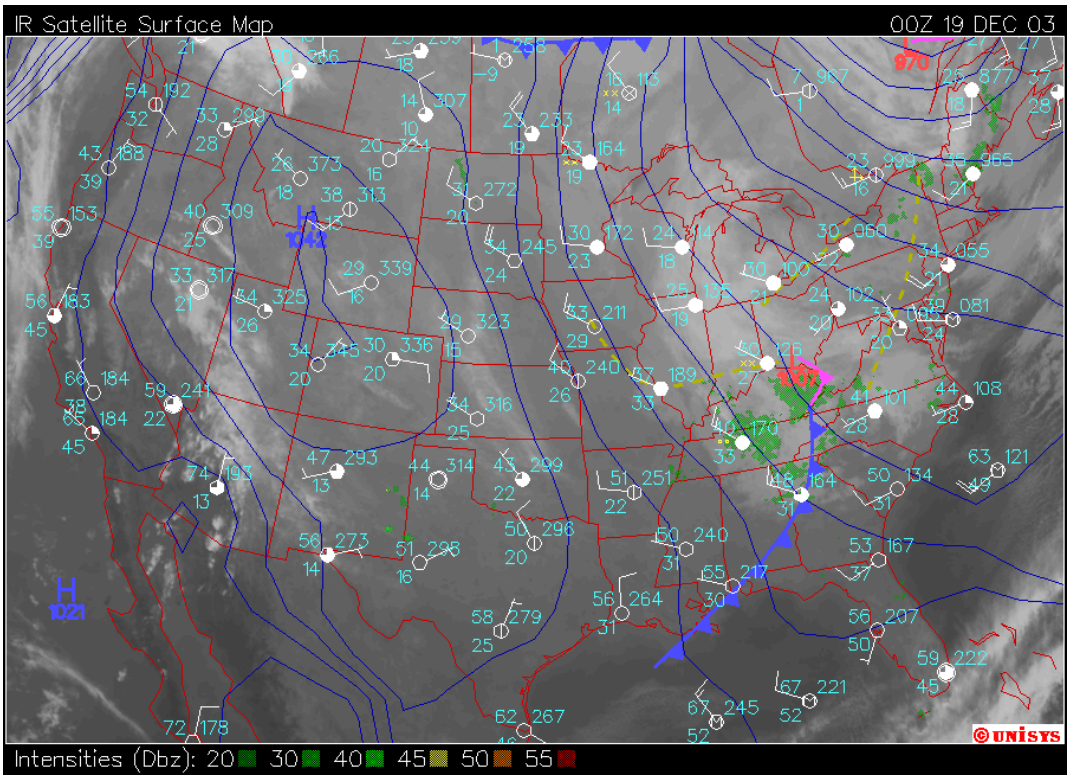

Figure 4.18. As in Figure 4.16 except for 0000 UTC 19 December 2003.

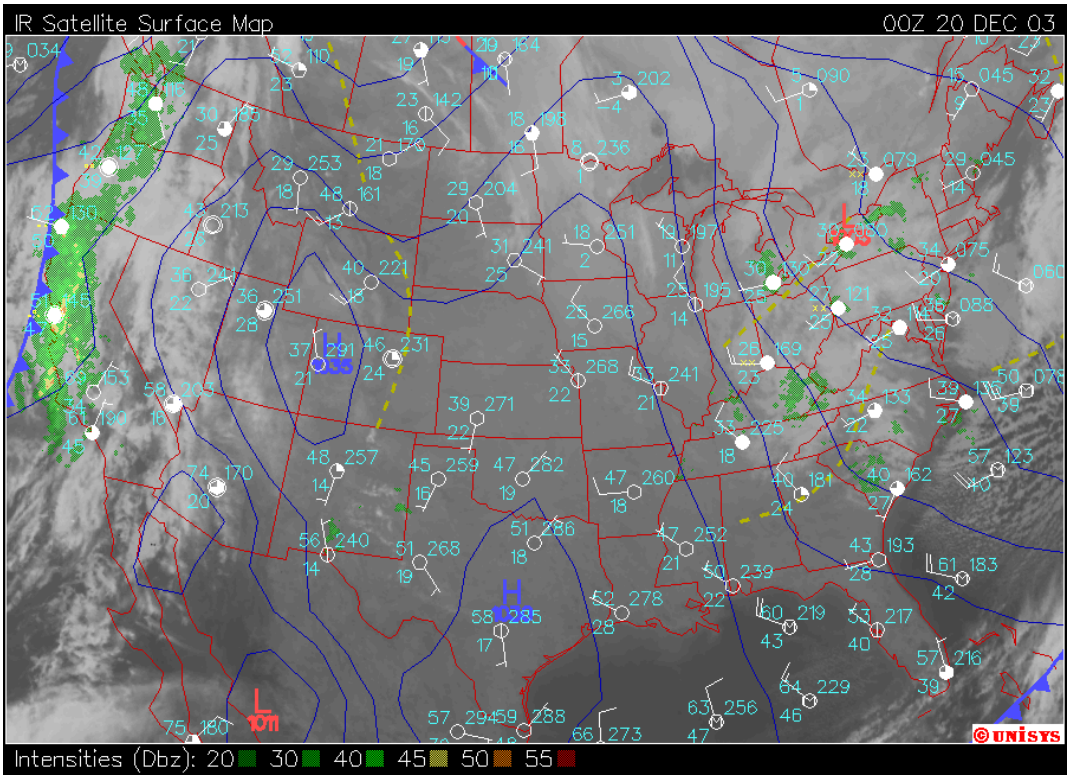

Figure 4.19. As in Figure 4.16 except for 0000 UTC 20 December 2003.

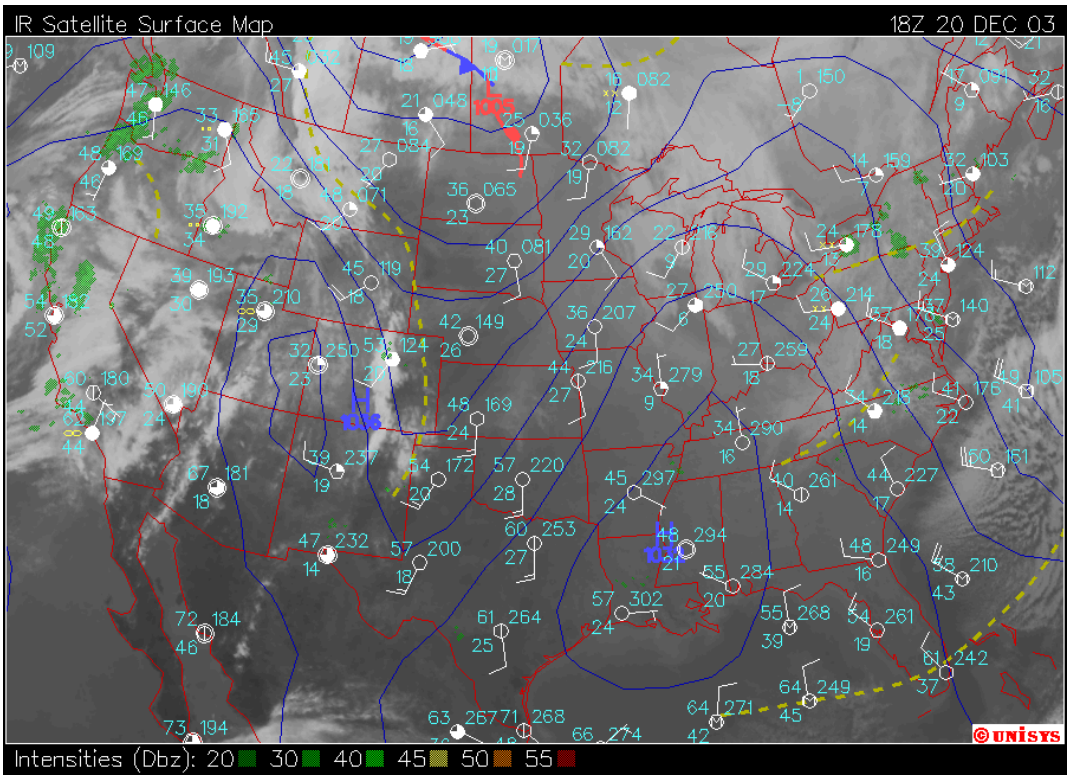

Figure 4.20. As in Figure 4.16 except for 1800 UTC 20 December 2003.

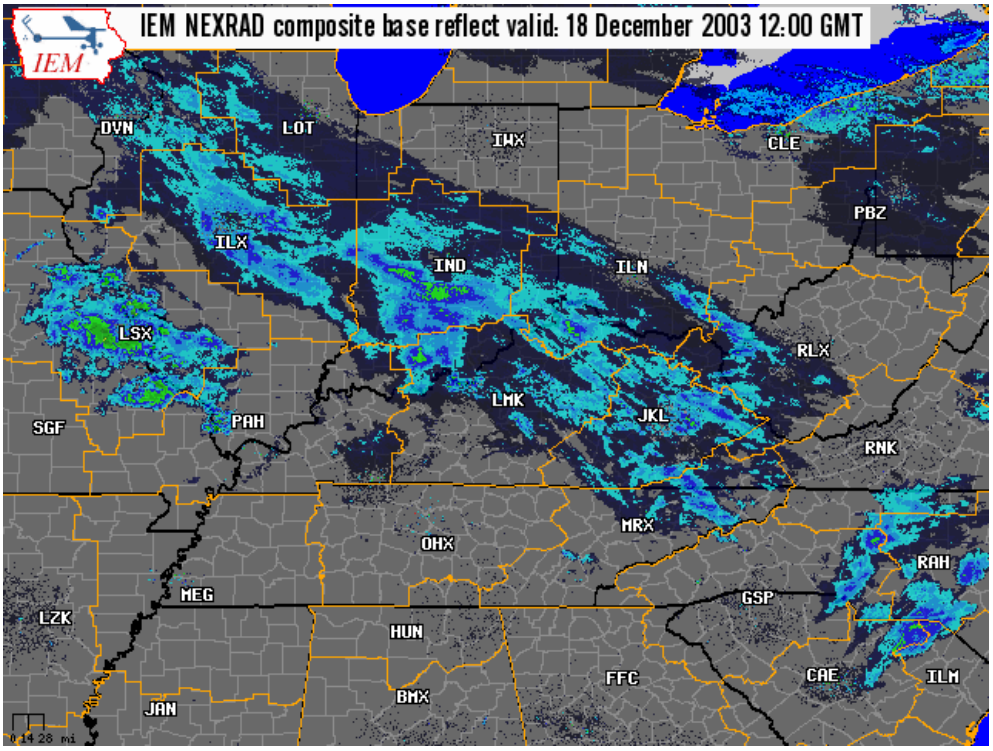

Figure 4.21. Composite radar reflectivity from 1200 UTC 18 December 2003. Image from http://mesonet.agron.iastate.edu/GIS/apps/rview/warnings.phtml.

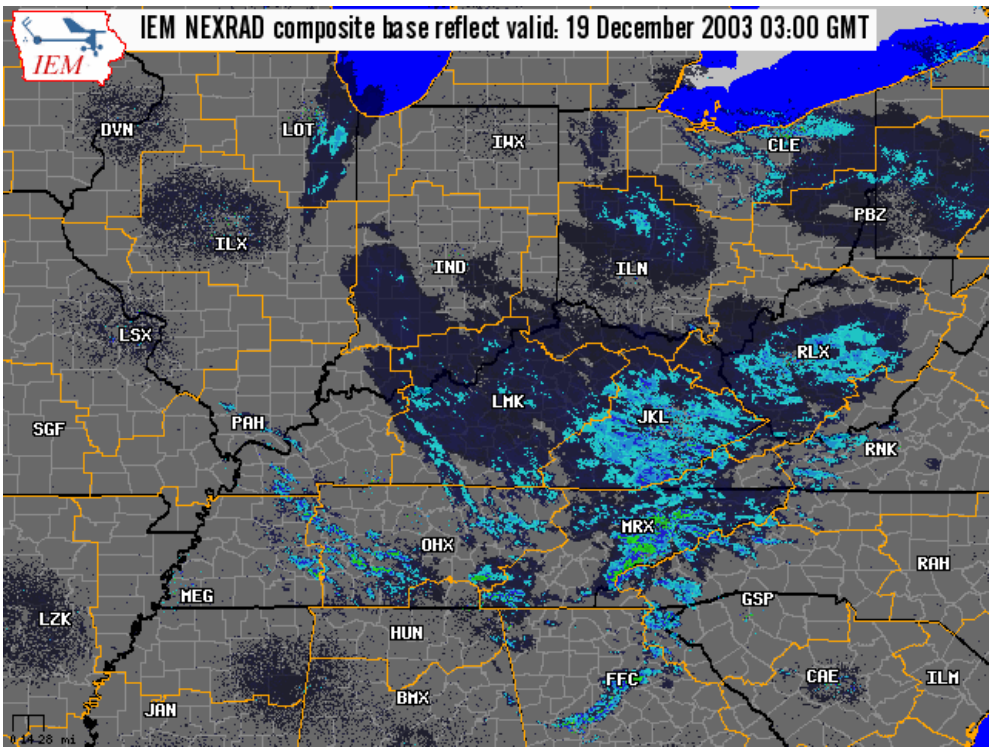

Figure 4.22. As in Figure 4.21 except for 0300 UTC 19 December 2003.

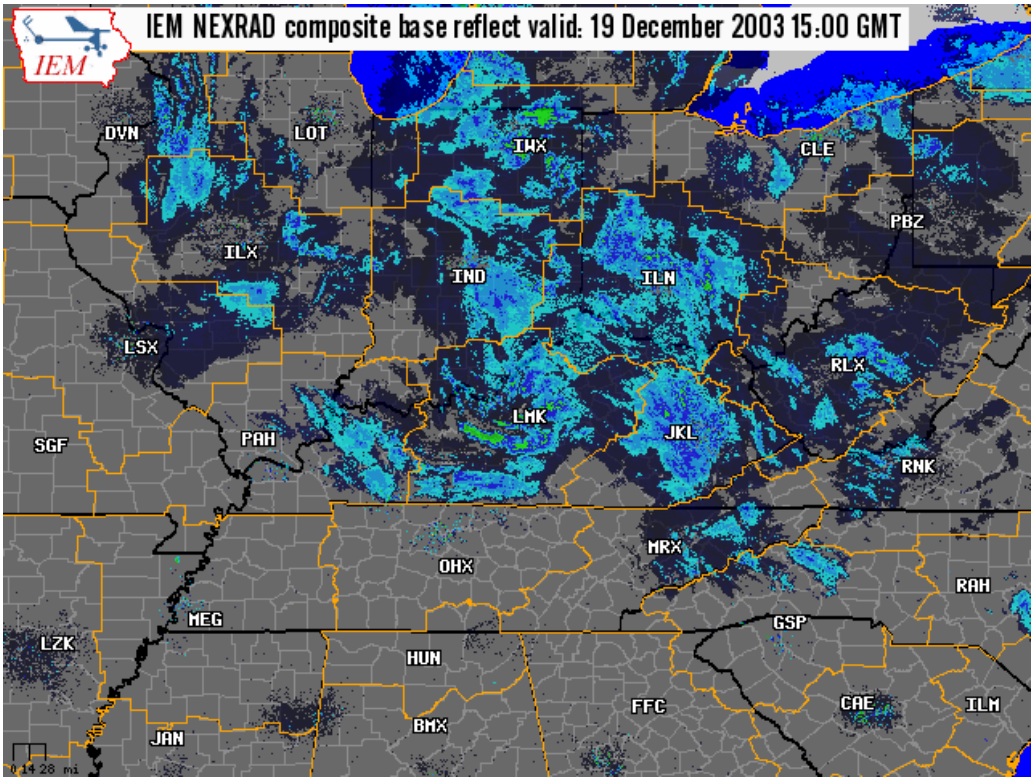

Figure 4.23. As in Figure 4.21 except for 1500 UTC 19 December 2003.

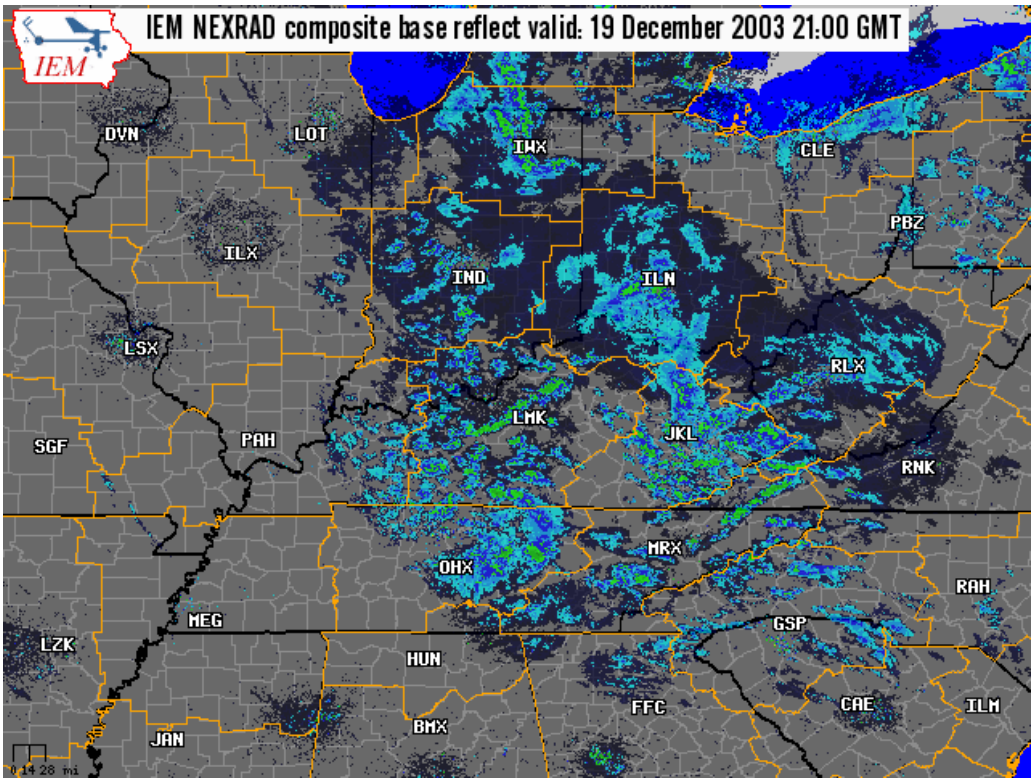

Figure 4.24. As in Figure 4.21 except for 2100 UTC 19 December 2003.

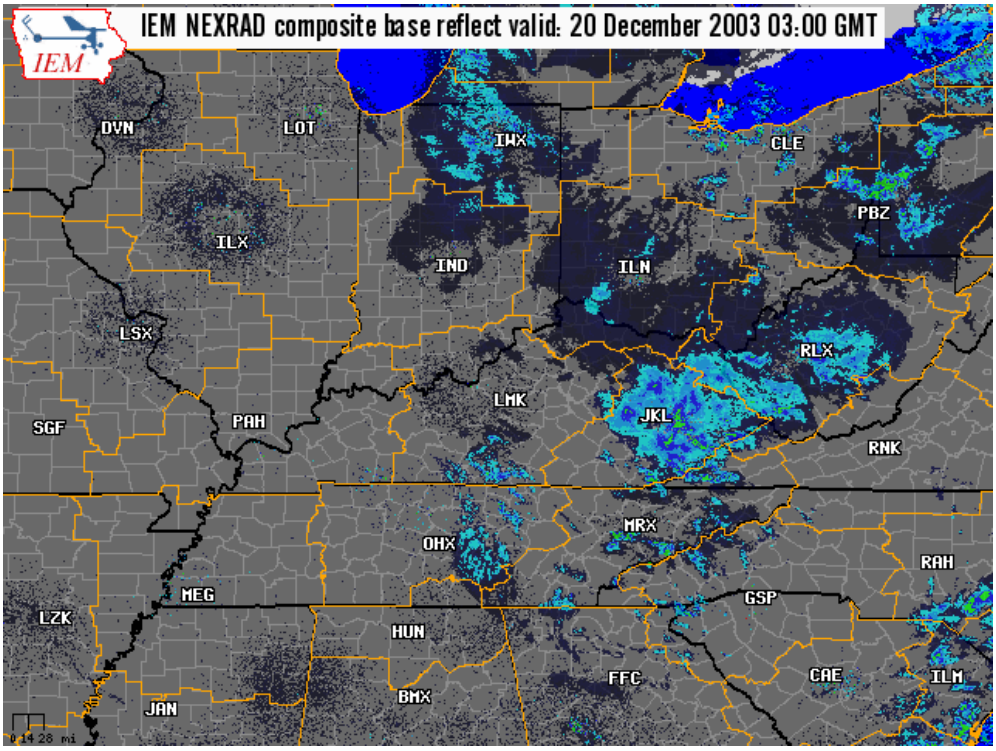

Figure 4.25. As in Figure 4.21 except for 0300 UTC 20 December 2003.

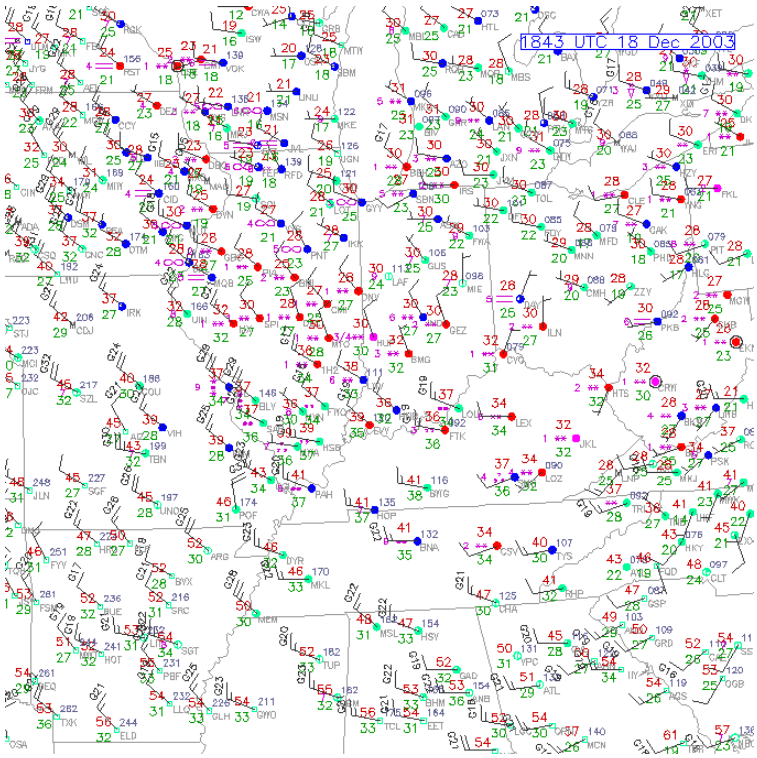

Figure 4.26. Surface observations from 1800 UTC 18 December 2003.

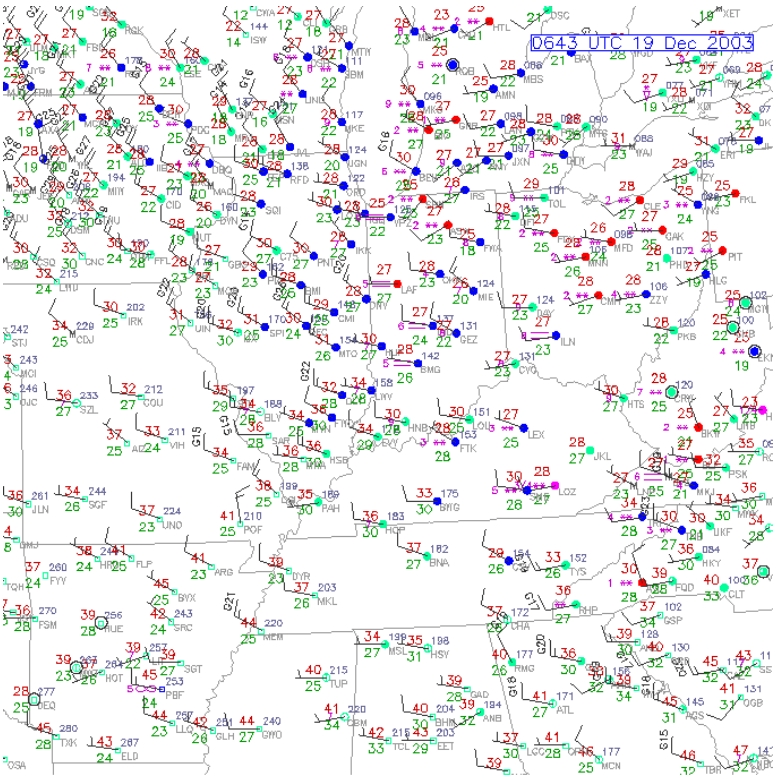

Figure 4.27. As in Figure 4.26 except for 0600 UTC 19 December 2003.

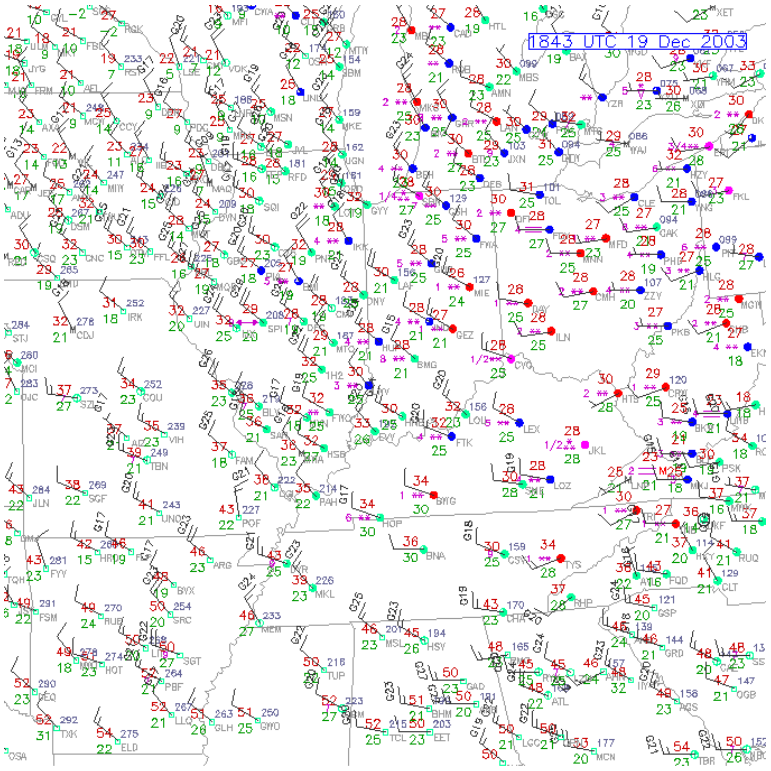

Figure 4.28. As in Figure 4.26 except for 1800 UTC 19 December 2003.

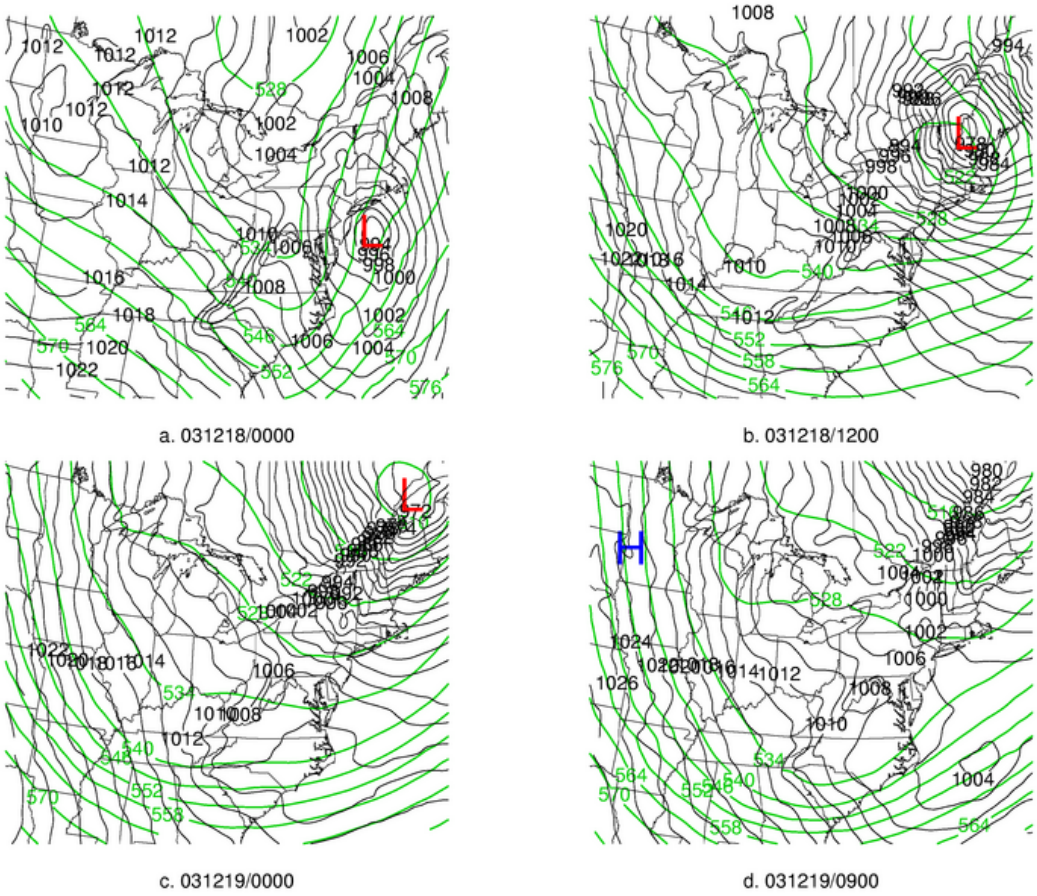

Figure 4.29. CTRL sea-level pressure (black solid contours, interval 2 hPa) and 500 hPa Geopotential height (green solid contours, interval 6 dam): (a) 0000 UTC 18 December 2003; (b) 1200 UTC 18 December 2003; (c) 0000 UTC 19 December 2003; (d) 0900 UTC 19 December 2003.

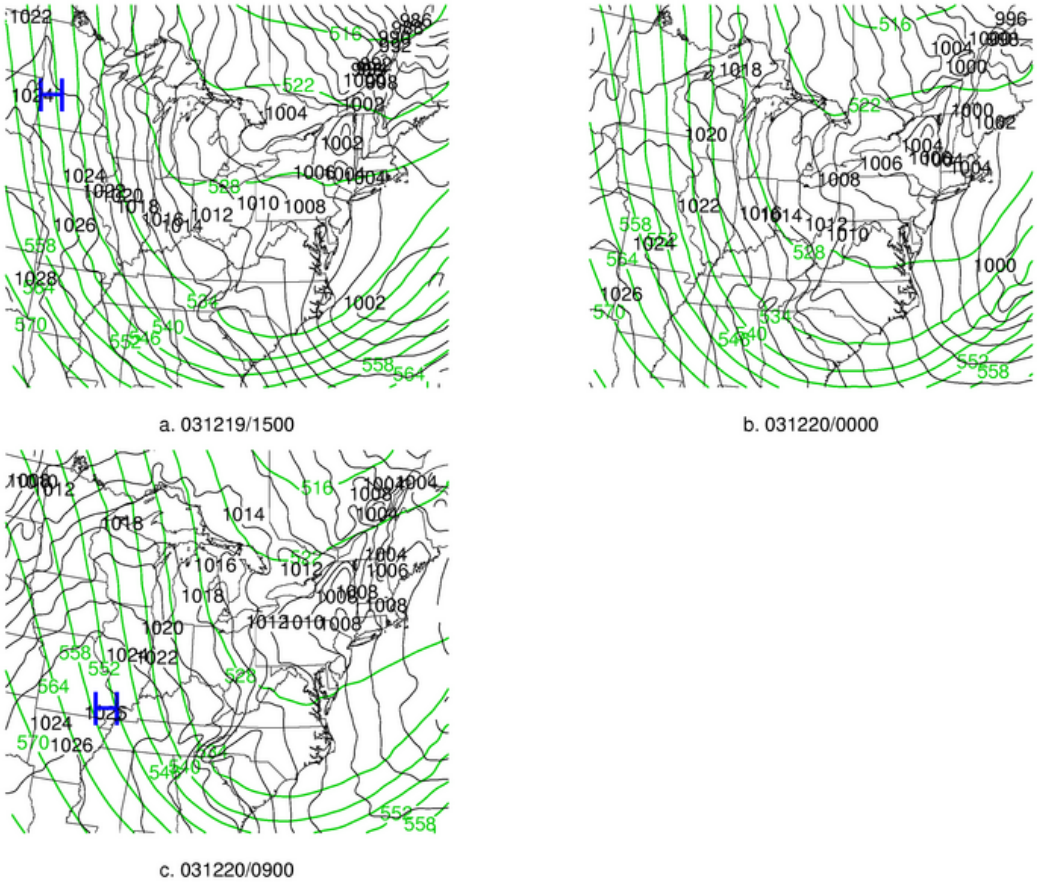

Figure 4.30. As in Figure 4.31 except for: (a) 1500 UTC 19 December 2003; (b) 0000 UTC 20 December 2003; (c) 0900 UTC 20 December 2003.

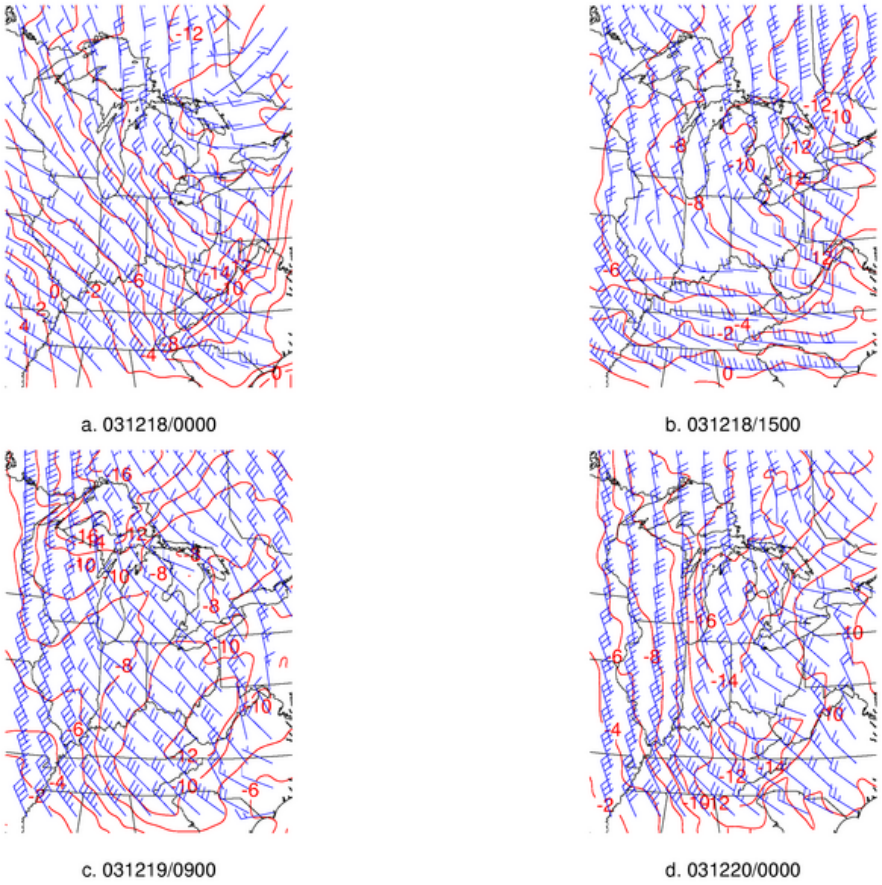

Figure. 4.31. CTRL 850 hPa temperature (°C, red solid, interval 2°C) and winds (kt, barbs): (a) 0000 UTC 18 December 2003; (b) 1500 UTC 18 December 2003; (c) 0900 UTC 19 December 2003; (d) 0000 UTC 20 December 2003.

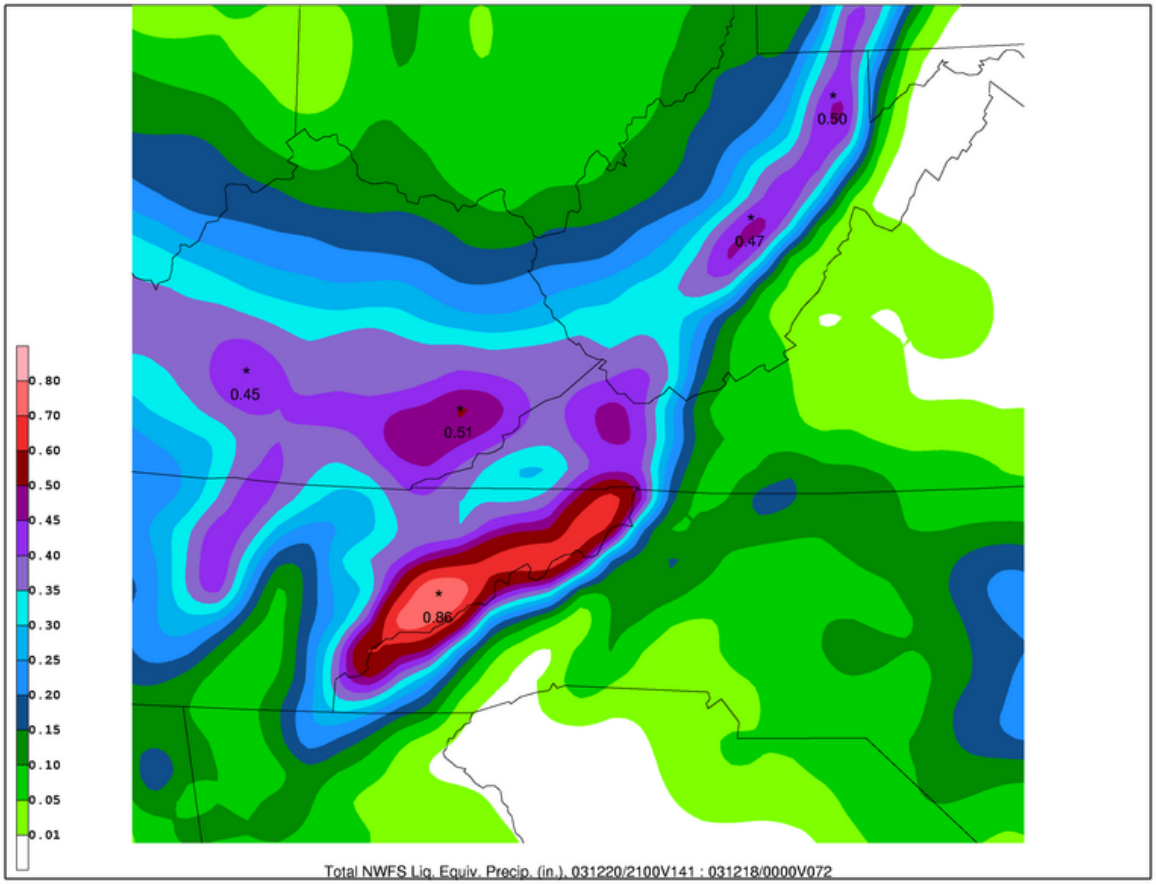

Figure 4.32. CTRL total liquid equivalent precipitation from 0000 UTC 18 December 2003 to 2100 UTC 20 December 2003 (inches, shaded as in colorbar in lower left corner).

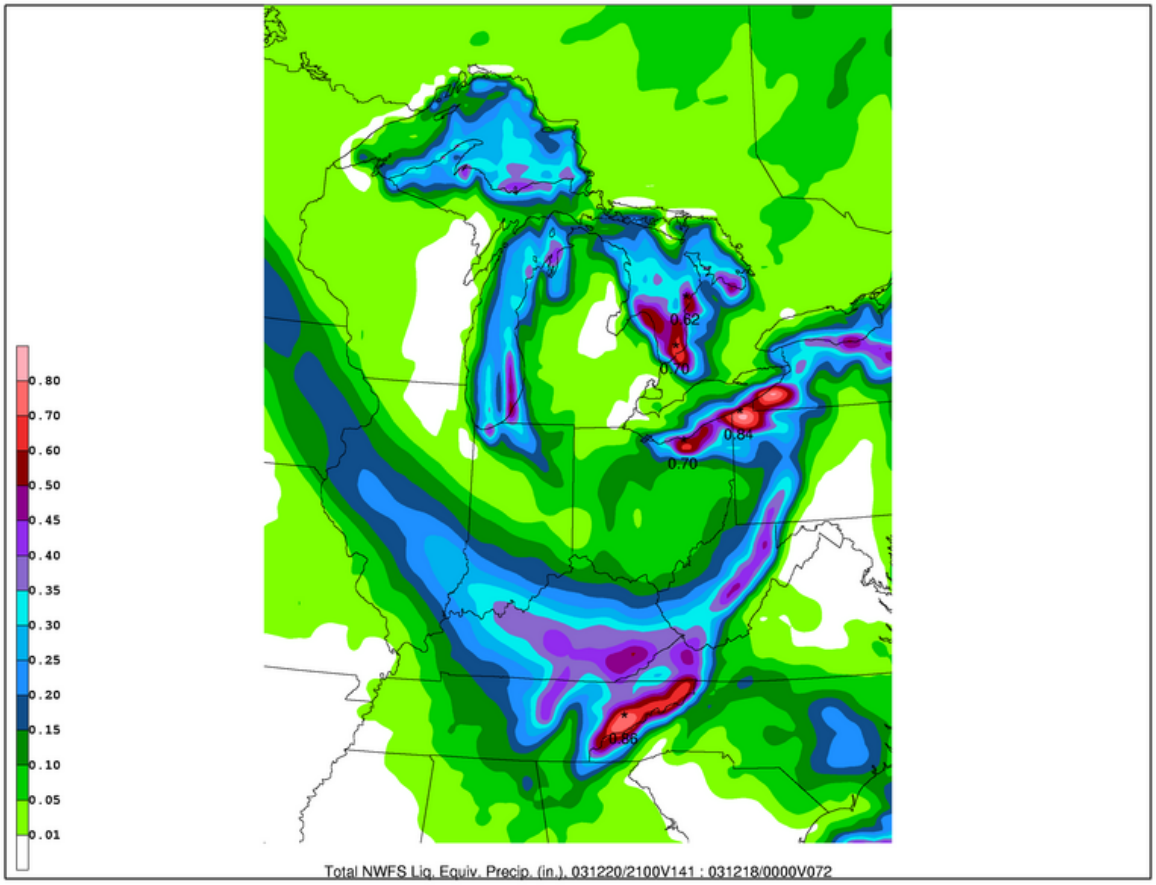

Figure 4.33. As in Figure 4.32 except larger view.

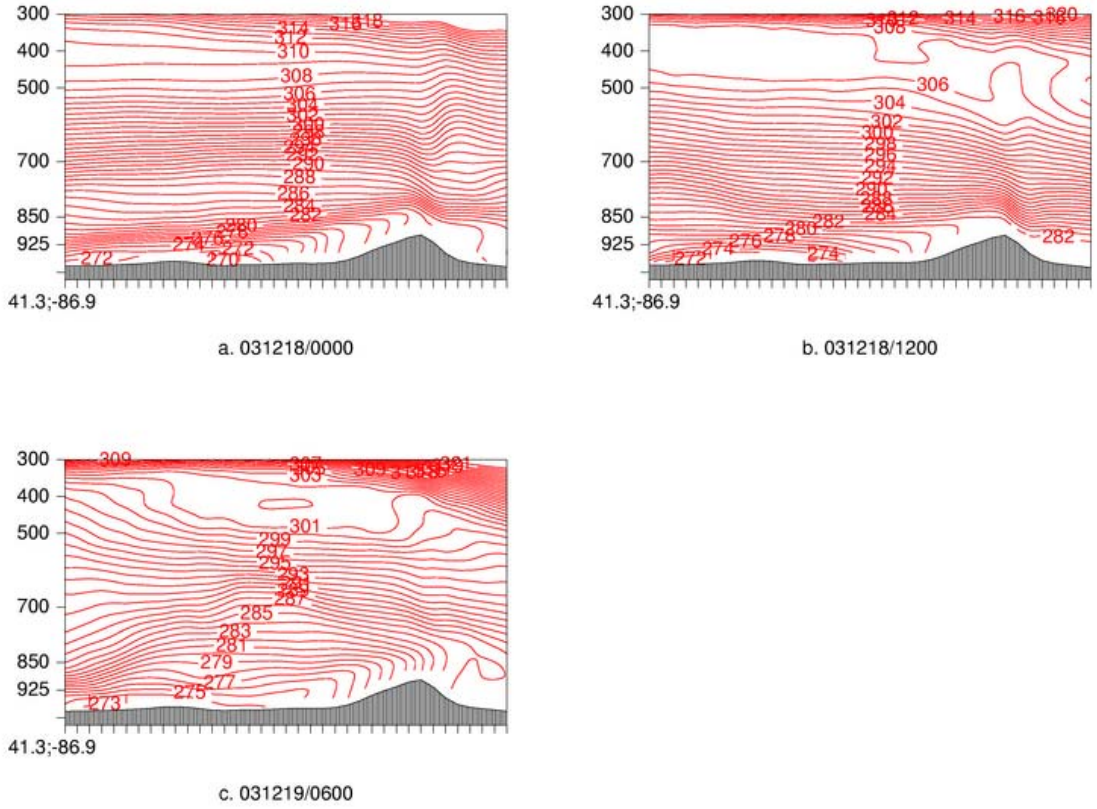

Figure 4.34. θ_e cross sections along the line shown in Figure 3.31 from CTRL: (a) 0000 UTC 18 December 2003; (b) 1200 UTC 18 December 2003; (c) 0600 UTC 19 December 2003.

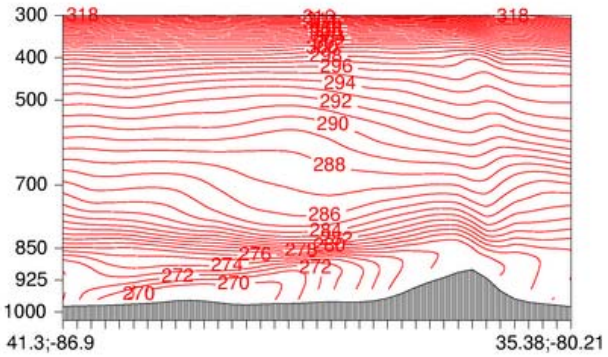

a. 031219/2100

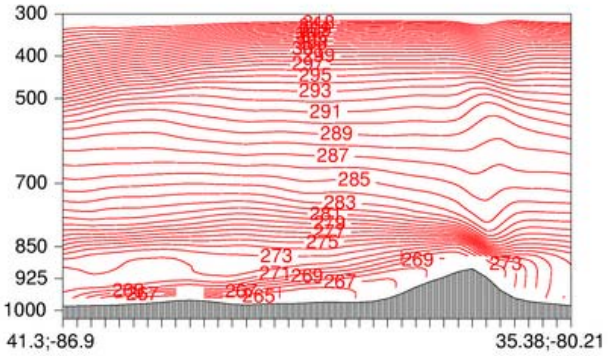

b. 031220/0600

Figure 4.35. As in Figure 4.38 except for: (a) 2100 UTC 19 December 2003; (b) 0600 UTC 20 December 2003.

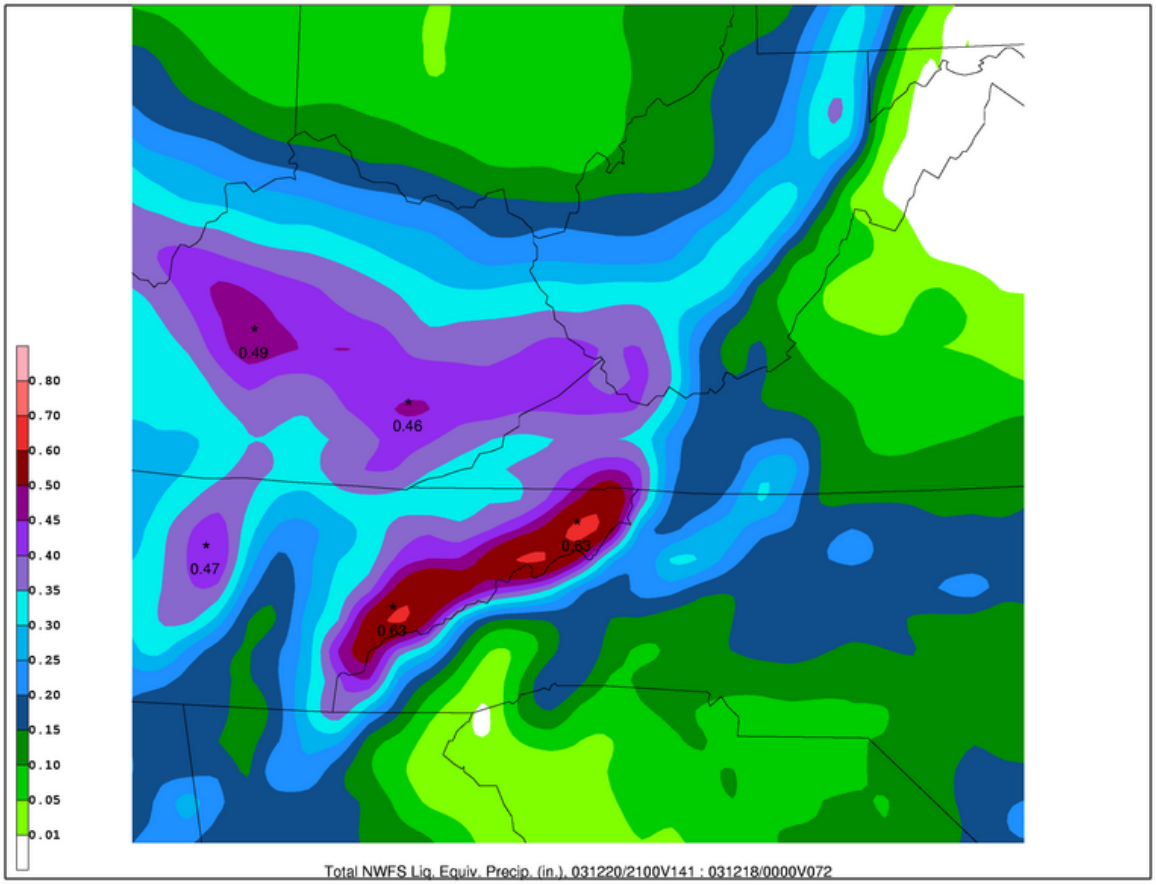

Figure 4.36. As in Figure 4.32 except for MYJPBL.

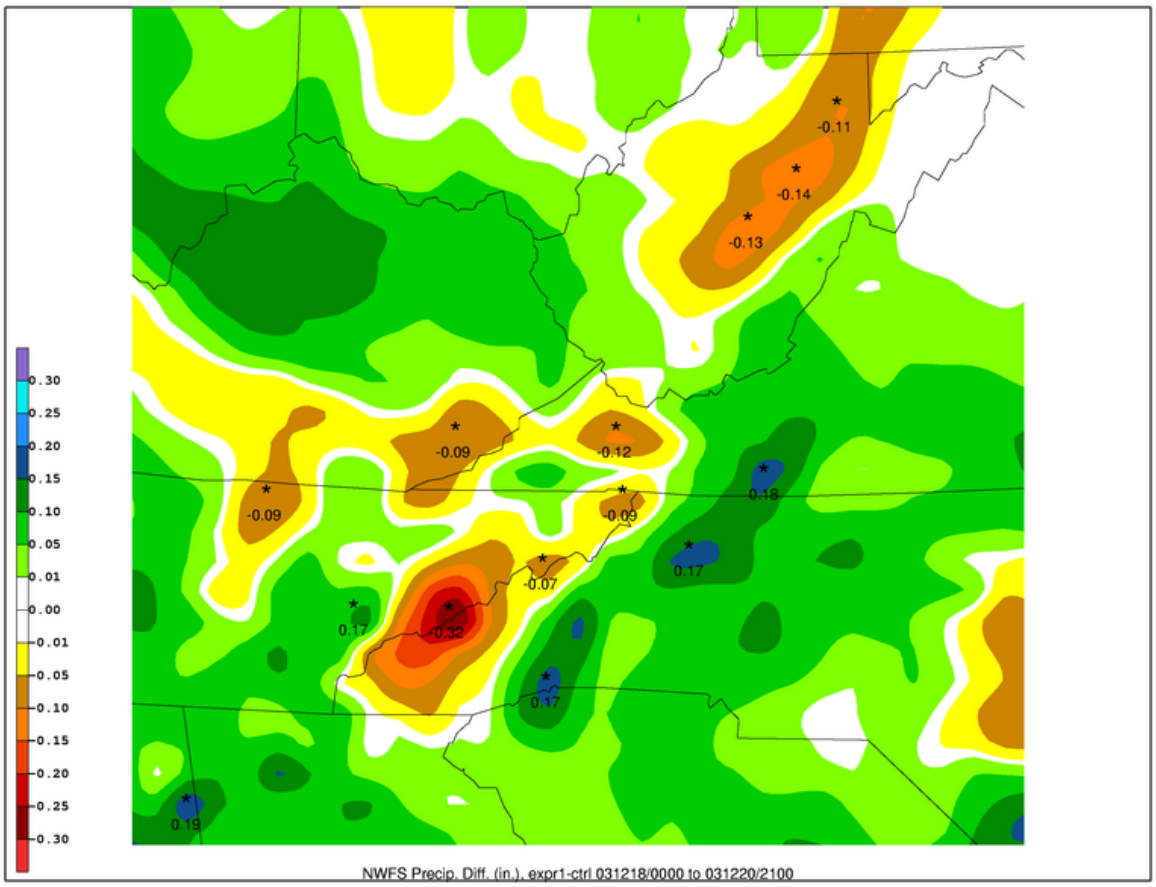

Figure 4.37. Difference field of liquid equivalent precipitation, MYJPBL-CTRL, from 0000 UTC 18 December 2003 to 2100 UTC 20 December 2003 (inches, shaded as in colorbar in lower left).

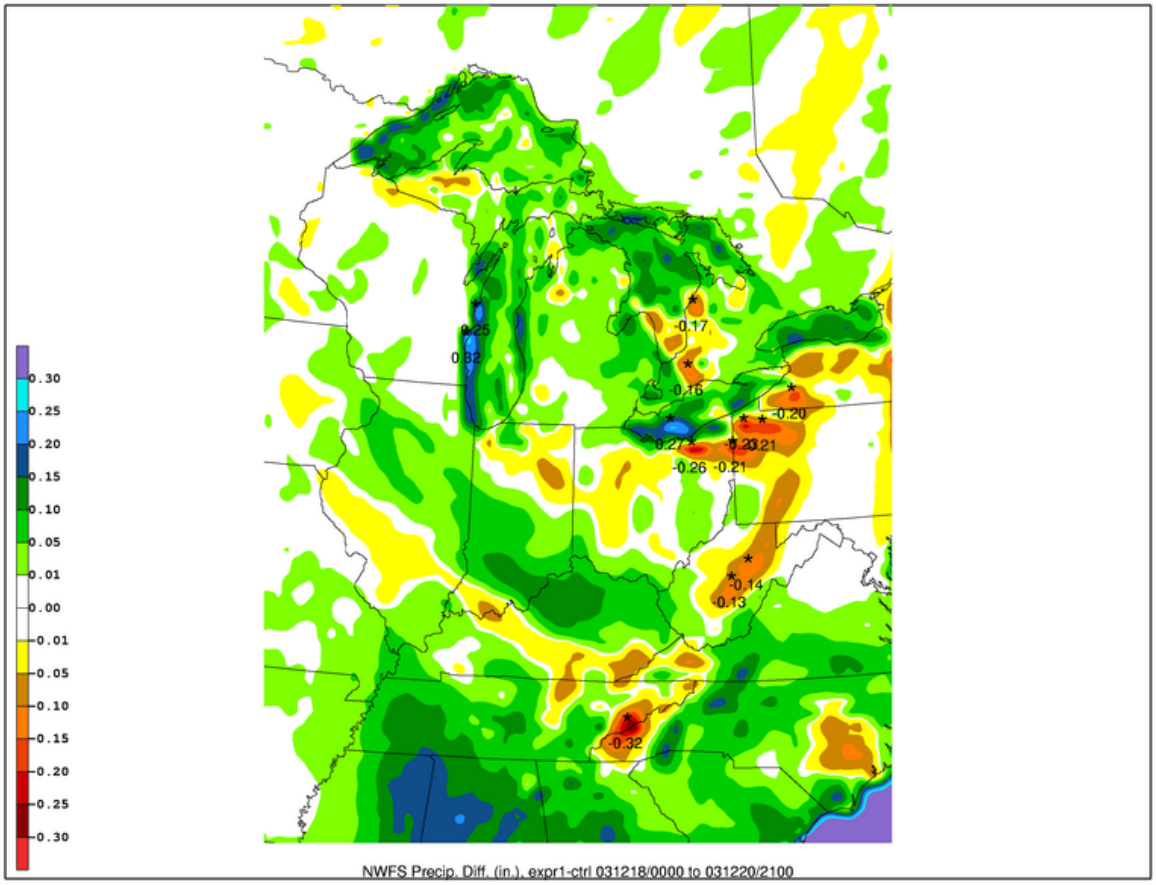

Figure 4.38. As in Figure 4.37 except larger view.

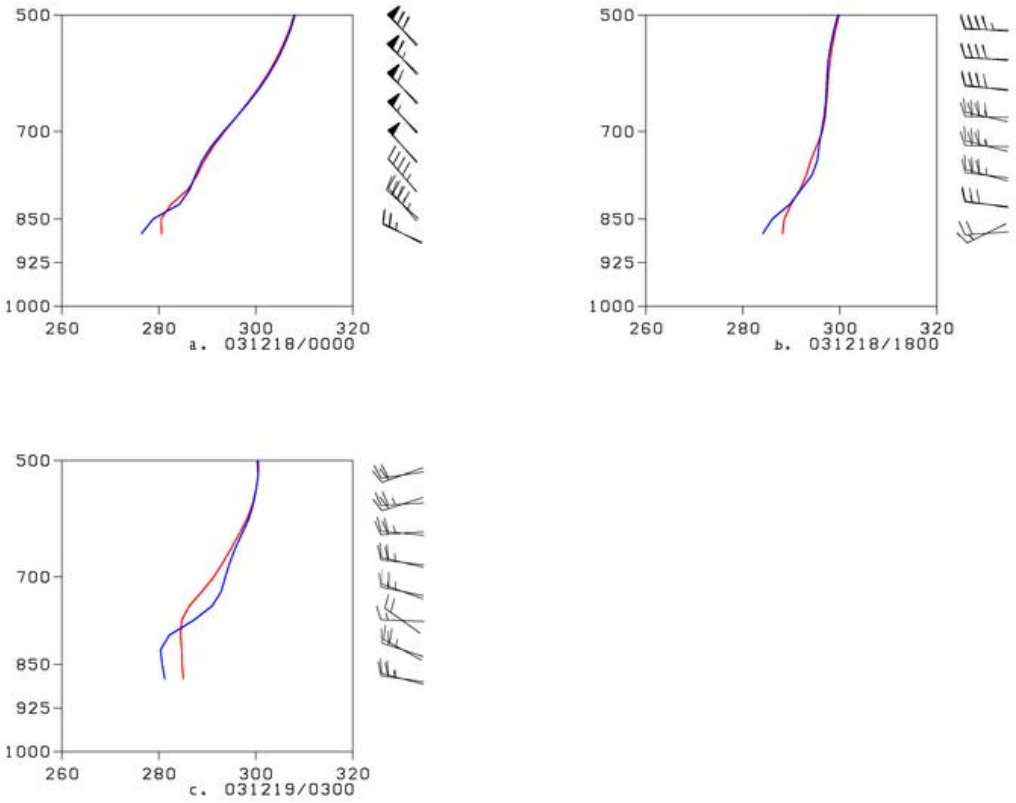

Figure 4.39. θ_e (K) profiles at Erwin, TN (36.14 N;-82.39 W) for CTRL (red) and MYJPBL (blue): (a) 0000 UTC 18 December 2003; (b) 1800 UTC 18 December 2003; (c) 0300 UTC 19 December 2003.

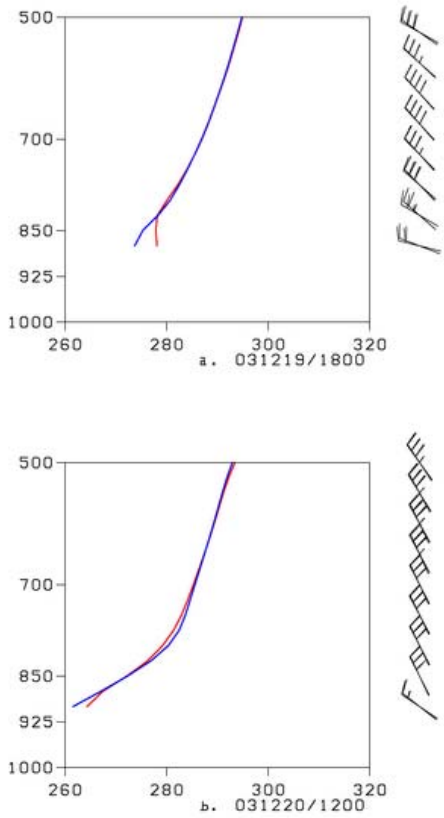

Figure 4.40. As in Figure 4.39 except for: (a) 1800 UTC 19 December 2003; (b) 1200 UTC 20 December 2003.

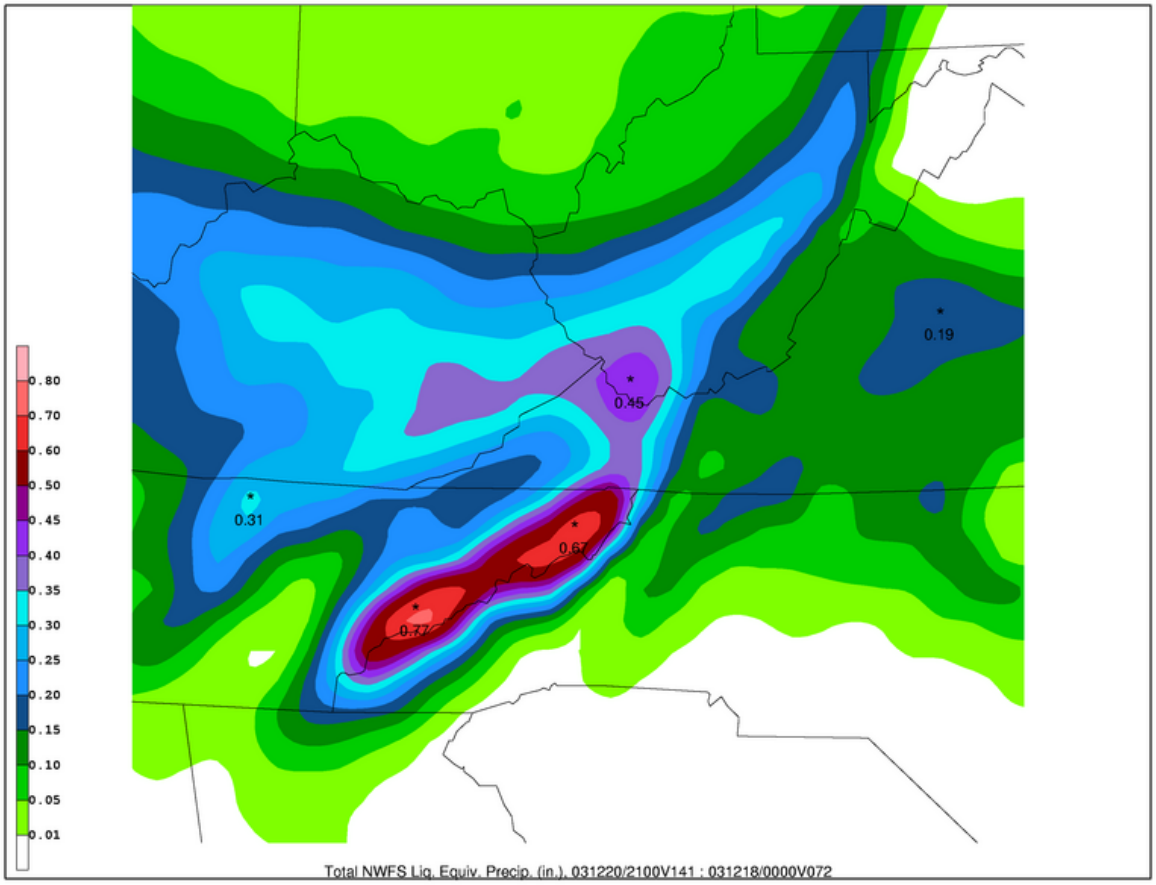

Figure 4.41. NOFLX total liquid equivalent precipitation from 0000 UTC 18 December 2003 to 2100 UTC 20 December 2003 (inches, shaded as in colorbar in lower left corner).

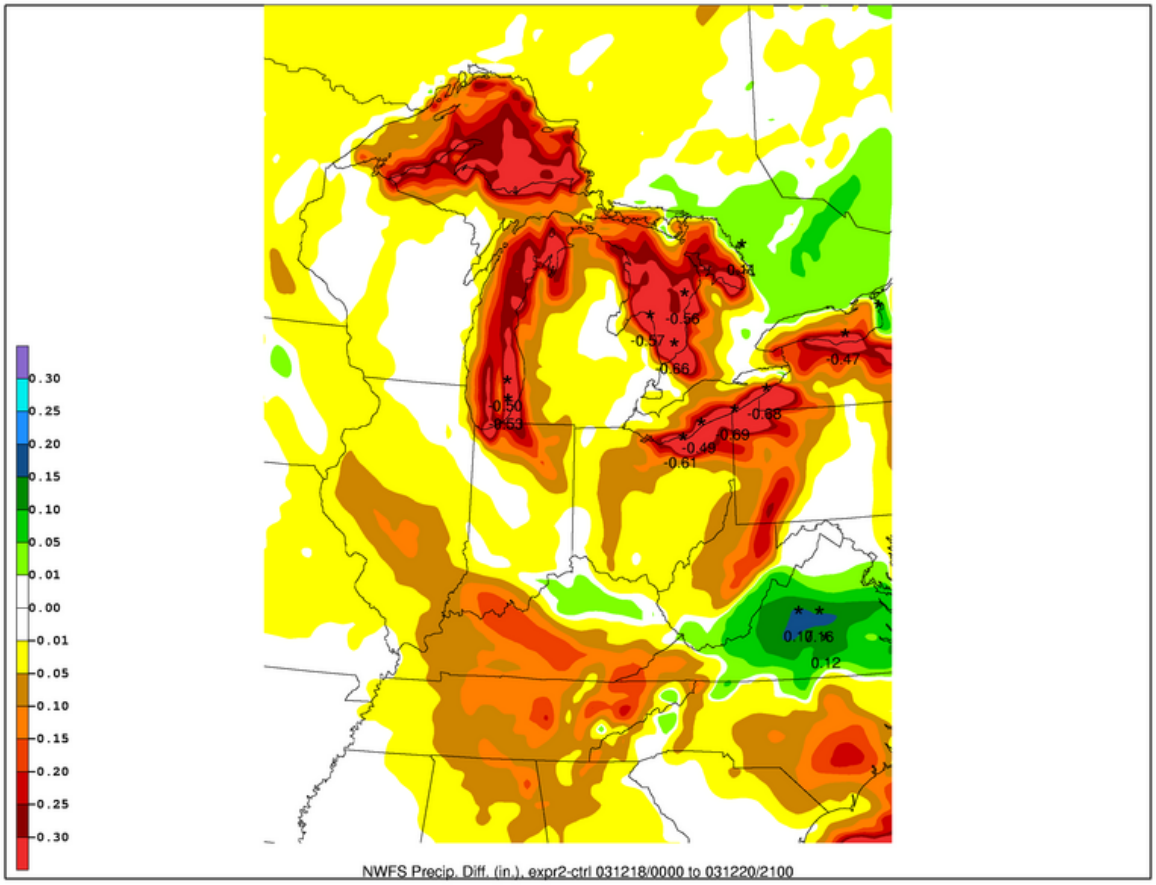

Figure 4.42. Difference field of liquid equivalent precipitation, NOFLX-CTRL, from 0000 UTC 18 December 2003 to 2100 UTC 20 December 2003 (inches, shaded as in colorbar in lower left).

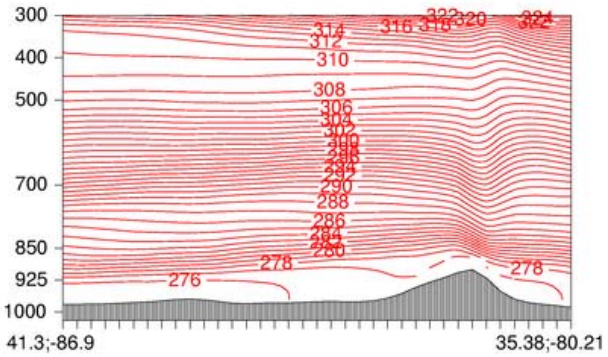

Figure 4.43. θ_e cross sections along the line shown in Figure 3.31 from NOFLX: (a) 0000 UTC 18 December 2003; (b) 1200 UTC 19 December 2003.

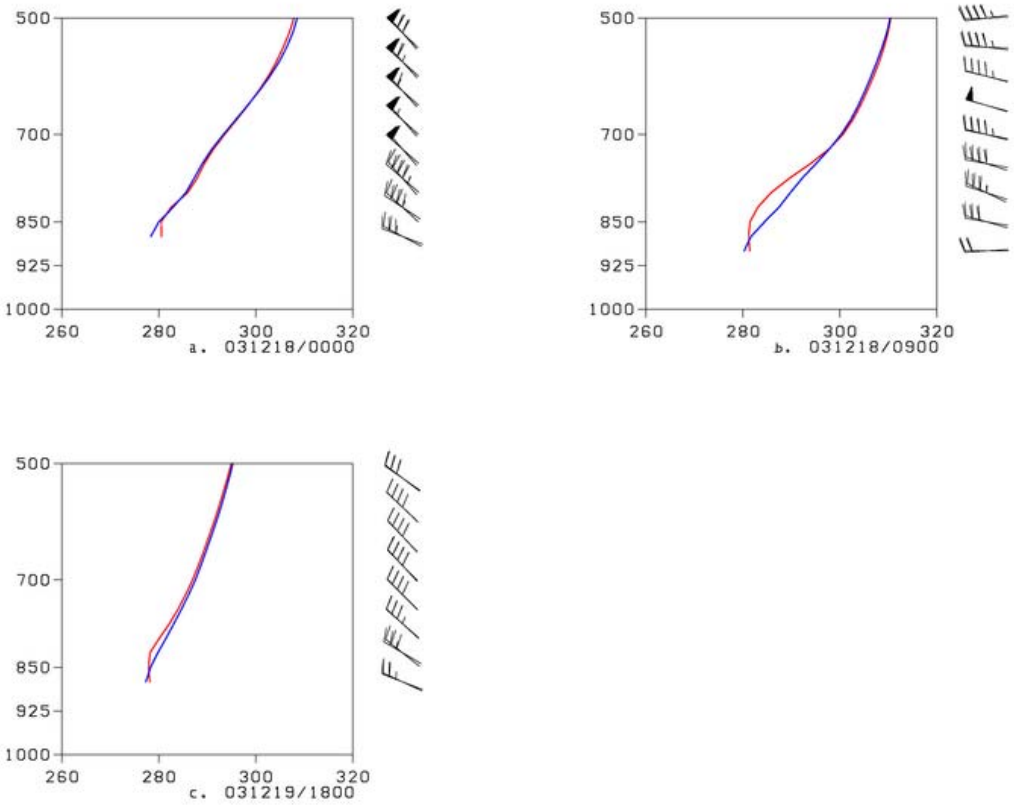

Figure 4.44. θ_e (K) profiles at Erwin, TN (36.14 N;-82.39 W) for CTRL (red) and NOFLX (blue): (a) 0000 UTC 18 December 2003; (b) 0900 UTC 18 December 2003; (c) 1800 UTC 19 December 2003.

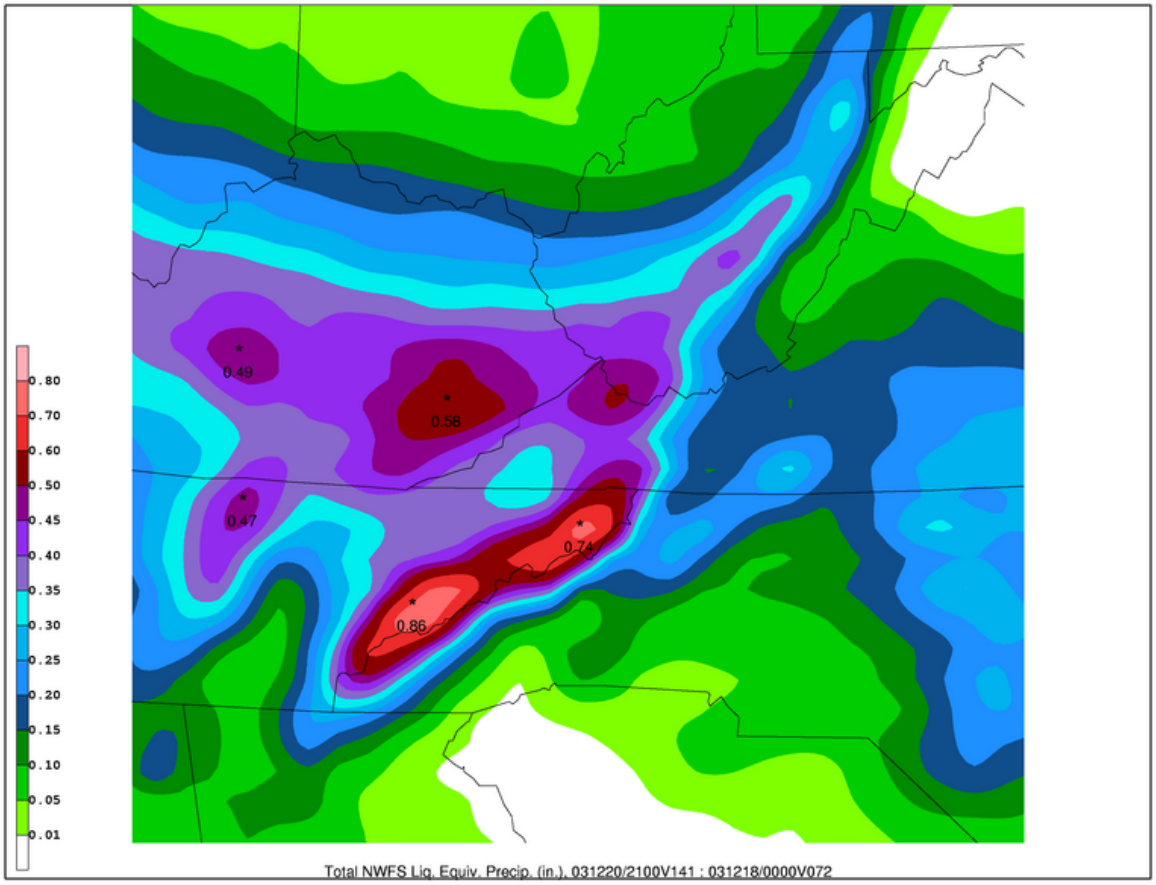

Figure 4.45. LKNOFLX total liquid equivalent precipitation from 0000 UTC 18 December 2003 to 2100 UTC 20 December 2003 (inches, shaded as in colorbar in lower left corner).

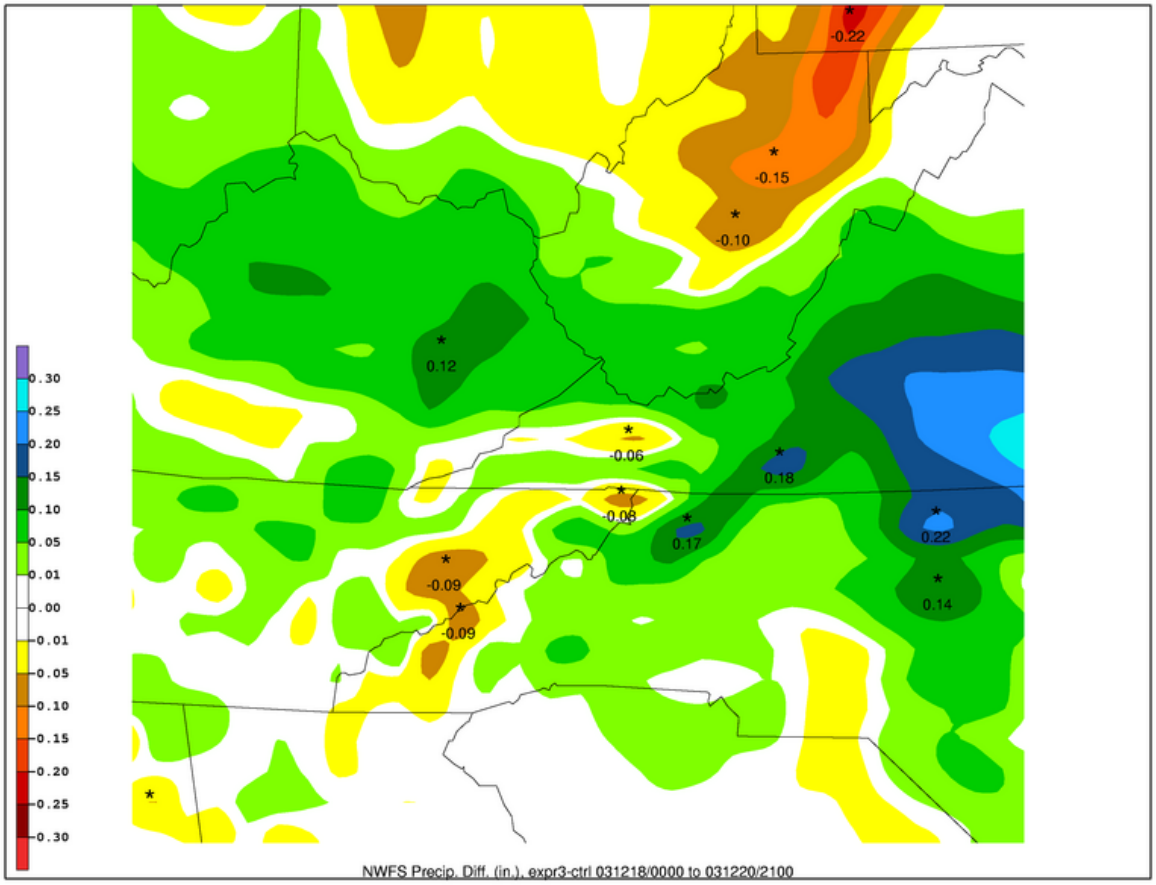

Figure 4.46. Difference field of liquid equivalent precipitation, LKNOFLX-CTRL, from 0000 UTC 18 December 2003 to 2100 UTC 20 December 2003 (inches, shaded as in colorbar in lower left).

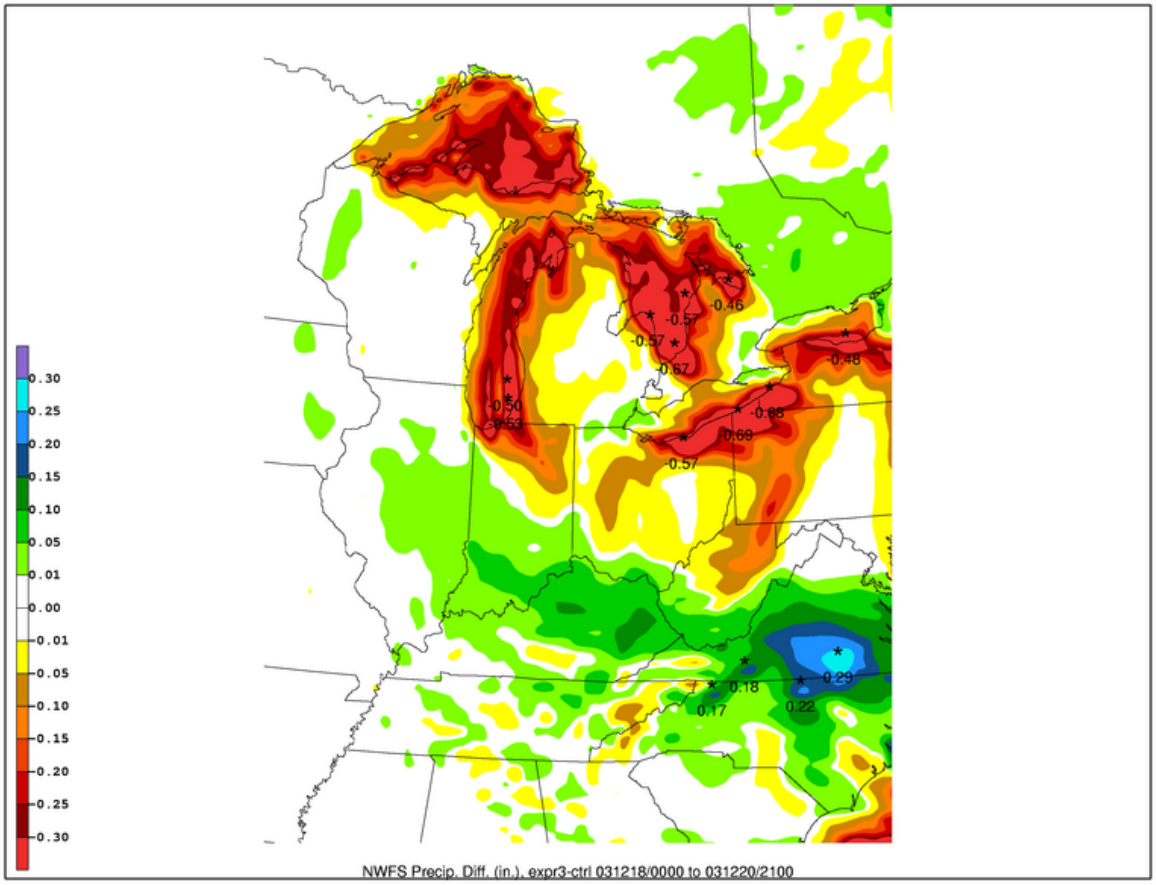

Figure 4.47. As in Figure 4.46 except larger view.

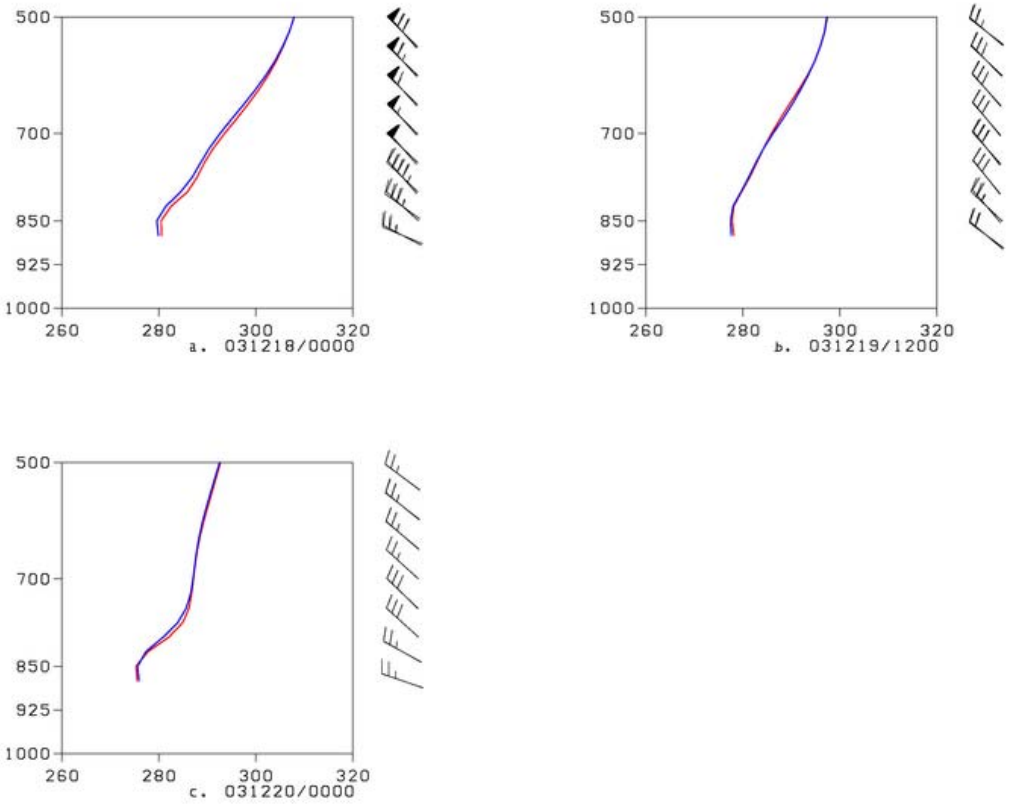

Figure 4.48. θ_e (K) profiles at Erwin, TN (36.14 N;-82.39 W) for CTRL (red) and LKNOFLX (blue): (a) 0000 UTC 18 December 2003; (b) 1200 UTC 19 December 2003; (c) 0000 UTC 20 December 2003.

5. Case 3: 5–7 March 2001

5.1. Event analysis

The third and final NWFS event considered in this study occurred on 5–7 March, 2001. This event is an example of a late winter, medium impact NWFS case that distinctly falls into the Type III category in the classification scheme discussed previously in section 1.3.3. Section 5.1 describes Case 3 from a synoptic and observational standpoint while section 5.2 discusses the model experiments conducted on the event.

5.1.1. Synoptic overview

The 5–7 March 2001 NWFS event is one marked by the development and southeastward movement of a large upper level low. Beginning on 1200 UTC on the 4th, this feature was located over southeastern Canada with southwesterly flow well entrenched across the southern Appalachians (Fig. 5.1). The upper low then slowly sinks southward over the Great Lakes by around 1200 UTC on the 5th (Fig. 5.2), with flow transitioning from southwesterly to northwesterly over the southern Appalachians. By 0000 UTC on the 6th the upper low is centered over Ohio (Fig. 5.3), and makes its closest approach to the southern Appalachians around 1200 UTC on the 6th (Fig. 5.4). Finally, the upper low pushes off the East Coast by 0000 UTC on the 7th (Fig. 5.5), continuing its eastward progression away from the eastern seaboard through 1200 UTC on the 7th (Fig. 5.6).

At lower levels in the atmosphere, flow at the 850-hPa level over the southern Appalachian Mountains undergoes a transition to northwesterly from southwesterly around 0000 UTC on the 5th (Fig. 5.7). By 1200 UTC on the 5th, 30–40 kt northwesterly flow is

prevalent across the southern Appalachians (Fig. 5.8), and temperatures at the 850-hPa level have cooled from around +6°C at 0000 UTC on the 5th, to -6 °C at 1200 UTC. Winds remained northwesterly and increased to greater than 40 kt over the region by 1200 UTC on the 6th, with temperatures decreasing to between -12 and -14 °C at the same time (Fig. 5.9). With the upper low moving east and off the East Coast, winds at 850 hPa decreased to 25–30 kts as the height gradient began to relax over the southern Appalachians by 1200 UTC on the 7th (Fig. 5.10).

Surface analyses throughout the 5–7 March 2001 event also show the northwesterly flow seen at other levels of the atmosphere. Starting at 1200 UTC on the 5th, northwesterly flow is already well in place and extends from the southern Appalachians to areas upstream across the Great Lakes (Fig. 5.11). Similarly, northwesterly flow over this area persisted through 1200 UTC on the 6th (Fig. 5.12), before becoming more variable by 1200 UTC on the 7th as the pressure gradient weakened across the eastern portion of the country (Fig. 5.13).

5.1.2. Observational overview

Though the 5–7 March 2001 case can be defined as a medium level impact NWFS event, it still produced some rather impressive event totals of around one foot across the northern mountains of North Carolina (Fig. 2.2). Overall however, the majority of the snowfall totals ranged from trace amounts to around 4 inches along and near the North Carolina/Tennessee border. This event definitely falls in between the lighter totals of the 10–11 February 2005 event, and the extremely large totals reported in the 18–20 December 2003.

As shown before, synoptic scale northwesterly flow began across the southern Appalachians around 1200 UTC on the 5th. However, the precipitation period associated with this event began around 2100 UTC on the 5th as the first showers approached the southern Appalachians (Fig. 5.14). The coverage of the precipitation increased through 0300 UTC on the 6th, with bands extending southeastward from Lake Michigan (Fig. 5.15). Patches of precipitation remained across the southern Appalachians through 1200 UTC on the 6th (Fig. 5.16), and persisted through 1800 UTC (Fig. 5.17). By 0000 UTC on the 7th (Fig. 5.18), precipitation was mainly confined to northern sections of the southern Appalachians, before dwindling throughout the entire region by 1200 UTC on the 7th (Fig. 5.19).

Finally, as shown in the 10–11 February 2005 case, satellite imagery can be a useful source of information regarding NWFS events. One such image from 1826 UTC on the 6th shows a band of clouds that extends from the southern Appalachians, upstream to the Great Lakes region (Fig. 5.20). This band of clouds could perhaps be a strong indication of a Great Lakes influence in this case, and even takes on the appearance of a channel of clouds and moisture that extends southeastward from the lakes toward the higher terrain of the southern Appalachians.

5.2. Numerical simulations

In this section, the 4 model runs performed are discussed within the context of the 5–7 March 2001 NWFS event. These model runs are identical in setup to those discussed in chapter 3 and 4 regarding the 10–11 February 2005 event, and the 18–20 December 2003

event, respectively. A description of the individual model run specifics is available in chapter 2.

5.2.1. Control run (CTRL)

At 1200 UTC on the 5th, the CTRL has a strong upper low positioned over the Great Lakes with a tight surface pressure gradient across the eastern third of the country (Fig. 5.21a). By 0000 UTC on the 6th, the upper low tracks southeastward toward the mid-Atlantic (Fig. 5.21b), and makes its closest approach to the southern Appalachians around 1200 UTC on the 6th (Fig. 5.21c). The upper low pushes offshore by 0000 UTC on the 7th (Fig. 5.22a), progressing further east and away from the East Coast by 1200 UTC on the 7th (Fig. 5.22b), with a slackening surface pressure gradient over the eastern portion of the county.

At the 850-hPa level, CTRL shows 20–30 kt northwesterly flow at 1200 UTC on the 5th across the southern Appalachians with temperatures in the -6 to -8°C range (Fig. 5.23a). Temperatures cool slightly to around -8 to -10°C and strong northwesterly flow continues across the region through 0000 UTC on the 6th (Fig. 5.23b), before temperatures cool greatly to around -22 °C by 1200 UTC (Fig. 5.23c). By 0000 UTC on the 7th temperatures do warm a bit, to between -12 and -16 °C across the area, while northwesterly winds remain quite strong, around 50 kts (Fig. 5.24a). As the event comes to a close around 1200 UTC on the 7th, the 850-hPa level winds begin to decrease across the southern Appalachians and turn more westerly upstream across northern portions of the Great Lakes (Fig. 5.24b).

For the event, NWFS precipitation lasted from 2100 UTC on the 5th to 2100 UTC on the 7th. Over this time period, CTRL produced precipitation totals generally ranging from

0.20 inches, to around 0.50 inches (Fig. 5.24). Overall, CTRL does a good job of focusing the maximum of precipitation along the higher terrain as well as creating a tight precipitation gradient to the east of these same areas, similar to the actual event (Fig. 2.2). Considering snowfall totals reported during this event, and assuming a rather high snow to liquid ratio of 20:1, maximum snowfall totals of around 6 inches would be possible along the North Carolina/Tennessee border, with higher amounts further northeast. This is a reasonable representation of the event except for the fact that the highest totals recorded along the North Carolina/Tennessee border were in the vicinity of the northern North Carolina mountains (Fig. 2.2), and is a underdone in CTRL (Fig. 5.25). However, the area of approximately 4 inches of snowfall seen in observations is well represented in CTRL. On the large scale view, the precipitation even shows a pattern much like that of the 10–11 February 2005 event with precipitation stretching back upstream towards the Great Lakes (Fig. 5.26).

At the beginning of the event, 2100 UTC on the 5th, potential instability is present on cross sections from the Great Lakes to the southern Appalachians (Fig. 5.27a). This instability continues to move downstream toward the southern Appalachians through 0600 UTC on the 6th, despite its decrease further upstream toward the Great Lakes (Fig. 5.27b). By 1200 UTC only small amounts of potential instability are present and are confined to the vicinity of the southern Appalachians (Fig. 5.27c). Potential instability increases once again by 1800 UTC on the 6th (Fig. 5.28a), only to decrease by 0600 UTC on the 7th (Fig. 5.28b). This variability in the magnitude of potential instability between 1800 UTC on the 6th and 0600 UTC on the 7th is perhaps indicative of a diurnal influence in the surface fluxes in this case. A diurnal trend in both the latent and sensible heat fluxes is easily seen at 1800 UTC on the 6th (Fig. 5.29) and 0600 on the 7th (Fig. 5.30). Also of note is the fact surface fluxes

in excess of 50 W/m^2 are only present across portions of Lake Michigan. This shows the effect of the significantly cooler lake surface present in this late-winter NWFS event, relative to the other cases discussed in chapter 3 and chapter 4.

5.2.2. Experimental run 1 (MYJPBL)

For the event, MYJPBL produces precipitation amounts and structure similar to that seen in the CTRL (Fig. 5.31), but a difference plot of the two shows that MYJPBL quite dramatically increases precipitation across most of the southern Appalachians (Fig. 5.32). Except for a small area in southwestern Virginia where less precipitation occurs, increases are generally 0.10 inches or greater, mainly along and near the North Carolina/Tennessee border. Even more striking is the fact that on a larger scale view nearly all areas across the model domain experience an increase in precipitation during the NWFS period (Fig. 5.33). This is very similar to the results from MYJPBL in Case 1 which also produced a substantial increase in precipitation across the southern Appalachians.

Differences between the CTRL and MYJPBL are not limited to precipitation. The amount and magnitude of potential instability also appears to be greatly altered in MYJPBL. A cross section of θ_e from the beginning of the NWFS event, 2100 UTC on the 5th, shows less instability in the lower levels in the atmosphere (Fig. 5.34) between the Great Lakes and the southern Appalachians when compared to the same plot from the CTRL (Fig. 5.27a). Profiles of θ_e at various locations also highlight this difference. At La Crosse, IN, MYJPBL produces a shallower boundary layer starting around 0600 UTC on the 6th (Fig. 5.35a). These differences continue through 1800 UTC on the 6th (Fig. 5.35b), and 0000 UTC on the 7th (Fig. 5.35c), before both model simulations greatly stabilize around 1500 UTC on the 7th

(Fig. 5.35d). Similar differences appear downstream of the Great Lakes at Erwin, TN where the CTRL is much more unstable and deeply mixed at 2100 UTC on the 5th (Fig. 5.36a). The MYJPBL simulation showed increased instability by around 0300 UTC on the 6th but is still much more stable than the CTRL (Fig. 5.36b). The differences decreased substantially by 1200 UTC on the 6th (Fig. 5.36c), but would again increase by 2100 UTC on the 6th as MYJPBL provided a much more stable solution (Fig. 5.37a). Finally, as the event was nearing its end, both simulations stabilized (Fig. 5.37b).

5.2.3. Experimental run 2 (NOFLX)

Surface fluxes of heat and moisture were set to zero across the model domain in the NOFLX experimental run. Overall, a significant amount of precipitation still fell across the southern Appalachians during the NWFS period (Fig. 5.38). However, precipitation decreases occurred across the entire region with the greatest differences seen along southern and central sections of the North Carolina/Tennessee border (Fig. 5.39). This decrease in precipitation extends back to the northwest to the Great Lakes, mainly across Lake Michigan (Fig. 5.40), and strongly resembles the structure of precipitation decreases produced in NOFLX from Case 1 (Fig. 3.46).

However, unlike NOFLX in Case 1, more potential instability appears at locations from the Great Lakes to the southern Appalachians in NOFLX from Case 3. Starting at La Crosse, IN at 2100 UTC on the 5th, NOFLX still has potential instability present, though to a much lesser magnitude than the CTRL (Fig. 5.41a). By 0300 UTC on the 6th, NOFLX began stabilizing while the CTRL still produced a deep mixed layer up to about 850 hPa (Fig.

5.41b). At 1200 UTC on the 6th, NOFLX was still much more stable than the CTRL which featured waning potential instability, compared to 6 hours previous (Fig. 5.41c).

Similar differences occurred further downstream at Lexington, KY. At 2100 UTC on the 5th, the CTRL is considerably more unstable over a deeper layer than NOFLX (Fig. 5.42a). This trend continues through 0300 UTC on the 6th, as the NOFLX is more stable than the CTRL, despite showing potential instability from the surface up to ~900 hPa (Fig. 5.42b). This continues through 0000 UTC on the 7th (Fig. 5.42c), before both are quite stable by 0600 UTC (Fig. 5.42d).

Finally, these differences in potential instability between NOFLX and the CTRL are seen in the southern Appalachians. At Erwin, TN at 2100 UTC on the 5th, NOFLX is quite stable in the lower levels compared to the CTRL (Fig. 5.43a). By 0600 UTC on the 6th, NOFLX displays some destabilization, though still considerably less than the CTRL (Fig. 5.43b). Both are much more stable by 1500 UTC on the 6th (Fig. 5.43c), with both runs devoid of potential instability by 1200 UTC on the 7th (Fig. 5.43d).

5.2.4. Experimental run 3 (LKNOFLX)

In the final experimental run, LKNOFLX simulated the NWFS event in question with the surface fluxes of heat and moisture over water in the model domain set to zero. The total precipitation for the event appears quite similar to the CTRL over the southern Appalachians (Fig. 5.44), with the exception of the absence of precipitation just downwind of the lakes, as expected (Fig. 5.45). When directly compared to the CTRL, it is quite clear that LKNOFLX produced less precipitation across the entire southern Appalachian region by nearly a tenth of an inch in some locations (Fig. 5.46). On the larger scale view, the swath of decreased

precipitation extends from the southern Appalachians upstream to Lake Michigan (Fig. 5.47). For the event, this decrease in precipitation equates to a general 20–30% reduction compared to CTRL across the southern Appalachian region (Fig. 5.48). In some locations, the percentage decrease is closer to 50%. Overall, this result is similar to the 10–11 February 2005 event, with more a more widespread decrease noted here.

In the southern Appalachians, profiles of θ_e feature some differences between LKNOFLX and the CTRL, mainly during the middle and latter parts of the NWFS event. At Erwin, TN near the beginning of the event, 2100 UTC on the 5th, the CTRL and LKNOFLX are virtually identical (Fig. 5.51a). Small differences do occur later in the event, by 0900 UTC on the 6th, as LKNOFLX is a bit more stable than the CTRL (Fig. 5.51b). This continues through 1200 UTC (Fig. 5.51c), before both model runs again become very similar and stabilize greatly by the end of the NWFS event (Fig. 5.51d).

5.3. Froude number calculations

In order to further quantify the effect of the Great Lakes during this NWFS event, a layer-averaged Froude number was calculated following the procedure discussed in section 2.4. This calculation was done for Lexington, KY, located roughly half-way between the lakes and mountains for the 950–850 hPa layer. The time period investigated runs from 2100 UTC on the 5th to 0600 UTC on the 7th, which covers the core of the NWFS event. Throughout this time period, F_r values are higher in CTRL, except for a few individual hours near the beginning of the event where LKNOFLX is close to if not slightly higher (Fig. 5.50). The diurnal variation in F_r is clear in both the CTRL and LKNOFLX where maximum values are reached on both the 5th and the 6th during the afternoon and evening hours, generally

around 2100–0000 UTC both days. The lake influence is quite clear during this event as F_r is lower in LKNOFLX is consistently lower than CTRL from around 0000 UTC on the 6th onward. Overall for the time period considered, the average 950–850 hPa F_r value for each model run is as follows: CTRL=1.70, NOFLX=0.80, and LKNOFLX=1.28. Again, much like the 10–11 February 2005 event, the average F_r is lower for the LKNOFLX model run compared to the CTRL, pointing to the effect of the Great lakes on this NWFS event. With a lower F_r in LKNOFLX, more blocking would occur concerning air flowing up and over the southern Appalachians. This matches up quite well with the decrease in precipitation that occurs when the effect of the Great Lakes is removed.

5.4. Summary

The 5–7 March 2001 NWFS case is an example of a middle impact, late winter NWFS event. Synoptically, the event is defined by a southeastward moving upper level low that passed just to the north of the southern Appalachians, and clearly falls into the Type III NWFS category. Overall, snowfall accumulations generally ranged around 4 inches at most locations along the North Carolina/Tennessee border, with some higher totals of around a foot reported in portions of the northern mountains of North Carolina. The event began around 2100 UTC on the 5th, and ended as snow showers tapered off around 1200 UTC on the 7th. The event is marked by strong northwesterly flow across the southern Appalachians for the duration of the event, with almost due northerly flow noted across the Great Lakes. In this regard, it is more similar to Case 1 than to Case 2.

Overall for this event, the Great Lakes are responsible for 20–30% of NWFS precipitation across most of the southern Appalachians, and up to 50% in some isolated

locations. The effect of the Great Lakes can be seen in profiles of θ_e in the vicinity of the southern Appalachians, as less potential instability is present in the LKNOFLX experimental run where the surface fluxes of heat and moisture from the lakes are removed. The role of the Great Lakes in this case is even more strongly reflected in values of low-level F_r upstream of the southern Appalachians. The average F_r in the LKNOFLX run for this NWFS event is 1.28, which is 0.42 less than the CTRL value of 1.70 for the same time period. Much like the 10–11 February 2005 event discussed in chapter 3, this reduction in F_r represents how the Great Lakes can help determine how much NWFS precipitation occurs. Due to surface fluxes of heat and moisture from the lakes being removed, the response is to produce a lower F_r in the low-level airmass, which in turn increases the degree of blocking as the airmass interacts with the southern Appalachians.

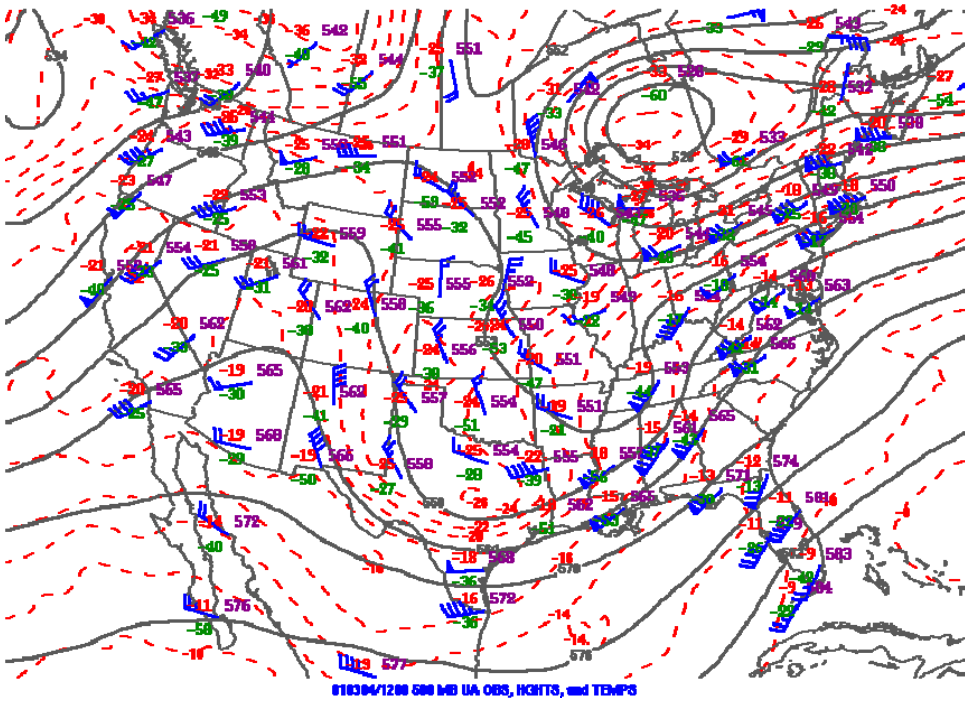

Figure 5.1. Plot of 500 hPa upper air observations, heights (solid black contours), and temperatures (dashed red contours) from 1200 UTC 4 March 2001. Image from http://www.spc.noaa.gov/obswx/maps/.

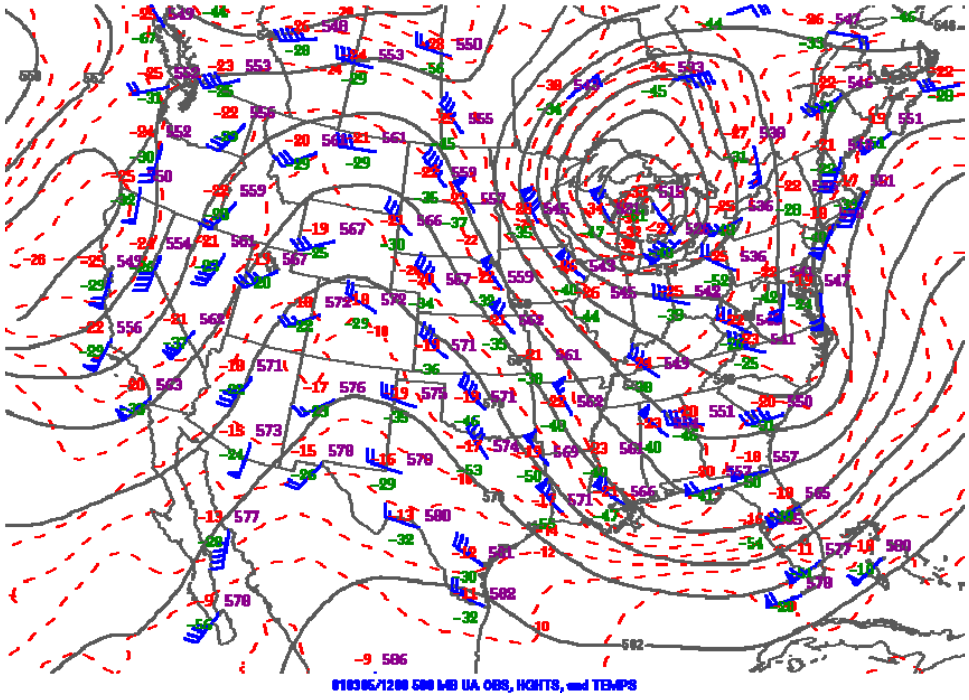

Figure 5.2. As in Figure 5.1 except for 1200 UTC 5 March 2001.

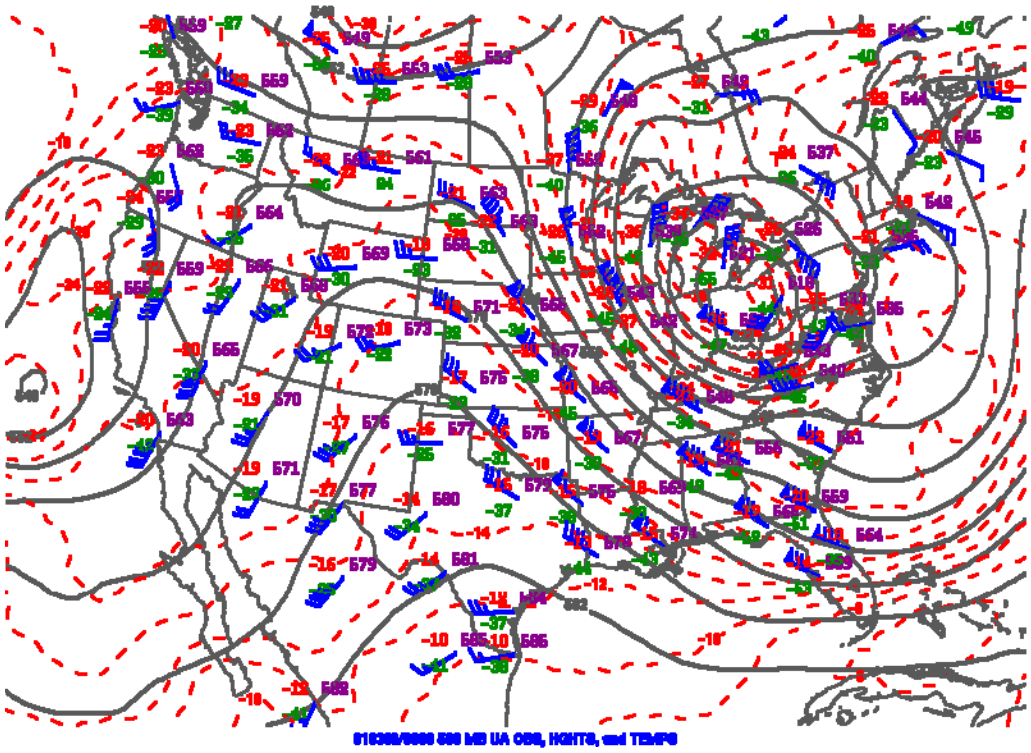

Figure 5.3. As in Figure 5.1 except for 0000 UTC 6 March 2001.

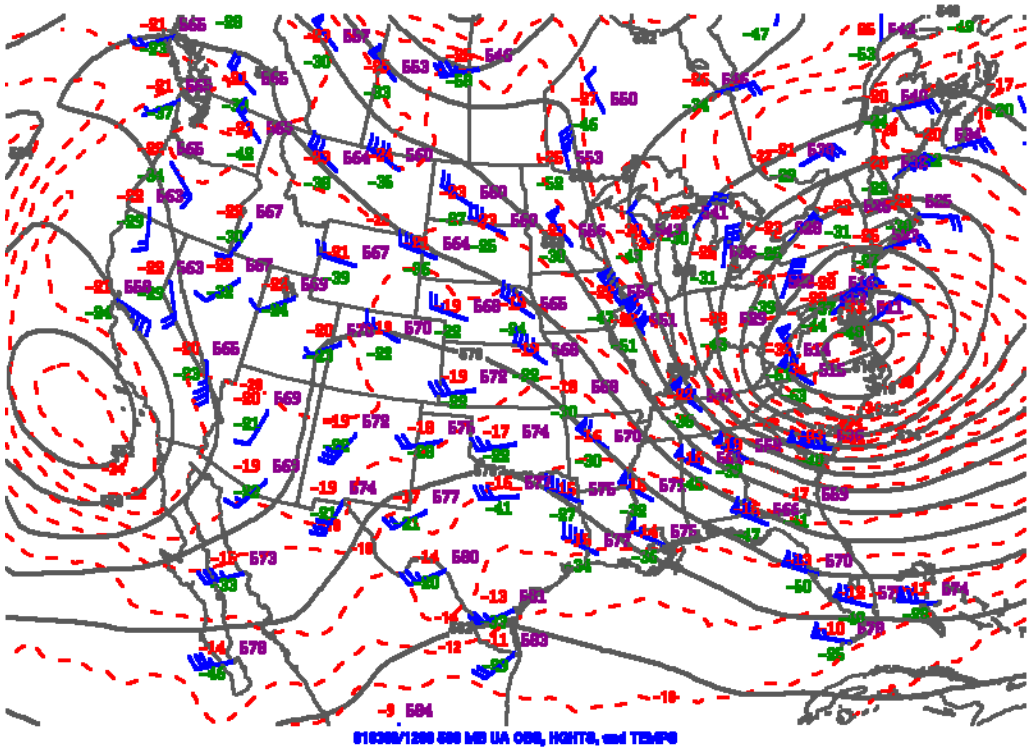

Figure 5.4. As in Figure 5.1 except for 1200 UTC 6 March 2001.

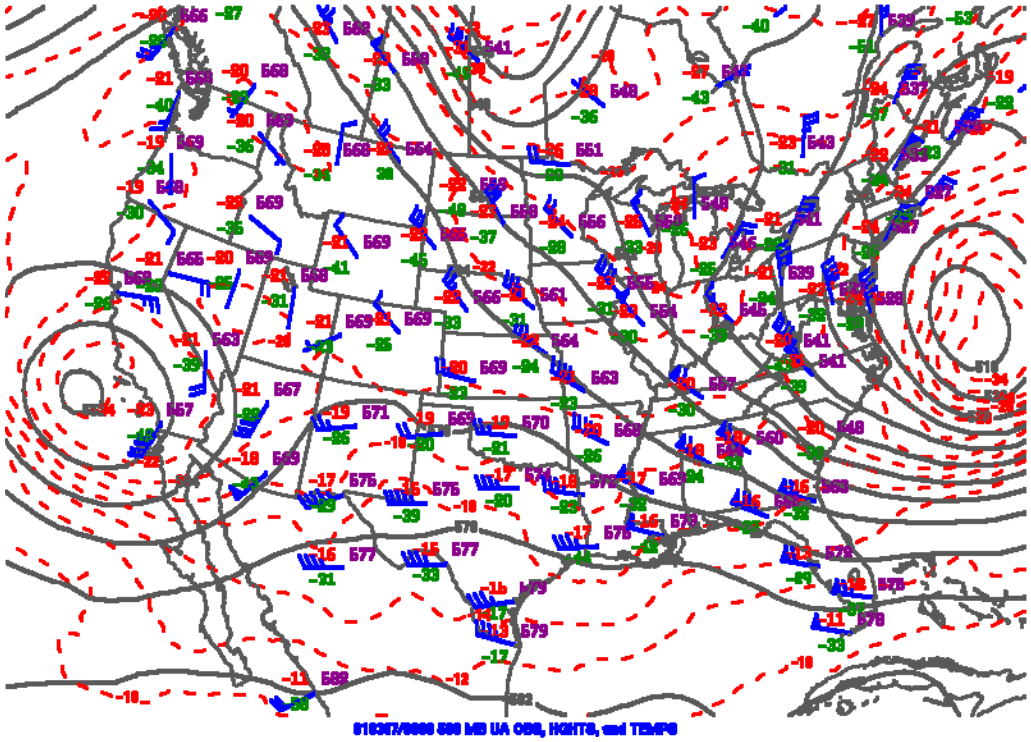

Figure 5.5. As in Figure 5.1 except for 0000 UTC 7 March 2001.

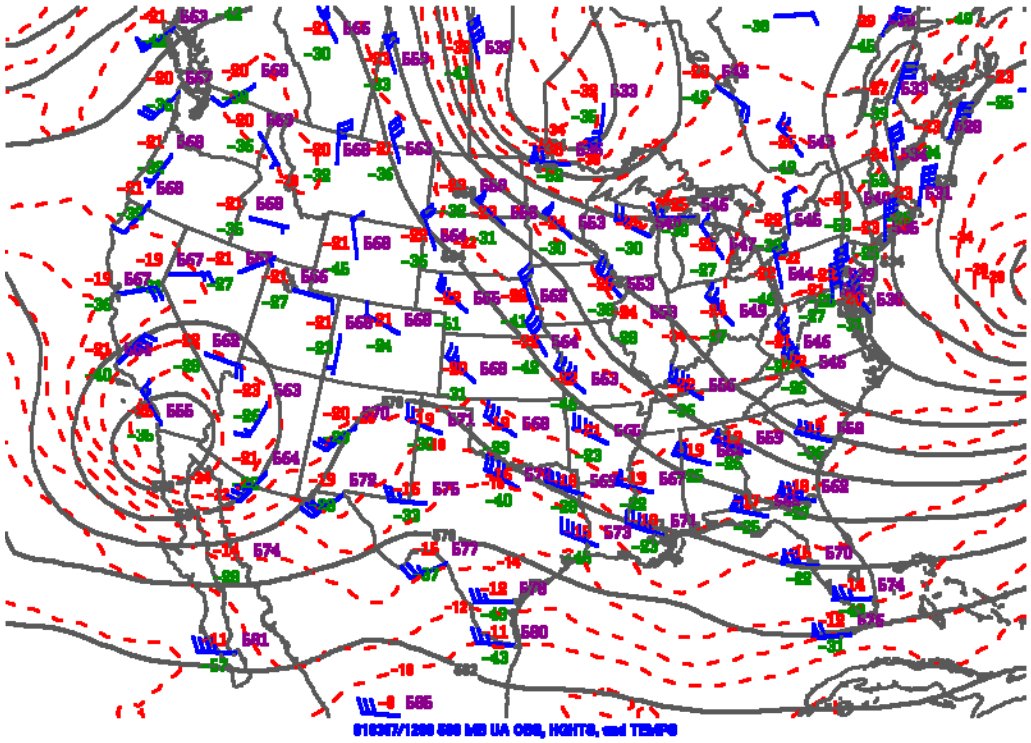

Figure 5.6. As in Figure 5.1 except for 1200 UTC 7 March 2001.

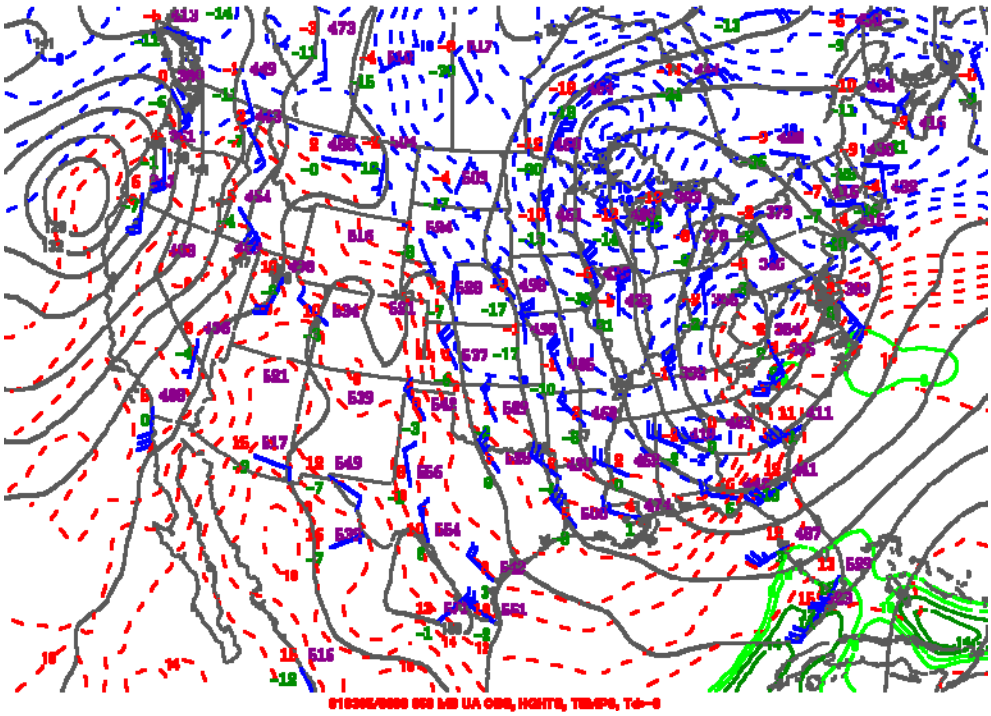

Figure 5.7. Plot of 850 hPa observations, heights (solid dark contours), temperatures (dashed contours), and dew point (solid green contours) from 0000 UTC 5 March 2001.

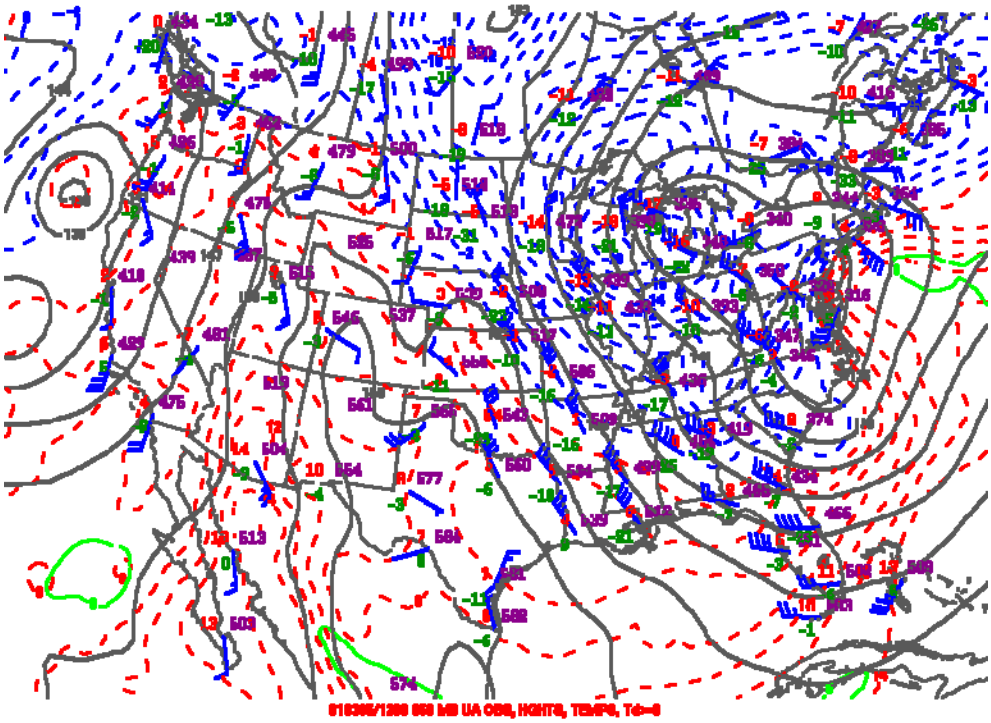

Figure 5.8. As in Figure 5.7 except for 1200 UTC 5 March 2001.

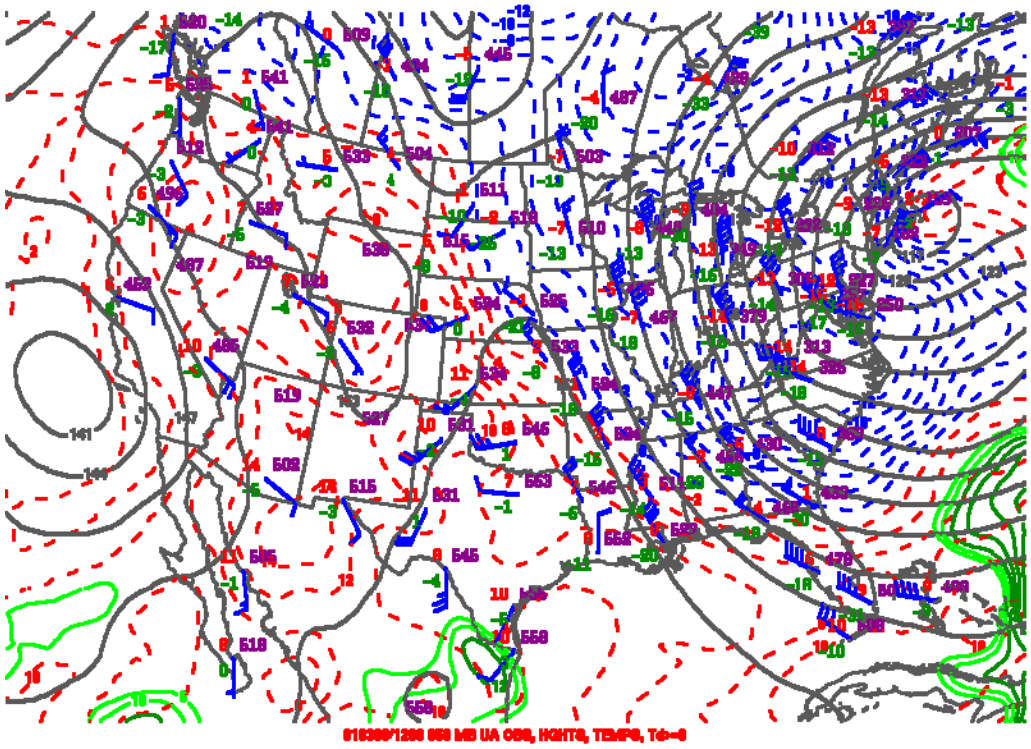

Figure 5.9. As in Figure 5.7 except for 1200 UTC 6 March 2001.

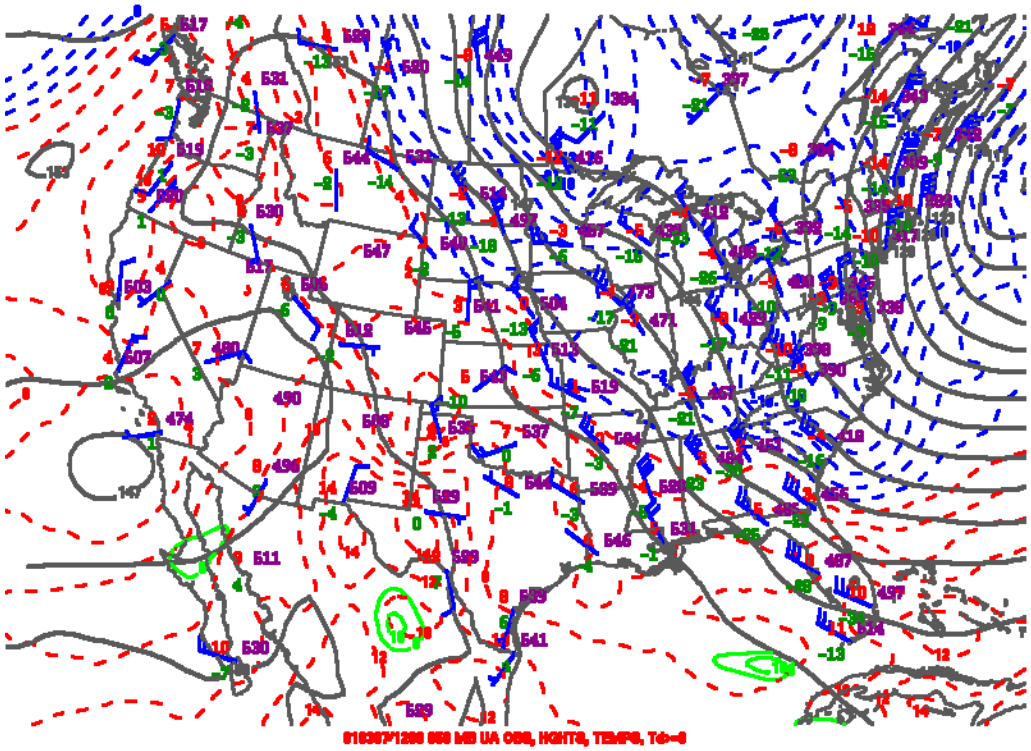

Figure 5.10. As in Figure 5.7 except for 1200 UTC 7 March 2001.

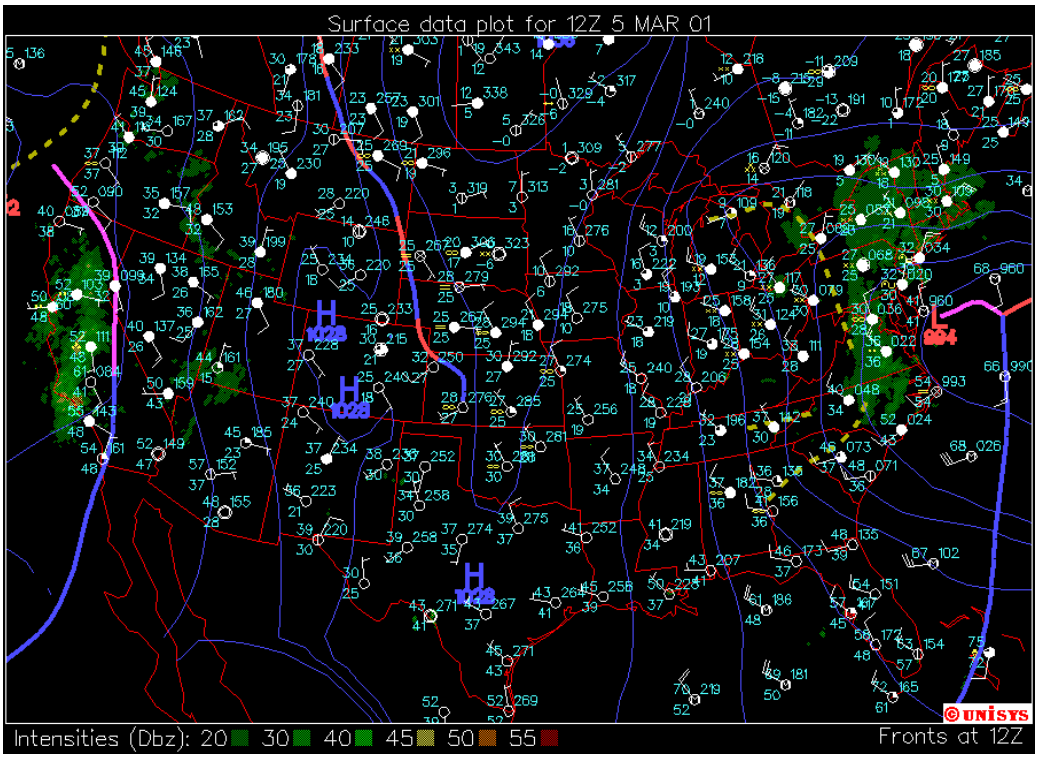

Figure 5.11. Plot of surface analysis, surface observations, and composite radar reflectivity from 1200 UTC 5 March 2001. Image from http://weather.unisys.com/archive/sfc_map/.

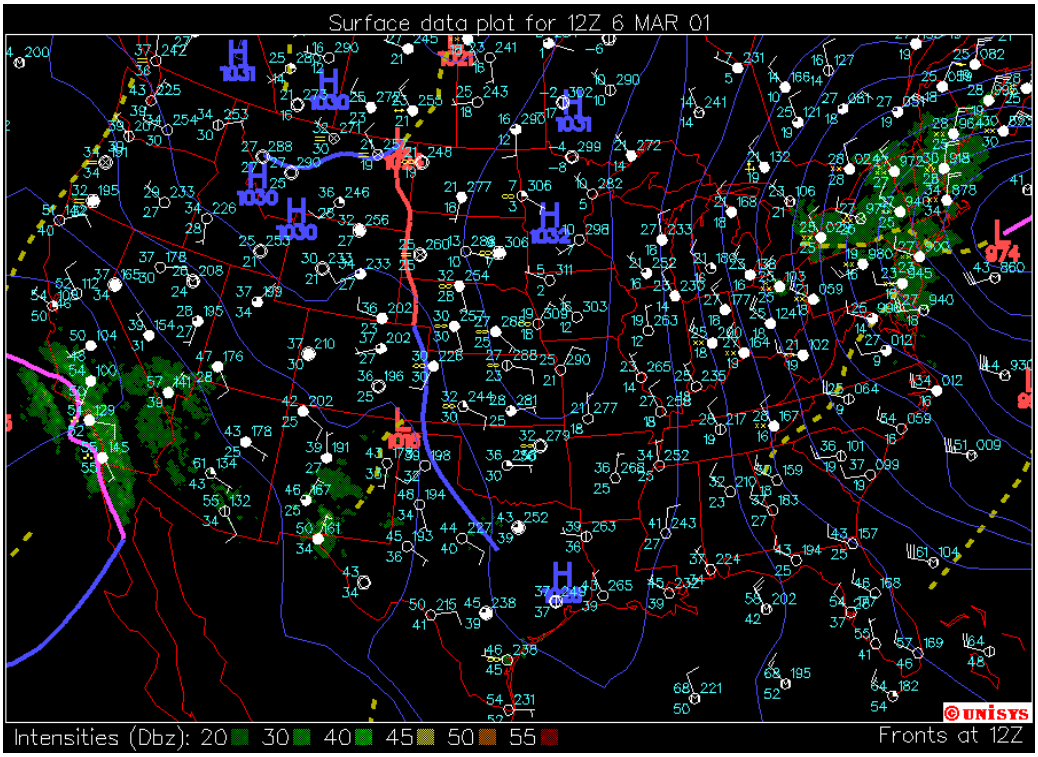

Figure 5.12. As in Figure 5.11 except for 1200 UTC 6 March 2001.

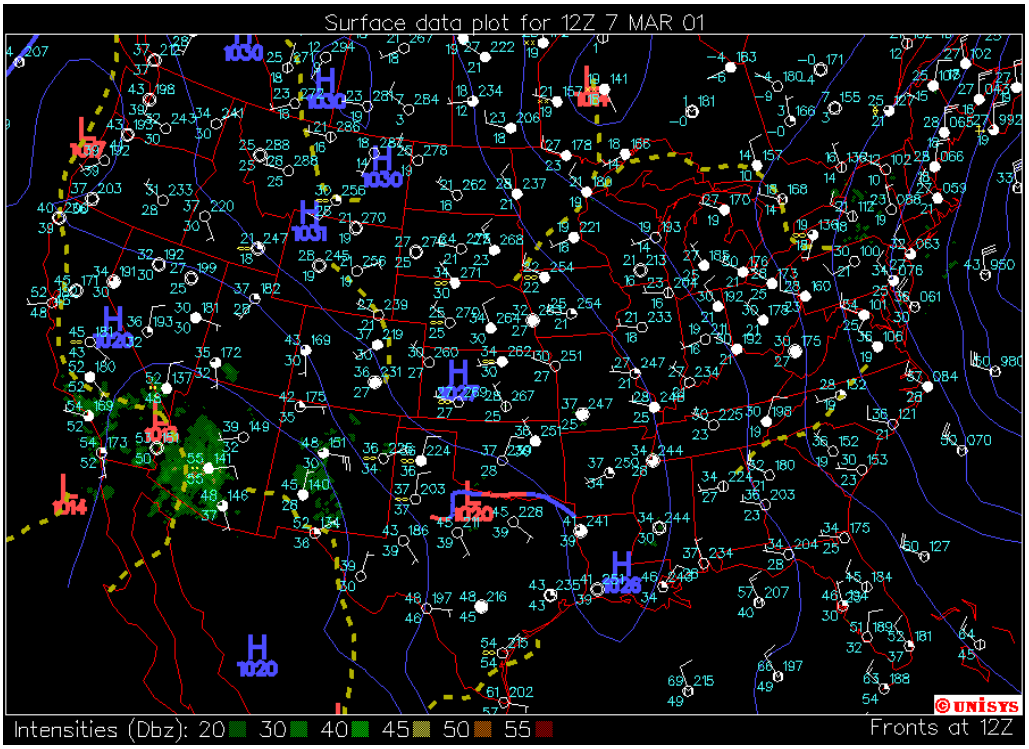

Figure 5.13. As in Figure 5.11 except for 1200 UTC 7 March 2001.

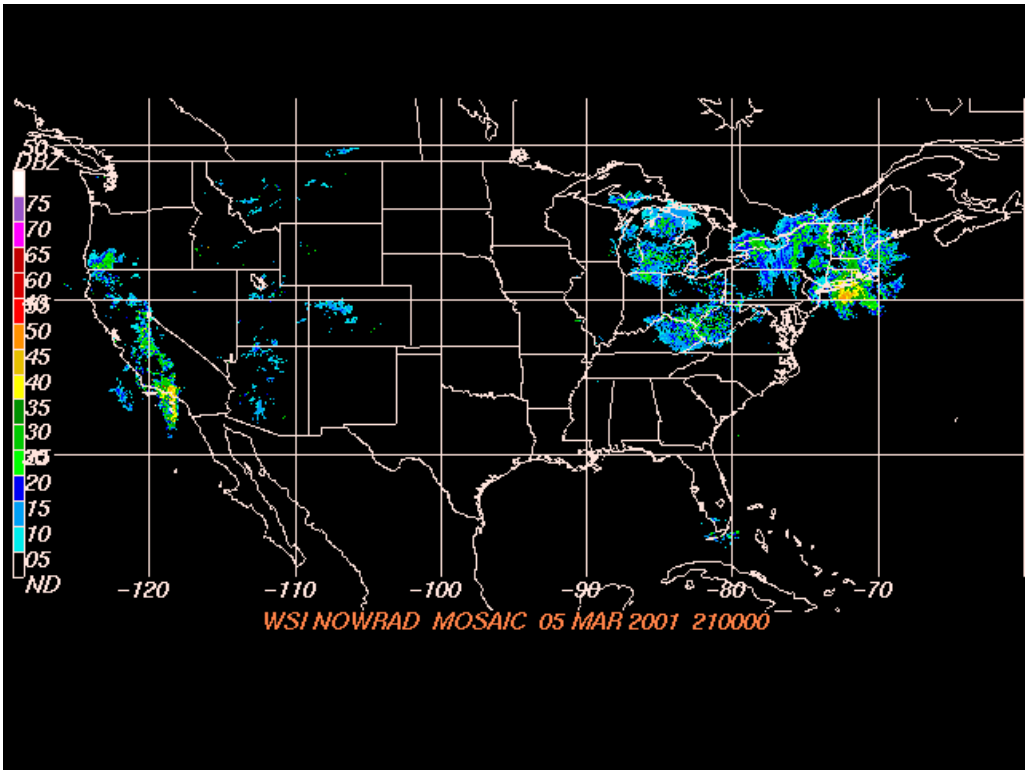

Figure 5.14. National mosaic composite reflectivity image from 2100 UTC 5 March 2001. Image from http://www4.ncdc.noaa.gov/cgi-win/wwcgi.dll?WWNEXRAD~Images2.

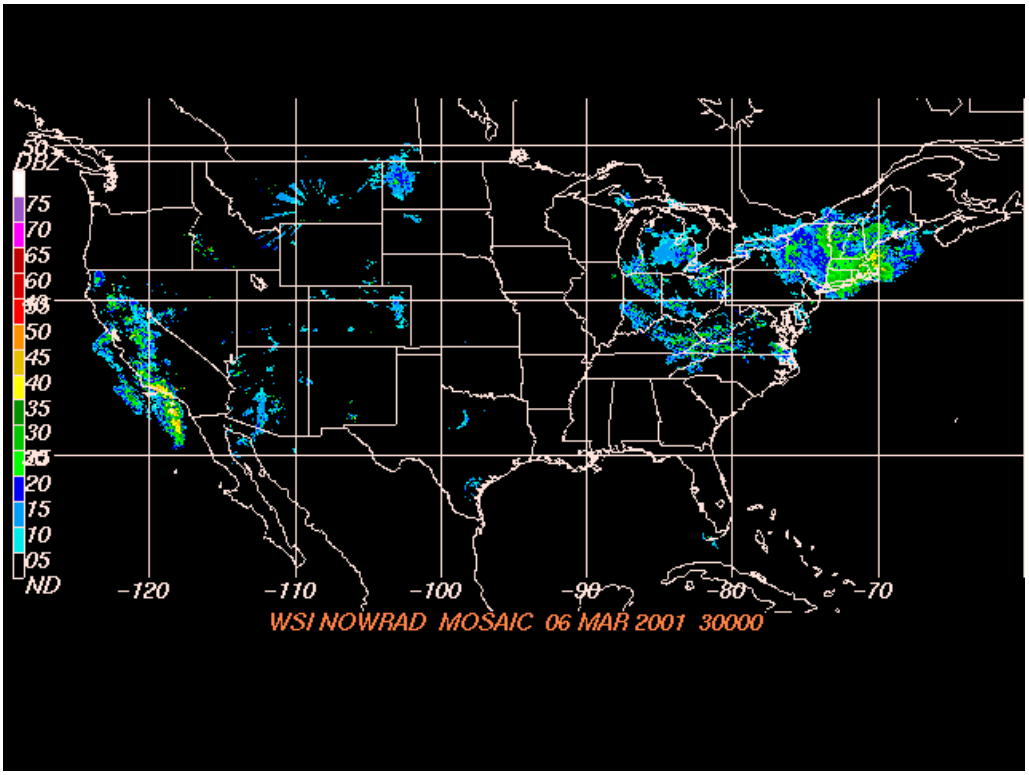

Figure 5.15. As in Figure 5.14 except for 0300 UTC 6 March 2001.

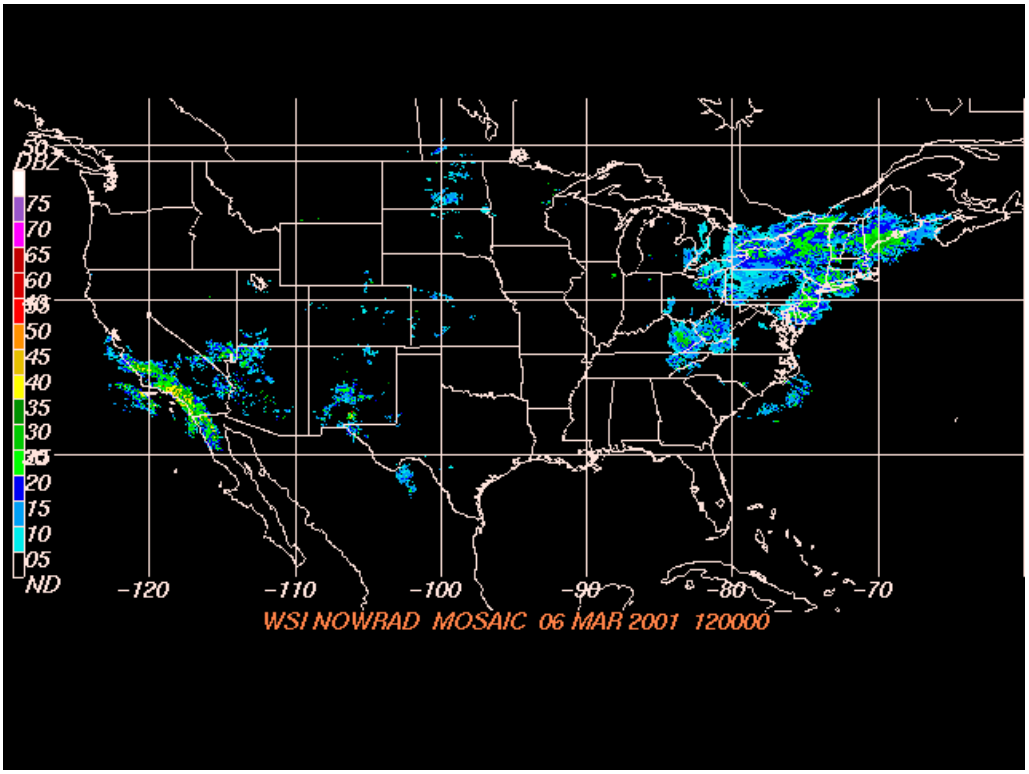

Figure 5.16. As in Figure 5.14 except for 1200 UTC 6 March 2001.

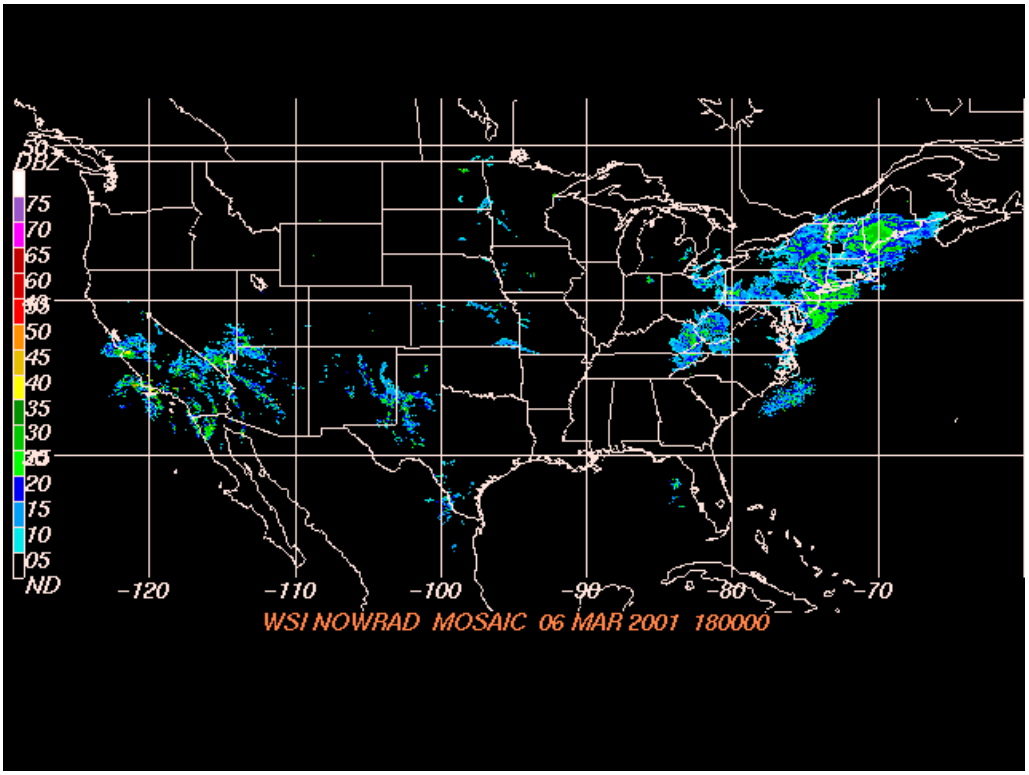

Figure 5.17. As in Figure 5.14 except for 1800 UTC 6 March 2001.

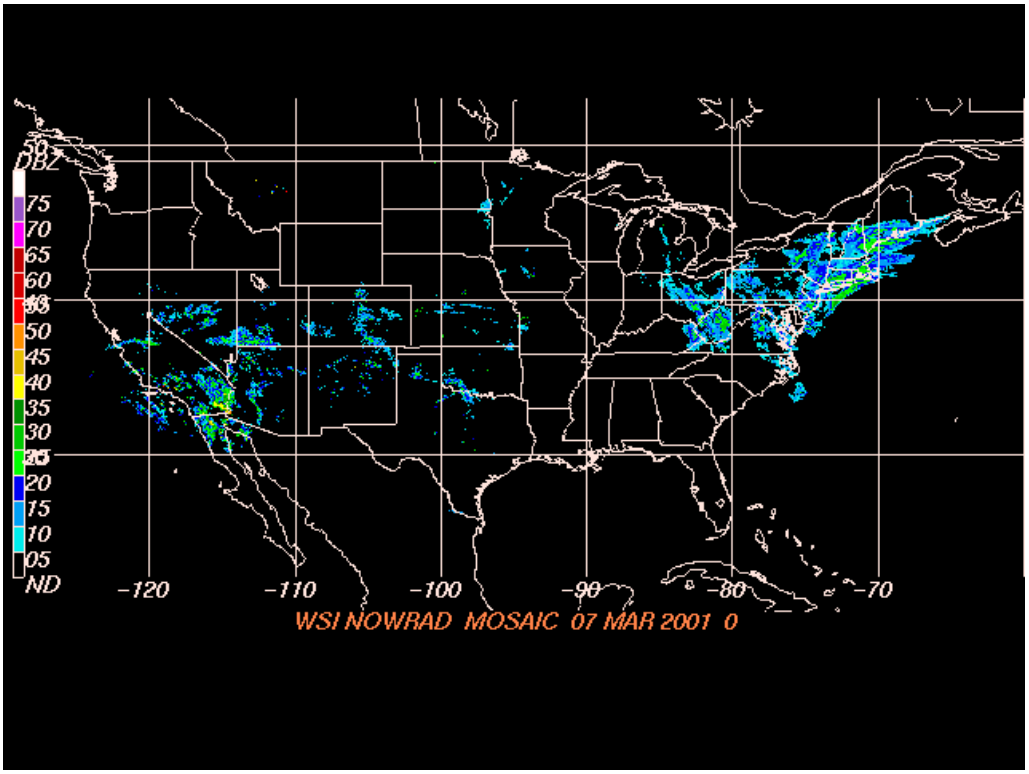

Figure 5.18. As in Figure 5.14 except for 0000 UTC 7 March 2001.

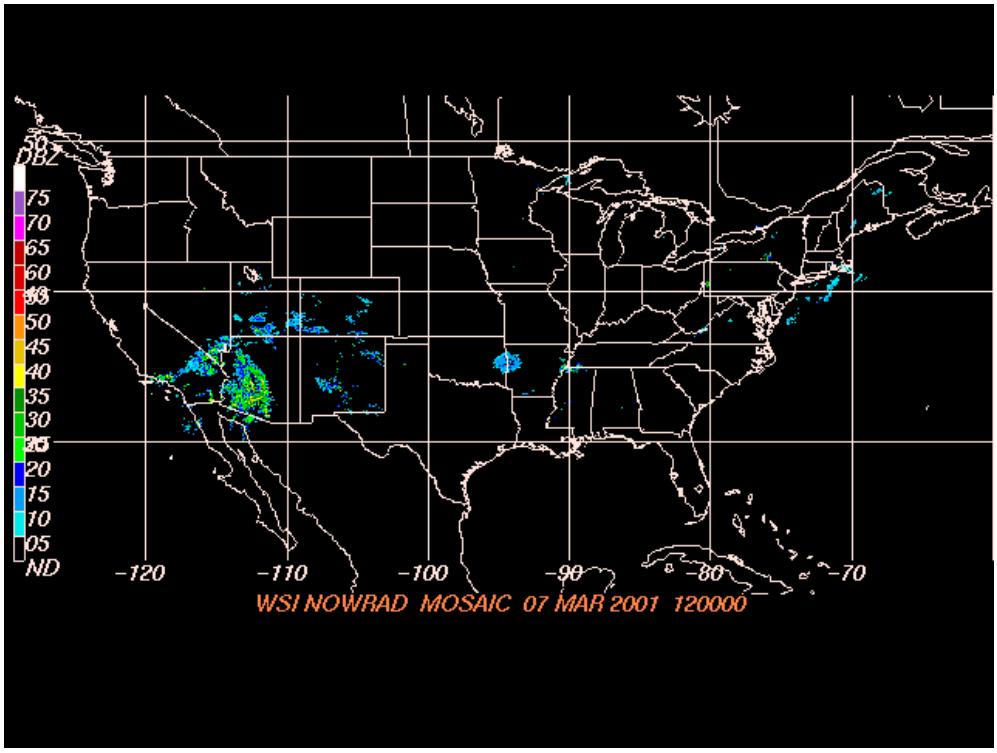

Figure 5.19. As in Figure 5.14 except for 1200 UTC 7 March 2001.

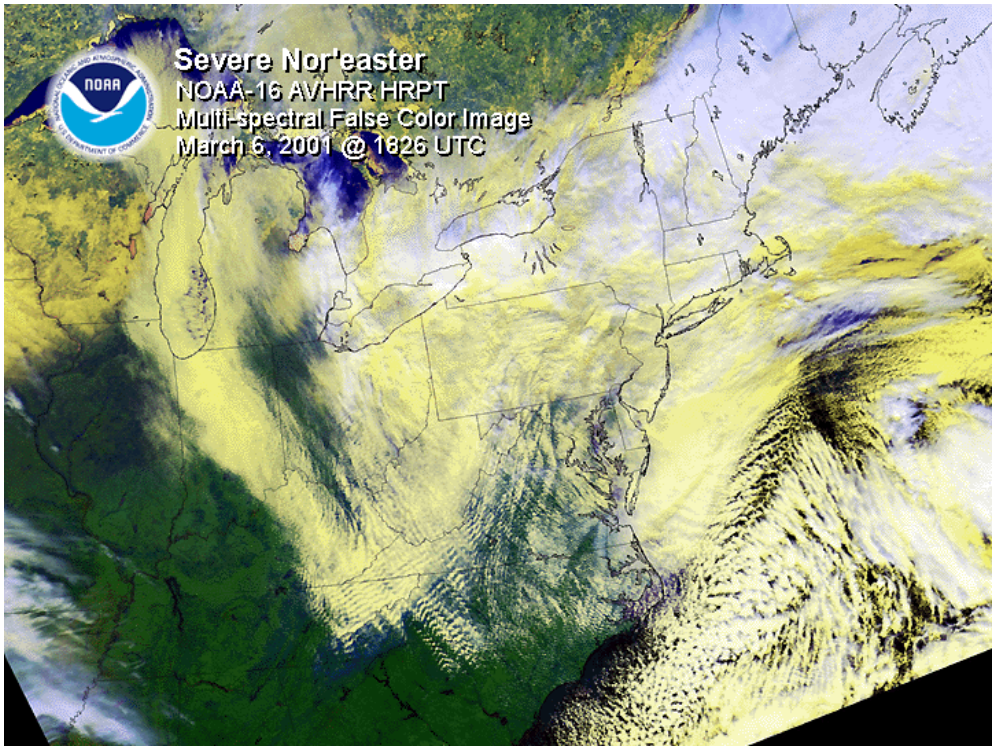

Figure 5.20. NOAA-16 multi-channel color composite image from 1826 UTC 6 March 2001. Image from http://www.osei.noaa.gov/.

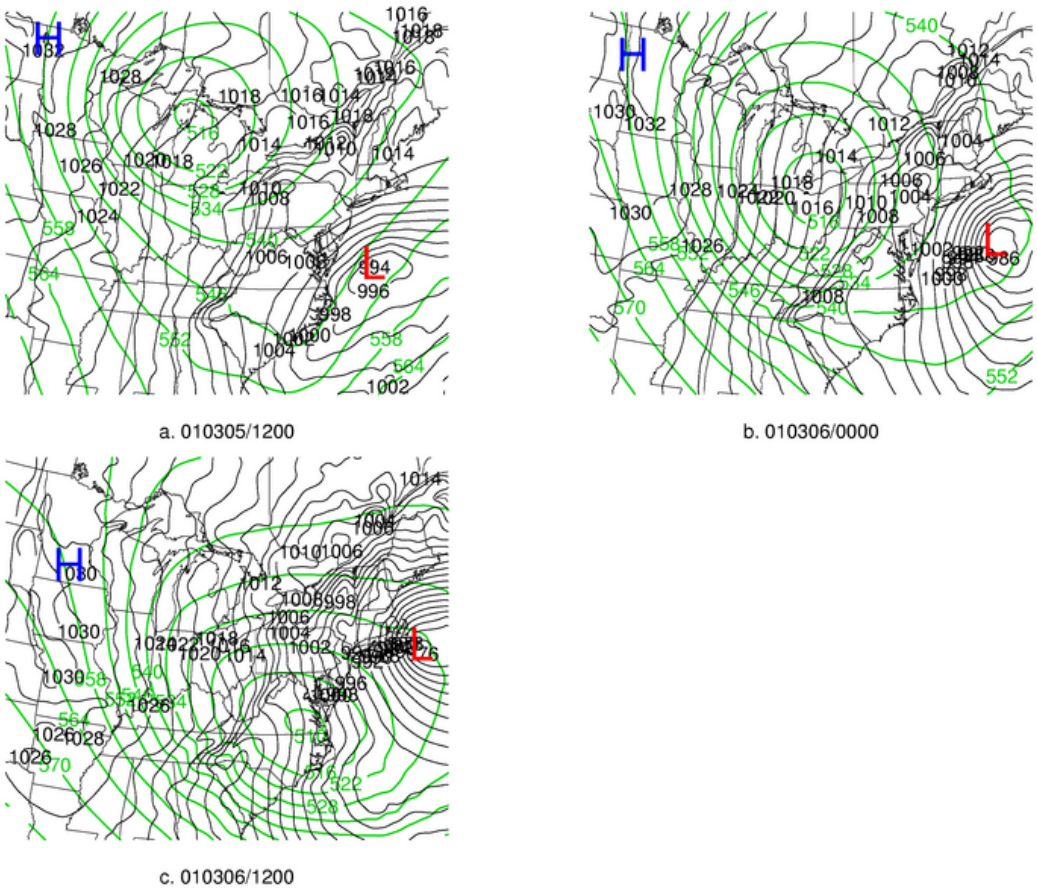

Figure 5.21. CTRL sea-level pressure (black solid contours, interval 2 hPa) and 500 hPa Geopotential height (green solid contours, interval 6 dam) for: (a) 1200 UTC 5 March 2001; (b) 0000 UTC 6 March 2001; (c) 1200 UTC 6 March 2001.

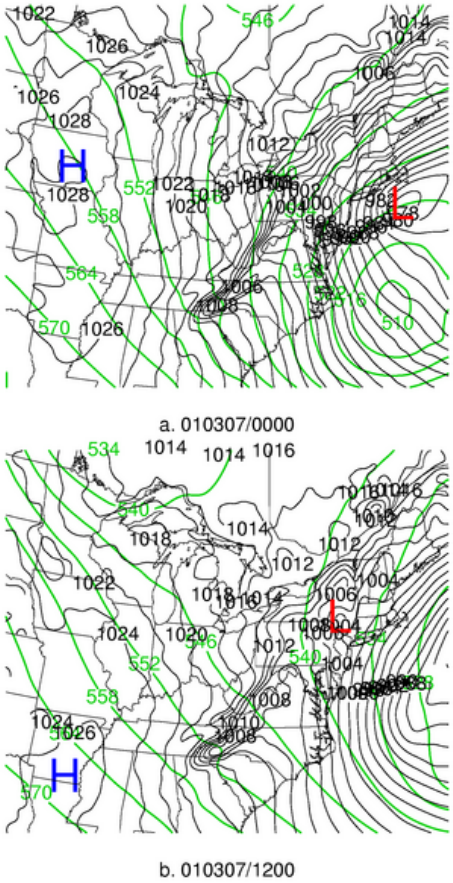

Figure 5.22. As in Figure 5.21 except for: (a) 0000 UTC 7 March 2001; (b) 1200 UTC 7 March 2001.

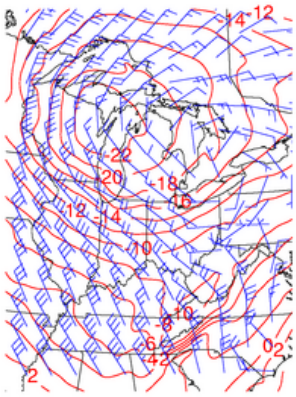

a. 010305/1200

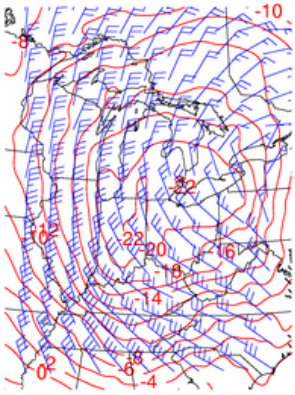

b. 010306/0000

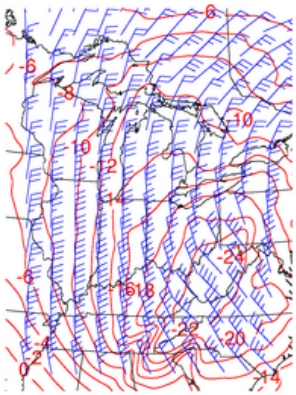

c. 010306/1200

Figure 5.23. CTRL 850 hPa temperature (°C, red solid, interval 2 °C) and winds (kt, barbs) for: (a) 1200 UTC 5 March 2001; (b) 0000 UTC 6 March 2001; (c) 1200 UTC 6 March 2001.

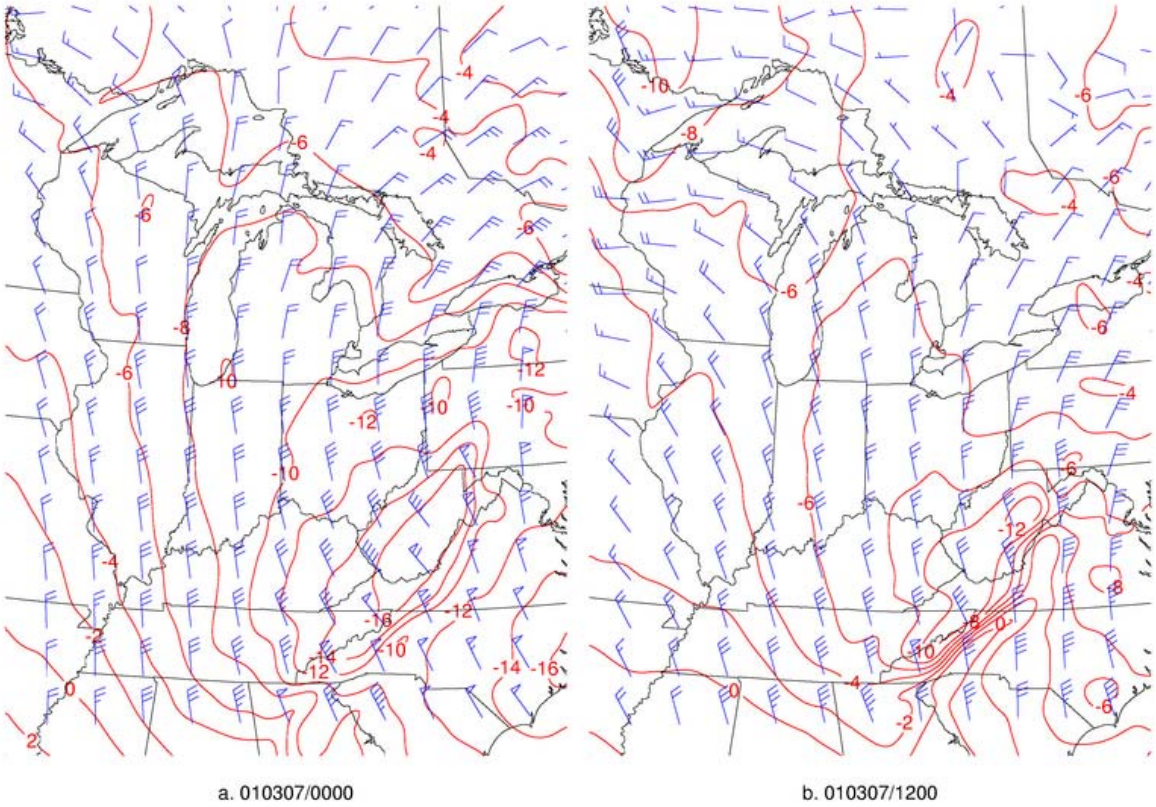

Figure 5.24. As in Figure 5.23 except for: (a) 0000 UTC 7 March 2001; (b) 1200 UTC 7 March 2001.

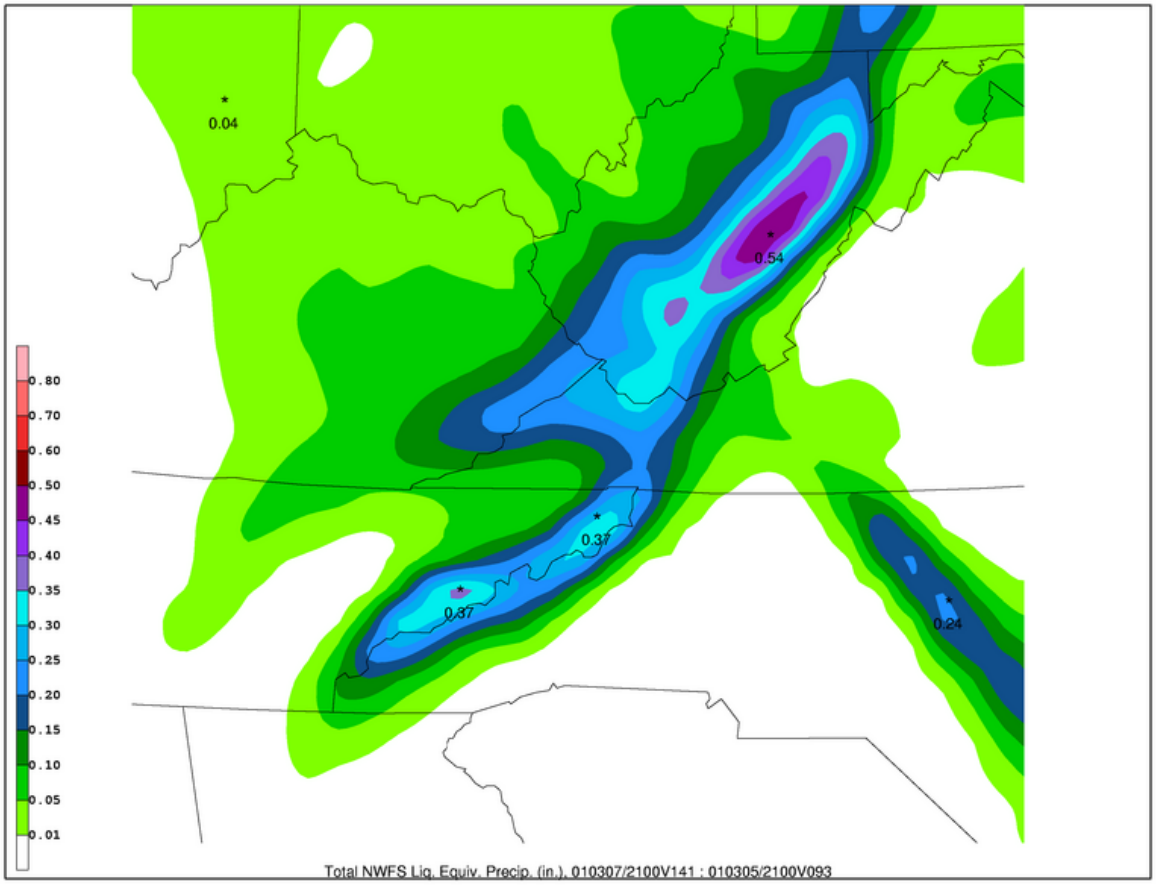

Figure 5.25. CTRL total liquid equivalent precipitation from 2100 UTC 5 March 2001 to 2100 UTC 7 March 2001 (inches, shaded as in colorbar in lower left corner).

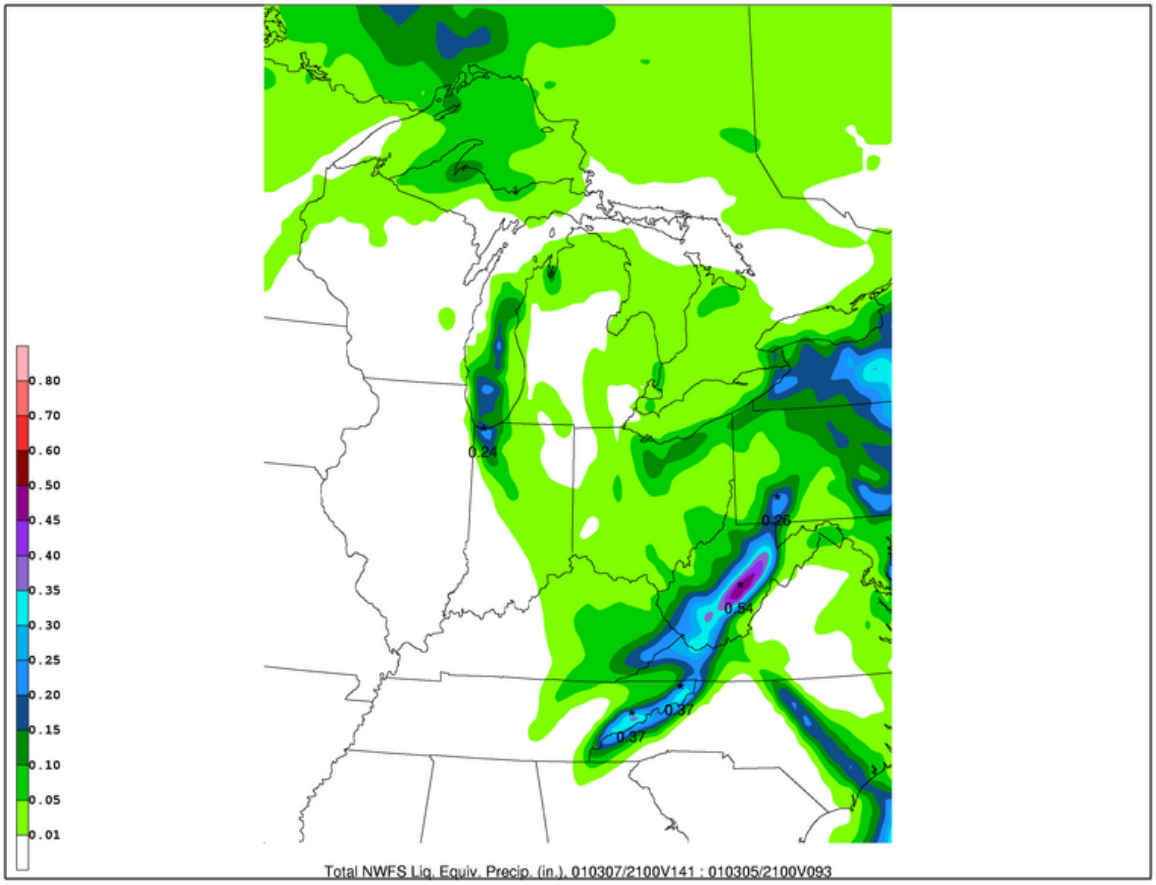

Figure 5.26. As in Figure 5.25 except larger view.

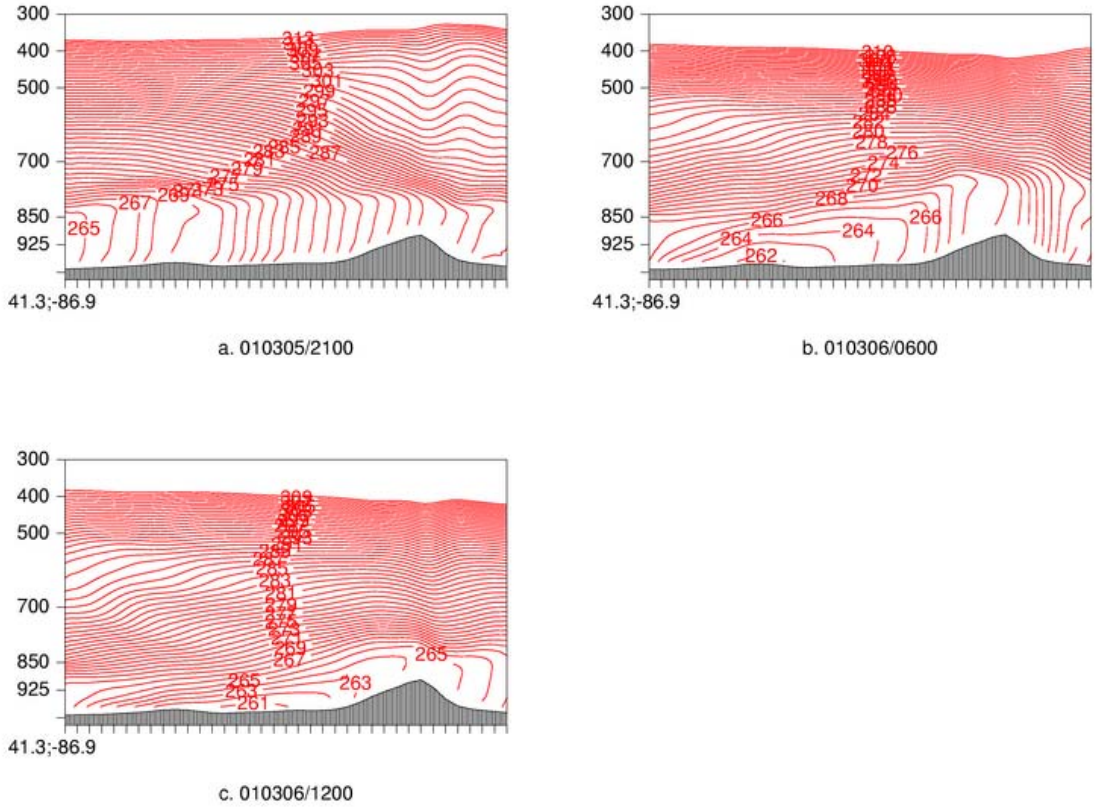

Figure 5.27. θ_e cross sections along the line shown in Figure 3.31 from CTRL: (a) 2100 UTC 5 March 2001; (b) 0600 UTC 6 March 2001; (c) 1200 UTC 6 March 2001.

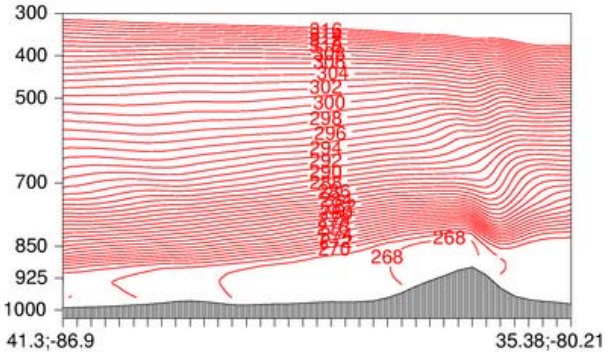

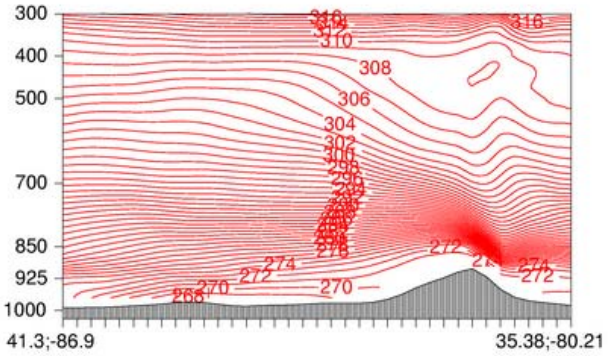

Figure 5.28. As in Figure 5.27 except for: (a) 1800 UTC 6 March 2001; (b) 0600 UTC 7 March 2001.

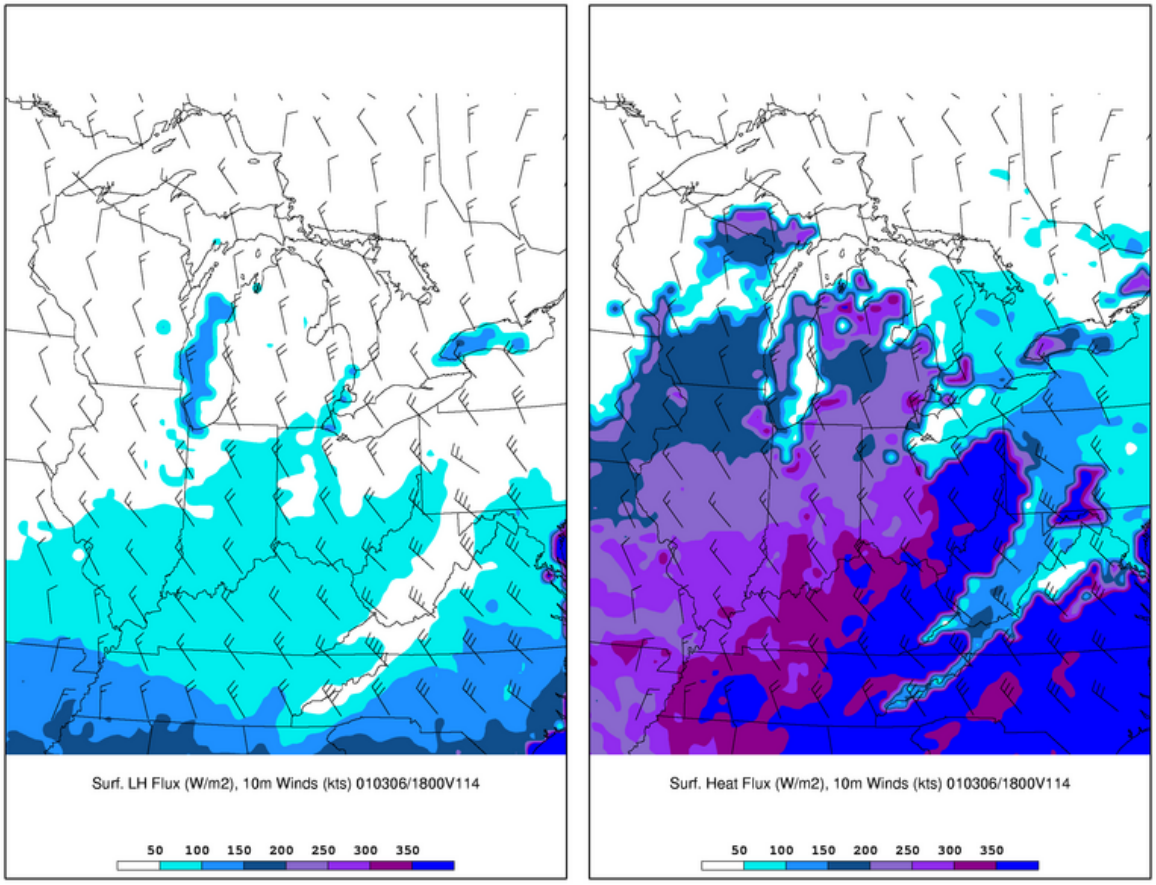

Figure 5.29. CTRL surface latent and sensible heat fluxes (W/m^2, shaded as in colorbar in lower center), and 10 m winds (kt, barbs) for 1800 UTC 6 March 2001.

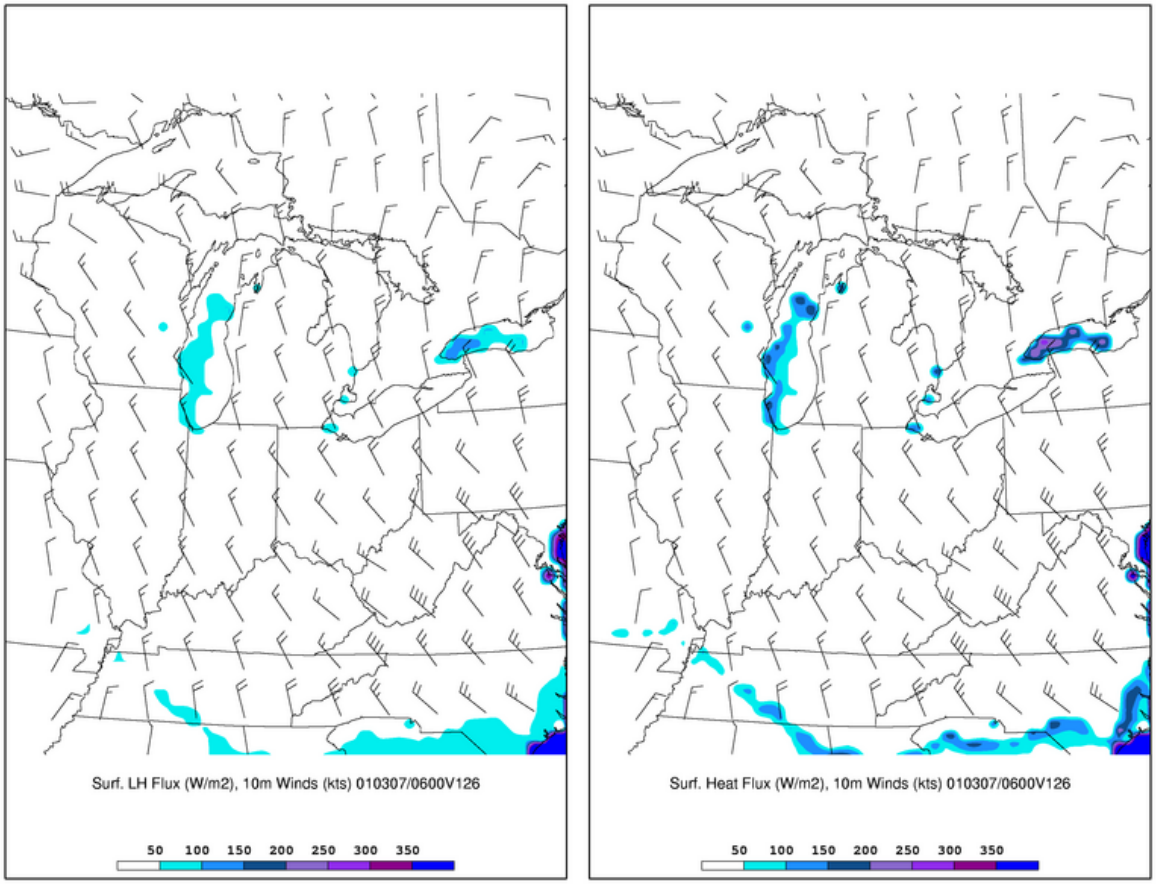

Figure 5.30. As in Figure 5.29 except for 0600 UTC 7 March 2001.

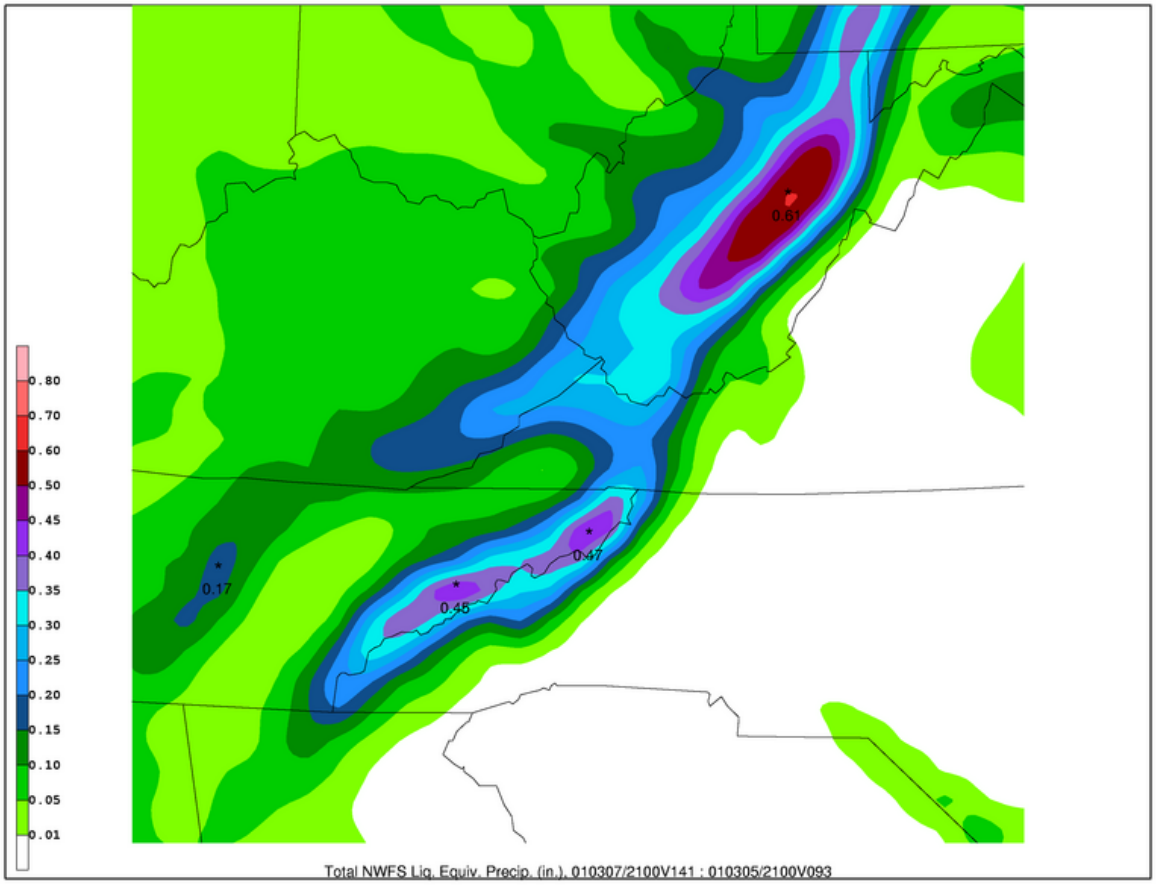

Figure 5.31. MYJPBL total liquid equivalent precipitation from 2100 UTC 5 March 2001 to 2100 UTC 7 March 2001 (inches, shaded as in colorbar in lower left corner).

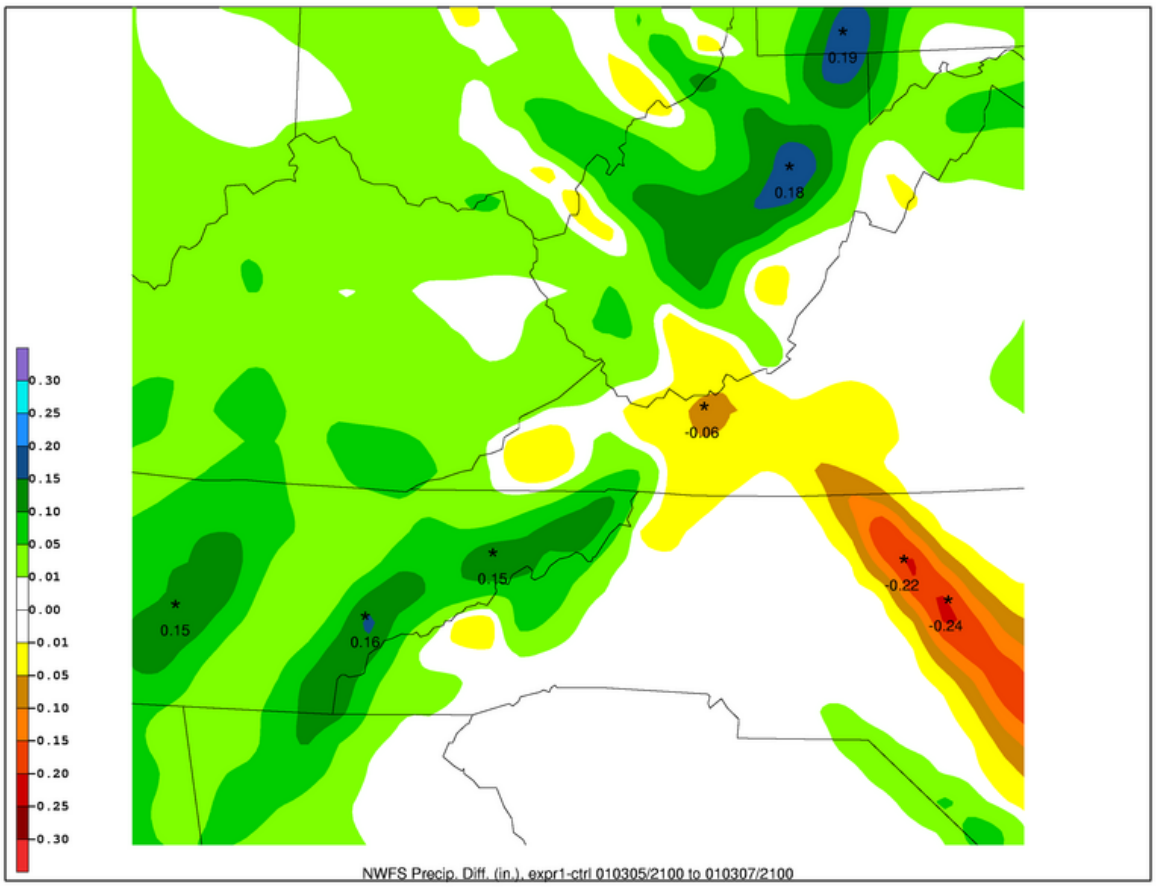

Figure 5.32. Difference field of liquid equivalent precipitation, MYJPBL-CTRL, from 2100 UTC 5 March 2001 to 2100 UTC 7 March 2001 (inches, shaded as in colorbar in lower left).

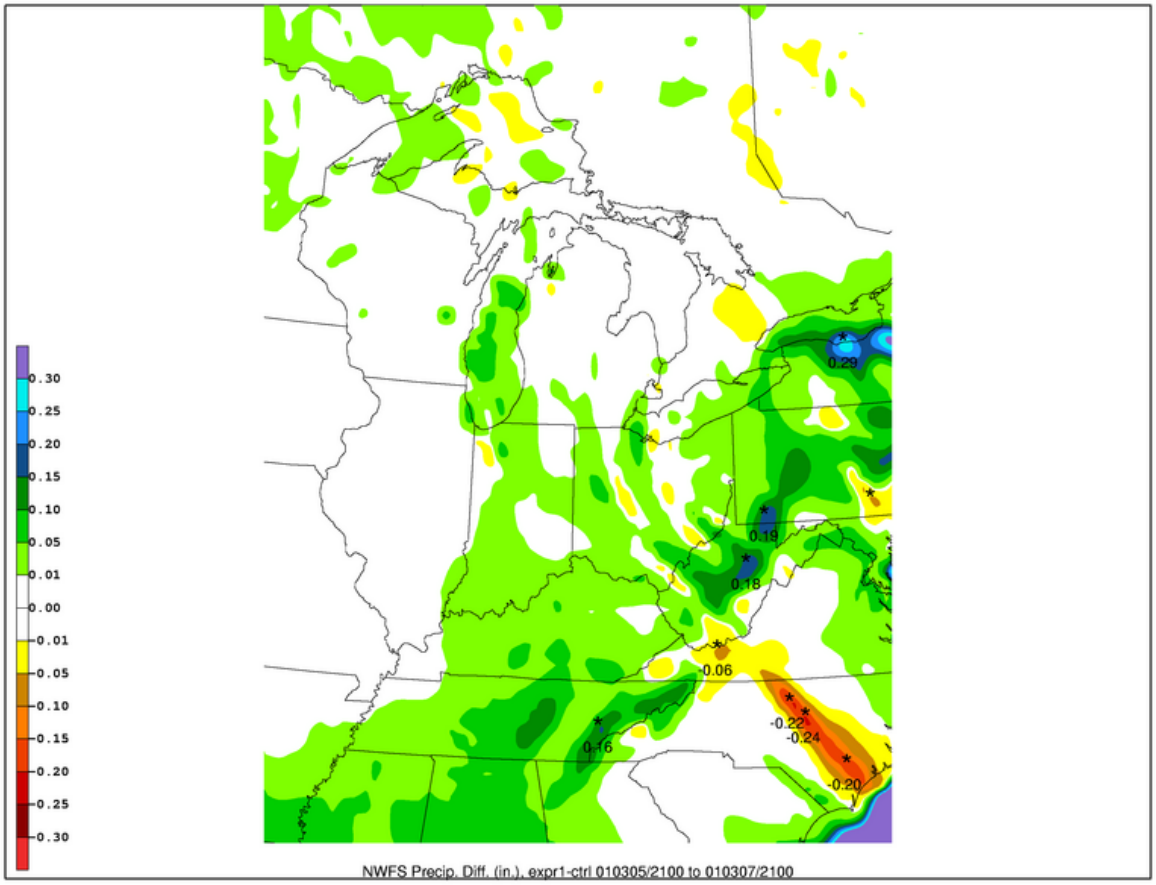

Figure 5.33. As in Figure 5.32 except larger view.

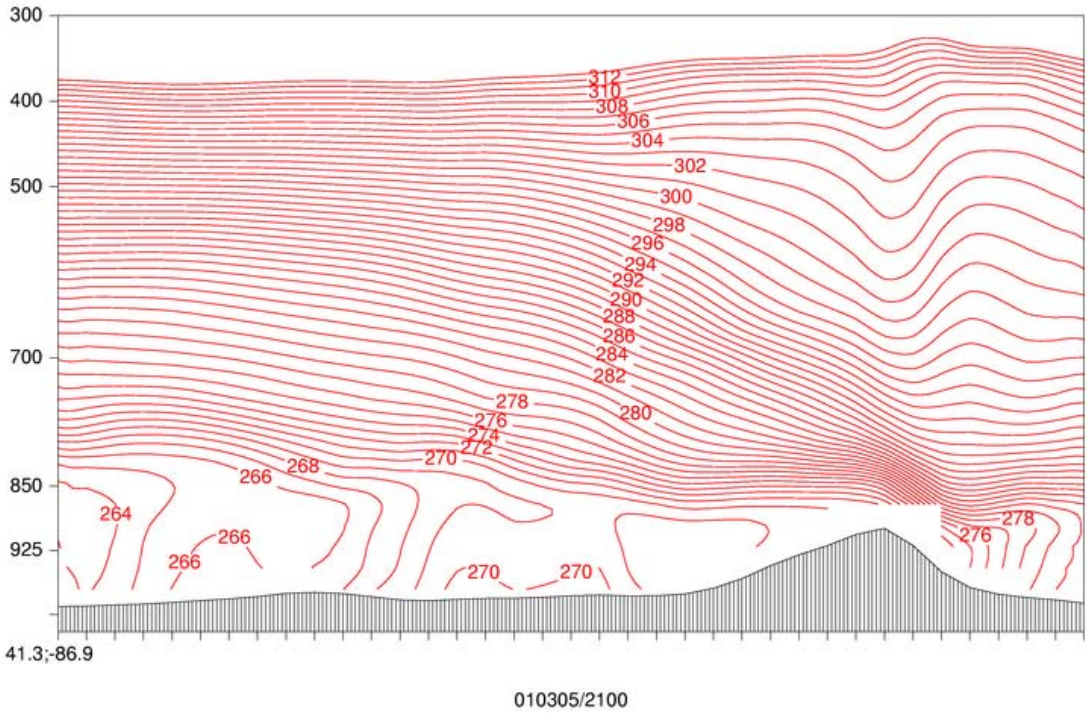

Figure 5.34. As in Figure 5.27 except from MYJPBL for 2100 UTC 5 March 2001.

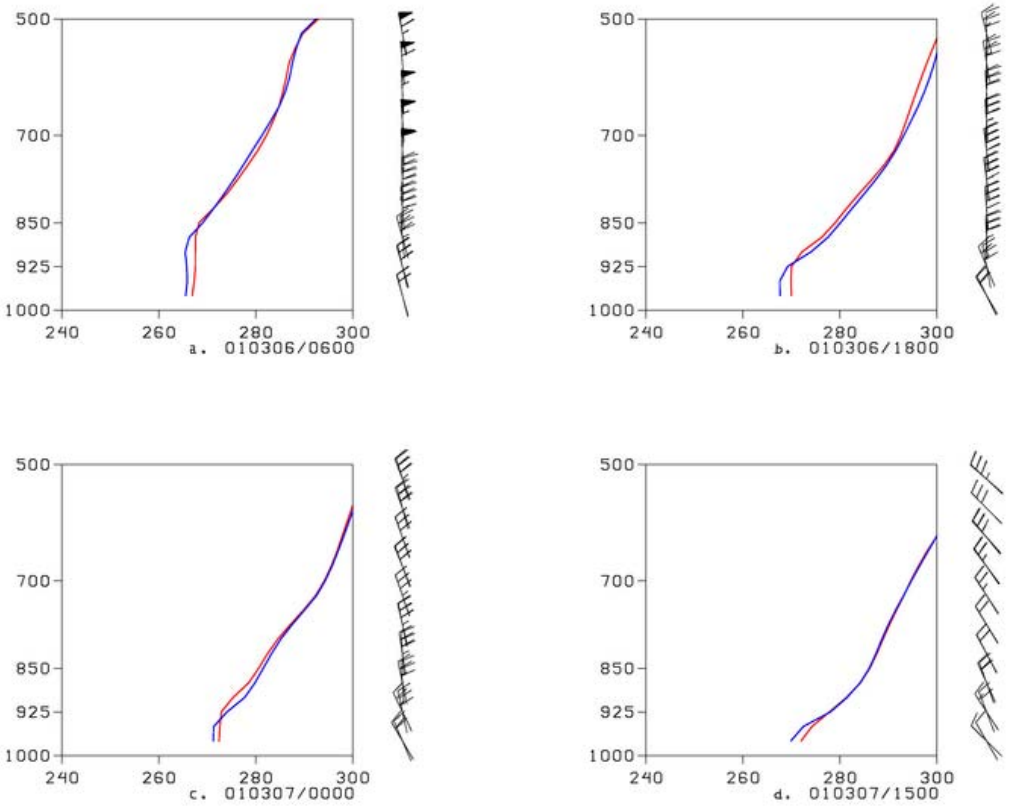

Figure 5.35. θ_e (K) profiles at La Crosse, IN (41.3 N;-86.9 W) for CTRL (red) and MYJPBL (blue) at: (a) 0600 UTC 6 March 2001; (b) 1800 UTC 6 March 2001; (c) 0000 UTC 7 March 2001; (d) 1500 UTC 7 March 2001.

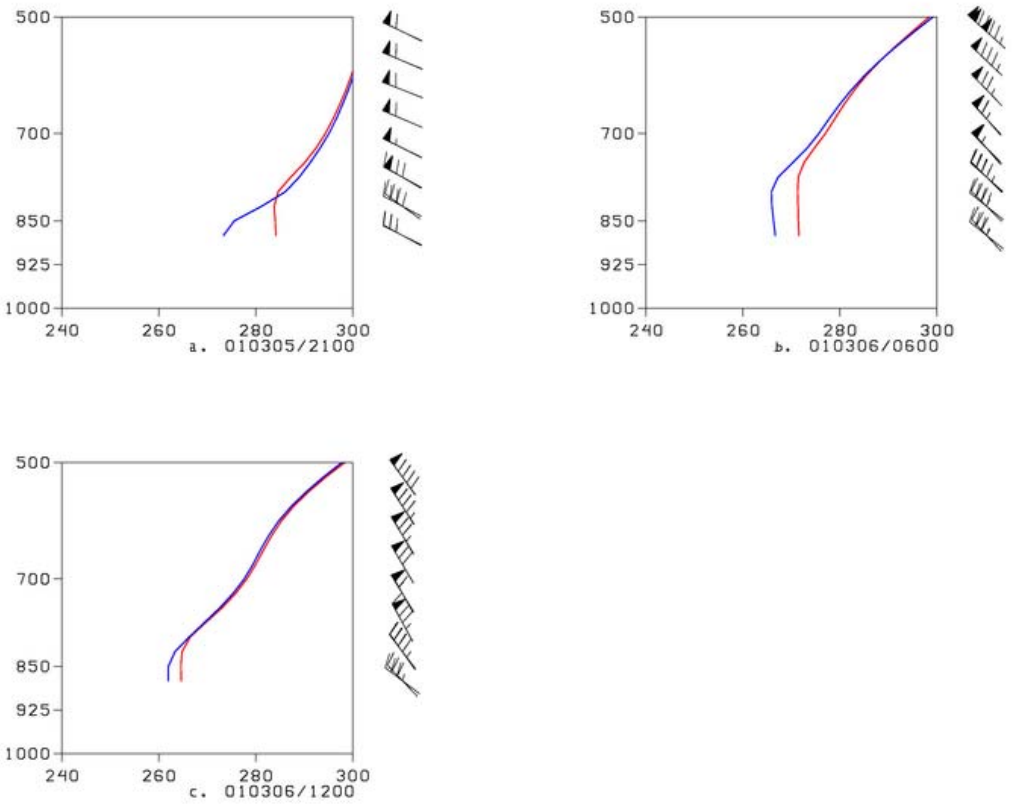

Figure 5.36. θ_e (K) profiles at Erwin, TN (36.14 N;-82.39 W) for CTRL (red) and MYJPBL (blue) at: (a) 2100 UTC 5 March 2001; (b) 0600 UTC 6 March 2001; (c) 1200 UTC 6 March 2001.

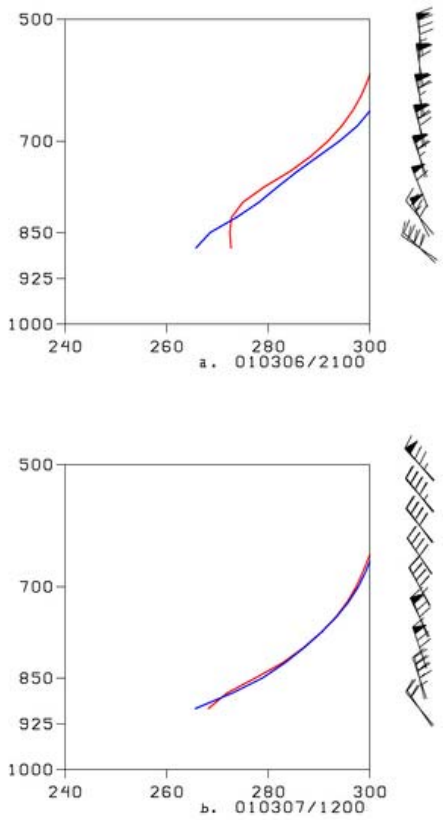

Figure 5.37. As in Figure 5.36 except for: (a) 2100 UTC 6 March 2001; (b) 1200 UTC 7 March 2001.

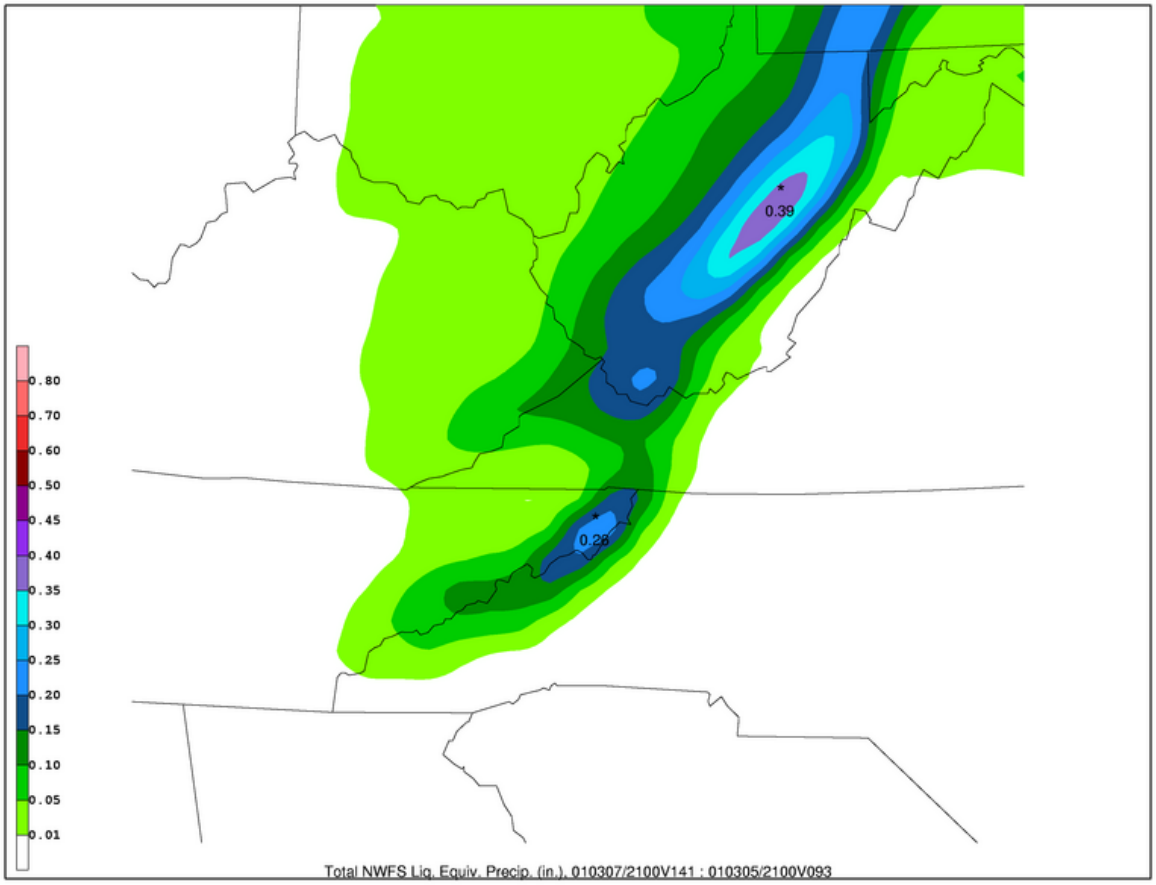

Figure 5.38. NOFLX total liquid equivalent precipitation from 2100 UTC 5 March 2001 to 2100 UTC 7 March 2001 (inches, shaded as in colorbar in lower left corner).

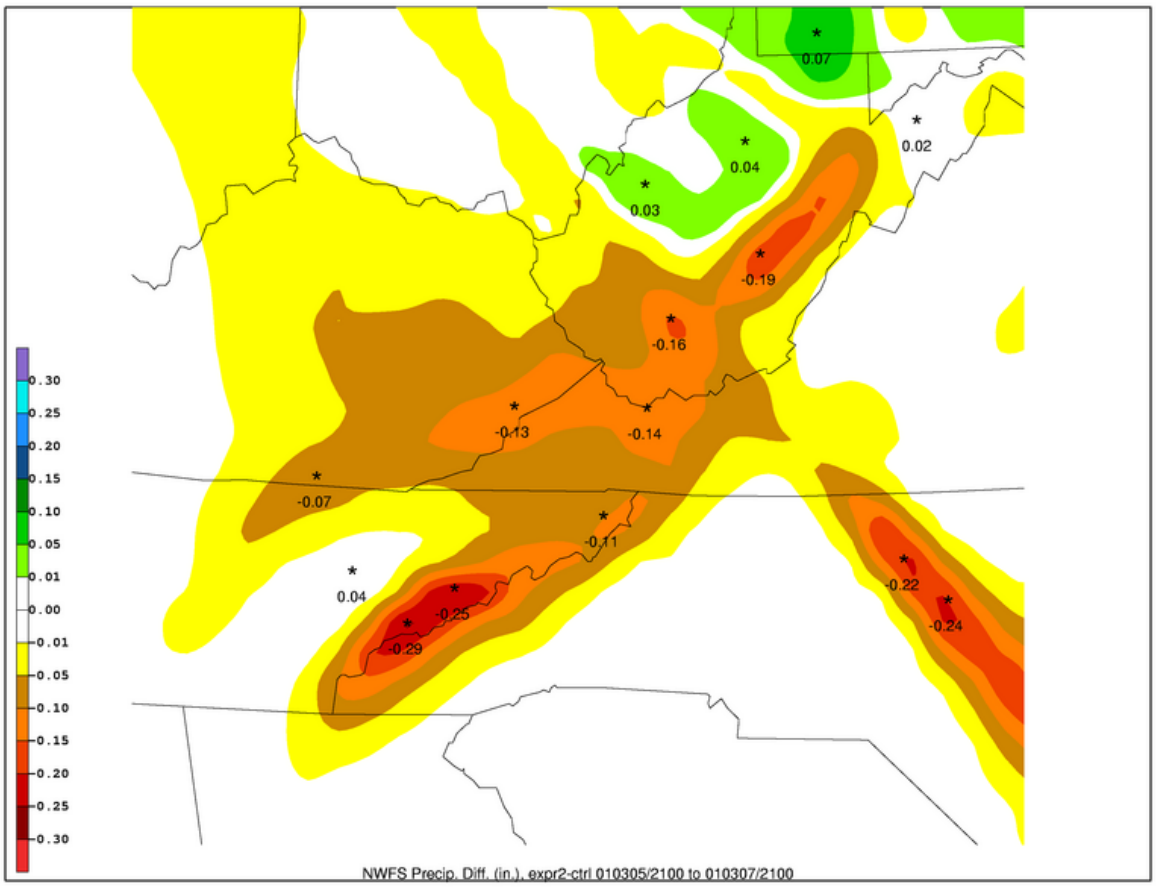

Figure 5.39. Difference field of liquid equivalent precipitation, NOFLX-CTRL, from 2100 UTC 5 March 2001 to 2100 UTC 7 March 2001 (inches, shaded as in colorbar in lower left).

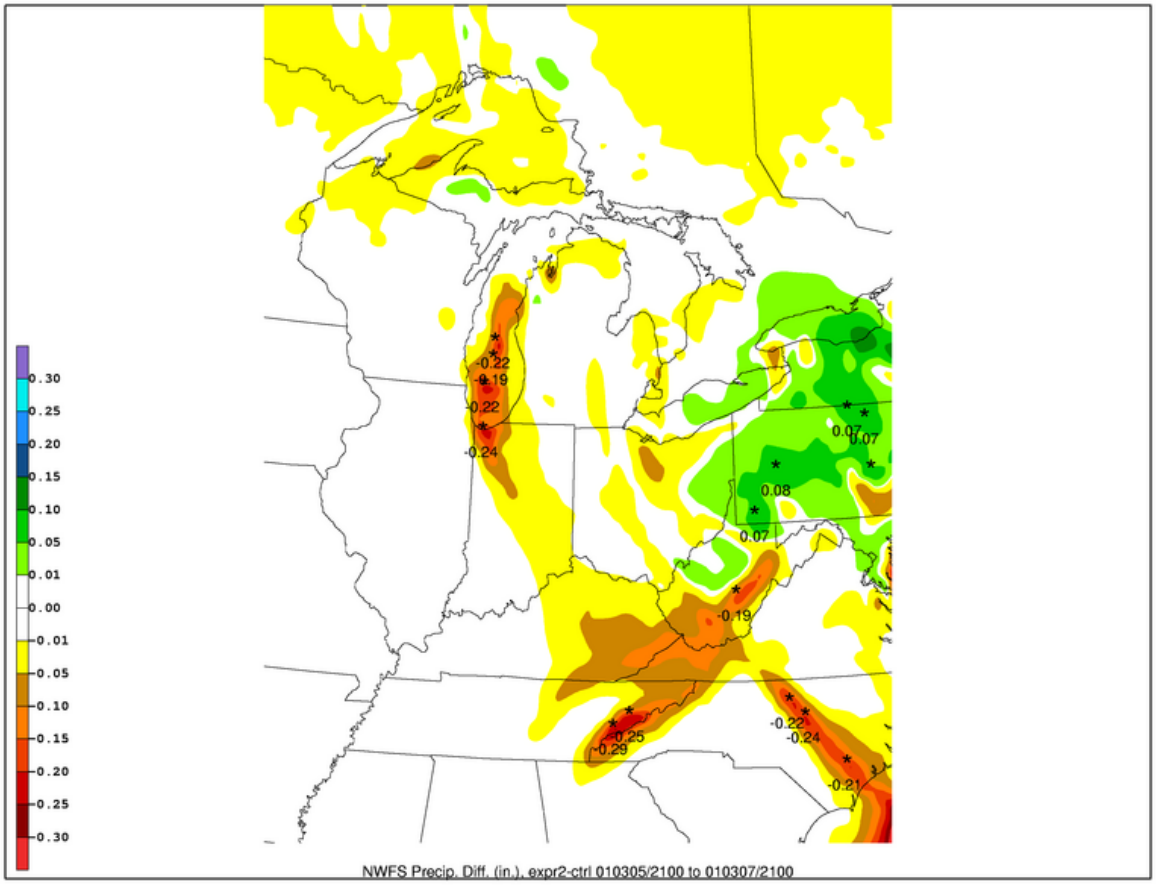

Figure 5.40. As in Figure 5.39 except larger view.

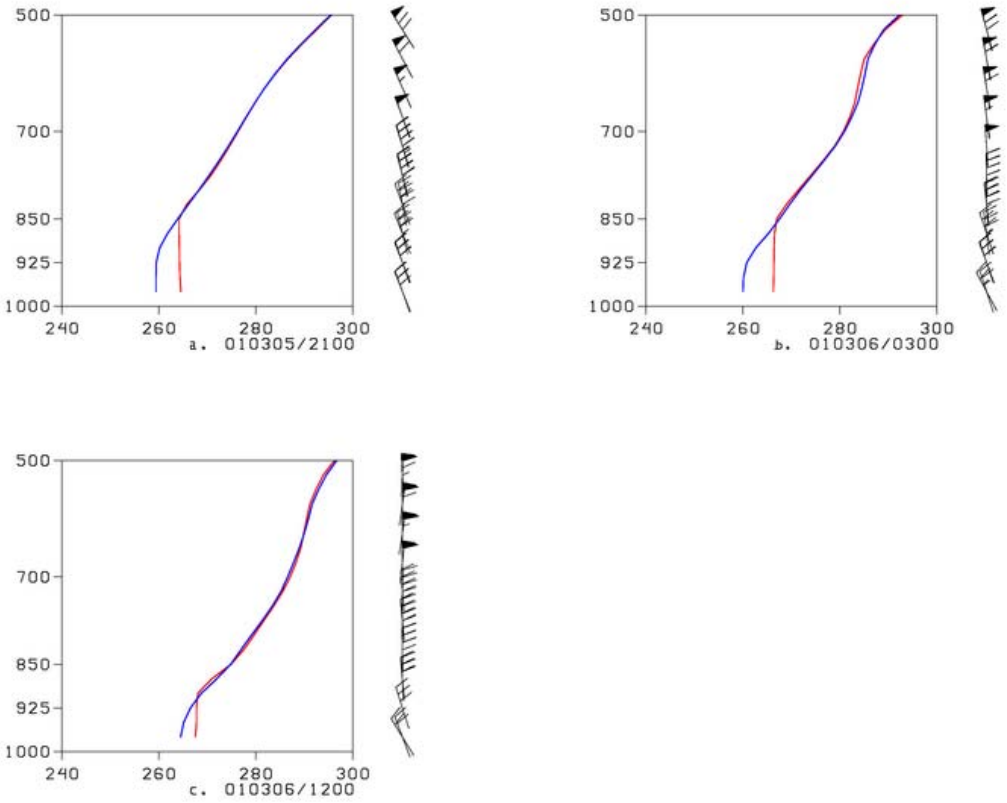

Figure 5.41. θ_e (K) profiles at La Crosse, IN (41.3 N;-86.9 W) for CTRL (red) and NOFLX (blue) at: (a) 2100 UTC 5 March 2001; (b) 0300 UTC 6 March 2001; (c) 1200 UTC 6 March 2001.

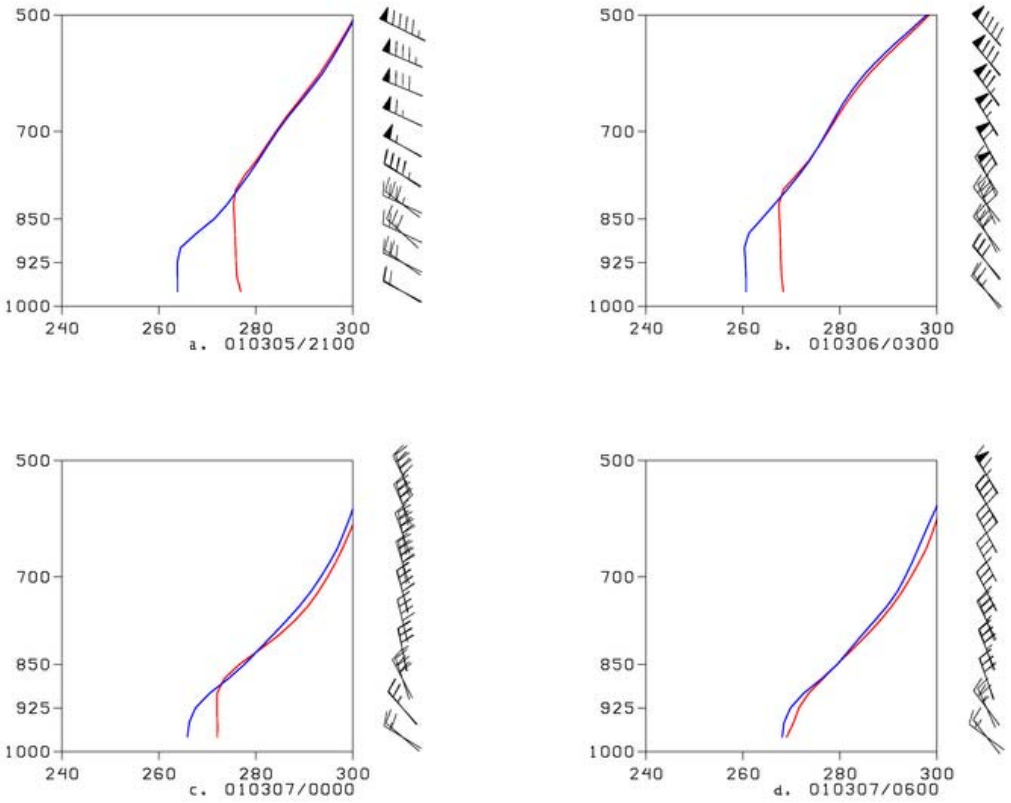

Figure 5.42. θ_e (K) profiles at Lexington, KY (38.03 N; -84.44 W) for CTRL (red) and NOFLX (blue) at: (a) 2100 UTC 5 March 2001; (b) 0300 UTC 6 March 2001; (c) 0000 UTC 7 March 2001; (d) 0600 UTC 7 March 2001.

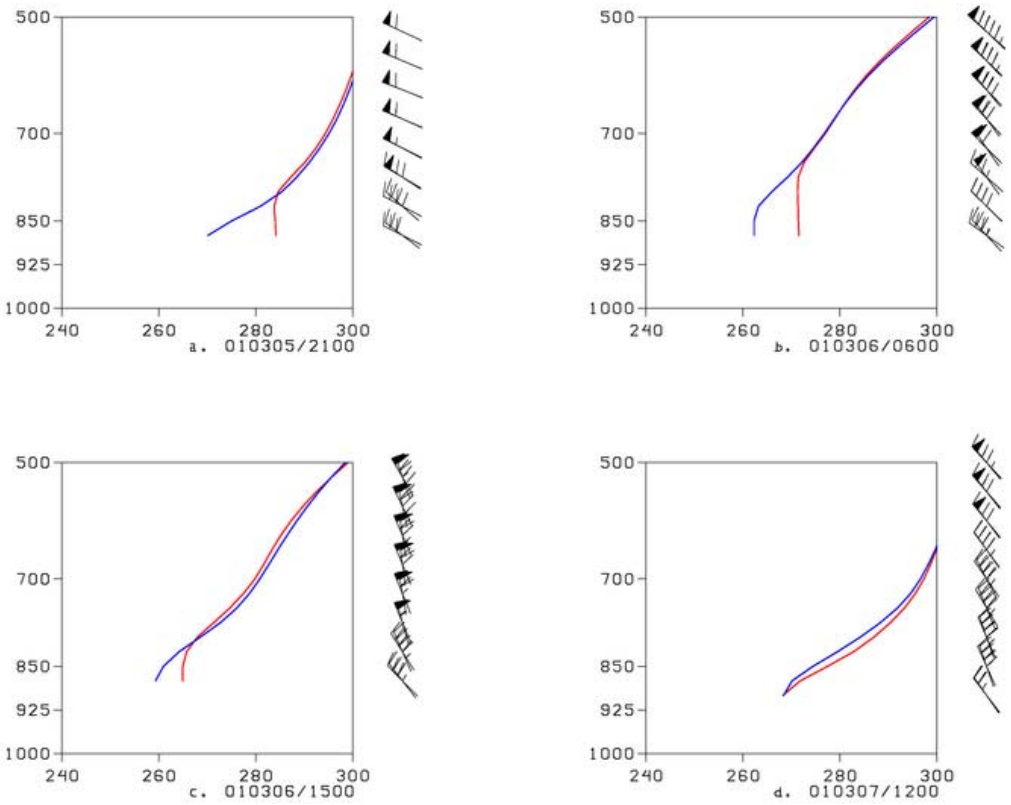

Figure 5.43. θ_e (K) profiles at Erwin, TN (36.14 N;-82.39 W) for CTRL (red) and NOFLX (blue) at: (a) 2100 UTC 5 March 2001; (b) 0600 UTC 6 March 2001; (c) 1500 UTC 6 March 2001; (d) 1200 UTC 7 March 2001.

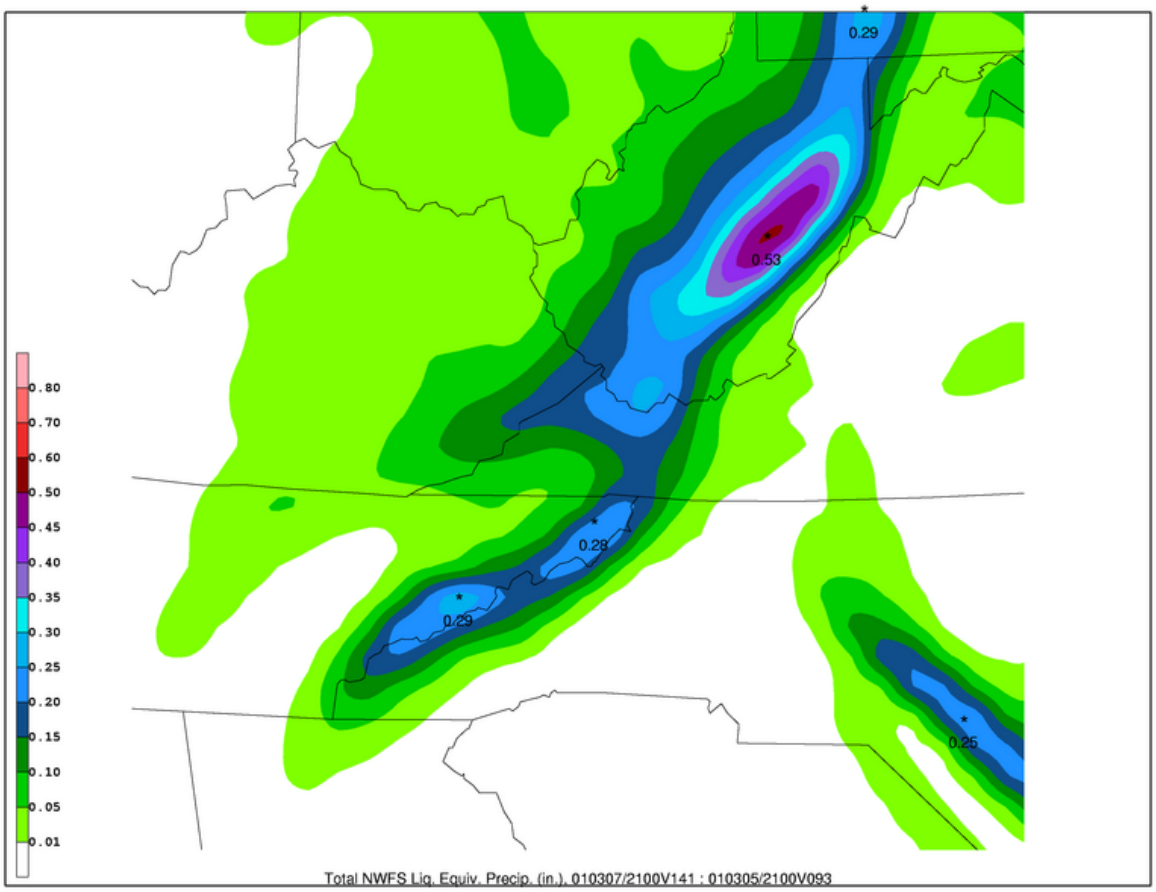

Figure 5.44. LKNOFLX total liquid equivalent precipitation from 2100 UTC 5 March 2001 to 2100 UTC 7 March 2001 (inches, shaded as in colorbar in lower left corner).

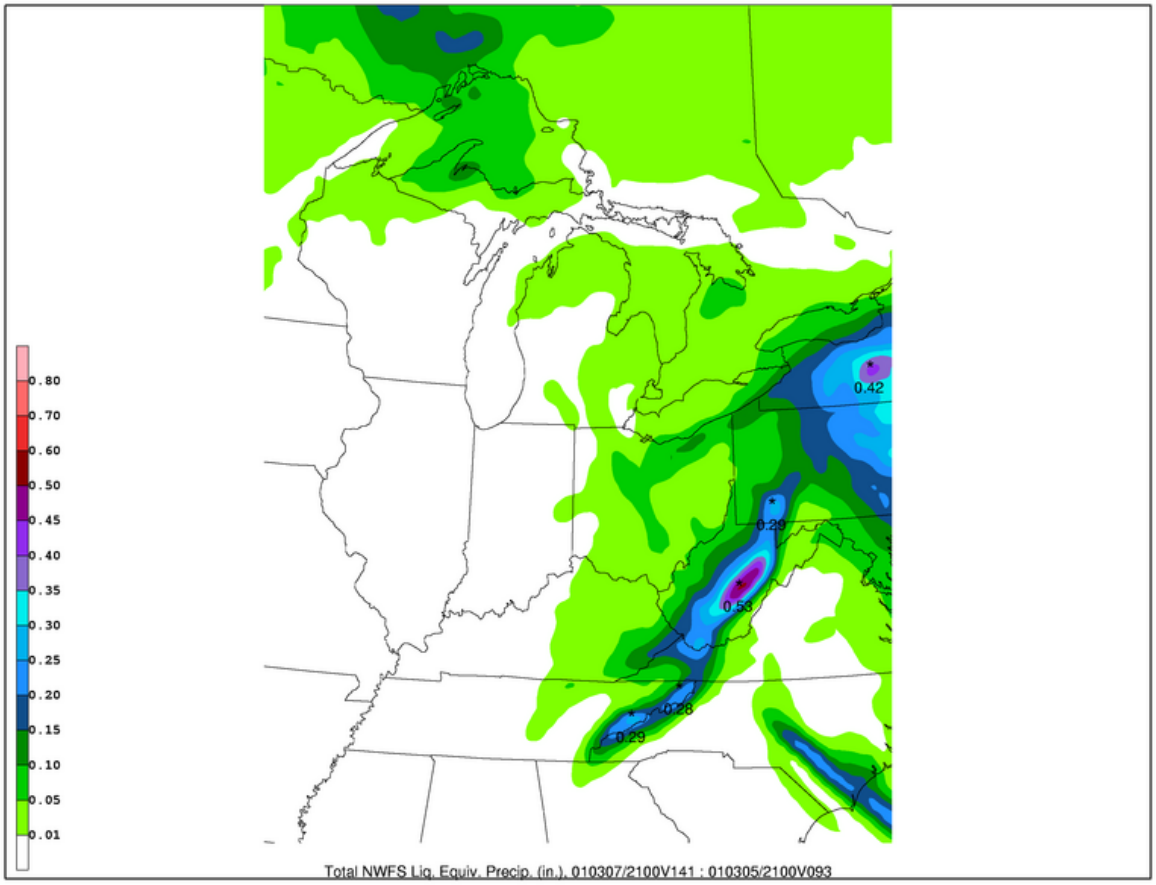

Figure 5.45. As in Figure 5.44 except larger view.

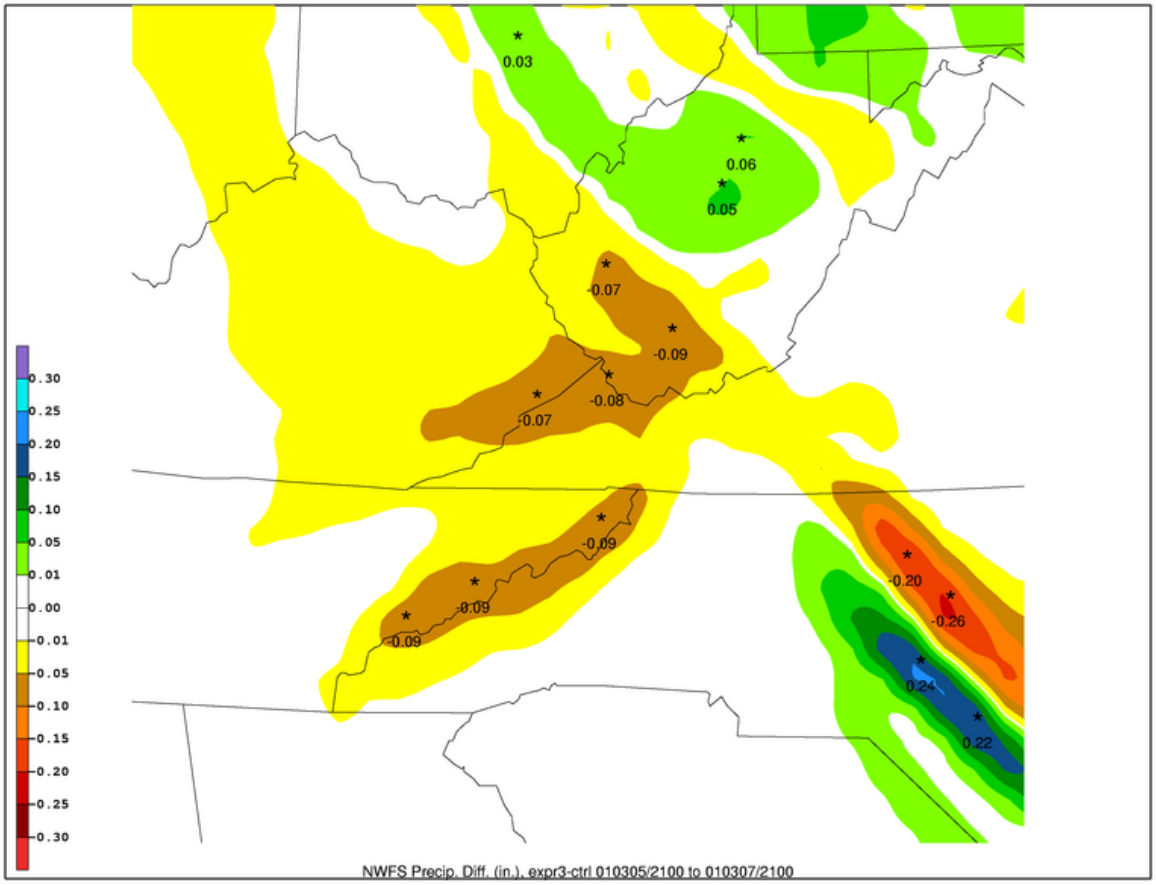

Figure 5.46. Difference field of liquid equivalent precipitation, LKNOFLX-CTRL, from 2100 UTC 5 March 2001 to 2100 UTC 7 March 2001 (inches, shaded as in colorbar in lower left).

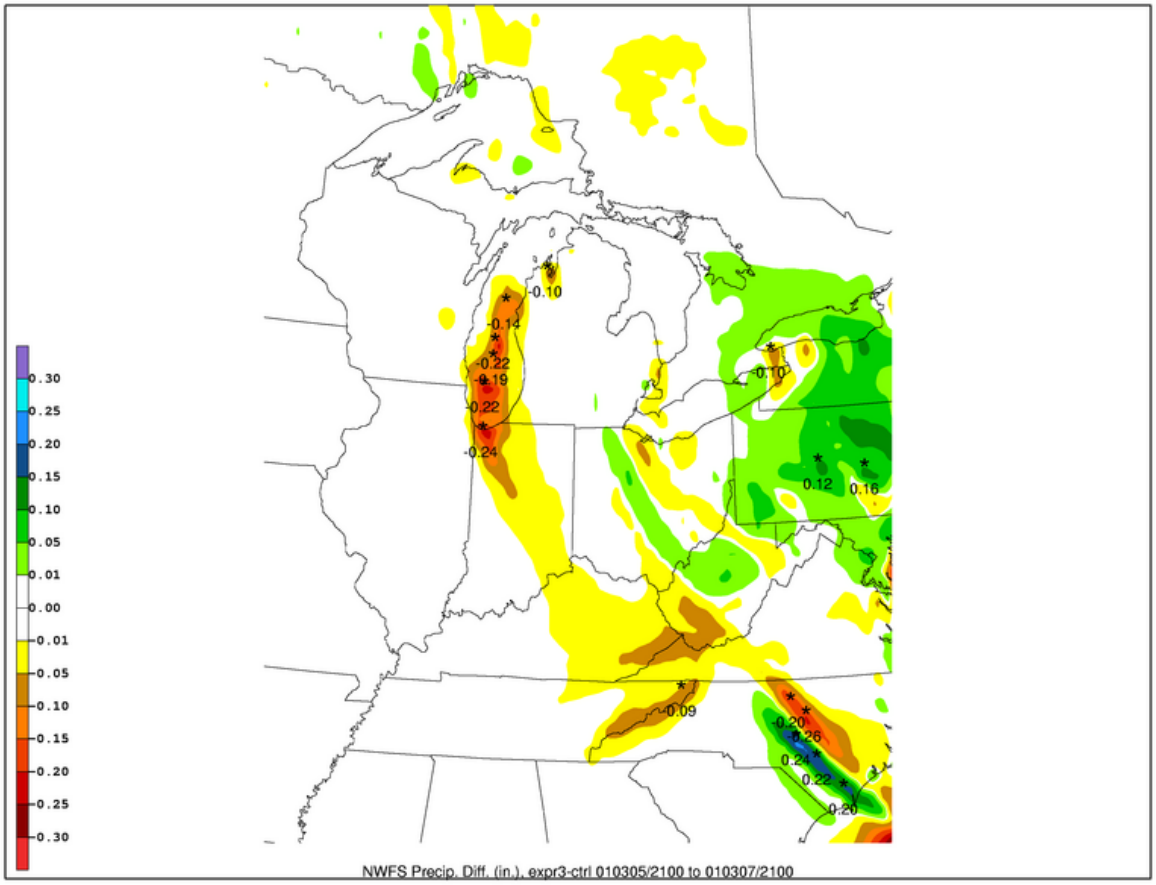

Figure 5.47. As in Figure 5.46 except for larger view.

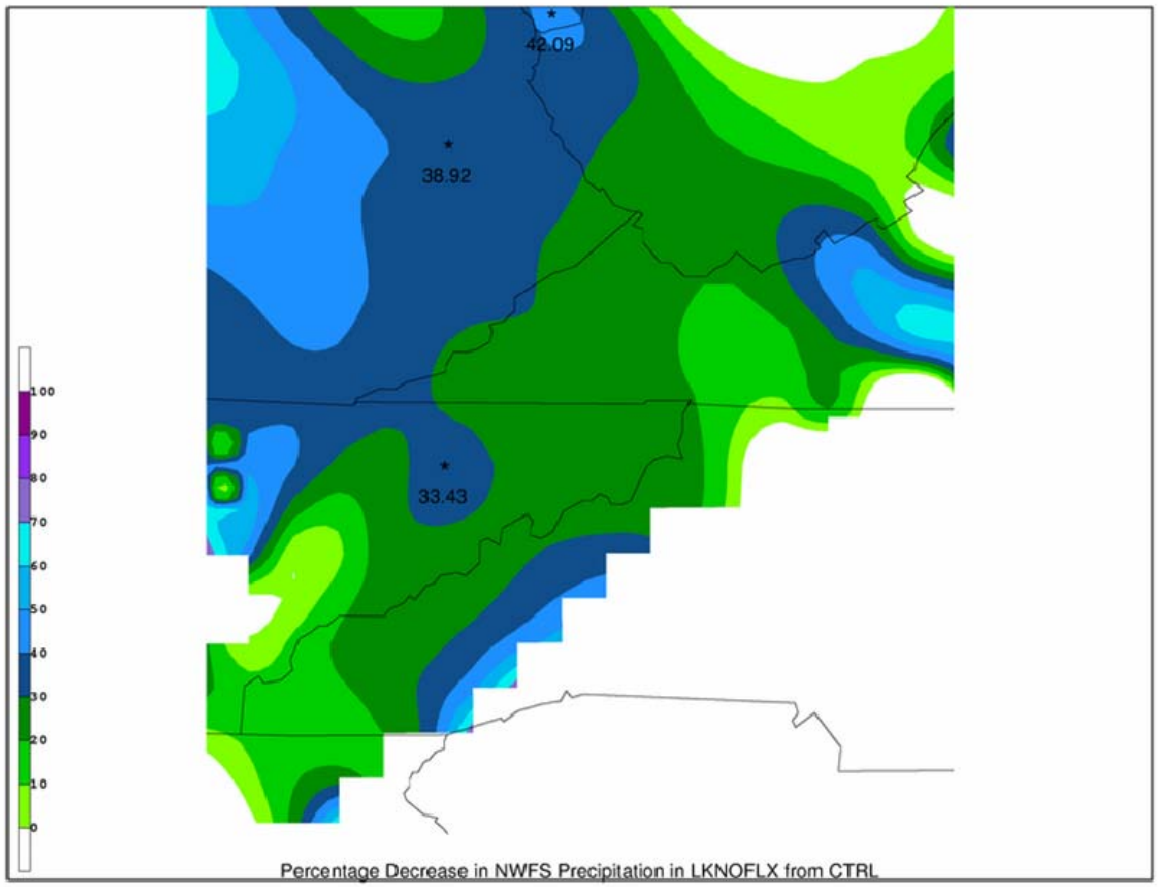

Figure 5.48. Percent of decrease in liquid equivalent precipitation for total NWFS precipitation in LKNOFLX from CTRL for areas of decreased precipitation (shaded as in colorbar in lower left corner).

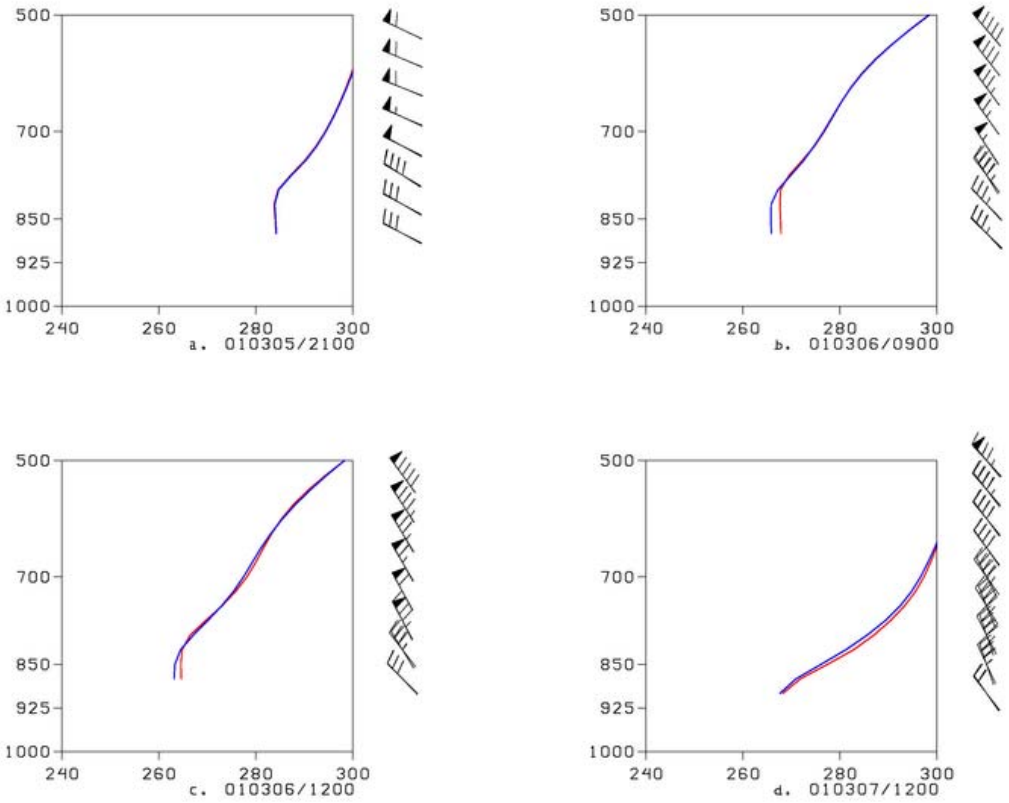

Figure 5.49. θ_e (K) profile at Erwin, TN (36.14 N;-82.39 W) for CTRL (red) and LKNOFLX (blue) at: (a) 2100 UTC 5 March 2001; (b) 0900 UTC 6 March 2001; (c) 1200 UTC 6 March 2001; (d) 1200 UTC 7 March 2001.

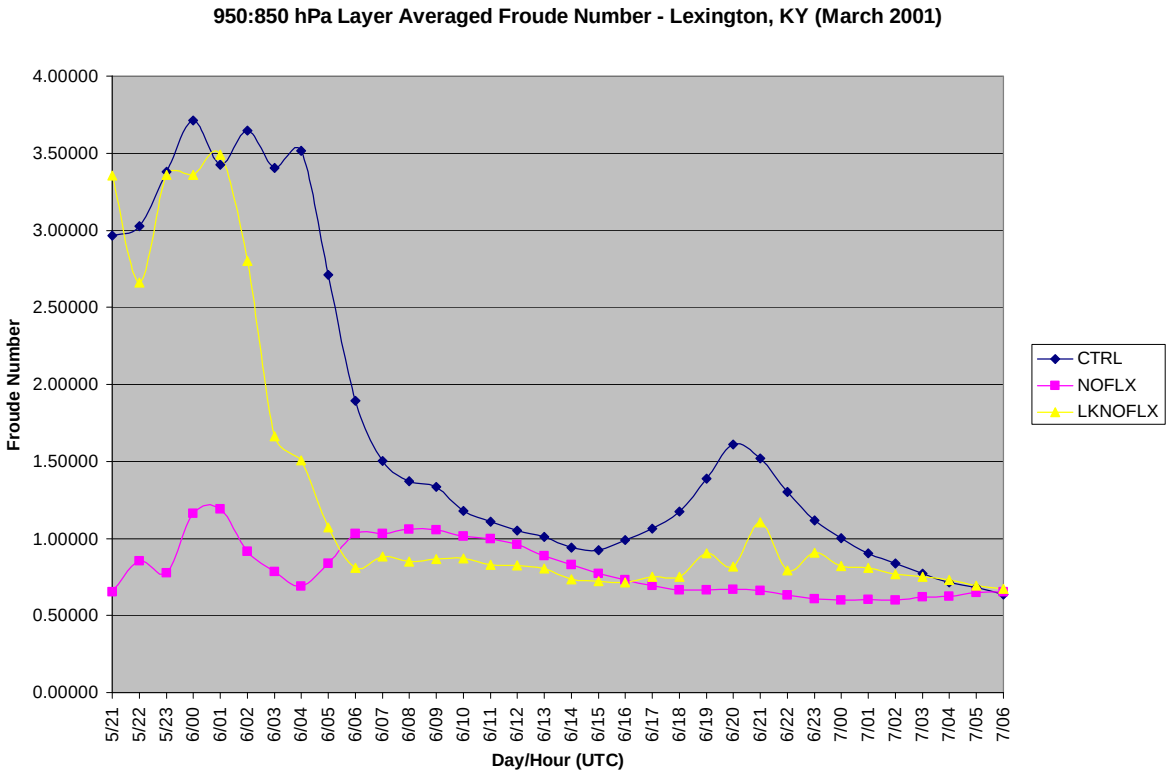

Figure 5.50. 950–850 hPa layer averaged Froude number for Lexington, KY (38.03°N;-84.44°W) from 2100 UTC 5 March to 0600 UTC 7 March for CTRL (blue), NOFLX (pink), and LKNOFLX (yellow).

6. Conclusions, application, and future work

6.1. Conclusions

The main objective of this study was to quantify and evaluate the role of the Great Lakes in NWFS events for select cases via model experiments using the WRF model. These model experiments were designed in a way that removed the effect of the Great Lakes for the purpose of quantifying the resulting changes in NWFS precipitation in the southern Appalachian Mountains. The role of the Great Lakes was then further quantified based on changes in the Froude number of the low-level upstream airmass which was calculated and compared amongst the model runs. Below, is a list of conclusions based on the results of the model runs performed of the selected cases presented in this study.

1. *The Great Lakes play an important role in some NWFS events, and can be responsible for 20–30% of the precipitation that occurs in these events.* In the LKNOFLX run of both the February 2005, and March 2001 NWFS events, large decreases in precipitation occurred across the southern Appalachians in comparison to the CTRL. A percentage of precipitation decrease calculation revealed a ~20% decrease in the February 2005 case in the region. Similarly, the March 2001 case showed a 20–30% decrease with some locations featuring a decrease in precipitation upwards of 50% in the southern Appalachians.
2. *In NWFS events that are favorable for a Great Lakes influence, the role of the lakes is to destabilize the upstream low-level airmass and increase the Froude number.* By increasing the Froude number, more air is able to rise up and over the southern Appalachians and less blocking occurs. This effect of the Great Lakes on the Froude

number of the low-level upstream airmass is best shown in Froude number calculations done roughly half-way between the lakes and the mountains. In the February 2005 event, the LKNOFLX run had an average 950–850 hPa Froude number of 0.99, which was 0.40 less than the CTRL value of 1.39. Similarly, the LKNOFLX run of the March 2001 event had and average low-level Froude number of 1.28, which was 0.42 less than the CTRL value of 1.70. These variations in the Froude number shows that by removing surface fluxes of heat and moisture from the lakes, a more stable airmass results upstream of the southern Appalachians, and thus a lower Froude number.

3. *Overall, the spatial extent and distribution of NWFS precipitation appears to be largely determined by the terrain of the southern Appalachians, and not the presence and magnitude of lake-induced instability.* The precipitation extent and distribution in the NOFLX and LKNOFLX runs of both the February 2005 and March 2001 was generally quite similar to the CTRL. In both cases, both experimental runs featured a maximum in precipitation along the higher terrain of the southern Appalachians, as well as a tight precipitation gradient on both the west and east sides of the terrain axis. Instead, the precipitation amount was altered more than the spatial extent and distribution.
4. *Influence from the Great Lakes is not a necessary ingredient for a NWFS event to occur.* This can easily be seen in the December 2003 case where a favorable low-level trajectory did not exist for a lake influence, but yet a high impact event occurred with over two feet of snow in some locations. Instead, this result points to the Great

Lakes as a source of precipitation enhancement for only those cases that exhibit low-level trajectories from the southern Appalachians upstream to the lakes.

6.1.1. Limitations of the study

One of the main limitations of this study is the fact that the WRF model runs were performed with 24 km grid spacing. This not only reduced the resolution on the model domain, but is also responsible for a significant decrease in the model terrain of the southern Appalachian Mountains. It is believed that this under representation of the southern Appalachians in the WRF model runs could be responsible for the lack of more localized precipitation maxima produced by the model runs for the selected cases. Also, this study only focuses on three NWFS events. Analyzing more events across the entire winter time period would be beneficial to solidify the results and conclusions discussed here.

Another potential limitation of the study is the difficulty of comparing the model results to observations in a region often devoid of data. Snowfall observations for the cases presented were gathered from the network of cooperative observers throughout the region. However, the combination of complex terrain and sparsely populated area makes the distribution of observations quite irregular.

Finally, the NOFLX and LKNOFLX experimental runs do contain surface fluxes of heat and moisture despite the fact that these same fluxes are set to zero over the entire model domain and just over water respectively. These fluxes are introduced via the initial conditions and the lateral boundary conditions provided by the NARR data used to complete the model runs. These data contain surface fluxes of heat and moisture at the times when the boundary conditions are updated, but at all other subsequent times are set to zero by the

process described in section 2.3.2. Despite this potential limitation of the study, both the NOFLX and LKNOFLX experimental model runs are believed to provide a useful test of the scientific questions and hypotheses examined in this study.

6.2. Application

6.2.1. Operational significance

The operational significance of this study is apparent in two main ways. First, there are several NWS forecast offices that stand to benefit from a greater understanding of NWFS events in the southern Appalachians. These offices encompass the entire stretch of the southern Appalachians and include the local offices in Greenville-Spartanburg, SC, Morristown, TN, Blacksburg, VA, Jackson, KY, and Charleston, WV. The sheer number of these offices and their coverage of the southern Appalachians show that NWFS events are not a local forecasting phenomenon and are instead a regional forecasting consideration. Also, as the selected cases in this study and others show, NWFS events are possible across many months during the year and are a forecasting situation that operational forecasters have to consider on a consistent basis.

Finally, the operational significance of this study extends further into the individual NWS forecast offices due to the use of the workstation WRF on localized domains (Rozumalski 2006). At many of the offices in the southern Appalachian region, the workstation WRF is being setup and utilized to model local weather phenomena on a much smaller scale than the operational forecast models such as the NAM and the GFS. Though the workstation WRF is being used with intent for many forecasting applications such as fire

weather and aviation among others, its potential benefit can be extended into NWFS events. Due to the fact that the workstation WRF is being run independently at many individual offices, the configuration of the model at each office could potentially be different because of the flexibility of the WRF infrastructure. This flexibility allows for the model to be tuned and setup with the desired specifications of model parameterizations such as the PBL scheme among others. For example, in this study, the sensitivity of selected NWFS events to the selection of PBL scheme was tested. Overall, from the results of this study, the YSU PBL scheme provided the best representation of NWFS precipitation in the three selected cases. Therefore, the NWS offices in the southern Appalachians could consider using the YSU PBL scheme in the workstation WRF during the NWFS season.

6.2.2. Forecasting considerations

The results of this study are perhaps best applied with consideration of the presence of convective instability in NWFS events. Currently operational forecasters in the southern Appalachians use a variety of parameters to forecast the amount and spatial extent of snowfall expected from NWFS events (Lee 2005). These parameters include moisture characteristics of the air mass west of the mountains, temperature, stability, and wind speed and direction (Lee 2005). In addition to the current methodologies used, the results of this study suggest that further investigation of the low-level stability between the Great Lakes and the southern Appalachians could be important. Also, identifying events that have low-level trajectories conducive to a Great Lakes influence could alert forecasters to the possibility of the lakes modifying stability of the airmass upstream of the southern Appalachians. This could be accomplished in a similar manner to this study by using cross-sections of θ_e taken

along a plane extending from the southern Appalachians upstream toward the Great Lakes. Such cross-sections would allow for forecasters to identify whether potential instability is present for a particular case. Also, use of the Froude number could be potential enhancement to NWFS forecast methodologies. Local workstation WRF output could be used to derive the Froude number of the low-level upstream airmass to gauge the degree of blocking that will occur when this airmass impinges upon the southern Appalachian region.

6.3. Future work

There are a plethora of possible avenues for future research concerning NWFS events in the southern Appalachians to take. First, higher resolution WRF modeling needs to be performed on the cases in this study as well as others. As stated in section 2.3.2, all of the model runs discussed in this study were run on a domain with 24-km grid spacing. This is a rather coarse model grid, though it is encouraging that the WRF was still able to reasonably depict the selected NWFS events. Higher resolution model runs could be nested down to ~4km grid spacing or less and may reveal even more significant details about NWFS events. Reducing the grid spacing on the model domain in the southern Appalachians would have two other benefits including allowing for explicit convection model runs, and a much better representation of the southern Appalachian terrain. As outlined in section 2.3.1.2, the coarse 24km grid spacing used in this study was the cause of the underestimation of the height of the southern Appalachians.

Two other areas of future work include an observational study of NWFS events and an operational model climatology. From an observational standpoint the benefits include a better understanding of the snow-to-liquid ratio of NWFS events as well as the cloud physics

and snowfall production that occurs. This type of study could really shed light on the small-scale physical processes that are important to NWFS events in the southern Appalachians. Also, an operational model climatology of these events would be greatly beneficial. Such a study could help highlight what characteristics of NWFS events that the models represent with success as well as those that they fail to adequately capture. This type of study would be especially beneficial to forecasters in the region where model biases could have significant impacts on forecasting operations and methodologies.

Finally, continued collaboration between the academic and operational forecasting community is necessary to further improve understanding of NWFS events in the southern Appalachians. Forecaster feedback on events of varying scales in conjunction with future research studies on NWFS events is the best way to continue the progress made concerning this regional forecasting problem. Useful tools and applications are expected to be developed with time, improving forecaster performance and awareness of NWFS events in the southern Appalachians.

7. List of References

Bluestein, H. B., 1992: Synoptic-Dynamic Meteorology in Midlatitudes, Vol. I., Oxford University Press.

Chang, S. S., and R. R. Braham Jr., 1991: Observational study of a convective internal boundary layer over Lake Michigan. *J. Atmos. Sci.*, **48**, 2265–2279.

desJardins, M. L., K. F. Brill, and S. S. Schotz, 1991: GEMPAK 5 Part I-GEMPAK 5 programmer's guide. National Aeronautics and Space Administration. [Available from Scientific and Technical Information Division, Goddard Space Flight Center, Greenbelt, MD 20771.]

Draxler, R. R. and G. D. Rolph, 2003. HYSPLIT (HYbrid Single-Particle Lagrangian Integrated Trajectory) Model access via NOAA ARL READY Website (http://www.arl.noaa.gov/ready/hysplit4.html). NOAA Air Resources Laboratory, Silver Spring, MD.

Dudhia, J., 1989: Numerical study of convection observed during the winter monsoon experiment using a mesoscale two-dimensional model, *J. Atmos. Sci*., **46**, 3077–3107.

Fishel, G. B., and S. Businger, 1993: Heavy orographic snowfall in the southern Appalachians: a late season case study. *Postprints, Third National Heavy Precipitation Workshop*, 275–284. Pittsburgh, PA: NWS/NOAA.

Gurka, J. G., E. P. Auciello, A. F. Gigi, J. S. Waldstreicher, K. K. Keeter, S. Businger, and L. G. Lee, 1995: Winter weather forecasting throughout the eastern United States. Part II: An operational perspective of cyclogenesis. *Wea. Forecasting,* **10**, 21–41.

Hjelmfelt, M. R., 1992: Orographic effects in simulated lake-effect snowstorms over Lake Michigan. *Mon. Wea. Rev.*, **120**, 373–377.

Hong, S.-Y., and H.-L. Pan, 1996: Nonlocal boundary layer vertical diffusion in a medium-range forecast model, *Mon. Wea. Rev*., **124**, 2322–2339.

Hong, S.-Y., Y. Noh, and J. Dudhia, 2006: A new vertical diffusion package with an explicit treatment of entrainment processes. *Mon. Wea. Rev.*, **134**, 2318–2341.

Janjic, Z. I., 1990: The step-mountain coordinate: physical package, *Mon. Wea. Rev*., **118**, 1429–1443.

———, 1994: The step-mountain eta coordinate model: further developments of the convection, viscous sublayer and turbulence closure schemes, *Mon. Wea. Rev*., **122**, 927–945.

———, 1996: The surface layer in the NCEP Eta Model, Eleventh Conference on Numerical Weather Prediction, Norfolk, VA, 19–23 August; Amer. Meteor. Soc., Boston, MA, 354–355.

———, 2000: Comments on ”Development and Evaluation of a Convection Scheme for Use in Climate Models”, *J. Atmos. Sci*., **57**, p. 3686.

———, 2002: Nonsingular Implementation of the Mellor-Yamada Level 2.5 Scheme in the NCEP Meso model, NCEP Office Note, No. 437, 61 pp.

Keeter, K. K., S. Businger, L.G. Lee, and J. S. Waldstreicher, 1995: Winter weather forecasting throughout the eastern United States. Part III: The effects of topography and the variability of winter weather in the Carolinas and Virginia. *Wea. Forecasting,* **10**, 42–60.

Keyser, D. and L. W. Uccellini, 1987: Regional models: Emerging research tools for synoptic meteorologists. *Bull. Amer. Met. Soc.,* **68**, 306–320.

Kristovich, D. A. R., N. F. Laird, and M. R., Hjelmfelt, 2003: Convective evolution across Lake Michigan during a widespread lake-effect snow event. *Mon. Wea.Rev.*, **131**, 643–655.

Lee, L. G., 2005: *Northwest Flow Snow Events*. CSTAR Workshop Presentation, October 7, 2005.

Lin, Y.-L., R. D. Farley, and H. D. Orville, 1983: Bulk parameterization of the snow field in a cloud model. *J. Climate Appl. Meteor*., **22**, 1065–1092.

———, 2007: *Mesoscale Dynamics*. Cambridge University Press.

Maglaras, G. J., J. S. Waldstreicher, P. J. Kocin, A. F. Gigi, and R. A. Marine, 1995: Winter weather forecasting throughout the eastern United States. Part I: An overview. *Wea. Forecasting,* **10**, 5–20.

Mesinger, F., and Coauthors: North American Regional Reanalysis. *Bull. Amer. Met. Soc*., **87**, 343–360.

Michalakes, J., S. Chen, J. Dudhia, L. Hart, J. Klemp, J. Middlecoff, and W. Skamarock (2001): *Development of a Next Generation Regional Weather Research and Forecast Model. Developments in Teracomputing: Proceedings of the Ninth ECMWF Workshop on the Use of High Performance Computing in Meteorology*. Eds. Walter Zwieflhofer and Norbert Kreitz. World Scientific, Singapore. pp. 269–276.

Mlawer, E. J., S. J. Taubman, P. D. Brown, M. J. Iacono, and S. A. Clough, 1997: Radiative transfer for inhomogeneous atmosphere: RRTM, a validated correlated-k model for the longwave. *J. Geophys. Res*., **102** (D14), 16663–16682.

Niziol, T. A., W. R. Snyder, and J. S. Waldstreicher, 1995: Winder weather forecasting throughout the eastern United States. Part IV: Lake Effect Snow. *Wea. Forecasting,* **11**, 61–76.

Perry, L.B., 2006: Synoptic Climatology of Northwest Flow Snowfall in the Southern Appalachians. Ph.D. dissertation, Dept. of Geography, University of North Carolina at Chapel Hill, 176 pp. [Available from Dept. of Geography, University of North Carolina at Chapel Hill, Chapel Hill, NC 27599.]

———, and C. E. Konrad, 2004: Northwest flow snowfall in the southern Appalachians: spatial and synoptic patterns. *Proceedings of the 61st Eastern Snow Conference*, 179–189.

———, and ———, 2005: The Influence of the Great Lakes on snowfall patterns in the southern Appalachians. *Proceedings of the 62nd Eastern Snow Conference*, 279–289.

———, and ———, 2006: Relationships between NW flow snowfall and topography in the Southern Appalachians, USA. *Clim. Res.*, **32**, 35–47.

———, C. E. Konrad, and T. W. Schmidlin, 2007: Antecedent upstream air trajectories associated with northwest flow snowfall in the southern Appalachian Mountains. *Wea. Forecasting*, **22**, 334–352.

Rozumalski, R. A., 2006: National Weather Service SOO Science and Training Resource Center - WRF Environmental Modeling System User's Guide, 89 pp.

Sabones, M. E., and K. K. Keeter, 1989: Late season snowfalls in the North Carolina Mountains associated with cutoff lows. In, *Postprints, Second National Winter Weather Workshop*, pp. 230–236. Raleigh, NC: NWS/NOAA. (NOAA Technical Memorandum NWS ER-82).

Schmidlin, T. W., 1992: Does lake-effect snow extend to the mountains of West Virginia? *Proceedings of the 49th Eastern Snow Conference*, 145–148.

Skamarock, W. C., J. B. Klemp, J. Dudhia, D. O. Gill, D. M. Barker. W. Wang, and J. G. Powers, 2005: A description of the Advanced Research WRF Version 2. NCAR Tech. Note, NCAR/TN-468+STR, 100 pp.

Smirnova, T. G., J. M. Brown, and S. G. Benjamin, 1997: Performance of different soil model configurations in simulating ground surface temperature and surface fluxes. *Mon. Wea. Rev*., **125**, 1870–1884.

———, ———, ———, and D. Kim, 2000: Parameterization of coldseason processes in the MAPS land-surface scheme. *J. Geophys. Res*., **105** (D3), 4077–4086.

Sousounis, P. J., and J. M. Fritsch, 1994: Lake-aggregate mesoscale disturbances. Part II: A case study of the effects on regional and synoptic-scale weather systems. *Bull. Amer. Met. Soc.,* **75,** 1793–1811.

———, and G. E. Mann, 2000: Lake-aggregate mesoscale disturbances. Part V: Impacts on lake-effect precipitation. *Mon. Wea. Rev.,* **128**, 728–745.